



University
of Glasgow

Schachtner, Hannah (2013) *Investigation of the structural and functional role of podosomes in megakaryocytes*. PhD thesis.

<http://theses.gla.ac.uk/4032/>

Copyright and moral rights for this thesis are retained by the author

A copy can be downloaded for personal non-commercial research or study, without prior permission or charge

This thesis cannot be reproduced or quoted extensively from without first obtaining permission in writing from the Author

The content must not be changed in any way or sold commercially in any format or medium without the formal permission of the Author

When referring to this work, full bibliographic details including the author, title, awarding institution and date of the thesis must be given

**Investigation of the functional and structural role
of podosomes in megakaryocytes**

by

Hannah Schachtner

**Submitted in fulfillment of the requirements for the
Degree of Doctor of Philosophy**

Beatson Institute for Cancer Research

University of Glasgow

February 2013

Abstract

Megakaryocytes (Mks) give rise to platelets via extension of proplatelet arms, which are released through the vascular sinusoids into the bloodstream. Mks and their precursors undergo varying interactions with the extracellular environment in the bone marrow during their maturation and positioning in the vascular niche. The dynamic remodeling of the actin cytoskeleton and the formation of cell-matrix contacts such as podosomes are fundamental for this process. However, the role and function of podosome structures in Mks are poorly understood.

Podosomes are well characterized in different cell-types of the myeloid lineage such as macrophages and dendritic cells. Their formation is associated with a dynamic F-actin turnover, facilitated cell migration and the degradation of extracellular matrix (ECM). The function of podosome organelles is multifaceted and is described in association with cell adhesion, motility, ECM lysis, invasion and mechanosensors.

A fundamental analysis of podosomes was necessary to define a potential function for these structures in Mks. I determined an abundant formation of classical podosomes with an F-actin core and a Vinculin ring in primary murine Mks, which were adherent on different physiological relevant ECM substrates such as fibrinogen, collagen I and a native basement membrane. Lifetime analysis was performed and was demonstrated to be dependent on the substrate as well as on Myosin-II activity. Another key feature of podosomes, the degradation of ECM proteins, could be detected and was mediated in an MMP associated manner. Furthermore, I verified that podosomes are necessary to penetrate a native basement membrane, which is amongst others part of blood vessels.

In this thesis I therefore demonstrate multifaceted properties of Mk podosomes and direct a potential function of these structures in the process of Mk maturation and possibly in platelet formation

Acknowledgement

I would sincerely like to thank my supervisor Prof. Laura Machesky, who always was supportive with guidance, help and new inspiring ideas. I also would like to thank Prof. Steve Watson, his critical input often changed my perspective of interpreting data of the “red protein” in the context of megakaryocytes and platelets. I acknowledge my advisor Prof. Robert Insall for interesting discussions, which helped the progress of my project. A special thank goes to Simon Calaminus, who was always a “big” help in the lab, during scientific discussions and a moral support.

I also want to thank the members of the Machesky, the Insall and the Anderson lab, especially Heather, Amber, Tobi and Juli; it was great fun to work with or beside you. I really appreciated the company of Max and Elena, which were very helpful with any kind of (scientific) business, moral support and the increase of my coffee consumption.

I also want to thank my family, especially my Dad and my aunt, who were always interested in my work and tried to understand this. I am very thankful for my brother, who helped me to believe in myself. I also thank my sisters and my Mum for supporting me during the ups and downs of the last three years.

Finally a huge thanks to Janis Vogt for his patients and sympathy, for all the proof-reading and support especially in the last few months. I dedicate this thesis to him, my family and friends, without whom my life would be a much poorer place.

Declaration

I, Hannah Schachtner, declare that I am the sole author of this thesis. All the research presented here is my own unless where I have declared otherwise. I have consulted all of the references cited within this thesis and none of this research has previously been accepted for a higher degree.

Hannah Schachtner

Publications arising from this work

Schachtner H*, Li A*, Stevenson D, Calaminus S, Thomas S, Watson SP, Sixt M, Wedlich-Soldner R, Strathdee D, Machesky LM. **Tissue inducible lifeact expression visualizes actin dynamics *in vitro* and *in vivo*.** May, 2012, European Journal of Cell Biology

*denotes equal contribution

Calaminus S, Guitart A, Sinclair A, **Schachtner H**, Watson S, Holyoake T, Kranc K, Machesky LM. **Lineage tracing of Pf4-Cre marks hematopoietic stem cells and their progeny.** November, 2012, PlosOne

Schachtner H., Calaminus S, Sinclair A, Moneypenny J, Blundell M, Jones G, Thimas S, Watson S, Machesky LM. **Megakaryocyte assemble podosomes that degrade matrix and protrude through basement membrane.** February, 2012, Blood

Abbreviations

2D – two-dimensional

3D – three-dimensional

Abi – Abl-kinase interactor

ACD – Acid-Citrate Dextrose

ACK – Ammonium-chloride-potassium buffer

ADF – Actin depolymerizing factor

AFAP-110 – Actin filament-associated protein 1

AMP – Adenosine monophosphate

ANOVA – Analysis of variance

Arp – Actin related protein

ATP – Adenosine triphosphate

BM – Basement membrane

BSA – Bovine serum albumin

Cdc42 – Cell division control protein 42 homolog

CR16 – Corticosteroid and regional expression protein 16 homolog

DAPI – 4',6-Diamidino-2-Phenylindole, Dihydrochloride

DMEM – Dulbecco's Modified Eagle Medium

DNA – Deoxyribonucleic acid

ECL – Enhanced chemiluminescence

ECM – Extracellular matrix

F-actin – Filamentous actin

FA – Focal adhesion

FAK – Focal adhesion kinase

FBS – Fetal bovine serum

FGD1 – Faciogenital dysplasia 1 protein

FITC – Fluorescein isothiocyanate

G-actin – globular actin

GAP – GTPase activating protein

GAPDH – Glyceraldehyde 3-phosphate dehydrogenase

GDP – Guanosine diphosphate

GEF – Guanine nucleotide exchange factor

GFP – Green fluorescent protein

GPVI – Glycoprotein VI

GTP – Guanosine triphosphate

Hck – Hemopoietic cell kinase

HEK – Human embryonic kidney

HS1 – Hematopoietic lineage cell-specific protein 1

HSPC300 – Haematopoietic stem/progenitor cell protein 300

HUVEC – Human umbilical vein endothelial cells

IF - Immunofluorescence

Ig G – Immunoglobulin G

IRSp53 – Insulin receptor substrate p53/p58

IQGAP – IQ motif containing GTPase activating proteins

KO – Knockout

LIMK – LIM domain kinase

Ly6G – Lymphocyte antigen 6 complex, locus G

mDia – Diaphanous homolog 1

Mk – Megakaryocyte

MLCK – Myosin light chain kinase

MMP – Matrix metalloprotease

MOI – Multiplicity of infection

MT1-MMP – Membrane-type 1 matrix metalloproteinase

N-Wasp – Neural Wiskott-Aldrich syndrome protein

Nap – Nck-associated protein

Nck – Non-catalytic region of tyrosine kinase adaptor protein

NPF – Nucleation-promoting factor

p130Cas – Breast cancer anti-estrogen resistance protein 1

PAK – p21 protein (Cdc42/Rac)-activated kinase

PBS – Phosphate buffered saline

PEI – Polyethylimine

Pf4 – Platelet factor 4

PGI₂ – Prostaglandin I₂, Prostacyclin

PIP2 – Phosphatidylinositol 4,5-biphosphate

PKC – Protein kinase C

PPL – Proplatelet

PRP – Platelet-rich plasma

Pyk2 – Protein tyrosine kinase 2 beta

qRT-PCR – Quantitative reverse transcriptase polymerase chain reaction

Rac – Ras-related C3 botulinum toxin substrate

RFP – Red fluorescent protein

Rho – Ras homolog family member

ROCK – Rho-associated coiled-coil containing protein kinase

RIPA buffer – Radioimmunoprecipitation assay buffer

SCF – Stem Cell Factor

SDF-1 α – Stromal derived factor-1 α

SFK – Src family kinases

SFM – Serum free medium

SH2 – Src homology 2

SH3 – Src homology 3

Sra – Specifically Rac-1-associated protein

Src – Sarcoma

TBS-T – Tris-buffered saline and tween 20

TGF- β – Transforming growth factor beta

TIRF – Total internal reflection

TPO – Thrombopoietin

VCA – Verprolin central acidic domain

VSV-G – Vesicular stomatitis virus-protein G

vWF – von Willebrand Factor

Was – Wiskott-Aldrich syndrome

Wasp – Wiskott-Aldrich syndrome protein

Wave – Wasp family verprolin homologs

Wip – Wasp-interacting protein

WIRE – Wip-related

wt – Wild type

Abstract	I
Acknowledgement	III
Declaration	IV
List of Tables	- 1 -
List of Figures	- 2 -
1 Introduction	- 5 -
1.1 Cell types forming podosomes.....	- 5 -
1.2 Core structure	- 8 -
1.2.1 F-actin nucleation	- 10 -
1.2.2 Rho GTPases.....	- 11 -
1.2.3 Wasp and Wip	- 14 -
1.2.4 The Wave complex.....	- 19 -
1.2.5 The Arp2/3 complex.....	- 20 -
1.2.6 Cortactin	- 23 -
1.2.7 Myosin II	- 25 -
1.3 Ring structure.....	- 26 -
1.3.1 Integrins.....	- 27 -
1.3.2 Src family kinases – Src kinase	- 30 -
1.3.3 Vinculin interacting with α -actinin, Talin and Paxillin	- 31 -
1.3.4 Kindlins	- 33 -
1.3.5 Matrix metalloproteases and serine proteases.....	- 34 -
1.4 Other podosome relevant proteins	- 37 -
1.4.1 Microtubules	- 37 -
1.4.2 Formins.....	- 38 -
1.4.3 Fascin	- 39 -
1.5 Podosome properties and functions	- 40 -

1.5.1	Podosomes in migration	- 40 -
1.5.2	Adhesion.....	- 41 -
1.5.3	Size and lifetime	- 42 -
1.5.4	Degradation	- 44 -
1.5.5	Mechanosensor	- 45 -
1.6	Podosome versus invadopodia and focal adhesions – a comparison.....	- 46 -
1.6.1	Invadopodia	- 46 -
1.6.2	Focal adhesions	- 49 -
1.7	Megakaryocytes, proplatelets and platelets	- 51 -
1.7.1	Megakaryopoiesis and the bone marrow environment	- 51 -
1.7.2	Proplatelet formation.....	- 55 -
1.7.3	Platelets spreading and activation	- 58 -
1.8	Aims	- 60 -
2	Materials and Methods	- 61 -
2.1	Antibodies and reagents:	- 61 -
2.2	Inhibitors:	- 62 -
2.3	Extracellular matrix proteins:	- 62 -
2.4	Mice	- 63 -
2.5	Cell Culture	- 63 -
2.5.1	Isolation and cultivation of bone marrow derived megakaryocytes	- 63 -
2.5.2	Cultivation of HEK 293T cells and virus production	- 65 -
2.5.3	Determination of virus titre.....	- 66 -
2.5.4	Infection of Mks.....	- 67 -
2.5.5	Preparation of washed platelets	- 67 -
2.5.6	Immunoblotting.....	- 68 -
2.6	Fluorescence Microscopy	- 69 -

2.6.1	Preparation of coverslips	- 69 -
2.6.2	Immunofluorescence of fixed cells.....	- 69 -
2.6.3	Quantification of podosome numbers.....	- 70 -
2.6.4	Real-time spreading of Mks.....	- 71 -
2.6.5	Quantification of podosome lifetime.....	- 71 -
2.6.5.1	Fluorescent Labelling of ECM proteins	- 71 -
2.6.6	Degradation Assay	- 72 -
2.6.7	Quantification of matrix degradation	- 72 -
2.6.8	Basement Membrane Assay.....	- 72 -
2.6.9	Quantification of the basement membrane assay	- 73 -
2.6.10	Statistics	- 74 -
3	Megakaryocytes assemble podosomes on fibrinogen and collagen-	75 -
3.1	Summary	- 75 -
3.2	Introduction.....	- 75 -
3.3	Results.....	- 78 -
3.3.1	Podosome assembly depends on the underlying substrate	- 78 -
3.3.2	Wasp is essential for podosome formation in Mks.....	- 87 -
3.3.3	The presence of serum influences podosome assembly and the spreading behaviour of Mks seeded on collagen.....	- 90 -
3.3.4	DMSO does not influence Mk podosome assembly	- 93 -
3.3.5	Dose response curve for CK666 and Blebbistatin.....	- 95 -
3.3.6	F-actin nucleation and the Arp2/3 complex is essential for podosome assembly and spreading on collagen and fibrinogen	- 99 -
3.3.7	MMP activity and microtubules are not fundamental for podosome formation in Mks spread on collagen or fibrinogen.....	- 105 -
3.3.8	Integrin $\alpha_{IIb}\beta_3$ is involved in podosome formation on horn collagen	- 110 -
3.4	Discussion.....	- 112 -

4	Podosome lifetime and matrix degradation depends on the underlying substrate	- 117 -
4.1	Summary	- 117 -
4.1.1	Introduction	- 117 -
4.1.2	The Lifetime of podosomes is dependent on the underlying matrix .	- 119 -
4.1.3	The activity of Myosin II plays a significant role in podosome turnover.....	- 122 -
4.1.4	Mk Podosomes degrade fibrinogen but not gelatin or collagen I.....	- 129 -
4.1.5	Podosome driven degradation of fibrinogen is MMP and Myosin II dependent.....	- 131 -
4.1.6	Establishment of a native basement membrane assay	- 134 -
4.1.7	Mks form podosomes and protrusive actin-rich structures to cross a native basement membrane	- 138 -
4.1.8	Mks form podosomes to cross a native basement membrane	- 141 -
4.2	Discussion	- 146 -
5	The role of Cortactin and Abi in podosome formation	- 150 -
5.1	Summary	- 150 -
5.2	Introduction	- 150 -
5.3	Results.....	- 152 -
5.3.1	The loss of Cortactin in Mks changes podosome size but not its degradative activity	- 152 -
5.3.2	Podosome formation and spreading behavior is not changed in Abi-1 ^{+/-} Abi-2 ^{-/-} deficient Mks	- 156 -
5.3.3	Abi-1 ^{+/-} Abi-2 ^{-/-} platelets have a reduced spread area on fibrinogen in the presence of thrombin	- 159 -
5.4	Discussion	- 164 -
6	General Discussion	- 167 -
6.1	Summary	- 167 -
6.2	The ECM directs podosome properties and function	- 167 -

6.3	Podosome formation in 3D and <i>in vivo</i>	- 168 -
6.4	Podosome structures in Mks – a direction of functionality	- 171 -
6.5	Future directions	- 175 -
	References.....	- 177 -
	Appendix	

List of Tables

Table 2.1: Antibodies and reagents used in this study.....	- 61 -
Table 2.2: Inhibitors used in this study.....	- 62 -
Table 2.3: Extracellular matrix proteins used in this study	- 62 -

List of Figures

Figure 1.1: Different forms of podosome structures	- 7 -
Figure 1.2: Podosome architecture	- 9 -
Figure 1.3: Structure of Wasp family proteins	- 18 -
Figure 1.4: Actin rearrangement in podosomes and lamellipodia formation ...	- 22 -
Figure 1.5: Fundamental transmembrane receptor trafficking	- 29 -
Figure 1.6: Differentiation of the megakaryocytic lineage	- 54 -
Figure 1.7: Mks, platelet formation and the potential role of podosomes	- 57 -
Figure 3.1: Mks fully spread in 3 hours and undergo proplatelet formation on fibrinogen.	- 80 -
Figure 3.2: The underlying substrate influences the number of podosomes and the spreading behaviour of Mks.	- 81 -
Figure 3.3: Identification of podosome-core-associated proteins on horm collagen.	- 83 -
Figure 3.4: Identification of podosome-core-associated proteins on fibrinogen.	- 84 -
Figure 3.5: Visualization of adhesion-associated proteins on horm collagen..	- 85 -
Figure 3.6: Visualization of adhesion-associated proteins on fibrinogen.....	- 86 -
Figure 3.7: Wasp is necessary for podosome formation in Mks spreading on horm collagen.	- 88 -
Figure 3.8: Wasp is necessary for podosome formation in Mks spreading on fibrinogen.	- 89 -
Figure 3.9: Serum influences podosome assembly and spreading behaviour of Mks plated on horm collagen.	- 91 -
Figure 3.10: Serum does not influence podosome assembly in Mks spreading on fibrinogen.	- 92 -
Figure 3.11: DMSO does not influence podosome formation or spreading behaviour of Mks.....	- 94 -
Figure 3.12: Dose response of actin related inhibitors on Mk podosome formation and cell spreading.	- 97 -

Figure 3.13: Dose response of actin related inhibitors on Mk podosome formation and cell spreading.	98 -
Figure 3.14: Inhibition of actin-associated proteins and the influence on Mks podosome formation and spreading on horm collagen.	101 -
Figure 3.15: F-actin polymerization and Arp2/3 complex activity is essential for podosome formation on horm collagen.....	102 -
Figure 3.16: Inhibition of actin-associated proteins and the influence on Mk podosome formation and spreading on fibrinogen.	103 -
Figure 3.17: F-actin polymerization and Arp2/3 complex activity is essential for podosome formation on fibrinogen.	104 -
Figure 3.18: Dose response of GM6001 on Mk podosome formation and cell spreading.....	107 -
Figure 3.19: MMP activity and microtubule assembly is not involved in podosome formation in Mks spreading on horm collagen.....	108 -
Figure 3.20: MMP activity and microtubule assembly is not involved in podosome formation in Mks spreading on fibrinogen.....	109 -
Figure 3.21: The inhibition of integrin $\alpha_{IIb}\beta_3$ induces a reduction in podosome assembly by Mks spreading on horm collagen.....	111 -
Figure 4.1: Podosome lifetime is dependent on the underlying matrix.....	120 -
Figure 4.2: Podosome lifetime is dependent on the underlying matrix.....	121 -
Figure 4.3: Podosome lifetime is independent of MMP activity but dependent on Myosin II in Mks spreading on fibrinogen	124 -
Figure 4.4: Podosome lifetime is independent of MMP activity but dependent on Myosin II in Mks spreading on fibrinogen	125 -
Figure 4.5: Podosome lifetime is independent of MMP activity but dependent on Myosin II in Mks spreading on collagen I	126 -
Figure 4.6: Podosome lifetime is independent of MMP activity but dependent on Myosin II in Mks spreading on collagen I	127 -
Figure 4.7: Summary of Mk podosome lifetime on collagen and fibrinogen with MMP and Myosin II inhibition.....	128 -
Figure 4.8: Podosome degrade fibrinogen but not gelatin and collagen I	130 -
Figure 4.9: Podosome-mediated degradation of fibrinogen is dependent on MMP and Myosin II activity	132 -

Figure 4.10: Podosome-mediated degradation of fibrinogen is dependent on MMP and Myosin II activity	133 -
Figure 4.11: Establishment of a native basement membrane assay	136 -
Figure 4.12: Permeability of the basement membrane	137 -
Figure 4.13: Mks form podosomes on a native basement membrane	139 -
Figure 4.14: Mks form podosomes and actin-rich protrusions to cross a basement membrane	140 -
Figure 4.15: Mks use podosomes to cross a basement membrane	143 -
Figure 4.16: Mks use podosomes to cross a basement membrane	144 -
Figure 4.17: Mks use podosomes to cross a basement membrane	145 -
Figure 5.1: Cortactin ^{-/-} Mks form podosomes on fibrinogen	153 -
Figure 5.2: Cortactin ^{-/-} Mks form podosomes on fibrinogen	154 -
Figure 5.3: Cortactin ^{-/-} Mks perform podosome mediated degradation of fibrinogen	155 -
Figure 5.4: The loss of Abi-2 does not influence podosome formation in Mks-	157 -
Figure 5.5: The loss of Abi-2 does not influence podosome formation in Mks-	158 -
Figure 5.6: The heterozygous expression of Abi-1 does not affect platelet spreading on collagen I	161 -
Figure 5.7: The heterozygous expression of Abi-1 does not affect platelet spreading or actin nodule formation on fibrinogen	162 -
Figure 5.8: The heterozygous expression of Abi-1 does not affect platelet spreading or actin nodule formation on fibrinogen in the presence of thrombin	163 -
Figure 6.1: Mks form podosome-like structures in a 3D collagen I matrix	170 -
Figure 6.2: Mks with larger nuclei have an increased ability to degrade a fibrinogen matrix	174 -

1 Introduction

1.1 Cell types forming podosomes

Podosomes are dynamic F-actin based adhesion structures associated with motile cells of the myeloid lineage such as macrophages (Linder *et al.*, 2000a), monocytes (Cougoule *et al.*, 2010), dendritic cells (Olivier *et al.*, 2006) or osteoclasts (Saltel *et al.*, 2008) but also endothelial cells (Rottiers *et al.*, 2009), smooth muscle cells (Kaverina *et al.*, 2003) or Src-transformed fibroblasts (Berdeaux *et al.*, 2004). Macrophages form evenly distributed podosomes during spreading and assemble at the leading lamella of a migrating cell similar to dendritic cells (Banon-Rodriguez *et al.*, 2011; Evans *et al.*, 2003; Linder *et al.*, 2000b). This is in contrast to osteoclasts, which form a podosome belt along the rim of the cell or podosome clusters on glass and a so-called sealing zone, which is related to podosome structures, on a bone substrate (Luxenburg *et al.*, 2007). Similar structures are formed in endothelial cells exposed to TGF- β , in which podosomes assemble into large ring-shaped formations called podosome rosettes (Varon *et al.*, 2006). Independently of TGF- β , podosomes are assembled in the same rosette-like appearance in Src transformed fibroblasts (Pan *et al.*, 2011). Another trigger for podosome assembly are phorbol esters, which activate integrins, in smooth muscle cells (Eves *et al.*, 2006).

The podosome formations in the mentioned cell types differ from each other in the appearance and the structural organization (Figure 1.1). However, there are hallmarks for podosome structures like the subdivision into an F-actin core and an Integrin-associated ring structure, the degradation of extracellular matrix (ECM)

proteins and a very dynamic F-actin turnover rate displayed by a short lifetime of podosomes (Linder *et al.*, 2011).

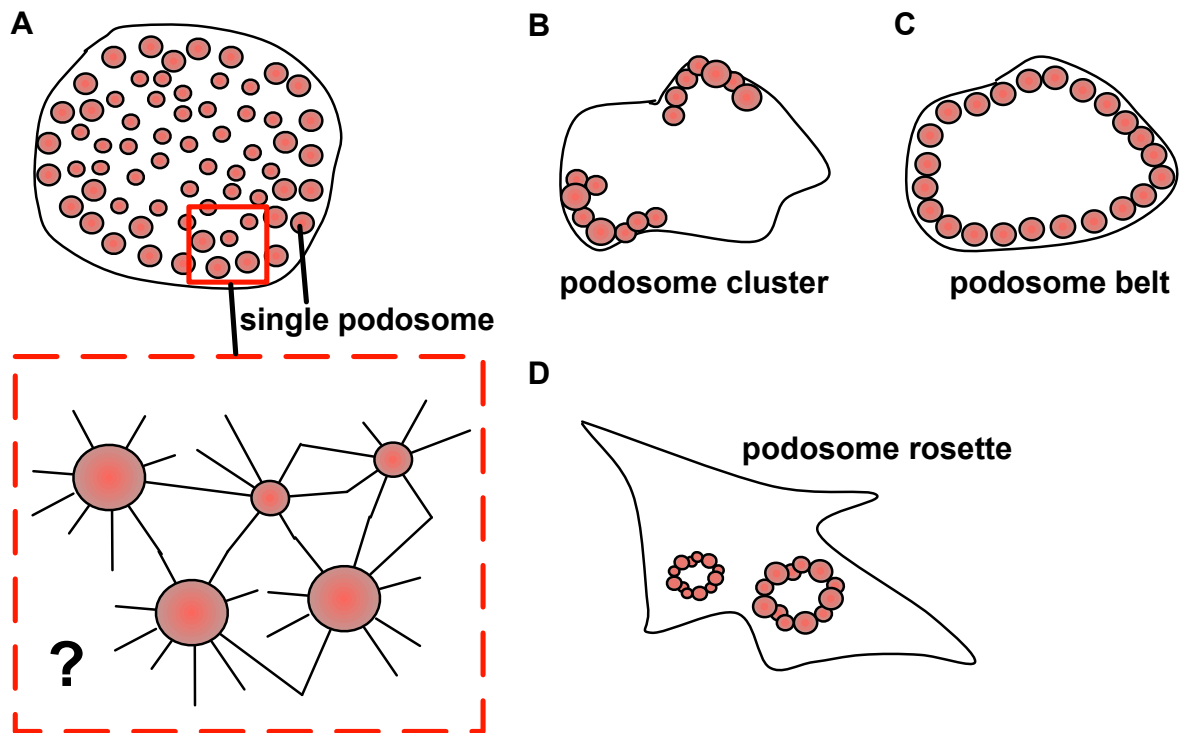


Figure 1.1: Different forms of podosome structures

There are different arrangements of podosome formation. (A) Single podosomes, which have a random distribution and are regular shaped. The red square represents a blow up of a few podosomes, indicating a hypothetical network of podosomes throughout the cell connected via radial fibers. (B) Podosome cluster formation is most common in osteoclasts, in which the formation of podosomes correlates with the cell's differentiation state. (C) Podosome belt formation, which is associated with the previous presence of podosome cluster and rings and ultimately evolve into an absorbing F-actin rich sealing zone. (D) Podosome rosettes are well established in Src-transformed fibroblasts and endothelial cells, which form smaller rosettes but more numerous compared to transformed fibroblasts. Figure was adapted from Linder *et al.*, 2011.

1.2 Core structure

Podosomes can be subdivided into a ring and a core structure, in which both parts are characterized by specific proteins (Figure 1.2). F-actin and its associated proteins, which are required for F-actin nucleation, polymerization and stabilization, dominate the core structure of podosomes. The formation of the F-actin core was shown to be based on a branched actin network and is therefore dependent on the Actin-related protein 2/3 complex (Arp2/3 complex). Nevertheless, it is also reported that radial F-actin fibers are formed, which connect the core with the adhesion proteins of the ring structure, as well as single podosomes with each other (Cox *et al.*, 2012; Luxenburg *et al.*, 2007). The actual F-actin core is also reported to be surrounded by an actin cloud containing not only F-actin but also G-actin (Akisaka *et al.*, 2001).

The most important proteins for the podosome core and its regulators are discussed in detail below.

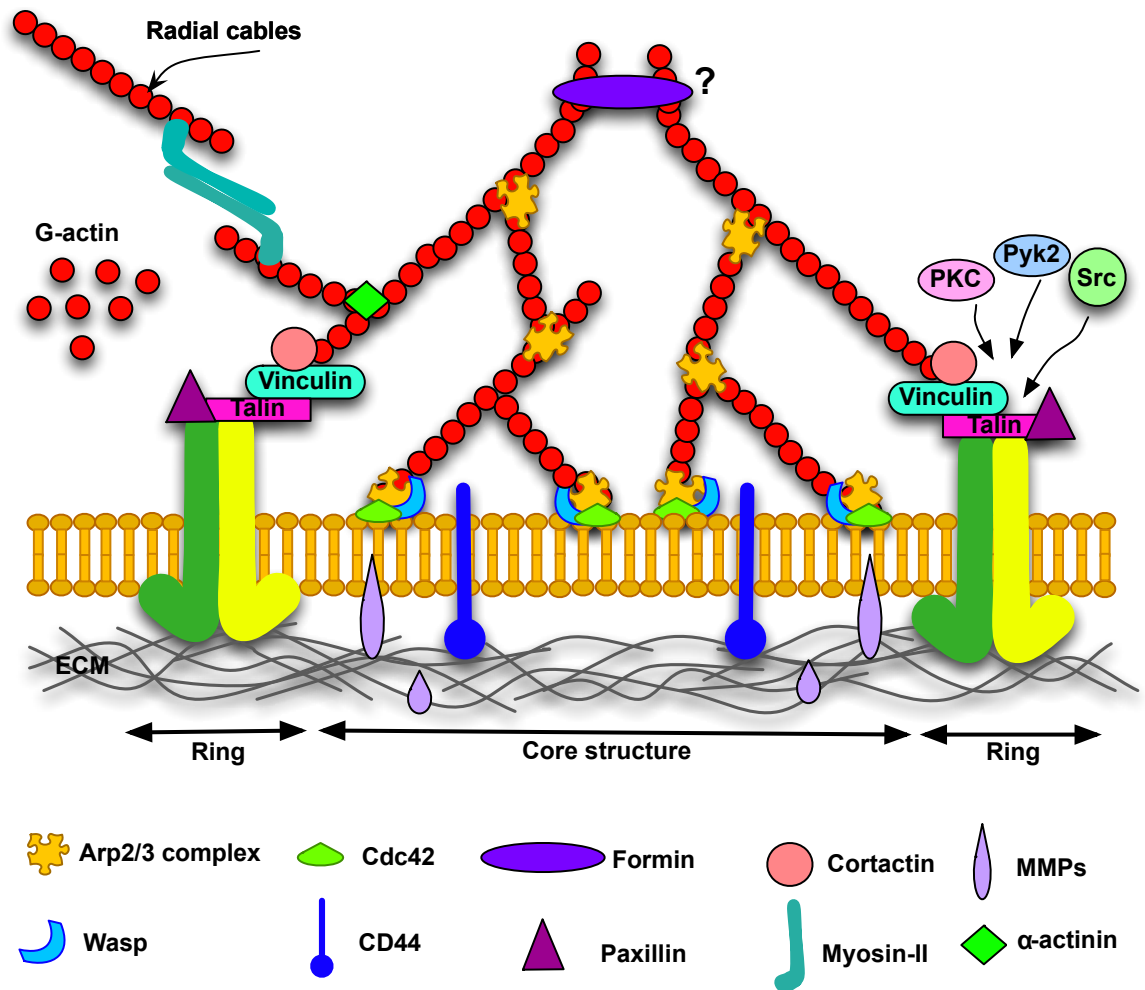


Figure 1.2: Podosome architecture

The architecture of a podosome can be subdivided into a ring and core structure with characteristic proteins for the different compartments. Integrins and adaptor proteins such as Talin, Paxillin and Vinculin dominate the ring structure. The core structure predominantly contains F-actin associated proteins such as the Arp2/3 complex, Wasp and Cortactin. Radial actin fibers contain Myosin II and are thought to influence podosome dynamics. Formins and actin bundling proteins such as Fascin were identified on the top of the actin core and might be involved in actin stabilization. Figure was adapted from Linder and Aepfelbacher, 2003.

1.2.1 F-actin nucleation

An intact F-actin network underpins formations like filopodia, lamellipodia as well as adhesion structures such as podosomes, invadopodia or focal adhesions (Kirchenbuchler *et al.*, 2010; Lee and Dominguez, 2010; Linder *et al.*, 2000a). The actin cytoskeleton is based on the nucleation process of globular actin monomers (G-actin) assembled by the Arp 2/3 complex, Formins or Spire into double-helical actin filaments (F-actin) (Nicholson-Dykstra *et al.*, 2005). The created filaments have a polarity with a barbed end (+) and a pointed end (-). The elongation of the filament takes place at the barbed end. However, there are several proteins, which regulate the assembly and disassembly of the formed actin filaments. These proteins can be subdivided into classes of bundling proteins, capping proteins, sequestering proteins, severing proteins and depolymerizing proteins (Revenu *et al.*, 2004). Prominent bundling and crosslinking proteins are Fascin, α -actinin or fimbrin, which connect F-actin strands with each other (Ishikawa *et al.*, 1998; Pelletier *et al.*, 2003; Volkmann *et al.*, 2001). Capping proteins such as Gelsolin bind to barbed ends to prevent further elongation or to pointed ends to stop depolymerization (Sun *et al.*, 1999). Gelsolin can also act as severing proteins by intercalating into the actin strand causing its fragmentation (Selden *et al.*, 1998). Another sequestering protein is Thymosin β 4, which binds G-actin and prevents the assembly of actin filaments (Cassimeris *et al.*, 1992). This is in contrast to severing proteins such as Profilin, which catalyzes the exchange of ADP to ATP on actin monomers and thereby facilitates polymerization (Athman *et al.*, 2002; Carlier and Pantaloni, 1997). The depolymerization of actin is promoted by proteins such as Cofilin, Destrin or actin depolymerizing factor (ADF) by binding to actin subunits of a filament, which induce a twist of the actin strand and leads to an increase in the dissociation rate of an filament (McGough *et al.*, 1997; Revenu

et al., 2004). However, Cofilin has also functions as a severing protein, creating new filament ends (Staiger and Blanchoin, 2006; Theriot, 1997).

The continuous turnover of F-actin drives podosome dynamics and impinges on their organization as well as the molecular composition (Luxenburg *et al.*, 2012). Further evidence for the requirement of rapid actin polymerization provides the detection of G-actin around the podosome structure, which represents a potential source for new actin filament nucleation (Akisaka *et al.*, 2001). To initiate new actin filament assembly a so-called nucleator is needed. In podosome structures the most abundant nucleator is the Arp2/3 complex, the function of which is described later in this chapter (Linder *et al.*, 2000a).

1.2.2 Rho GTPases

Rho GTPase are key regulators of cytoskeletal dynamics such as cell migration, adhesion or vesicle trafficking, which are mediated by interactions with actin nucleators, protein kinases and phospholipases (Heasman and Ridley, 2008). The Rho GTPase family describes a group of 20 signaling molecules (in humans), of which Rac, RhoA and Cdc42 are the best studied (Sit and Manser, 2011). Rho GTPases switch between an active-GTP-bound form and an inactive GDP-bound form. This process is regulated by guanine-nucleotide-exchange factors (GEFs), GTPase-activating proteins (GAPs) and guanine nucleotide-dissociation inhibitors (GIDs) (Bishop and Hall, 2000).

Humans have three Rac isoforms: Rac1, Rac2 and Rac3. Rac proteins are involved in the formation of lamellipodia and membrane ruffles. Rac1 is ubiquitously expressed, while Rac2 is expressed mainly in hematopoietic cells and Rac3 is predominantly found in the brain (Grill and Schrader, 2002; Kalfa *et al.*,

2006). The importance of Rac is underlined by the embryonic lethal $Rac1^{-/-}$ mice. Cells from these embryos indicated a role for Rac1 in lamellipodia formation, cell adhesion and cell migration *in vivo* (Sugihara *et al.*, 1998). Tissue-specific knockout models of Rac1 in platelets and melanoblasts confirmed these observations (Li *et al.*, 2011; McCarty *et al.*, 2005). However, macrophages deficient in Rac1 and Rac2 have no defect in migration and move like wild type cells, which indicates an Rac-independent migration mechanism (Wheeler *et al.*, 2006). A well studied role of Rac is the regulation of the Wave complex by binding to Sra (Chen *et al.*, 2010). Other down stream targets of Rac are PAK, PAR6 or IQGAP, which are involved in lamellipodia formation, cell polarity and cell-cell adhesions (Natale and Watson, 2002; Nishimura *et al.*, 2005; Vidal *et al.*, 2002).

Rac is primarily known to be involved in cell migratory processes (Raftopoulou and Hall, 2004). However, Rac was also demonstrated to be involved in adhesion structures in T-cells (Garcia-Bernal *et al.*, 2005). This is in agreement with Rac1-deficient dendritic cells, which are unable to form podosomes (Burns *et al.*, 2001). In addition, in macrophages Rac2 was identified to be essential for podosome formation, while Rac1-deficient macrophages form F-actin foci but no clear ring structures (Wheeler *et al.*, 2006).

The three Rho isoforms RhoA, RhoB and RhoC are highly homologues (Heasman and Ridley, 2008). However, $RhoB^{-/-}$ and $RhoC^{-/-}$ mice only display minor developmental defects (Hakem *et al.*, 2005; Liu *et al.*, 2001). Conditional knockout mice of RhoA demonstrated that RhoB and RhoC could compensate the regulation of actomyosin processes. However, cells had proliferation defects indicating a requirement of RhoA during mitosis (Melendez *et al.*, 2011). Furthermore, it was reported that the loss of RhoA in neural progenitor cells leads

to the disruption of adherens junctions and hyperproliferation (Katayama *et al.*, 2011). In addition, RhoA is prominently known to be involved in podosome formation, stress fiber assembly, filopodia generation and epithelial polarity (Heasman and Ridley, 2008). Its activity can be linked to the Rho-associated kinase (ROCK), which induces myosin light chain (MLC) phosphorylation leading to actomyosin contractile forces (Bhadriraju *et al.*, 2007). Activated ROCK also interacts with Lim kinase (LIMK), which can be associated with stress fibers, focal adhesion or collective cell invasion (Amano *et al.*, 2001; Scott *et al.*, 2010). Nonetheless, RhoA also interacts with mDia Formins, which in this context assembles unbranched actin-filaments or aligns microtubules (Sun *et al.*, 2011; Yamana *et al.*, 2006).

The involvement of RhoA in adhesion structures is well established in several studies, although most of the reports focus on focal adhesion structures and the ongoing actomyosin dynamics (Barry and Critchley, 1994; Ren *et al.*, 2000). However, there are a few reports mentioning Rho as a requirement for podosome assembly such as in dendritic cells or osteoclasts (Burns *et al.*, 2001; Ory *et al.*, 2008). In Src-transformed fibroblast RhoA was demonstrated to be involved in the formation of podosome rosettes as well as in matrix degradation (Berdeaux *et al.*, 2004). Interestingly, RhoU, which has structural similarities with Cdc42, was located to podosomes in osteoclasts. This is linked to osteoclast differentiation and the transition from podosome rings to belts (Brazier *et al.*, 2006; Ory *et al.*, 2008). However, because these investigations were only done in osteoclasts, the role of RhoU requires further investigations in other podosome forming cell types.

The Rho GTPase Cdc42 has been implicated in several actin-associated processes such as cell polarity, migration, chemotaxis or filopodia formation (Allen

et al., 1998; Cau and Hall, 2005; Nobes and Hall, 1995). The relevance of Cdc42 is underlined in the embryonic lethality of Cdc42 knockout mice (Chen *et al.*, 2000). Cdc42 has several effector proteins including Wasp/N-Wasp, Insulin receptor substrate p53/p58 (IRSp53) or PAK, which regulate actin polymerization and actin turnover (Bu *et al.*, 2010; Lim *et al.*, 2008; Symons *et al.*, 1996).

Cdc42 activity was also detected at podosome structures. A constitutively active form of Cdc42 was shown to induce podosome formation, which is in line with its direct regulation of Wasp (Linder *et al.*, 2011; Symons *et al.*, 1996). This is also observed in dendritic cells, which were microinjected with a dominant-negative form of Cdc42 inducing the loss of podosomes and cell polarity (Burns *et al.*, 2001). In HUVECs the activation of Cdc42 induced the formation of podosome structures and controlled these in aortic endothelial cells (Moreau *et al.*, 2003; Tatin *et al.*, 2006).

1.2.3 Wasp and Wip

Wasp is a key activator of the Arp2/3 complex and thus important in the remodeling of the actin cytoskeleton (Figure 1.4). The relevance of Wasp is underlined by the Wiskott-Aldrich syndrome, which is the result of X-linked inherited mutations of the *WASP* gene. Patients suffer from immunodeficiency characterized by eczema, recurrent infections and microthrombocytopenia, an abnormal low thrombocyte count and small platelets (Ariga, 2012). On cellular level Wasp expression is restricted to cells of the myeloid lineage (Monypenny *et al.*, 2011). However, there is a homologue called neural Wasp (N-Wasp), which shares 50% homology with Wasp (Cotta-de-Almeida *et al.*, 2007). Despite the name, N-Wasp is ubiquitously expressed. N-Wasp is prominently involved in

invadopodia formation and cancer metastasis and will be discussed in a later section of the chapter (Lorenz *et al.*, 2004; Yu *et al.*, 2012).

Wip is a ubiquitous interaction partner for Wasp and is thought to regulate Wasp activity, stability, interactions and subcellular localization (Chou *et al.*, 2006; Konno *et al.*, 2007). To maintain these processes Wip has several functional domains interacting directly with F-actin or Cortactin (Anton *et al.*, 2007). Further members of the Wip family are CR16, sharing 25% of the structure with Wip, and Wire, which is 30-40% identical to Wip (Anton *et al.*, 2007). CR16-N-Wasp complexes have been identified in the brain, however, the role of CR16 is still unknown. Nonetheless, the knockout of CR16 induce a male-specific sterility (Suetsugu *et al.*, 2007). Wire was shown to bind to Wasp/N-Wasp and was associated with microspikes and cross-linked actin filaments (Aspenstrom, 2002; Kato *et al.*, 2002; Kato and Takenawa, 2005).

Wasp contains several functional domains, the most important are the WH1 (Wasp-Homology 1) domain, a GBD (GTPase binding domain)/CRIB (Cdc42 or Rac-interactive binding) region connected via a proline-rich motif with the VCA domain (Verprolin-homology also called WASP-homology-2 (WH-2), central (C), acidic (A)) (Calle *et al.*, 2004; Nonoyama and Ochs, 2001). The VCA domain was mentioned before and describes the interaction site with the Arp2/3 complex. The proline-rich region is thought to be involved in the signal transduction of different SH3 domain containing proteins like members of the Src family kinases (Nonoyama and Ochs, 2001; Scott *et al.*, 2002). Furthermore, this domain interacts with Profilin (Takenawa and Miki, 2001). The WH-1 motif is necessary to bind to a specific region of Wip which regulates the expression and the stability of Wasp (Konno *et al.*, 2007). Wip also links Wasp to adaptor proteins like CrkL and

Nck, which are involved amongst others in T-cell receptor regulation (Sasahara *et al.*, 2002; Yablonski *et al.*, 1998). Interestingly, around 80% of Was patients show mutations in this sequence, which underlines the relevance of Wip in the signaling cascade with Wasp (Volkman *et al.*, 2002). The other regulatory domain of Wasp is GBD/CRIB, which is described as the region of interaction with different Rho GTPases such as Cdc42 (Aspenstrom, 2002). This is in contrast to the GTPases Rac and Rho, the involvement of which, if any, in the regulation of Wasp is not well understood (Burbelo *et al.*, 1995; Sit and Manser, 2011; Symons *et al.*, 1996). Beside these regulative regions the Wasp molecule can undergo an autoinhibitory conformation, in which the VCA domain is masked and cannot interact with the Arp2/3 complex. This conformation can be reverted by Rac or Cdc42 binding to the CRIB motif (Takenawa and Suetsugu, 2007).

Wasp appears to be crucial for podosome structure and dynamics, differentiating podosomes from focal adhesions, which generally do not contain Wasp. Wasp deficient cells are unable to form podosomes (Calle *et al.*, 2004; Isaac *et al.*, 2010; Sabri *et al.*, 2006). Even a partial downregulation of Wasp by 60% is sufficient to block podosome formation as demonstrated in dendritic cells (Olivier *et al.*, 2006). Wip has a similar important role. It facilitates the localization of Wasp to sites of actin polymerization at podosomes and also regulates calpain-mediated cleavage of Wasp and therefore podosome dynamics (Calle *et al.*, 2006; Chou *et al.*, 2006). However, Wasp is not only essential for podosome formation but plays also a role in several other actin based processes such as cell polarization, motility, chemotaxis and vesicle trafficking (Calle *et al.*, 2004; Dovas *et al.*, 2009; Pollitt and Insall, 2009).

Another prominent regulator involved in some of the aforementioned events is the Wave complex, the composition and function of which in terms of actin polymerization will be described in the next passage.

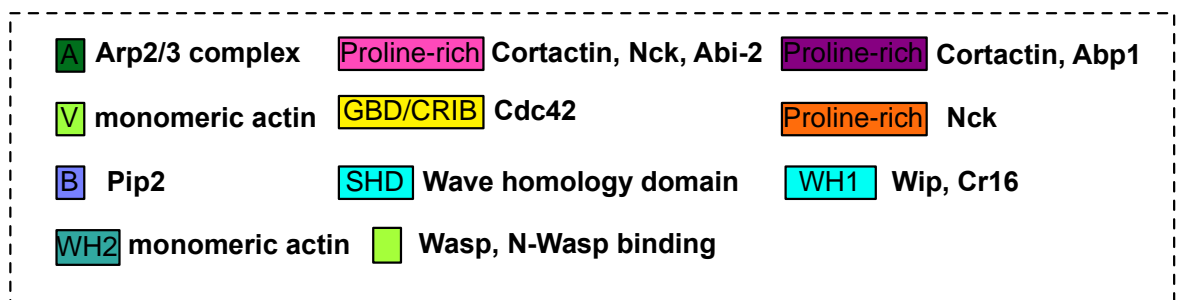
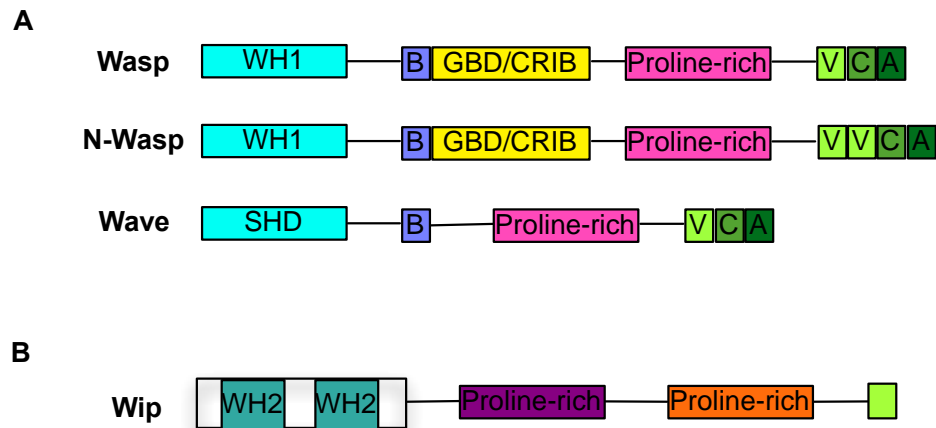


Figure 1.3: Structure of Wasp family proteins

(A) Wasp family proteins contain a C-terminal VCA domain, which is necessary for Arp2/3 complex and actin binding, followed by a proline-rich region. Wasp and N-Wasp contain a GBD/CRIB domain, which is responsible for Cdc42 interactions. The basic domain of the Wasp family proteins binds to PIP₂. Wasp and N-Wasp have a WH1 domain at their N-terminal, in which Wave has a Wave/Scar homology domain. (B) The Structure of Wip has several N-terminal WH2 domains interacting with actin. Proline-rich regions mediate binding to Cortactin, Abp1 or Nck. The C-terminal contains a domain required for Wasp and N-Wasp interactions.

1.2.4 The Wave complex

The Wave complex is a 5-protein complex that controls actin assembly by the Arp2/3 complex primarily in lamellipodia assembly (Figure 1.4). Because two groups discovered the Wave complex at the same time, it is also called Scar (suppressor of the cyclic AMP receptor) which describes the same protein in *Dictyostelium discoideum* (Bear *et al.*, 1998). However, the mammalian homologue is called Wave. So far there are three Wave isoforms; Wave-2, which is ubiquitously expressed in mammals as well as Wave-1 and Wave-3, which are expressed predominantly in the brain (Sossey-Alaoui *et al.*, 2002; Westphal *et al.*, 2000; Yan *et al.*, 2003). The structure of these proteins consists of a Wave homology/Scar homology domain (WHD), a basic region, a proline-rich motif and a VCA domain (Figure 1.3). The composition of these domains shows similarities to Wasp/N-Wasp, however, Wave proteins do not have a GBD/CRIB domain indicating that the regulation of these proteins is different. As Wave occurs in a heteropentameric complex consisting of Wave, Sra1, Nap1, Abi, and HSPC300 it is likely that another member of the complex can interact with its regulators such as Rac. It is known that the binding of the GTPase Rac to Sra1 activates the complex (Ismail *et al.*, 2009). Regulation of Wave is also induced by its phosphorylation, which induces a conformational change of the complex and leads to its activation (Chen *et al.*, 2010).

A requirement of the intact functionality of the Wave complex is the presence of all members in a complete and intact manner (Kunda *et al.*, 2003; Steffen *et al.*, 2006).

Interestingly, the Wave complex is located to lamellipodia protrusions and is an important regulator of cell migration. However, so far, the complex could not be

detected in podosome structures. Nevertheless, Abi, a member of the complex can be associated with cell-cell adhesion structures, which indicates a function of Abi independent of the Wave complex (Stradal *et al.*, 2001). Furthermore, Abi was detected in invadopodia structures in breast cancer cells and linked to matrix degradation via interactions with Diaphanous formins (Sun *et al.*, 2009).

1.2.5 The Arp2/3 complex

The nucleation of branched actin filaments, as they occur in podosomes and lamellipodia, is initiated by the Arp2/3 complex (Nolen *et al.*, 2009; Suraneni *et al.*, 2012). The Arp2/3 complex is composed of 7 subunits named in mammals as followed: the actin related subunits are Arp2 and Arp3 and the remaining subunits are actin-related protein complex-1 to 5 called ARPC-1, ARPC-2, ARPC-3, ARPC-4, ARPC-5 (Goley and Welch, 2006; Welch *et al.*, 1997). The major function of the complex is to bind to actin monomers or to preexisting actin strands to initiate the elongation of the filaments, which causes γ -side branches and a dendritic network of actin (Machesky and Gould, 1999). In order to initiate this process, the complex needs to undergo a conformational change by binding to a nucleation-promoting factor (NPF) like Wasp or WAVE (Mullins and Pollard, 1999; Robinson *et al.*, 2001). Both of these NPFs contain a VCA domain, in which the WH-2 domain promotes binding of G-actin, which enables polymerization and the CA region mediates binding to the Arp2/3 complex (Chereau *et al.*, 2005; Marchand *et al.*, 2001). In this way Arp2 and Arp3 bind to the pointed end of the daughter filament initiating elongation, in which the other subunits connect to the mother filament. Due to filament ageing the interaction between the complex and filaments gets weakened until the filament disassembles and the complex is released and recycled (Goley and Welch, 2006).

This process highlights the crucial requirement of the Arp2/3 complex in podosome formation and reflects a similar relevant role as F-actin itself. It is reported that without the Arp2/3 complex, the actin cytoskeleton is still able to remodel but at least two previous studies have implicated Arp2/3 in podosome formation and maintenance (Hurst *et al.*, 2004; Kaverina *et al.*, 2003). Podosomes also were compromised in monocytes treated with a chemical compound, called CK666, which blocks the activity of the Arp2/3 complex (Nolen *et al.*, 2009).

Another aspect of this process is the regulation of the Arp2/3 complex and therefore the relevance of the Wasp family members in podosome formation.

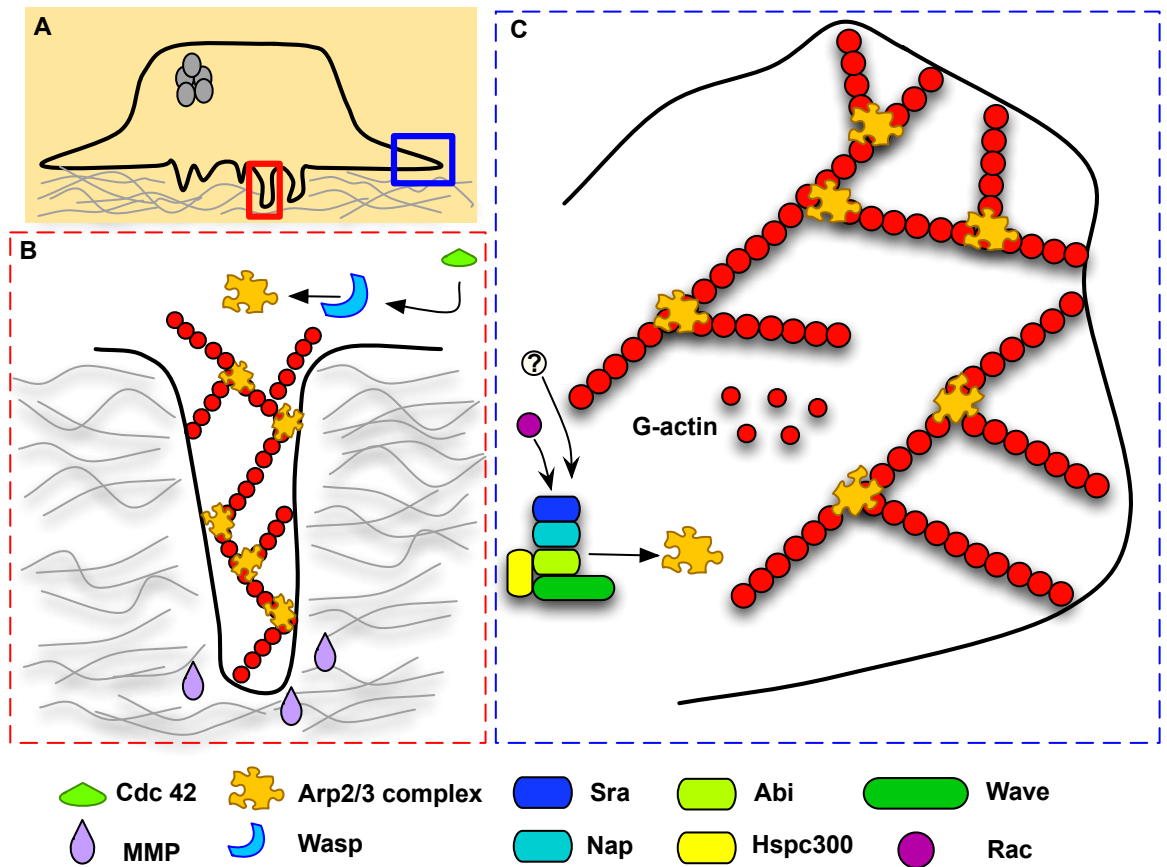


Figure 1.4: Actin rearrangement in podosomes and lamellipodia formation

(A) Adhesive cell forming podosomes (red box) and lamellipodia (blue box) during spreading. (B) F-actin arrangement based on the Arp2/3 complex activated by Wasp, which is recruited by Cdc42 but also interacts with Wip and Cortactin (not shown). This process takes place not only at the top of the podosome structure but also at its protrusive ends. MMPs are released to degrade the surrounding matrix proteins. (C) Lamellipodia formation of a spreading cell, which is also present in migrating cells. The actin cytoskeleton of a lamellipodia is predominantly based on a branched network mediated via the Arp2/3 complex regulated by the heteropentameric Wave complex. The activity of the Wave complex is controlled by the RhoGTPase, Rac but might also have other unidentified regulators.

1.2.6 Cortactin

Cortactin is an actin-filament binding protein, which is involved in several important cell processes such as cell motility, vesicle transport and cell invasion (Bowden *et al.*, 1999; Kirkbride *et al.*, 2012; Weed *et al.*, 2000). The structure of Cortactin can be subdivided into six functional domains. The N-terminal acidic region (NTA) contains the binding site for Arp3 of the Arp2/3 complex. This region is followed by a repeat of amino acids responsible for binding F-actin (Cosen-Binker and Kapus, 2006). Next to this domain, there is an α -helical motif, of unknown function. The proline-serine-threonine-rich region (PST) and some crucial tyrosine residues compose the next domain, which displays interaction sites for serine/threonine kinases such as PAK and ERK as well as for members of the Src family kinases (Huang *et al.*, 1997; Martinez-Quiles *et al.*, 2004; Vidal *et al.*, 2002). The last domain is a Src-homology 3 (SH3) domain, which is a hotspot of interaction with key proteins like Wasp/N-Wasp, Wip or Cdc42 activator faciogenital dysplasia protein (FGD1) (Hou *et al.*, 2003; Kinley *et al.*, 2003; Mizutani *et al.*, 2002). In hematopoietic cells there is a Cortactin homologue called hematopoietic cell-specific protein (HS1). Cortactin and HS1 share around 65% amino acid sequence identity, in which the SH3 domain (86%) and the actin binding region (86%) are the most similar motifs (Urano *et al.*, 2003a; van Rossum *et al.*, 2005). However, the expression of the different proteins is cell type dependent and HS1 is only expressed in hematopoietic cells, whereas Cortactin is expressed in the remaining cell types. There are only a few cell types known to express both proteins, such as platelets and megakaryocytes (Thomas *et al.*, 2007; Zhan *et al.*, 1997).

One of the most important functions of Cortactin is probably the coupling of F-actin filaments with the Arp2/3 complex and is therefore associated with a dendritic actin

network. The relevance of this role is highlighted by the fact, that Cortactin has a 20 fold higher affinity for F-actin than the Arp2/3 complex does (Urano *et al.*, 2003b). Cortactin can also act via Wasp or Wip to enhance actin polymerization (Tehrani *et al.*, 2007). Furthermore, Cortactin is able to stabilize preexisting filaments and connects these with the Arp2/3 complex (Pant *et al.*, 2006).

Based on this background, it is not surprising that there are several reports about Cortactin involvement in podosome formation in several cell types such as smooth muscle cells, osteoclasts or macrophages (Tehrani *et al.*, 2007; Van Goethem *et al.*, 2011; Zhou *et al.*, 2006). However, the relevance of Cortactin in podosome assembly and maintenance seems to be cell type specific. Osteoclasts, in which cortactin expression was down-regulated, were unable to form podosomes to degrade a bone substrate (Tehrani *et al.*, 2007). A similar effect was observed in smooth muscle cells, where the number of podosomes correlated with the degree of Cortactin knockdown and Src-mediated phosphorylation played a key role in the assembly of podosomes (Zhou *et al.*, 2006). Furthermore, it was demonstrated that the SH3 domain of Cortactin, which interacts with Src kinases as well as with Wasp, is essential for podosome formation (Webb *et al.*, 2006). Another report describes disorganized podosome structures and a loss of podosome mediated matrix degradation induced by the lack of the Cortactin/HS1-binding domain of Wip (Banon-Rodriguez *et al.*, 2011). This observation indicates a crucial role for Cortactin/HS1 and Wip not only in podosome organization but also in recruitment of MMPs to podosomes. However, HS1 deficient dendritic cells were able to form loosely packed podosomes, which did not show a deficiency in matrix degradation (Dehring *et al.*, 2011). Nevertheless, Cortactin is associated with matrix

degradation in other actin based structures like invadopodia, which will be discussed later in this chapter (Artym *et al.*, 2006).

1.2.7 Myosin II

Non-muscle Myosin II is a member of a motor protein superfamily and describes an actin-binding protein that functions in cross-linking and contractility processes during adhesion, migration and cell division (Laevsky and Knecht, 2003; Straight *et al.*, 2003). There are three isoforms in mammals, Myosin IIA, Myosin IIB and Myosin IIC. However, because megakaryocytes and platelets only express Myosin IIA, I will focus on this isoform (Murakami *et al.*, 1990). The structure of Myosin II can be subdivided into three pairs of peptides; two heavy chains, two regulatory light chains (RLC), which control the activity and two essential light chains (ELC), which stabilize the heavy chains (Vicente-Manzanares *et al.*, 2009). Each heavy chain contains a globular head, which present the actin and Mg^{2+} -ATPase binding domain and is in direct proximity with the light chains composing the neck region. This part is connected via an α -helical coiled coil with an C-terminal nonhelical tailpiece (Bresnick, 1999). The regulation of Myosin II activity depends on the phosphorylation of serine and threonine residues in the RLC domain, which increase actin-activated Mg^{2+} -ATPase activity leading to a conformational change of the myosin head domain (Sellers *et al.*, 1982; Somlyo and Somlyo, 2003). Dephosphorylation of Myosin abrogates movement of actin and its activation of the ATPase (Burgess *et al.*, 2007). In this way, Myosin II is able to walk along actin filaments in the direction of the plus end and induce contractile forces between the filaments.

Myosin IIA is found in macrophage, dendritic cell, osteoclast and Src-transformed fibroblast podosomes (Gawden-Bone *et al.*, 2010; Kopp *et al.*, 2006; Ory *et al.*, 2008). The localization of Myosin II was detected in dendritic cells in the ring structure, whereas in osteoclasts and macrophages Myosin was found in the cloud domain of podosomes connected by radial actin cables (Bhuwania *et al.*, 2012; Saltel *et al.*, 2008; van Helden *et al.*, 2008). Furthermore, the inhibition, by Blebbistatin, or the knockdown of Myosin II expression induced a decrease in matrix degradation and an increase in podosome lifetime. Also fibroblasts completely lose the ability to form podosome rosettes (Bhuwania *et al.*, 2012; Collin *et al.*, 2006; Saltel *et al.*, 2008; van Helden *et al.*, 2008). Another report highlighted the essential role of myosin-light-chain kinase (MLCK) in podosome ring structures (Collin *et al.*, 2008). Myosin II was not only detected in the ring structure, where it might play a role in podosome stiffness regulation, but it was also localized to actin cables connecting single podosomes with each other and might function in the turnover through contractile actions (Bhuwania *et al.*, 2012; Labernadie *et al.*, 2010).

1.3 Ring structure

The ring structure of the podosome is characterized by adhesion plaque proteins such as integrins and adaptor proteins like Vinculin, Paxillin, Talin as well as kinases such as members of the Src family, Phosphoinositide 3-kinase (PI3K) and Protein kinase C (PKC) (Linder *et al.*, 2011; Quintavalle *et al.*, 2010). How and why the arrangement of Integrins assembles in a ring structure is still unknown. So far the Vinculin ring structure was a hallmark of podosome structures, but recently it was reported that specific breast cancer cells form invadopodia with Vinculin

rings (Branch *et al.*, 2012). This discovery makes the differentiation of podosomes and invadopodia more difficult.

1.3.1 Integrins

Integrins are heterodimer cell surface transmembrane glycoproteins, which function as adhesion receptors and connect the cell to the extracellular matrix (ECM) environment. The Integrin family consists of 24 members (in humans), each built by an α - and a β -subunit (Berman *et al.*, 2003). The overall structure of a dimer is composed of an extracellular head domain, which binds ligands and is connected via two long stalk regions to the transmembrane and the cytoplasmic region (Shimaoka *et al.*, 2002). The activity of Integrins is determined by a conformational change into a bent form of both subunits regulated amongst others by a salt-bridge tethering the α - and β -subunits (Luo *et al.*, 2007). The interaction with different binding partners such as Talin, Paxillin or Kindlin, can remove this bridge inducing a swap into an active conformation (Plow *et al.*, 2009; Schaller, 2001; Ye *et al.*, 2010).

In podosomes the most prominent Integrin β -subunits are β_1 -, β_2 - and β_3 -Integrins, of which the first occurs in the core structure and the latter in the ring structure (Destaing *et al.*, 2010; Duong and Rodan, 2000; Faccio *et al.*, 2002; Marchisio *et al.*, 1988). Furthermore, β_1 -Integrins were shown to be essential for podosome rosette formation, in contrast to β_3 -Integrins, whose loss induced only a less intense F-actin staining in clear podosome ring structures (Destaing *et al.*, 2010). Which Integrins are involved in detail is dependent on the cell type as well as on the extracellular matrix. The majority of β_1 -Integrin ligands are collagen isoforms but also fibronectin and laminin, whereas β_3 -Integrins predominantly bind to

vitronectin, fibronectin, fibrinogen and osteopontin (Lal *et al.*, 2009). β_2 -Integrins are leukocyte specific and bind to plasminogen, ICAM-2 (intercellular adhesion molecule 2) and VCAM-1 (vascular cell adhesion molecule) (Niu and Chen, 2011). Besides their adhesive task, podosomes are also believed to have a mechanosensory function, in which Integrins sense the substrate stiffness and induce an appropriate signaling cascade involving potential motor proteins such as Myosin II (Collin *et al.*, 2008; Peng *et al.*, 2012). Furthermore, the stimulation of Integrins by their specific ligand was shown to activate several phosphorylation cascades, predominantly by Src kinases, inducing adhesion complex assembly, actin nucleation and possibly matrix metalloprotease (MMPs) expression (Galvez *et al.*, 2002; Vicente-Manzanares *et al.*, 2009). The detailed interactions between Integrins, adaptor proteins and the actin cytoskeleton will be discussed in the next paragraph.

There are also non-Integrin adhesion receptors involved in podosome assembly. One of these is the recently described transmembrane receptor CD44 in osteoclasts, which localizes to the F-actin core of podosomes and mediates adhesion to hyaluronan, collagen, osteopontin and laminin (Avigdor *et al.*, 2004; Chabadel *et al.*, 2007; Ponta *et al.*, 2003). However, more investigations are needed to understand the full function and regulation of this receptor.

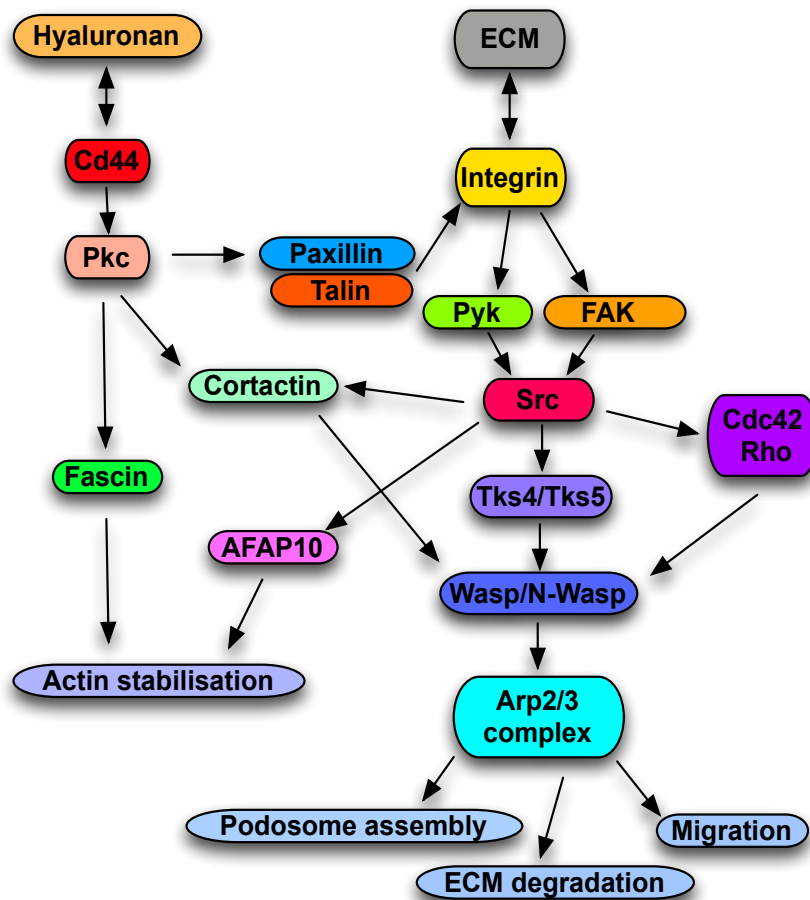


Figure 1.5: Fundamental transmembrane receptor trafficking

Integrin binding to the ECM induces a conformational change and the recruitment of kinases such as FAK and Pyk2, which activate Src. Src has numerous substrates such as the adaptor proteins Tks4 or Tks5 but also interacts with Cortactin or Cdc42, which are able to interact with Wasp initiating Arp2/3 activity. The Arp2/3 complex accumulates a branched actin network and provides the requirement for migration, ECM degradation and novel podosome assembly. A recently identified transmembrane receptor is CD44, which binds to Hyaluronan, which is also present in the sinusoids of the bone marrow. This interaction causes recruitment of PKC, which interacts with several proteins such as Cortactin and Paxillin but also Fascin, which might be involved in actin stabilization mechanisms in podosomes.

1.3.2 Src family kinases – Src kinase

The Src family kinases (SFKs) describe 9 nonreceptor tyrosine kinases (in humans). The most characterized role of SFKs is the phosphorylation of tyrosine residues in certain key proteins causing their activation or deactivation (Cougoule *et al.*, 2010; Huang *et al.*, 1997; Zhou *et al.*, 2006). However, because Src is well known for its involvement in adhesion complexes, cell spreading and migration, I focused on this member of the Src family kinases (Boateng *et al.*, 2012; Huveneers and Danen, 2009; Sen and Johnson, 2011).

The structure of Src is composed of an amino-terminal myristoylation sequence (M), a unique region (U), a Src-homology-2 (SH2) and a SH3 domain, a kinase domain containing a phosphorylation site and a carboxy-terminal regulatory motif (R). C-terminal Src kinase (Csk) phosphorylates a specific tyrosine residue of c-Src and induces a conformational change, which leads to inactivity (Frame, 2002; Levinson *et al.*, 2008).

The importance of Src is highlighted by a constitutively active form of Src (v-Src), which is able to induce the formation of podosome rosettes in fibroblasts (Berdeaux *et al.*, 2004). Furthermore, it was shown that podosome belts are not formed in Src deficient osteoclasts (Sanjay *et al.*, 2001). Interestingly, Src gets activated in wildtype cells shortly after integrin clustering and was demonstrated to be involved in the dynamic turnover of podosome structures (Luxenburg *et al.*, 2007; Sanjay *et al.*, 2001). There are several interacting partners of Src, which are involved in the assembly of podosomes such as Cortactin, Wasp, β_1 - and β_3 -Integrins, Paxillin but also Focal adhesion kinase (FAK), Pyk2 or the adaptor protein Tks5 (Baba *et al.*, 1999; Datta *et al.*, 2001; Huang *et al.*, 1997; Mitra and Schlaepfer, 2006; Sakai *et al.*, 2001; Stylli *et al.*, 2009; Webb *et al.*, 2004).

However, the numerous substrates and their different nature (actin regulation, adhesion plaque or signaling) make it difficult to determine a defined role for Src in podosome assembly (Figure 1.5).

Besides Src, the SFK Hck and the FAK family member Pyk2 were shown to play an important role in podosome signaling cascades (Cougoule *et al.*, 2010; Duong and Rodan, 2000).

1.3.3 Vinculin interacting with α -actinin, Talin and Paxillin

Vinculin is one of the most commonly used podosome markers and is characterized by its ring appearance in these structures. Besides its functions in podosomes, Vinculin is also involved in other cell-matrix and cell-cell interactions as well as cell migration and invasion processes (Grashoff *et al.*, 2010; Kirchenbuchler *et al.*, 2010; Mierke *et al.*, 2010; Weiss *et al.*, 1998). However, Vinculin functions here as a connector between the actin cytoskeleton and transmembrane proteins such as Integrins via other adaptor proteins. The relevance of Vinculin during development is highlighted by the embryonic lethality of knockout mice, which is resulting from heart and brain defects (Xu *et al.*, 1998). The structure of Vinculin is composed of a globular head domain and a tail region. The most important domains of the globular head, which is the N-terminus of the protein, is the binding site for Talin as well as α -actinin a proline-rich region, which is essential for binding of the Arp2/3 complex and a V8-protease cleavage site. The tail domain contains binding sites for F-actin and Paxillin (Bakolitsa *et al.*, 2004; Price *et al.*, 1989; Weekes *et al.*, 1996). The interactions of Vinculin with α -actinin, Talin and Paxillin are well known and furthermore all of these proteins are present in podosomes and localized to the ring structure (Badowski *et al.*, 2008;

Kaverina *et al.*, 2003; Wiesner *et al.*, 2010). α -actinin consists of two identical anti-parallel peptides, which can bind directly to Integrin subunits but is also known to crosslink actin filaments into bundles and networks (Brakebusch and Fassler, 2003; Otey *et al.*, 1990; Pelletier *et al.*, 2003). The binding of α -actinin to Vinculin induces a conformational change, which allows Vinculin binding to F-actin (Bois *et al.*, 2005). However, in smooth muscle cells, Vinculin activity appears later than α -actinin does and in osteoclasts α -actinin is localized to the actin core (Kaverina *et al.*, 2003; Luxenburg *et al.*, 2012). These observations might indicate a Vinculin independent function of α -actinin and implies a possible involvement in crosslinking actin filaments into bundles. Similar to α -actinin-Vinculin interactions are the interactions between Talin and Vinculin (Bois *et al.*, 2005). Talin comprises a globular head region and a flexible stalk domain. The head domain displays binding sites for F-actin, Integrins, FAK and other kinases. The rod domain contains additional Integrin and F-actin binding sites and several interaction sites for Vinculin connection. A C-terminal α -helix facilitates the formation of an antiparallel dimer with another Talin monomer (Critchley and Gingras, 2008). In focal adhesions, Talin binds to the activated Integrin and F-actin via its head domain, in which Vinculin binds to its rod domain and crosslinks Talin to another or the same F-actin strand (Ziegler *et al.*, 2006). The most important signaling proteins in this process are FAK and the enzyme phosphatidylinositol phosphate kinase type IY (PIPKIY), which produces the second messenger phosphatidylinositol (4,5) bis-phosphate (PIP2), which in turn promotes binding of Talin with Integrins (Martel *et al.*, 2001). Talin has a similar functionality and importance in podosome structures, which is underlined by its presence in several cell types (Allavena *et al.*, 1991; Cox *et al.*, 2012; Duong and Rodan, 2000).

Another Vinculin interactor, which is localized at the membrane-cytoskeleton interface of podosomes, focal adhesions and invadopodia is paxillin (Bowden *et al.*, 1999; Pfaff and Jurdic, 2001; Schaller, 2001). Paxillin contains an array of different binding sites for several protein-protein interactions with actin-binding proteins, different GAPs and kinases (Schaller, 2001). In this context, Vinculin binds to the N-terminal domain of Paxillin and links it to the F-actin strands (Turner *et al.*, 1990). Another direct binding partner of Paxillin and F-actin is Actopaxin (Turner *et al.*, 1990). Nevertheless, the presence of Paxillin in the ring structure was detected in several podosome formations (DeFife *et al.*, 1999; Destaing *et al.*, 2003; Duong and Rodan, 2000). A crucial regulator of Paxillin is thereby the nonreceptor tyrosine kinase Pyk2, both proteins colocalized with Integrins in podosome structures (Pfaff and Jurdic, 2001). Furthermore, the knockdown of Paxillin induces podosome cluster (instead of podosome belt) formation in osteoclasts (Badowski *et al.*, 2008). A similar dramatic effect was caused by the lack of Paxillin phosphorylation in Src-transformed cells, in which podosome clusters instead of rosettes were formed, which additionally only had a reduced ability to degrade ECM proteins (Badowski *et al.*, 2008). These observations underline the complexity of the protein network involved in podosome regulation.

1.3.4 Kindlins

The Kindlin family has three members Kindlin-1, Kindlin-2 and Kindlin-3, in which Kindlin-3 expression is restricted to the hematopoietic cell lineages. However, all three Kindlin isoforms are involved in Integrin activation (Herz *et al.*, 2006; Montanez *et al.*, 2008; Moser *et al.*, 2008). This activation can also take place with the cooperation of Talin (Moser *et al.*, 2008). Kindlins are also able to link Integrins to the cytoskeleton via interaction with α -actinin, FAK or Integrin-linked kinase

(IKL) (Has *et al.*, 2009; Montanez *et al.*, 2008). Kindlin-3 knockout mice are characterized by general hemorrhage, leukocyte adhesion defects and osteopetrosis (Karakose *et al.*, 2010). The latter is caused by osteoclast dysfunction leading to increased bone mineralization. Interestingly Kindlin-3 deficient osteoclasts show impaired podosome formation, with a smaller F-actin core, dispersed Vinculin and Integrin localization and no defined ring structure surrounded by a loose network of radial actin filaments (Schmidt *et al.*, 2011). These results underline the role of Kindlin as another adaptor protein of membrane-cytoskeleton interactions, which are essential for functional podosome organization.

1.3.5 Matrix metalloproteases and serine proteases

The enzymatic lysis of matrix proteins is a hallmark of podosome structures (Linder and Aepfelbacher, 2003). Matrix metalloproteases (MMPs) are the most prominent mediators of this process in podosomes. In contrast, invadopodia-driven degradation is mediated by MMPs and serine proteases, which will be discussed later in the chapter in the context of invadopodia structures. However, there are also different cysteine cathepsin proteases, which have been recently reported to be involved in podosome-driven ECM degradation (Tu *et al.*, 2008). Nevertheless, first I will focus on MMPs and then on cysteine cathepsin proteases.

There are 25 human MMPs, which can be subdivided into soluble MMPs, membrane-associated MMPs or cysteine array (CA) MMPs (Ziegler *et al.*, 2006). Most MMPs share a basic structure composed of a pro-domain, a catalytic domain, a hinge region and a hemopexin domain. The pro-domain is an autoinhibitory domain, regulated by Zn^{2+} -binding, and prevents the catalytic

domain from cleaving other proteins (substrate). The C-terminal hemopexin domain is responsible for protein-protein interactions such as substrate recognition and activation of the enzyme (Ziegler *et al.*, 2006). Depending on the specific MMP, there are some additional structural features such as a fibronectin type II repeat, mediating binding to collagen, or a transmembrane domain or a glycosylphosphatidylinositol linkage (GPI), which associates the MMP with the plasma membrane (Page-McCaw *et al.*, 2007). Initially these proteases are synthesized as zymogens and only become activated if the pro-domain is cleaved (Golubkov *et al.*, 2010). Other regulatory functions are held by the group of tissue inhibitors of metalloproteinases (TIMPs), which bind to the catalytic domain of the active MMP (Visse and Nagase, 2003).

MMPs are located to podosome formations in several cell types and were shown to drive the matrix degradation, which is associated with these structures (Johansson *et al.*, 2004; Sato *et al.*, 1997). The regulation of this process is associated with several proteins, which are cell type and podosome structure specific. Thus, it was shown that knockdown of tight junction protein Zona occludens, which also binds to Cortactin, causes a reduced ability of matrix degradation (Kremerskothen *et al.*, 2011). Similar results are reported for the loss of Hck (a member of the Src-family) and for impaired Wasp phosphorylation (Cougoule *et al.*, 2010; Dovas *et al.*, 2009). However, because the related phenotypes are always associated with the loss or reduction of podosome structures, a decreased ECM degradation is not surprising. A prominent regulator of MMP recruitment is Cortactin, which localizes to different MMPs such as MMP-2 at podosome structures (Aga *et al.*, 2008; Xiao *et al.*, 2009). Furthermore, the loss of the Cortactin-binding domain of WIP results in decreased matrix degradation

(Banon-Rodriguez *et al.*, 2011). Interestingly, the interaction between the Src kinase, protein kinase C (PKC) and Cortactin was described before in podosome formation and PKC is associated with MMP-9 release at these structures (Xiao *et al.*, 2013; Xiao *et al.*, 2009; Zhou *et al.*, 2006). Nevertheless, there are other proteins associated with MMP mobilization. The transport of MMPs was reported to be maintained by motor proteins moving along microtubules called KIFs (Hirokawa *et al.*, 2009). In this context, KIF5B, KIF3A/B and KIF1C were demonstrated to be involved in the transport of MT1-MMPs to podosome structures and the knockdown correlated with reduced ECM lysis (Wiesner *et al.*, 2010). Another interesting aspect of MMP regulation is the influence of different substrate properties, which will be discussed later in the chapter.

Not as well described as MMPs are Cysteine Cathepsin proteases and their function in podosome-mediated ECM degradation. There are 11 human Cysteine Cathepsins, which are predominantly endopeptidases, meaning that they cleave peptide bonds within their substrates at nonterminal amino acids (Mohamed and Sloane, 2006). There are also some Cathepsins, which are involved in extracellular functions. Cathepsin S for example plays a crucial role in the process of antigen loading via the major histocompatibility complex (MHC) class II by degrading a protein, which blocks the binding site (Shi *et al.*, 1999). Another example is the loss of Cathepsin K in mice, which cause osteopetrosis based on impaired bone resorption by osteoclasts (Saftig *et al.*, 1998). Dendritic cells, in which cathepsin X activity was inhibited, were not able to form podosomes, possibly by impaired activation of integrin $\alpha\text{M}\beta_2$ (Shi *et al.*, 1999). Furthermore Cathepsin X is known to interact with heparin sulfate proteoglycans, which occur in basement membrane meshworks (Nascimento *et al.*, 2005). Cathepsin mediated

ECM degradation was also reported at podosome structures in transformed fibroblasts. In this report Cathepsin B-loaded vesicles were identified at podosome structures and the presence of lysosomes correlated with the degree of matrix degradation (Tu *et al.*, 2008). The role of Cathepsin B is highlighted by several functions that support ECM lysis such as the degradation of TIMPs (Kostoulas *et al.*, 1999) or the activation of urokinase-type plasminogen activator (uPA) and its receptor uPAR, which can activate different MMPs (Lijnen, 2001). Recently, Cathepsin B was detected at degradative podosome structures in 3D and colocalized with Vinculin, Cortactin and β_3 -Integrins (Jevnikar *et al.*, 2012a; Jevnikar *et al.*, 2012b).

These observations underline the potential role of Cathepsins in podosomes, which need more investigations in order to understand their regulation and recruitment into the podosome structure.

1.4 Other podosome relevant proteins

1.4.1 Microtubules

Microtubules are cytoskeletal fibers, which polymerize from α -tubulin and β -tubulin dimers into a short nucleus. This elongates and folds into a cylinder-shaped arrangement of 12-15 protofilaments per row (Jordan and Wilson, 2004). The filaments have an inherent polarity, with a rapidly growing and more rapidly shrinking end, which is essential for motor proteins such as kinesins to transport cargo directionally along the microtubules (Cheeseman and Desai, 2008). A prominent reversible inhibitor of microtubule polymerization is Nocodazole, which induces depolymerization of the filament by binding to the tubulin dimers and

inducing a conformational change resulting in splaying of the filament (Eilers *et al.*, 1989). The microtubule cytoskeleton is reported to affect podosome dynamics in several cell types such as macrophages and osteoclasts (Destaing *et al.*, 2003; Linder *et al.*, 2000b). Macrophages treated with Nocodazole were unable to form podosomes, however, after wash out of the drug, the cells assembled podosome structures (Destaing *et al.*, 2003; Linder *et al.*, 2000b). However, this effect could not be observed in osteoclasts where podosomes were still accumulated but the cell-specific transition from podosome clusters to belts was impaired (Jurdic *et al.*, 2006). Furthermore, microtubules were shown to have a role in the stabilization of osteoclast podosome belts (Destaing *et al.*, 2003). It is also demonstrated that Kinesins such as KIF1C interacts with Myosin II and regulates podosome dynamics (Kopp *et al.*, 2006). In contrast, KIF5B, KIF3A/3B and KIF9 transport MMP-loaded vesicles towards podosome structures and are also involved in the regulation of adhesion receptor CD44 (Cornfine *et al.*, 2011; Wiesner *et al.*, 2010).

1.4.2 Formins

In addition to the Arp2/3 complex, there are other mediators of F-actin nucleation, one group of these are Formins. In contrast to the Arp 2/3 complex, Formins favour the initiation of unbranched F-actin strands and are involved in the formation of filopodia, stress-fibers and actin cables (Hotulainen and Lappalainen, 2006; Mellor, 2010; Sagot *et al.*, 2002). However, the role in podosome formation was just recently illuminated. In macrophages Formin FRL1 (FMNL1) localizes to podosome cores, immunoprecipitates with β_3 -Integrins and its knockdown induces a reduction in adhesion as well as in podosome numbers. In a 3D reconstruction it was demonstrated that FMNL1 localizes at the podosome tip, where it is thought to sever actin filaments into cables and to mediate the stabilization of the

podosome structure (Mersich *et al.*, 2010). In contrast, Formin mDia2, was shown to be involved in microtubule dynamics in osteoclast podosomes (Destaing *et al.*, 2005). Interestingly, there has been a Formin-binding protein (FBP17) identified, which localizes to podosomes, interacting with the Wasp-Wip-complex and is thought to recruit them together with Dynamin to the plasma membrane (Tsuboi *et al.*, 2009).

1.4.3 Fascin

Another newly discovered protein in podosome dynamics is the actin-bundling protein Fascin. Fascin was first described in the context of cell adhesion structures such as focal contacts, but also microspikes, filopodia and stress fiber formation (Adams, 1997; Svitkina *et al.*, 2003; Yamashiro *et al.*, 1998). However, the evidence of the involvement of Fascin in podosome structures is so far limited. Fascin localises towards the actin core in dendritic cells, where it appears to be involved in the disassembly of these structures (Yamakita *et al.*, 2011). This function was hypothesized to correlate with the expression level of the protein, so perhaps Fascin competes with other podosome proteins and disrupts the structure of normal podosomes. In contrast, the knockout of microRNA-145, which targets Fascin, induces the formation of podosomes (Quintavalle *et al.*, 2010). However, in invadopodia the role of Fascin is better established, where it is known to stabilize these structures and to promote invasion (Li *et al.*, 2010; Schoumacher *et al.*, 2010).

1.5 Podosome properties and functions

1.5.1 Podosomes in migration

The functions of podosomes are multifaceted; the involvement of podosomes in cell migratory actions is well described and is underlined by the fact that only motile cells assemble these structures. The function of podosomes is highlighted by the reduction in migration velocity associated with their loss (Olivier *et al.*, 2006). Besides random migration, podosomes are also known to facilitate chemotaxis, transmigration or migration in a complex 3D environment (Cougoule *et al.*, 2010; Dehring *et al.*, 2011; Sabri *et al.*, 2006). These observations can be put into a physiologically relevant context. Immature dendritic cells migrate from their place of origin, such as the bone marrow, to peripheral tissues to reside there until detection of a pathogen. Signals from pathogens trigger the maturing dendritic cell to move to the nearby lymphatic vessel (Burns and Thrasher, 2004; Shortman and Liu, 2002). A similar example is the recruitment of cells such as monocytes, eosinophils or macrophages to a site of inflammation and the associated transmigratory actions through a blood vessel wall and the surrounding tissue in which podosomes might have an essential role (Ley *et al.*, 2007). Interestingly, the migration mode of leukocytes correlates with the ability of forming podosomes and supports the hypothesis that podosomes support migratory processes (Cougoule *et al.*, 2012). The *in vivo* evidence for these models still needs to be investigated. However, podosome rosettes, stained for Cortactin and Tks5, were detected in murine aorta samples by immunoelectron microscopy and describe the first manifestation of podosomes *in vivo* (Quintavalle *et al.*, 2010).

1.5.2 Adhesion

Podosomes form direct cell-matrix contacts, which also might explain their name, originating from the Greek word “podo” meaning “foot”. This term refers to the first described podosomes appearing at the bottom of the cell, which are used to “walk” along the substrate and display the cell’s feet (Tarone *et al.*, 1985). The essential elements of the adhesion to several matrix proteins are Integrins but also transmembrane receptors like CD44 (Chabadel *et al.*, 2007; Chellaiah, 2006). As these receptors are substrate specific, the Integrin composition of podosomes determines if the cell adheres to a certain matrix protein (Niu and Chen, 2011). However, the substrate can also influence the clustering of Integrins and trigger several signaling cascades which can lead to the recruitment of MMPs or a change in morphology (Galvez *et al.*, 2002; Kumar, 1998; Peng *et al.*, 2012). The role of the substrate stiffness will be discussed later in this chapter. Nevertheless, why the adhesive plaque of podosomes is arranged in a ring appearance is still unknown. In osteoclasts it was shown that during podosome assembly the actin core appears before the integrin ring structure accumulates, which indicates that an intracellular trigger induces podosome formation (Luxenburg *et al.*, 2011). Interestingly, osteoclasts do not only form single podosomes arranged in clusters but also podosome rosettes and a podosome belt at the periphery, which ultimately differentiate into a sealing zone. The formation of the different structures correlates with the maturation stage of the cells, in which the sealing zone mediates a tight attachment of the resorbing osteoclast to the bone matrix (Jurdic *et al.*, 2006; Vaananen and Horton, 1995). This pattern might display the requirement of adhesiveness during the migration process from the bone marrow to the bone substrate (Ishii *et al.*, 2009).

The cultivation of podosome-forming cells in a 3D matrix environment mimics less artificial circumstances and possibly reflects closer *in vivo* conditions. Macrophages in a 3D collagen I gel form multiple protrusions enriched in F-actin and different podosome markers such as Cortactin, Vinculin, Talin or Paxilin and even showed similarities in lifetime compared to 2D data (Van Goethem *et al.*, 2010). However, a defined ring structure could not be determined.

A crucial point in the context of adhesive function is the composition of the matrix, its stiffness and density. This fundamentally influences Integrin recruitment and therefore cell-matrix communication, which dictates the cell behavior.

1.5.3 Size and lifetime

The exact size of podosomes depends on the cell type and on the actual arrangement into cluster, rosettes, belts or single podosomes. The average size for single podosome varies from 0.1-1.5 μ m in diameter based on the actin core (Stolting *et al.*, 2012). Macrophages display a mixed population of podosomes, which undergo fission and fusion leading to different sized podosome dots. Interestingly the bigger podosomes (also called precursor) appear at the leading lamella, in which the smaller structures (also named successors) stay at the center or rear of the cell (Evans *et al.*, 2003; Bhuwania *et al.*, 2012). This is in contrast to smooth muscle cells, which form different sized podosomes but with a random arrangement predominantly at the rim of the cell (Burgstaller and Gimona, 2004; Kaverina *et al.*, 2003). Podosomes are predominantly described as columnar adhesion structures (side view) extending intracellular with a height of around 0.5 μ m but are not protrusive structures (Akisaka *et al.*, 2008; Labernadie *et al.*, 2010). However, recently it was shown that dendritic cells form podosomes, which

protrude in a Myosin-II dependent manner into a gelatin matrix with an average length of around 3 μ m (Gawden-Bone *et al.*, 2010). The size of podosome structures formed in a 3D environment are also larger compared to podosomes formed in 2D conditions possibly due to extended integrin clustering (Rottiers *et al.*, 2009; Tatin *et al.*, 2006).

The lifetime of podosomes display their dynamic nature and is characterized by an range of 2-12 min dependent on the cell type and the podosome structure (Cougoule *et al.*, 2012; Destaing *et al.*, 2003; Evans *et al.*, 2003). What exactly regulates the turnover of podosomes is not clearly defined. The loss of Cortactin or its homologue HS1 was shown to decrease podosome lifetime in dendritic cells, but led to a total loss of podosomes in osteoclasts (Dehring *et al.*, 2011; Tehrani *et al.*, 2007). Another actin crosslinking protein, AFAP-110, and its impaired phosphorylation led to the stabilization of podosomes, an increased lifetime and a larger size (Dorfleutner *et al.*, 2008). Other effectors of podosome turnover are Myosin-II and Supervillin, a member of the gelsolin family, which are both thought to promote dissolution of podosomes in macrophages (Bhuwania *et al.*, 2012; Pestonjamas *et al.*, 1997). In this context, Gelsolin-deficient dendritic cells did not show a change in podosome lifetime (Hammarfjord *et al.*, 2011). The role of MMPs in the turnover of podosomes is not well established. Thus, in osteoclasts the inhibition of MMPs induce increased podosome lifetime, while other proteases such as ADAM17 are associated with the disassembly of podosomes (Goto *et al.*, 2002; West *et al.*, 2008). Interestingly, podosome lifetime was only slightly different (from 2min to 5min), when formed in a 3D environment compared to the turnover rate on a 2D substrate (Van Goethem *et al.*, 2010).

1.5.4 Degradation

The degradation of matrix proteins is a key characteristic of podosomes, which is mediated by proteases. Classically, the ability of matrix lysis is detected by cell spreading on a fluorescently labeled matrix. Typical substrates are collagen I, collagen IV, gelatin, fibronectin and fibrinogen or Matrigel, a mixture of basement membrane components (Chen *et al.*, 1984; Van Goethem *et al.*, 2010; Varon *et al.*, 2006). All of the mentioned matrix proteins are physiological relevant as they occur in structures such as basement membranes, vascular sinusoids, the bone marrow environment or connective tissues, which need to be passed (Kalluri, 2003; Klein, 1995; Rowe and Weiss, 2008). The best studied proteases associated with podosome structures are MMP-2, MMP-9, MT1-MMPs but also cysteine cathepsins such as Cathepsin-K, -B, -X or Cathepsin-S (Delaisse *et al.*, 2000; Gawden-Bone *et al.*, 2010; Jevnikar *et al.*, 2012; Saftig *et al.*, 1998; Tatin *et al.*, 2006). The regulation of these proteases is partially illuminated and some key regulators are identified. At the first point of contact there are the different Integrins through which, depending on the ECM, MMPs get recruited (Galvez *et al.*, 2002). Other studies demonstrated with micropatterned ECM surfaces, that β_1 -Integrin activity and signaling through PKC controls ECM degradation (Destaing *et al.*, 2010). Other potential regulators are Cortactin and Wip. This hypothesis is supported by the fact that the impaired Cortactin-interaction domain of Wip were demonstrated to be essential for gelatin degradation in dendritic cells and is mentioned in several reports in the context of matrix degradation and protease recruitment (Banon-Rodriguez *et al.*, 2010; Artym *et al.*, 2006). Furthermore, Cortactin is a substrate of Src, which is associated with ECM degradation in endothelial cells, transformed fibroblasts and osteoclasts (Bruzzaniti *et al.*, 2005; Tatin *et al.*, 2006; Tu *et al.*, 2008). The limited reports demonstrating podosome-

mediated degradation in 3D underline the importance of MMPs but also the activity of Hck kinase activity (Rottiers *et al.*, 2009; Cougoule *et al.*, 2010)

1.5.5 Mechanosensor

The function of adhesion complexes as mechanosensors was previously associated with focal adhesions (Pelham and Wang, 1997). However, in the last few years, podosomes have been linked to mechanosensing. This function influences several properties of podosomes such as their lifetime or spatial arrangement (Collin *et al.*, 2006). In this context, the physical properties of the ECM such as rigidity, surface topography or interfiber cross-linking play a crucial role (Friedl and Wolf, 2010; Parekh and Weaver, 2009). Stiffer matrix proteins lead to more stable podosomes, which are more spatially separated from each other with a less defined individual morphology (Collin *et al.*, 2006; Linder *et al.*, 2011). Furthermore, podosome rosettes were described to exert traction on the matrix, which was increased with rising substrate stiffness (Collin *et al.*, 2008). Recently, it was demonstrated that vascular endothelial cells form larger podosomes correlated with increased substrate stiffness (Juin *et al.*, 2012b). Similar observations were made in osteoclasts seeded on “smooth” and “rough” calcite crystals (bone component). This resulted in the formation of small unstable sealing zones (lifetime ~8min) in contrast to large and stable (lifetime ~6h) actin rings on a rough substrate (Geblinger *et al.*, 2010). These processes are only just starting to be understood. However, it is clear that Integrins play a key role as they built the bridge between matrix and cell (Peng *et al.*, 2011). Another key regulator is possibly Myosin II, which was demonstrated to be involved in the stiffness of the actin core probably by actin filament tension in radial actin cables, which potentially connects podosomes with each other (Labernadie *et al.*, 2010; Linder *et*

al., 2011). The mechanosensory function of podosomes was also demonstrated in a 3D culture system, in which macrophages formed podosome-like structures when embedded in a loose fibrillar collagen gel but no podosomes formed in a dense collagen gel (Van Goethem *et al.*, 2010).

1.6 Podosome versus invadopodia and focal adhesions – a comparison

1.6.1 Invadopodia

There is a debate in the field about the difference between podosomes and invadopodia and whether they are the same structure or not. Today, both structures are collectively termed invadosomes, illustrating cell-matrix contacts with the ability to degrade ECM proteins (Linder *et al.*, 2011). Invadopodia share many proteins with Podosomes. Invadopodia are F-actin rich structures with a dot-like appearance and a size of up to 8µm in diameter, which is around 5 times larger than the average podosome (Linder *et al.*, 2011; Schoumacher *et al.*, 2010; Stolting *et al.*, 2012). Besides F-actin, well characterized invadopodia components are the Arp2/3 complex, N-Wasp, Cortactin, Fascin, Paxillin, Myosin II, β_1 - and β_3 -Integrins, and different MMP and Serine proteases (Alexander *et al.*, 2008; Ayala *et al.*, 2008; Destaing *et al.*, 2010; Li *et al.*, 2010; Monsky *et al.*, 1993; Yamaguchi *et al.*, 2005). Kinases such as FAK, members of the Src-family as well as PKC make up the regulative signaling component of invadopodia structures (Bowden *et al.*, 1999; Chan *et al.*, 2009; Hu *et al.*, 2011). Most of the mentioned components are present in both, invadopodia and podosomes. However, there are some proteins that are only present in one of the structures. The best known is Wasp,

which is only expressed in myeloid cells and therefore only occurs in podosome structures, while in invadopodia its homologue N-Wasp plays a crucial role (Monypenny *et al.*, 2011; Yu *et al.*, 2012). There are several other proteins described to localize in podosomes but not in invadopodia such as Kindlin-3, ZO-1 or Calponin (Gimona *et al.*, 2003; Kremerskothen *et al.*, 2011; Schmidt *et al.*, 2011), but because of the divergence of the multifaceted cell types it is difficult to determine a defined marker for the different structures. Thus, it might be only a matter of time until the mentioned components are identified in invadopodia formations as well.

Another structural difference between podosomes and invadopodia is the arrangement of an adhesion-plaque ring structure in podosomes, which is absent in invadopodia (Albrechtsen *et al.*, 2011; Cox *et al.*, 2012). However, this hallmark was rebutted by a recent publication describing invadopodia with Vinculin ring structures around actin dots in breast cancer and head and neck squamous carcinoma cells (Branch *et al.*, 2012). This result highlights the difficulty to differentiate the two structures, if there is a difference.

The assembly of invadopodia is in general associated with cancer cells of invasive nature (Yamaguchi *et al.*, 2005; Ayala *et al.*, 2007). Furthermore, invadopodia are described to be protrusive structures extending into the underlying matrix for several microns, which correlates with the invasive properties of the cells (Bowden *et al.*, 1999; Linder, 2007). However, invadopodia to my knowledge were not proven to have an essential role in adhesive functions, which is in contrast to podosome structures. Another functional distinction can be observed in the lifetime and the dependency on some proteins. Podosomes have a lifetime of several minutes, while invadopodia can persist for several hours (Hammarfjord *et al.*,

2011; Artym *et al.*, 2006). Furthermore, invadopodia assembly is dependent on MMP activity, Fascin and Cortactin. This is in contrast to podosomes, the formation of which is not necessarily dependent on MMP activity. However, some studies demonstrated an essential function for Fascin and Cortactin (Artym *et al.*, 2006; Dehring *et al.*, 2011; Li *et al.*, 2010; Quintavalle *et al.*, 2010; Tehrani *et al.*, 2007; Yamakita *et al.*, 2011). These results underline the difficulty to distinguish podosomes and invadopodia based on their protein composition. Similarities of invadopodia and podosomes are also demonstrated in the ability to degrade ECM proteins by different proteases, regulated by key proteins such as Cortactin, Wip or N-Wasp/Wasp (Banon-Rodriguez *et al.*, 2010; Ayala *et al.*, 2007; Yu *et al.*, 2012; Dovas *et al.*, 2009).

Podosomes are thought to play a role in mechanosensory processes (Geblinger *et al.*, 2010; Labernadie *et al.*, 2010). There is increasing evidence that invadopodia may be mechanosensitive. For example, the stiffness of the underlying substrate was reported to increase invadopodia formation and to trigger the recruitment of MMPs in a Myosin-II dependent manner (Parekh and Weaver, 2011; Alexander *et al.*, 2008). Another study reports the induction of linear arranged invadopodia by collagen I fibers, which is surprisingly independent of β_1 - or β_3 -Integrins as well as Vinculin and Paxillin and also formed in a 3D environment (Juin *et al.*, 2012a). These results indicate possible mechanosensing by invadopodia structures.

The formation of invadopodia-like structures containing Cortactin and N-Wasp was also demonstrated in cells invading into matrigel. Furthermore, these structures correlated with ECM degradation dependent on N-Wasp and MT1-MMP activity (Yu and Machesky, 2012; Yu *et al.*, 2012). Cells seeded in a 3D-like environment

on a dermis-based matrix showed similar formations rich in F-actin and located to proteolytic cleaved collagen (Friedl and Wolf, 2010; Tolde *et al.*, 2010).

The complex network of proteins regulating podosome and invadopodia assembly and their function makes it difficult to differentiate these structures. The identification of a pivotal marker for either podosomes or invadopodia would be crucial in order to determine a clear distinction of the two formations. Additionally, further investigations are needed in order to understand both structures better in a 3D environment as well as in *in vivo* conditions.

1.6.2 Focal adhesions

Focal adhesions (FA) are Integrin based cell-matrix contacts which, in contrast to podosomes, have an elongated shape and are associated with stress fiber formation (Chrzanowska-Wodnicka and Burridge, 1996). The structure of focal adhesions is based on Integrins, which are connected via adaptor proteins such as Talin, α -actinin, Paxillin and Vinculin with the actin cytoskeleton, which is arranged predominantly in parallel bundles enabling cellular contractility via Myosin-II activity (Bois *et al.*, 2005; Turner *et al.*, 1990). Crucial kinases in the regulation of these proteins and the maturation of these structures are FAK, Src and Integrin-linked Kinase (ILK) (Chan *et al.*, 2009; Schlaepfer and Mitra, 2004). The protein composition of focal adhesions and podosomes is not very different from each other. However, the various proteins have a distinct significance in the different structures. Thus, focal adhesions are highly dependent on Myosin-II activity and its recruitment of Vinculin to FAs by FAK-mediated regulation of Paxillin (Pasapera *et al.*, 2010). This is in contrast to podosomes, in which Myosin-II is involved in

disassembly but not essential for the formation of podosomes (Bhuwania *et al.*, 2012).

The most prominent task of FAs is their function in mechanosensory processes, in which Vinculin and Myosin-II play a pivotal role (Grashoff *et al.*, 2010). Similar to podosomes, FA properties are dependent on the underlying substrate (Pelham and Wang, 1997; Collin *et al.*, 2006; Labernadie *et al.*, 2010). The lifetime is another feature to distinct podosomes and FAs. FAs are less dynamic structures and have a lifetime varying between 40 and 60 minutes (compared to podosomes lasting 2-12min) (Ren *et al.*, 2000; Schober *et al.*, 2007; Webb *et al.*, 2004).

Beside protein composition, shape and lifetime, the degradative activity was another characteristic to differentiate podosomes from FAs. However, recently it was demonstrated that cells with FA structures are indeed able to lyse ECM proteins, in which MMP recruitment is mediated by FAK and the adaptor protein p130Cas (Wang and McNiven, 2012).

Focal adhesion formation was also demonstrated to occur in a 3-dimensional environment and supported invasion in a Vinculin dependent manner (Mierke *et al.*, 2010). Surprisingly, the appearance of these structures was not very different from the morphology in 2D conditions (Cukierman *et al.*, 2002).

The distinction of podosomes and FAs can be based on their properties such as size, morphology, lifetime or protein composition. Mature FAs for example do not contain Wasp, a Vinculin ring structure or the Arp2/3 complex, which display ideal marker for differentiation (Block *et al.*, 2008; Serrels *et al.*, 2007).

1.7 Megakaryocytes, proplatelets and platelets

1.7.1 Megakaryopoiesis and the bone marrow environment

Megakaryocytes (Mks) originate from hematopoietic stem cells (HSCs). HSCs can differentiate into all blood cell types, but in order to differentiate into Mks, they will first become common myeloid progenitors, then megakaryocyte/erythroid progenitors (MEPs), before committing their differentiation pathway to the megakaryocyte specific lineage. MEPs develop into promegakaryoblasts leading to megakaryoblasts and finally into mature megakaryocytes, which ultimately can produce platelets via proplatelet (PPL) formation (Deutsch and Tomer, 2006; Sun *et al.*, 2006). The development of Mks is called megakaryopoiesis and the different stages are influenced by several cytokines and characterized by different surface receptors or transcription factors (Shivdasani *et al.*, 1997; Wickenhauser *et al.*, 1995). Maturity of Mks correlates with increased hematopoietic stem cell marker CD34 (Debili *et al.*, 1992; Huss, 2000). The differentiation stage of Mks can also be linked to the expression of specific glycoproteins (Gps) such as von Willebrand factor (vWF), CD41a (GpIIb/IIIa complex, Integrin $\alpha_{IIb}\beta_3$), Cd42 (GpIb), CD61 (GpIIIa) or platelet factor-4 (PF4) (Ferkowicz *et al.*, 2003; Tomer, 2004). An essential cytokine during Mk maturation, secreted by bone marrow endothelial cells, is thrombopoietin (TPO), which increases Mk size and polyploidization by Janus Kinase 2 (Jak2) signaling (Kaushansky *et al.*, 1994; Nagahisa *et al.*, 1996; Neubauer *et al.*, 1998). Other important cytokines are Interleukin-6 (IL-6) and stem cell factor (SCF), both of which induce nuclear and cytoplasmic maturation (Tajika *et al.*, 1998). A chemokine involved in megakaryopoiesis is stromal derived factor-1 α (SDF-1 α), the receptor of which, CXCR4, is expressed from progenitor cells to

platelets (Wang *et al.*, 1998). Furthermore, SDF-1 α was demonstrated to promote adhesion of Mks to endothelial cells, to initiate migration towards a gradient and to increase the expression of specific MMPs (Lane *et al.*, 2000; Mazharian *et al.*, 2009; Wang *et al.*, 1998).

The actual process of megakaryopoiesis is hypothesized to take place in the bone marrow niche (Figure 1.7). During this process, the Mks migrate towards the vascular niche, where the actual release of PPLs and ultimately platelets into the blood stream occurs. The matrix and cellular composition of both niches were demonstrated to influence Mk proliferation, adhesion, migration and proplatelet formation (Avecilla *et al.*, 2004; Balduini *et al.*, 2008; Larson and Watson, 2006b; Nagahisa *et al.*, 1996). The matrix of the osteoblastic compartment is dominated by collagen I (Psaila *et al.*, 2012; Reddi *et al.*, 1977). This is in contrast to the vascular niche, in which predominantly collagen IV, laminin, fibronectin and fibrinogen are present (Nilsson *et al.*, 1998). Interestingly, it was demonstrated that Mks undergo PPL formation on fibrinogen, fibronectin and collagen IV but not on collagen I (Balduini *et al.*, 2008; Larson and Watson, 2006a). A special component of the vascularity is the basement membrane, which displays a meshwork of different proteins but predominantly collagen IV and laminin, located between the endothelial cell layer and the outer smooth muscle cell layer (Hotary *et al.*, 2006; Kalluri, 2003). However, specific regions of the vessels have a low expression of basement membrane components, which might facilitate the penetration of Mks or proplatelets (Nourshargh *et al.*, 2010). The process of proplatelet release by Mks was described *in vivo* and displayed the cytoplasmic fragmentation of Mks into a bone marrow sinusoid (Junt *et al.*, 2007). However, this study did not visualize the actin cytoskeleton, so that the formation of podosomes by Mks during PPL release

in vivo is unknown. Nevertheless, podosomes potentially could support the migratory processes through the osteoblastic niche by adhering to the ECM and remodeling this. Furthermore, podosomes could facilitate the penetration of the vascularity to release platelets.

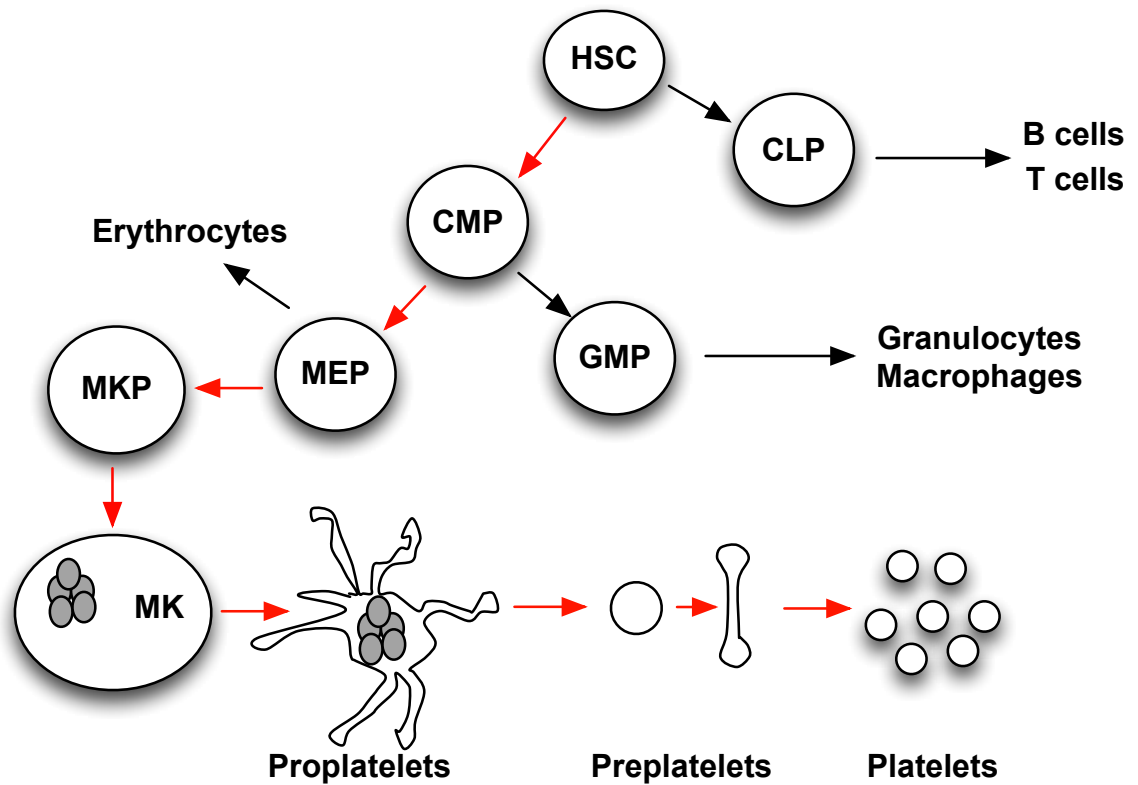


Figure 1.6: Differentiation of the megakaryocytic lineage

Mks origin from a hematopoietic stem cell (HSC), which differentiates into a common myeloid progenitor (CMP) further into a megakaryocyte/erythroid progenitor (MEP). This develops into a megakaryoblast and then into a megakaryocyte. If fully matured the Mks form cytoplasmic extensions called proplatelets, which are fragmented into preplatelets. These preplatelets divide via a microtubule dependent process into platelets. Red arrows indicate the proliferation from the HSC to the ultimately formed platelets. The differentiation of the different progenitors correlates with the essential presence of specific cytokines and chemokines such as TPO, SCF and SDF-1 α .

1.7.2 Proplatelet formation

After rounds of endomitosis the mature Mk starts to undergo proplatelet formation. During this process, several thousand platelets are produced per megakaryocyte via the fragmentation of the cytoplasm of the Mks and the release of PPLs (Mattia *et al.*, 2002; Tablin *et al.*, 1990). In order to produce platelets the Mk once mature increases the production of platelet-specific granules and the invaginated membrane system (IMS), which is possibly the source of PPL membrane (Beckstead *et al.*, 1986; Lordier *et al.*, 2012; Schulze *et al.*, 2006). PPL formation is a highly dynamic process, in which long tube-like formations containing bead shaped accumulations, which are roughly the size of a platelet, are formed. These PPL arms are dependent on a microtubule scaffold and can extend to a length of up to 50µm (Thon *et al.*, 2010). *In vitro* real-time studies of PPL formation demonstrated, that this process takes 4-10h and is dependent on the actin cytoskeleton, which provides necessary spreading dynamics. However, electron and confocal microscopy clearly demonstrated the concentration of microtubules in proplatelet extensions, which are arranged into loops in their bulbous ends (Italiano *et al.*, 1999). The microtubule filaments are also thought to serve as tracks for granule transport, which are essential for platelet function, via motor proteins such as kinesins (Richardson *et al.*, 2005). Nevertheless, there is another PPL membrane skeleton protein, called Spectrin. Spectrin is cross-linked by actin filaments, and influences the maturation of the IMS and is therefore essential for proplatelet formation (Patel-Hett *et al.*, 2011). Recently, it was hypothesized that there is an intermediate form between proplatelets and platelets, the preplatelet. The preplatelet has a circular morphology and breaks into a platelet by twisting microtubule forces (Thon *et al.*, 2012; Thon *et al.*, 2010).

What exactly triggers the formation of proplatelets is still not clearly defined, but the complex influence of maturity, the surrounding matrix proteins, the cellular environment, cytokines, and chemokines extend the understanding of this multifaceted process.

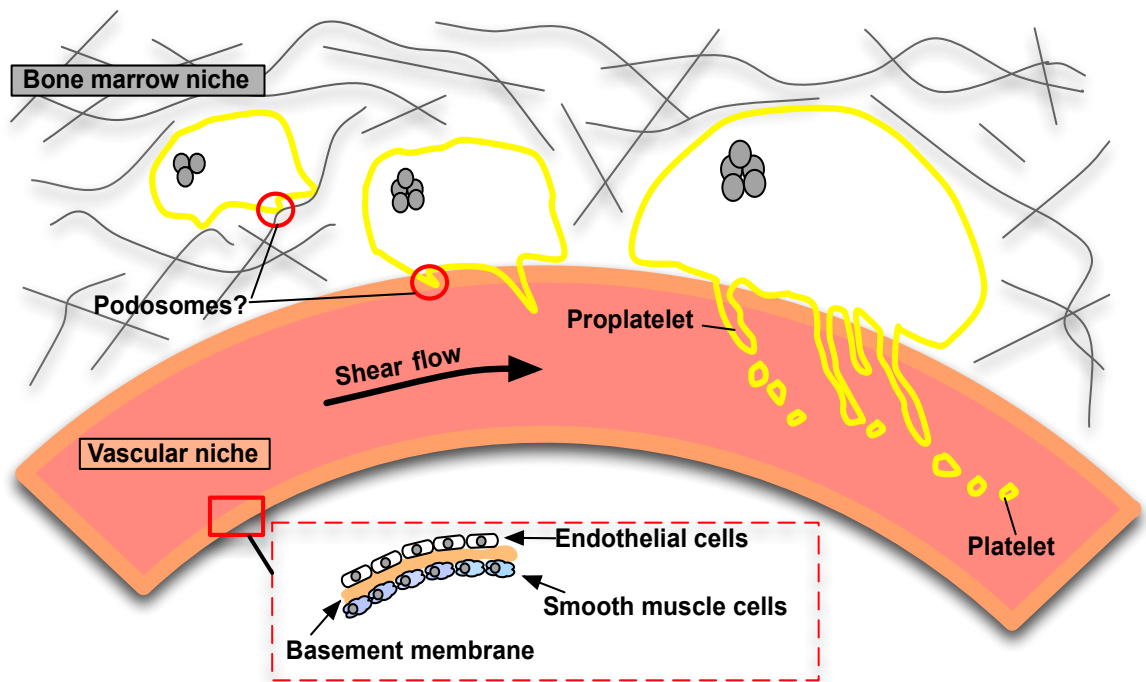


Figure 1.7: Mks, platelet formation and the potential role of podosomes

Mks originate from HSCs in the bone marrow compartment, which is predominantly composed of collagen I. During proliferation and differentiation Mks need to migrate from the bone marrow niche towards the vascular niche. This process is highly dependent on the cellular environment and the matrix composition, which provides necessary cytokines, chemokines and growth factors. The described migration step might be facilitated by podosomes, which interact with the matrix environment and possibly degrade it partially. The vascular niche is composed of fibrinogen, fibronectin as well as a basement membrane containing laminin and collagen IV. When the mature Mk reaches the vascularity of this compartment, the cell needs to cross the vessel wall including the basement membrane in order to release proplatelets. Podosomes might support this process by degrading parts of the basement membrane, to facilitate the penetration of the vessel, in order to finally shed of platelets supported by shear stresses of the blood stream.

1.7.3 Platelets spreading and activation

Platelets are small (2-3 μ m), discoid shaped, anucleated cell fragments, whose main function is the prevention of blood loss after vascular damage (Merten and Thiagarajan, 2000; Sim *et al.*, 2004). A crucial event is thereby the shape change of the platelet, which underlies a very dynamic cytoskeleton rearrangement and is activated by receptor signaling and the release of platelet-specific granules (Li *et al.*, 2002a; Morrell *et al.*, 2005; Polanowska-Grabowska *et al.*, 2003).

The secretion of the granules is fundamental to the thrombus formation as α -granules and dense granules contain proteins and polypeptides such as Integrin $\alpha_{IIb}\beta_3$, fibronectin, vWF or platelet-derived growth factor, serotonin, ADP and magnesium, all of which influence platelet spreading and thrombus formation (Italiano *et al.*, 2007; King and Reed, 2002; Reed *et al.*, 2000; Sehgal and Storrie, 2007).

The most important Integrin receptors involved in platelet activation are β_1 -Integrins, which bind to collagen, fibronectin and laminin and β_3 -Integrins, the most prominent ligands of which are fibrinogen, vWF and fibronectin (Bennett *et al.*, 2009). Another pivotal receptor is immunoglobulin GPVI, binding to collagen (Watson *et al.*, 2005b).

The role of the actin cytoskeleton during platelet activation is fundamental to thrombus stability and formation. Upon platelet activation, platelets undergo shape change, followed by the formation of filopodia, stress fibers, lamellipodia and actin nodules. These actin structures have been shown to be fundamental to the successful formation of thrombi in a high shear environment (Calaminus *et al.*, 2008; McCarty *et al.*, 2005). Furthermore, filopodia and lamellipodia formation in

spreading platelets on glass is Arp2/3 complex dependent and indicates a requirement of branched actin filament network for platelet activation (Li *et al.*, 2002b). Interestingly, Wasp deficient platelets display normal activation of the Arp2/3 complex and intact lamellipodia and filopodia structures (Falet *et al.*, 2002; Gross *et al.*, 1999). In agreement with this is the phenotype of Rac-1 deficient platelets, which are unable to assemble lamellipodia and have a spiky morphology (McCarty *et al.*, 2005). Similar results were observed in Wave-1^{-/-} platelets on laminin and on a collagen-related peptide (Calaminus *et al.*, 2008). These studies indicate the relevance of Rac-Wave complex-Arp2/3 complex interactions in platelet activation and therefore possibly in aggregation.

Interestingly, platelets form actin nodules containing the Arp2/3 complex, Rac as well as β_1 - and β_3 -Integrins. At present, the role of actin nodules in platelets is unknown. Furthermore, it is not yet clear whether the actin nodule is indeed the platelet version of the podosome. However, actin nodules are not dependent on Vinculin indicating a different structural organization (Mitsios *et al.*, 2010).

1.8 Aims

The goal of my project was to determine the characteristics of podosomes in Mks and to direct a possible functional role of these structures toward a physiologically relevant context. This is important to illuminate the process of proplatelet and platelet production. My thesis aims can be subdivided into following sections:

- 1.** Investigation of the influence of the underlying matrix and the identification of essential proteins, their effect on podosome numbers and the spreading behavior of Mks.
- 2.** Determination of podosome characteristics such as the lifetime, the ability to degrade ECM proteins and the identification of associated crucial regulators.
- 3.** Identification of the role of Cortactin and the Wave complex in podosome formation and cell spreading in Mks

2 Materials and Methods

2.1 Antibodies and reagents:

Antibody target	Details	Source	Experimental dilution
Wasp	Mouse, clone B9	Santa Cruz	1:200
P34-ARC/ARPC2	Rabbit	Millipore	1:400
Phosphotyrosine	Mouse, clone 4G10	Millipore	1:200
Cortactin	Mouse, clone 4F11	Millipore	1:200
Talin	Mouse, Ta205	Millipore	1:200
α -tubulin	Mouse, clone DM1A	Sigma-Aldrich	1:200
Rac1	Mouse	Abcam	1:200
Collagen IV	Rabbit	Abcam	1:200
Laminin	Mouse	Santa Cruz	1:200
Abi-1	Mouse	Santa Cruz	1:200
Abi-2	Mouse	Santa Cruz	1:200
Paxillin	Mouse	Millipore	1:200
CD41	Rat, FITC	BD Pharmingen	1:100
IgG	Rat, FITC	BD Pharmingen	1:100
F-actin	Texas Red	Life Technologies	1:200
F-actin	FITC-Phalloidin	Sigma-Aldrich	1:200
DNA	Hoechst 33342	Life Technologies	1:1000
CD11b	Rat	BD Pharmingen	3 μ l/mouse
CD16/32	Rat	BD Pharmingen	3 μ l/mouse
Ly-6G	Rat	BD Pharmingen	3 μ l/mouse
CD45R/B220	Rat	BD Pharmingen	3 μ l/mouse
SCF	Mouse	PeptoTech	20ng/ml
TPO	Mouse	PeptoTech	50ng/ml
SDF- α 1	Mouse	PeptoTech	250 or 300ng/ml

Table 2.1 Antibodies and reagents used in this study

2.2 Inhibitors:

Reagent target	Details	Source	Experimental concentration
MMPs	GM6001	Calbiochem	5 μ M
Arp2/3 Complex	CK666	Calbiochem	20 μ M
Negative control for CK666	CK689	Calbiochem	20 μ M
Myosin II	Blebbistatin (-)	Sigma-Aldrich	10 μ M
F-actin nucleation	Latrunculin A	Sigma-Aldrich	3 μ M
Microtubule polymerization	Nocodazole	Sigma-Aldrich	10 μ M
$\alpha_{11b}\beta_3$ integrins	Lotrafiban	Wyeth Pharmaceuticals	10 μ M

Table 2.2: Inhibitors used in this study

2.3 Extracellular matrix proteins:

Protein	Source	Experimental concentration
Horm collagen	Nycomed	100 μ g/ml
Fibrinogen	Enzyme research Laboratories	100 μ g/ml
FITC-Gelatin	Sigma-Aldrich	100 μ g/ml
Collagen G	Biochrom AG	100 μ g/ml
Fibronectin	Sigma-Aldrich	10 μ g/ml

Table 2.3: Extracellular matrix proteins used in this study

All chemicals if not otherwise stated were purchased from Sigma (St.Louis, USA).

2.4 Mice

Wild type mice from black 6 (B57BL/6) or mixed background between 6 weeks and 1 year old were used to isolate megakaryocytes from the bone marrow or platelets by vein puncture. Bone marrow from Wasp^{-/-} mice was a kind gift from Prof. A. Thrasher (Snapper *et al.*, 1998). The Lifeact-GFP mouse was a kind gift from R.Wedlich-Söldner (Riedl *et al.*, 2008).

Abi-1^{-/+}/Abi-2^{-/-} knockout mouse work was done in collaboration with the lab of Prof. Pendergast at the Duke University School of Medicine (Echarri *et al.*, 2004).

Genotyping of mice was completed by the company Transnetyx (Cordoca,USA) by established methods using quantitative PCR (McClive and Sinclair, 2001).

2.5 Cell Culture

2.5.1 Isolation and cultivation of bone marrow derived megakaryocytes

The isolation of bone marrow derived Mks was done according to the previously described methods (Dumon *et al.*, 2006). Mice from B57BL/6 or mixed background between 6 weeks and 1 year old were used to isolate megakaryocytes from the bone marrow. Mice were sacrificed by an approved Schedule I method using rising CO₂ and subsequently 2 femurs and 2 tibiae were removed. The following work was done in a tissue culture hood. The bones were briefly put in 70% ethanol followed by a PBS wash. 25G needles were used to flush the bones with 10ml complete Dulbecco's modified eagle medium (DMEM) (DMEM, 10% sterile filtered fetal bovine serum (FBS), 100 units/ml penicillin, 100µg/ml streptomycin, 2mM L-

Glutamine (Life Technologies, Carlsbad, USA)) per mouse. The resulting bone marrow was centrifuged for 5min at 1200rpm at room temperature. The pellet was resuspended in 6ml ACK lysis buffer (0.15mM NH₄Cl, 1mM KHCO₃, 0.1mM Na₂EDTA, pH 7.3) or red blood cell lysis buffer (0.8% NH₄Cl, 1mM Na₂EDTA, pH7.3) for 5min and centrifuged for 5min at 1200rpm at room temperature. With this step erythrocytes were eliminated from the cell suspension. The pellet was resuspended in 1ml DMEM containing 3µl of each of the following antibodies; biotin-conjugated rat anti-mouse CD45R/B220, purified rat anti-mouse CD16/CD32, anti-mouse Ly-6G, biotin anti-mouse CD11b and was incubated on ice for 30min. After incubation 1ml of DMEM was added and the suspension was centrifuged for 5min at 1200rpm at room temperature. 50µl of sheep anti-rat IgG dynabeads were washed 3 times in an equal amount of DMEM at 10000rpm for 2min with a microcentrifuge. The cell pellet was resuspended in 1ml DMEM and 50µl of washed beads. The suspension was centrifuged twice for 5min at 1200rpm and vortexed after every step. A magnet was used to separate the beads from the suspension, which was poured into a new tube. 750µl of DMEM were added to the remaining beads, centrifuged and the cells were added to the cell suspension. The used beads bind indirectly to a range of different leukocytes including B-cells, dendritic cells and natural killer cells. These cells were together with the beads discarded. The resulting cell suspension was centrifuged for 5min at 1200rpm and resuspended in 2ml DMEM containing 20ng/ml Stem Cell Factor (SCF). On day 2 new medium was added to the cells containing 20ng/ml SCF and 50ng/ml Thrombopoietin (TPO). On day 7 the mature Mks were separated with a BSA gradient. 3% BSA in PBS was warmed up in a 37°C waterbath. 4ml of 3% BSA was added and topped up by 4ml of 1.5% BSA, the cell suspension was carefully applied to the top and incubated for 45min at room temperature. The upper 6ml of

the gradient was removed to a separate tube. Both tubes were centrifuged for 5min at 1200rpm. The tube with the lower part of the gradient containing the mature Mks was resuspended in an appropriate volume of DMEM for the experiment but not more than 1ml per mouse in order to keep the cell number at an adequate level. The tube with the upper part of the gradient containing small, immature cells was resuspended in 2ml DMEM with 100ng/ml SCF and 50ng/ml TPO and incubated for further 3-4 days.

2.5.2 Cultivation of HEK 293T cells and lentiviral production

Human embryonic kidney (HEK) 293T cells were used as a packaging cell line to produce virus particles. Cells were cultured in DMEM with a confluency varying between 50-70% and split every 2-3 days in a ratio 1:4 or 1:6. To produce lentiviral particles, $12-15 \times 10^6$ HEK 293T cells were seeded in a T175 flask with 25ml complete DMEM 24h prior to transfection. In 5ml OptiMEM (Life Technologies, Carlsbad, USA) 32.5 μ g of plasmid p8.74 (gag-pol expressor), 17.5 μ g of plasmid pMDG (VSV-G expressor) and 50 μ g of the vector construct were added together in one tube. In another vial 10mM of polyethylimine (PEI) was added to 5ml OptiMEM. Both mixes were added together and incubated for 20min. This mixture was incubated on the prewashed 293T cells for 4h at 37°C with 5% CO₂ in a humidified incubator. After this incubation time, the medium was removed and replaced by complete DMEM. After 2 days, virus-containing medium was removed, filtered through a 0.45 μ m filter and stored until concentrated at 4°C, new medium was added to the cells. The next day the medium was removed and filtered again. Viral particles were concentrated by centrifugation with an Optima L-90K Ultracentrifuge and the SW28 9E473 Rotor at 23000rpm at 4°C for 2h. The supernatant was decanted and lentiviral particles were resuspended in a 100x less

volume than the initial volume (10ml -> 100µl diluent) of OptiMEM, aliquoted and stored at -80°C.

2.5.3 Determination of virus titre

To determine the virus titre a Lenti-X qRT-PCR kit (Clontech/Takara Bio Company, Kyoto, Japan) was used. The following Master mix was prepared per reaction:

RNase-free water:	8.5µl
Quant-X buffer (2x):	12.5µl
forward primer:	0.5µl
reverse primer:	0.5µl
Quant X-Enzyme:	0.5µl
K-Enzyme:	<u>0.5µl</u>
	23 µl + 2 µl virus solution

A standard dilution series of the virus template as well as from the virus of unknown concentration was prepared in Easy buffer and loaded to the PCR plate.

The following PCR program was applied:

Rt reaction:	42°C, 5min
	95°C, 10s
qPCR, 40 cycles:	95°C, 5min
	60°C, 30s
Melting curve:	95°C, 15s
	60°C, 30s
	60°C-95°C

With the results of the qPCR the infectious unit (IFU) was determined and the multiplicity of infections (MOI) was calculated.

2.5.4 Infection of Mks

Mks were isolated from the bone marrow and purified. On the same day, the cells were infected with a MOI (multiplicity of infection) of 30 with GFP-Wasp (plasmid was a kind gift of G. Jones, Kings College, London) virus particles with a cell concentration of 6×10^6 cells/ml. Complete medium was used containing 100µg/ml SCF, 50µg/ml TPO and 100 µg/ml polybrene. After 24h and 48h the medium was refreshed. After 5 days, mature Mks were purified with a BSA gradient and used for subsequent experiments.

2.5.5 Preparation of washed platelets

Mice were euthanized in a CO₂ chamber. Blood was taken by vein puncture with a 1ml syringe and 25G needle containing 100µl of prewarmed (37°C) Acid-Citrate Dextrose (ACD) buffer (120mM C₆H₇NaO₇, 110mM C₆H₁₂O₆, 79mM C₆H₈O₇). The needle was removed from the syringe and the blood was carefully transferred into a tube containing 200µl of prewarmed (37°C) Tyrode's buffer (134mM NaCl, 2.9mM KCl, 0.34mM Na₂HPO₄·7H₂O, 12mM NaHCO₃, 20mM HEPES, 1mM MgCl₂ and 5mM glucose, pH to 7.3). The blood was spun at 2000rpm with a microcentrifuge for 5min. The platelet rich plasma (PRP) and parts of the red blood cell layer were removed to a new tube and spun for 6min at 1000rpm with a bucket rotor centrifuge. The PRP containing the buffy coat was removed to a new tube, 2nM prostacyclin (PGI₂) (Sigma-Aldrich, St.Louis, USA) was added and spun at 2500rpm for 6min. The supernatant was discarded and the pellet was resuspended in 200µl Tyrode's buffer. To remove excess red blood cells, the

solution was centrifuged at 800rpm for 2min with a microcentrifuge and the supernatant containing platelets was removed carefully. The platelets were rested for 30min on the bench prior to experiments.

2.5.6 Immunoblotting

Purified mature Mks were lysed in 100µl ice-cold RIPA lysis buffer containing protease inhibitor (Thermo Fisher Scientific, Waltham, USA) and spun down at 12000rpm at 4°C for 10min in a microcentrifuge. The supernatant was removed and used for immunoblotting. The protein concentration was determined with a Bradford assay using Precision Red Advanced Protein Assay solution (Cytoskeleton, Denver, USA). Where necessary, samples were diluted to the same concentration with an appropriate volume of lysis buffer. 4x NuPAGE sample buffer and 10x NuPage reducing buffer (Life Technologies, Carlsbad, USA) was added to the samples and boiled for 5min. 30µl samples were loaded per lane onto 4-12% Bis-Tris gels and run at 150V for 1h. Samples were transferred to a PVDF transfer membrane (GE Healthcare Life Sciences, Little Chalfont, UK) with 240mA for 75min. The membrane was blocked with 5% skimmed milk solved in TBST-T for 1h at room temperature and incubated with the primary antibody diluted 1:500 in skimmed milk over night at 4°C. The membrane was washed 3 times for 5min in 0.1% TBST. The secondary antibody diluted in skimmed milk 1:1000 was incubated for 1h at room temperature and washed 3 times for 5min in 0.1% TBST. Membrane was analysed by enhanced chemiluminescence (ECL) with a kit from Thermo Fisher Scientific (Waltham, USA), a Syngene image analyser and Syngene GeneTools software (Cambridge, UK).

2.6 Fluorescence Microscopy

2.6.1 Preparation of coverslips

Coverslips were incubated for 1h at room temperature with 100µg/ml fibrinogen or horn collagen diluted in PBS or in collagen diluent solution. A 0.5% BSA (Sigma-Aldrich, St.Louis, USA) solution was prepared and heat inactivated for 13min at 85°C, after cooling down the BSA was run through a 0.45µm filter and added to the washed coverslips. After 1h incubation, any remaining BSA was removed by 3 washing steps with PBS. The same procedure was done with an initial nitric acid (HNO₃) wash for glass-bottom dishes used for real-time imaging.

2.6.2 Immunofluorescence of fixed cells

Mks were resuspended in an appropriated volume serum-free medium (SFM) (same content as complete DMEM but without FBS) containing 250ng/ml of Stomal cell-derived Factor-1α (SDF). Depending on the assay, 200-500µl of the cell suspension were added per coverslip. The cells were incubated for 3h at 37°C in a humidified incubator with 5% CO₂ supply.

Platelets were seeded with a density of 4×10^7 in Tyrode's buffer and in the presence of 100U/ml of apyrase (Sigma-Aldrich, St.Louis, USA) on coverslips coated with 100ug/ml horn collagen or fibrinogen. Spreading on fibrinogen was done with and without the addition of 1U/ml Thrombin (Sigma-Aldrich, St.Louis, USA). The platelets were spread for 45min at 37°C.

For both platelets and Mk spreading the cell suspension was removed and cells were incubated with 4% formaldehyde (Electron Microscopy Sciences, Hatfield,USA) for 10min followed by 3 PBS washes. The cells were incubated with

0.1% Triton X-100 (Sigma-Aldrich, St.Louis, USA) for 5min and washed 3 times with PBS. The primary antibody was added, diluted in PBS for 30min and washed 3 times with PBS. The Alexa-dye labelled secondary antibody and fluorescently labelled phalloidin were added together and applied for 30min followed by 3 PBS washes. The coverslips were washed once with distilled water before mounting onto a microscope slide with ProLong® Gold reagent with DAPI (Life Technologies, Carlsbad, USA) and dried overnight in the dark at room temperature.

2.6.3 Quantification of podosome numbers

Image J 1.45s and Fiji 1.46j were used to manually determine the number of podosomes, the cell surface and the size of podosomes. If not stated otherwise, fixed Mks stained for F-actin and Wasp were analysed. Dot-like structures positive for both Wasp and F-actin were counted. The cell area was divided according to the distribution of podosomes into 4 parts, only one part was analysed and the resulting number was multiplied by 4. Counting this way compared to counting podosomes of the entire cell did not show a significant difference. The cell surface was determined by measuring the cell shape based on the F-actin staining. The number of podosomes per μm^2 was calculated by dividing the number of podosomes by the cell surface. In this way at least 20 cells were analysed per experiment. The podosome size was analysed by measuring F-actin and Wasp positive dot-like structures, if not stated otherwise, at least 20 podosomes of 5 different cells were determined.

2.6.4 Real-time spreading of Mks

Mature Mks were purified with a BSA gradient and seeded on matrix coated glass-bottom dish. Mks were incubated for 30min to 1h at 37 °C before imaging. The confocal microscope Nikon A1R (Tokyo, Japan) was used for imaging and was equipped with a heating stage, CO₂ supply and a perfect focus. The Nikon total internal reflection microscope (TIRF) containing a heating insert was used as well. To stabilize the pH of the medium 20µM HEPES buffer was used (Life Technologies, Carlsbad, USA).

2.6.5 Quantification of podosome lifetime

Only podosomes that appeared and disappeared during the length of the movie could be analysed. F-actin rich, dot-like structures were evaluated and the lifetime was calculated based on the visual appearance in the movie. Images were taken every 10-20s for 20min up to 4h. Real-time Imaging was performed with a confocal or TIRF microscope.

2.6.5.1 Fluorescent Labelling of ECM proteins

An Alexa 488-protein labelling Kit from Life Technologies (Carlsbad, USA) was used according to the manufacturer's instructions to label fibrinogen and horn collagen. 150µl of a 1M NaHCO₃ solution was mixed with 1ml of 2mg/ml fibrinogen or 2mg/ml horn collagen dissolved in PBS or collagen diluent and added to a vial of Alexa-Fluor 488 reactive dye and stirred for 1h at room temperature. The solution was added with a syringe into a dialyzer cassette (Thermo Fisher Scientific, Waltham, USA), put with a swim device into a beaker filled with PBS and was stirred in the dark at 4°C for 3 days. The PBS was changed every day and the solution removed from the cassette and aliquoted.

2.6.6 Degradation Assay

Coverlips were mounted on a drop of 100µg/ml fluorescent labelled fibrinogen, horn collagen or gelatin and incubated at 4°C over night or alternatively 1h at room temperature. The coverslip was covered for 1h with DMEM at 37°C in an incubator and subsequently washed 3 times with SFM. Mks from the BSA gradient were resuspended in an appropriate volume of DMEM containing 100ng/ml SDF-1α and were incubated for 3h on fluorescently labelled matrix.

2.6.7 Quantification of matrix degradation

Image J 1.45s and Fiji 1.46j were used to write a plugin for the quantification of matrix degradation. The written plugin defines the cell shape according to the F-actin staining and measures the average pixel intensity of the matrix staining underneath the cell and around the cell of taken images from fixed cells. If the average pixel intensity underneath the cell is lower than the surrounding area the cell is defined as positive for degradation. In this way the percentage of degrading cells was determined. The amount of degradation was determined by calculating the percentage rate from the pixel intensity of the cell and the pixel intensity of the surrounding area. These values were normalized for the different treatments with a 100% degradation for control samples. At least 20 cells per experiment were analysed.

2.6.8 Basement Membrane Assay

The isolation of the basement membrane from the murine peritoneum was performed as previously described (Hotary *et al.*, 2006). Plastic cups from an invasion assay insert were used after removing the filter membrane. The basement membrane was directly transferred from the mouse to the plastic cup

and sealed at the edges with a 50:50 wax-paraffin mixture. The membrane was treated with 0.4mM ammonium hydroxide (NH₄OH) for 1h at room temperature followed by 3 washing steps with ice-cold PBS. The plastic cup with the membrane was put into a well of a 24-well plate containing 600µl SFM and 300ng/ml of SDF-1α. 4-8 x 10⁵ cells were seeded in SFM onto the membrane in a volume of 200µl and incubated for 3h at 37°C in an incubator. The medium was removed from both compartments and the cells were fixed with 4% formaldehyde for 10min. The formaldehyde was removed by PBS washes and 0.1% Triton X-100 was applied to the cells for 5min. PBS washes removed any remaining Triton. The primary antibody was applied for 30min in a volume of 100µl followed by PBS washing steps. The secondary antibody, fluorescently labelled phalloidin and Hoechst was incubated for 30min and removed by 3 washes of PBS and stored in PBS at 4°C until imaged. Imaging was done by removing the PBS but leaving the membrane wet and putting it onto a coverslip dish.

For real-time imaging the cells were added to the membrane whereas the plastic cup was put onto a 1-well glass-bottom dish containing SFM and 300ng/ml SDF-1α.

2.6.9 Quantification of the basement membrane assay

Analysis of the percentage of protrusions crossing the basement membrane and the determination the cell surface was done by evaluating z-stacks of fixed Mks spread on the BM and stained for Collagen IV or Laminin and F-actin. 3D reconstruction was done with Image J, Fiji or Imaris Bitplane (Zürich,Switzerland) imaging software. Random cross-sections of the z-stack were taken so that the thickness of the basement membrane was measured as well as the length of

single protrusions. If the protrusion was longer than the thickness of the BM the cell was counted as positive for forming crossing protrusions. If not stated otherwise at least 20 cells were analysed per experiment.

2.6.10 Statistics

Statistical analysis was performed by using Graph Pad Prism 5. In this way student's t-test and ANOVA analysis was done. Which test exactly was used is stated in the corresponding figure legends. If not otherwise stated experiments were performed 3 times with cells from different mice for each experiment. A result was defined as significant different with a P-value of <0.05 .

3 Megakaryocytes assemble podosomes on fibrinogen and collagen

3.1 Summary

Podosomes are F-actin based adhesion structures formed by different myeloid cells. My aim was to characterize podosomes in Mks, to determine involved proteins, and to investigate the influence of different matrix proteins on podosome assembly. I have found that Mks form the traditional actin-rich core, and a Vinculin ring structure associated with podosomes on both collagen I and fibrinogen. The formation of these podosomes is dependent on actin polymerisation and the activity of the Arp2/3 complex, but independent of Myosin II, matrix metalloproteases (MMPs) and microtubules.

3.2 Introduction

Podosomes are formed by several different cell types including dendritic cells, macrophages, osteoclasts, endothelial cells and Src-transformed fibroblasts (Linder *et al.*, 2011). In Mks there is only one report describing podosome assembly (Sabri *et al.*, 2006). The formation of Mk podosomes is dependent on the underlying matrix and the activity of the actin nucleator Wasp. However, Sabri and colleagues gave no detailed information about the number of podosomes, their size or the involvement of key proteins such as the Arp2/3 complex, Myosin II, MMPs or Integrins.

During maturation and proplatelet (PPL) formation, Mks need to migrate from the bone marrow niche towards the vascular niche and throughout this migration, they are exposed to a range of matrix proteins (Malara *et al.*, 2011b; Nilsson *et al.*, 1998). The most abundant matrix proteins in the Mk environment are collagen I and fibrinogen. Collagen I is mainly present in the bone marrow compartment, whereas fibrinogen occurs predominantly around the vascularity of the bone marrow (Psaila *et al.*, 2012). To verify the influence of these two physiological relevant substrates on podosome formation I performed Mk spreading on collagen I and fibrinogen. The adhesion to fibrinogen activates the Mk specific Integrin $\alpha_{IIb}\beta_3$, which has not been previously shown to have a role in podosome assembly.

Another fundamental aspect in the process of podosome assembly is the dynamic turnover of the actin cytoskeleton. One of the key regulators of this process is the Arp2/3 complex, which is controlled by members of the Wasp family, initiating the formation of branched actin filaments. The activity of the Arp2/3 complex as well as its regulator Wasp was shown to be essential for podosome assembly in several different cell types including dendritic cells and macrophages (Linder *et al.*, 2000a; Calle *et al.*, 2004). Another modulator of podosome turnover, focal adhesions and stress fibres, is Myosin II. Myosin II was described previously to be essential for the formation of podosome-like structures in osteoclasts but not in dendritic cells or macrophages (Bhuwania *et al.*, 2012; Collin *et al.*, 2008; Gawden-Bone *et al.*, 2010). This underlines the cell type specific protein composition of podosomes. Podosomes are also often compared with invadopodia, F-actin based protrusions formed by cancer cells and known to be involved in invasion (Ayala *et al.*, 2008), and sometimes defined as the same structures. However, a fundamental difference between podosomes and

invadopodia is the involvement of MMPs, which are essential for invadopodia formation but not for podosome assembly (Li *et al.*, 2010).

In this chapter I characterized the assembly of podosomes on collagen and fibrinogen. Furthermore, I investigated the role of proteins known to be involved in podosome assembly in other cell types and determined an essential function for F-actin and the Arp2/3 complex. Interestingly, I found a role for Mk integrin $\alpha_{11b}\beta_3$, which highlights the cell type specific involvement of proteins in podosome formation. Only a minor influence was determined for MMPs, Myosin II, and the microtubule cytoskeleton in Mk podosomes.

3.3 Results

3.3.1 Podosome assembly depends on the underlying substrate

Mks were allowed to spread on horn collagen I and fibrinogen and were imaged in real-time conditions for 12h (Figure 3.1 and supplemental movie 1 and 2). A dynamic spreading behaviour, indicated by lamellipodia formation, was observed on both matrices. Fully spread cells were detected after 3h and determined by clear retraction of the cell area after this timepoint on fibrinogen as well as on horn collagen (compare timepoint 3h versus 4h in Figure 3.1). Interestingly, after 4h Mks started to form long extensions on fibrinogen, which were identified as proplatelets, as these formations extended over several hours (black arrows, Figure 3.1A). However, Mks did not form such structures on horn collagen but spreading was performed along the collagen fibres (Figure 3.1B, red arrowheads). With these observations I determined the time, which is needed for a fully spread Mk, as 3h.

To investigate the formation of podosomes in Mks, the cells were allowed to spread on horn collagen I and fibrinogen. Immunofluorescence was performed for F-actin and Wasp in order to verify the influence on podosome formation of different physiologically relevant matrices. Podosomes were clearly formed on both substrates (Figure 3.2; Figure 3.3). Interestingly, Mks spread on collagen showed a different spatial arrangement with podosomes aligned along collagen fibres, which was not observed in spread cells on fibrinogen (Figure 3.2A,B and supplemental movie 3). The number of podosomes, the cell surface, podosomes formed per μm^2 and the podosome size was determined (Figure 3.2C-F). The total

number of podosomes was significantly higher in Mks spread on collagen compared to the ones spread on fibrinogen.

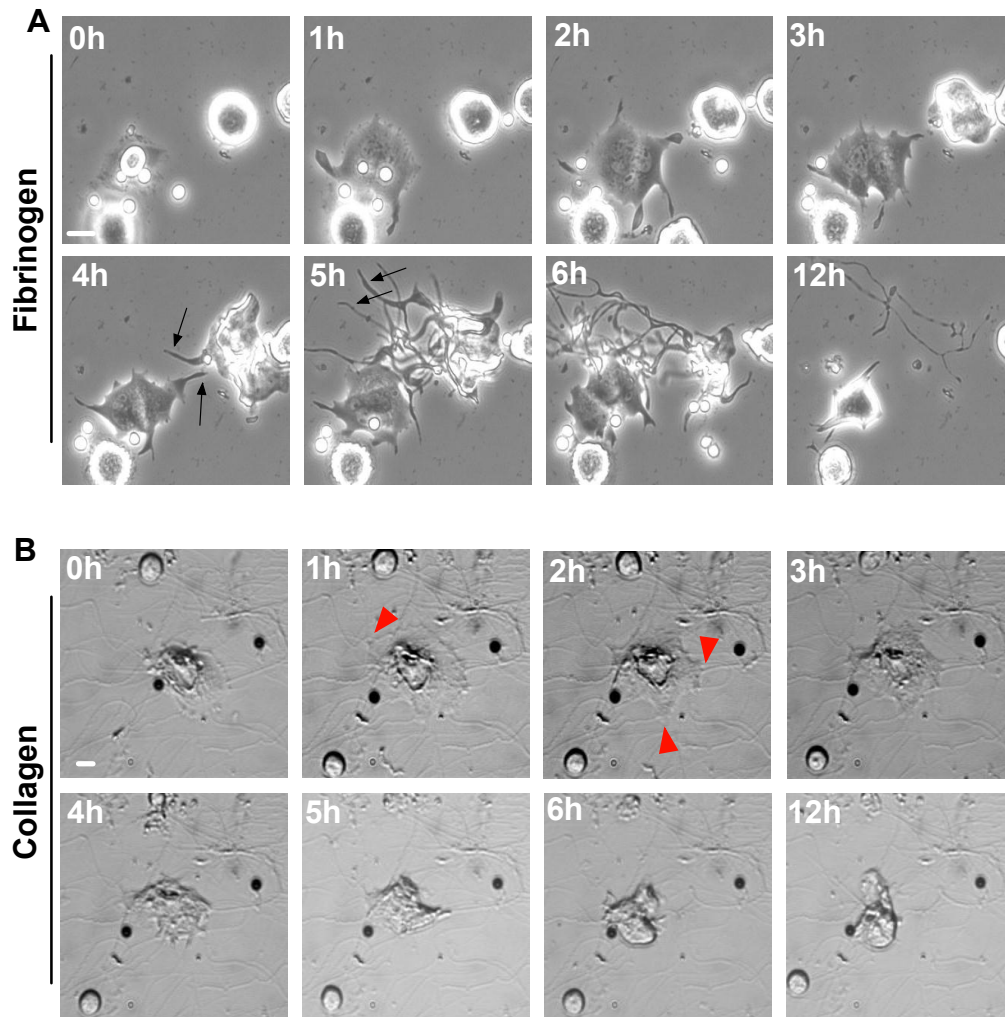


Figure 3.1: Mks fully spread in 3 hours and undergo proplatelet formation on fibrinogen.

Mks were allowed to spread on 100 μ g/ml fibrinogen (A) and 100 μ g/ml horn collagen-coated surfaces (B). Real-time imaging was performed at 37°C in humidified conditions with CO₂ supply. Images were taken every 5min for 12h. Black arrows represent proplatelet structures. Red arrowheads indicate cell spreading along collagen fibres. Scale bar show 10 μ m. Complete movies are included in the supplementary data (movie 1 and 2).

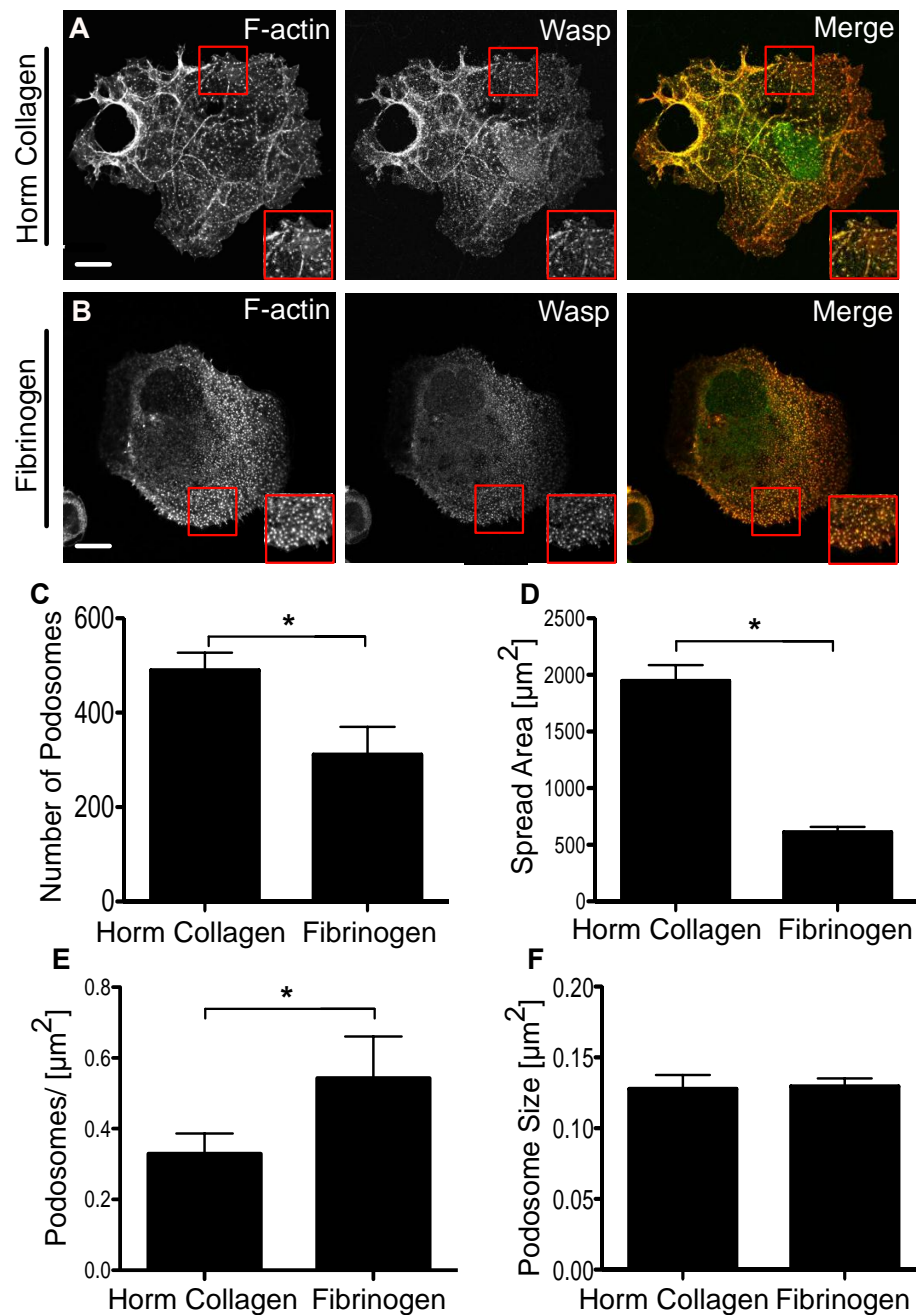


Figure 3.2: The underlying substrate influences the number of podosomes and the spreading behaviour of Mks.

Mks were spread for 3h on 100 $\mu\text{g}/\text{ml}$ horm collagen (A) or fibrinogen (B) coated surface in serum-containing medium at 37 $^{\circ}\text{C}$ in a humidified incubator. Cells were fixed with 4% formaldehyde and stained for F-actin (red) and Wasp (green). Right panel of images show the merge. The number of podosomes (C), the spread area (D) podosomes/ μm^2 (E) and the podosome size (F) was determined. Images were taken at the basolateral surface of the cell. Red square indicates magnified area. A two-tailed students t-test was performed, asterisk indicates a significant difference with a P-value < 0.05. Images are representative of at least three repeats. Scale bar represents 10 μm , error bars show $\pm\text{SEM}$.

However, Mks were able to spread more on collagen than on fibrinogen. Therefore, the podosomes formed per μm^2 was significantly lower on collagen (Figure 3.2C-E). Although there was a difference in the number of podosomes per area, the size of podosomes was unchanged (Figure 3.2F). To further investigate if the protein composition of podosomes depends on the matrix, the localization of the podosome-associated proteins, Cortactin, the Arp2/3 complex, Wasp, Talin, Vinculin and the presence of Phosphotyrosine was identified in Mks spread on both collagen and fibrinogen (Figure 3.3 - Figure 3.6). All proteins apart from Vinculin colocalized with most of the F-actin rich dot-like structures in Mks. Vinculin, however, formed a clear ring structure around the F-actin core, which is characteristic for podosome structures (red square, Figure 3.5; Figure 3.6). This observation was made for Mks spreading on both collagen and fibrinogen. Additionally, real-time spreading of Lifeact-RFP and GFP-Wasp Mks was performed, which were shown to colocalize in dot-like structures and in turn had a lifetime of several minutes confirming that I am looking at podosome formations (Figure 3.4D).

This data indicates that Mks form the traditional F-actin rich core surrounded by a Vinculin ring structure. This protein arrangement is unaffected by the underlying substrate. However, compared to fibrinogen, Horm collagen induces a change in the localisation of podosomes in a spread Mk, with some podosomes localised to collagen fibres.

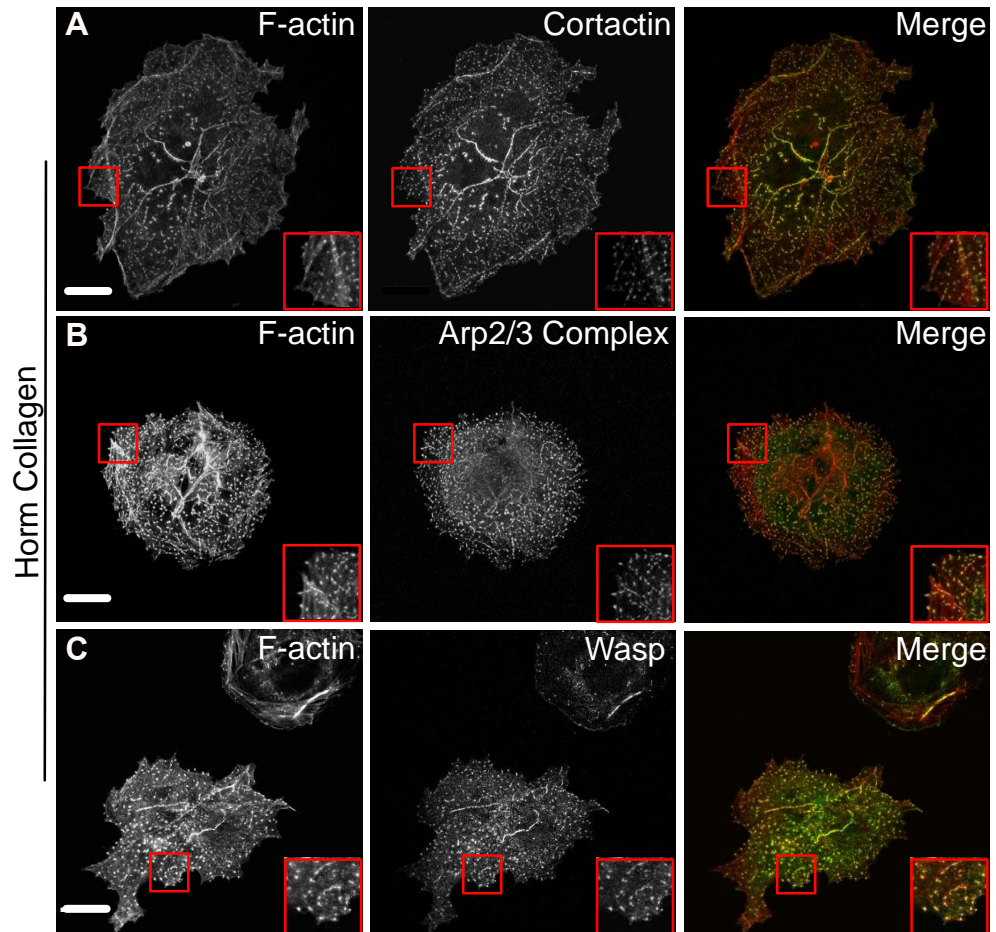


Figure 3.3: Identification of podosome-core-associated proteins on horm collagen.

Mks were spread for 3h on 100 μ g/ml horm collagen-coated surface in SFM, fixed and stained for F-actin (red) and Cortactin (A), Arp2/3 complex (B) or Wasp (C) (green). Right panel of images show the merge of both channels. Images were taken at the basolateral surface of the cell and are representative of three repeats. Red squares indicate the magnified area. Scale bar represents 10 μ m.

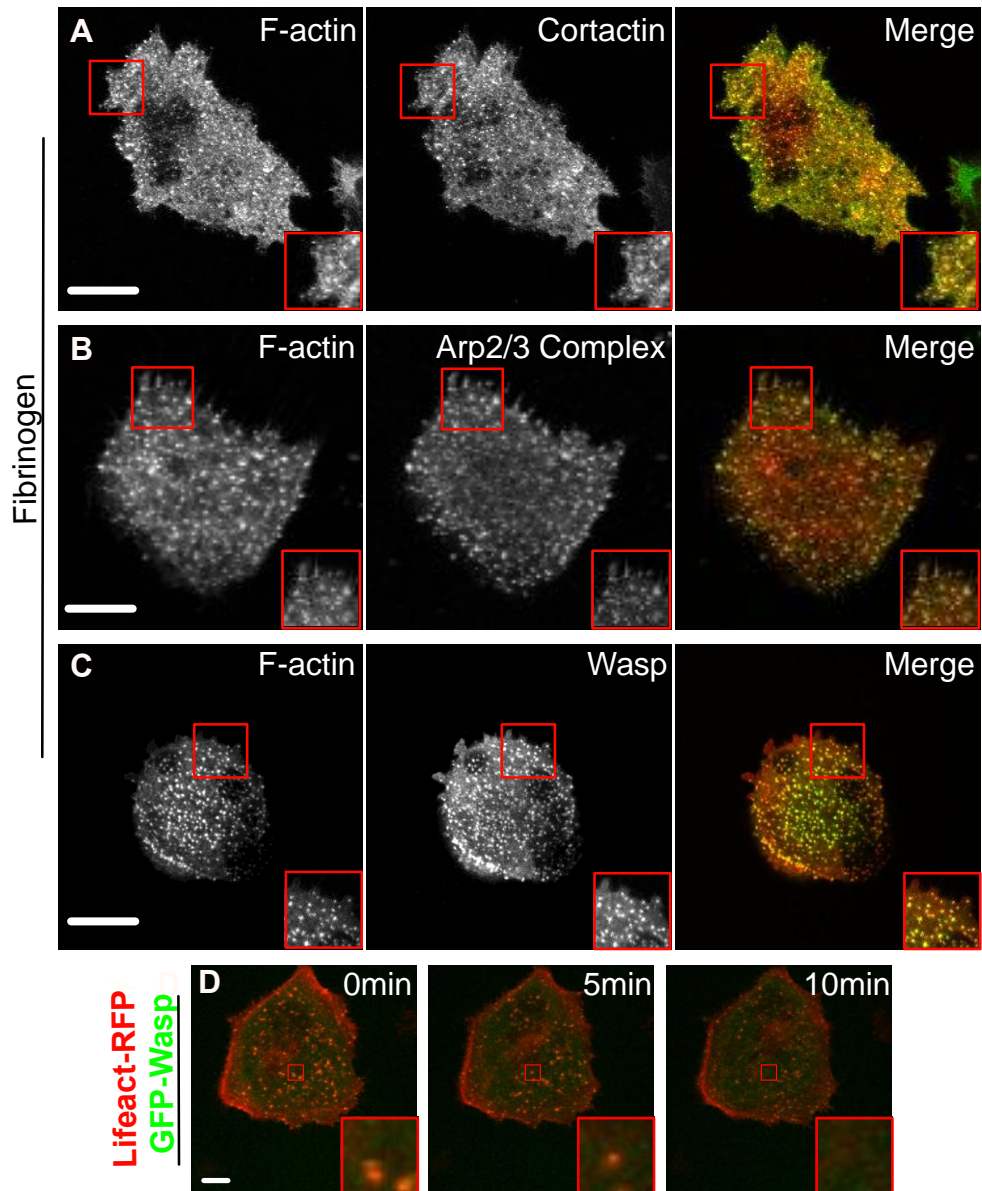


Figure 3.4: Identification of podosome-core-associated proteins on fibrinogen.

Mks were spread for 3h on 100 μ g/ml fibrinogen-coated surface in SFM, fixed and stained for F-actin (red) and Cortactin (A), Arp2/3 complex (B) or Wasp (C) (green). Right panel of images show the merge of both channels. Images were taken at the basolateral surface of the cell and are representative of three repeats. (D) Stills of Lifeact-RFP (red) and GFP-Wasp (green) positive Mks spreading on fibrinogen for 30min (D). Red squares indicate the magnified area. Scale bar represents 10 μ m. Complete movie is included in the supplementary data (movie 3).

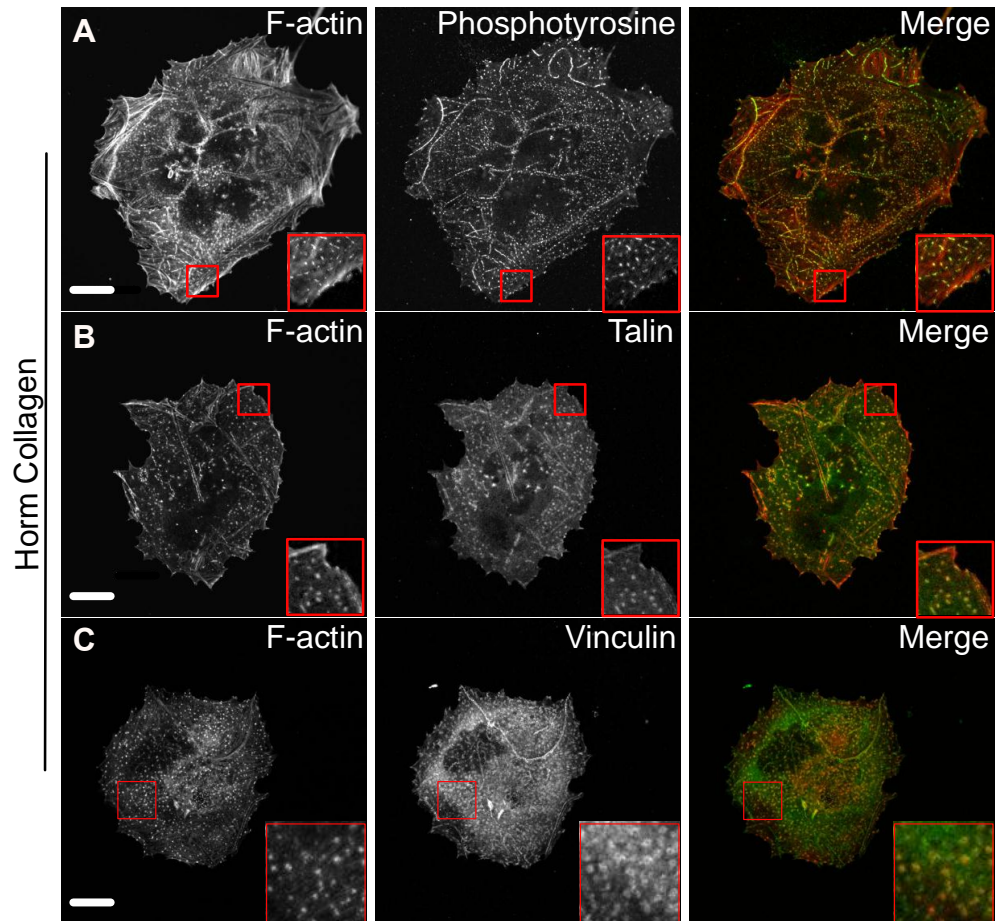


Figure 3.5: Visualization of adhesion-associated proteins on horm collagen.

Mks were spread for 3h on 100 μ g/ml horm collagen-coated surface in SFM, fixed and stained for F-actin (red) and Phosphotyrosine (A), Talin (B) or Vinculin (C) (green). Right panel of images show the merge of both channels. Red squares indicate the magnified area. Images were taken at the basolateral surface of the cell and are representative of three repeats. Red square indicates magnified area. Scale bar represents 10 μ m.

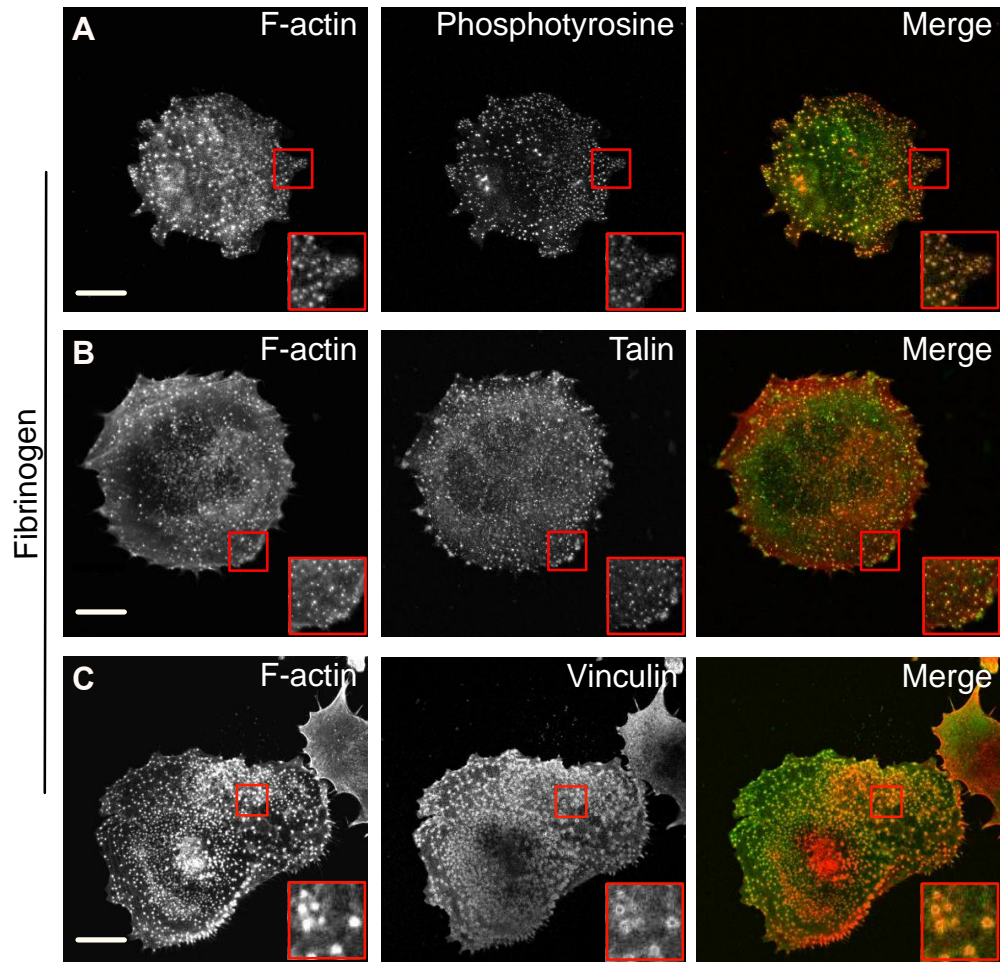


Figure 3.6: Visualization of adhesion-associated proteins on fibrinogen.

Mks were spread for 3h on 100 μ g/ml fibrinogen-coated surface in SFM, fixed and stained for F-actin (red) and Phosphotyrosine (A), Talin (B) or Vinculin (C) (green). Right panel of images show the merge of both channels. Red squares indicate the magnified area. Images were taken at the basolateral surface of the cell and are representative of three repeats. Scale bar represents 10 μ m.

3.3.2 Wasp is essential for podosome formation in Mks

To confirm that the punctate structures observed in Mks were real podosomes, I examined the dependence on Wasp (Olivier *et al.*, 2005; Dovas *et al.*, 2009). Mks were isolated from Wasp^{-/-} mice and litter-matched controls and were allowed to spread on collagen (Figure 3.7) and fibrinogen (Figure 3.8). Mks from control mice formed F-actin-rich structures identified as podosomes by the positive staining for Wasp. In contrast, Wasp^{-/-} Mks showed little formation of F-actin dot-like structures, and no staining for Wasp on either collagen or fibrinogen (Figure 3.7B; Figure 3.8B). Further confirmation of the lack of podosomes was identified by the lack of Vinculin ring structures around any actin puncta observed on both matrices (Figure 3.7C, Figure 3.8C). Interestingly, the loss of Wasp and therefore of podosomes did not influence the spreading area of Mks on fibrinogen or collagen (Figure 3.7D; Figure 3.8D).

These results confirm the identification of podosomes in Mks and underline the essential role of Wasp in podosome formation in Mks spread on collagen and fibrinogen.

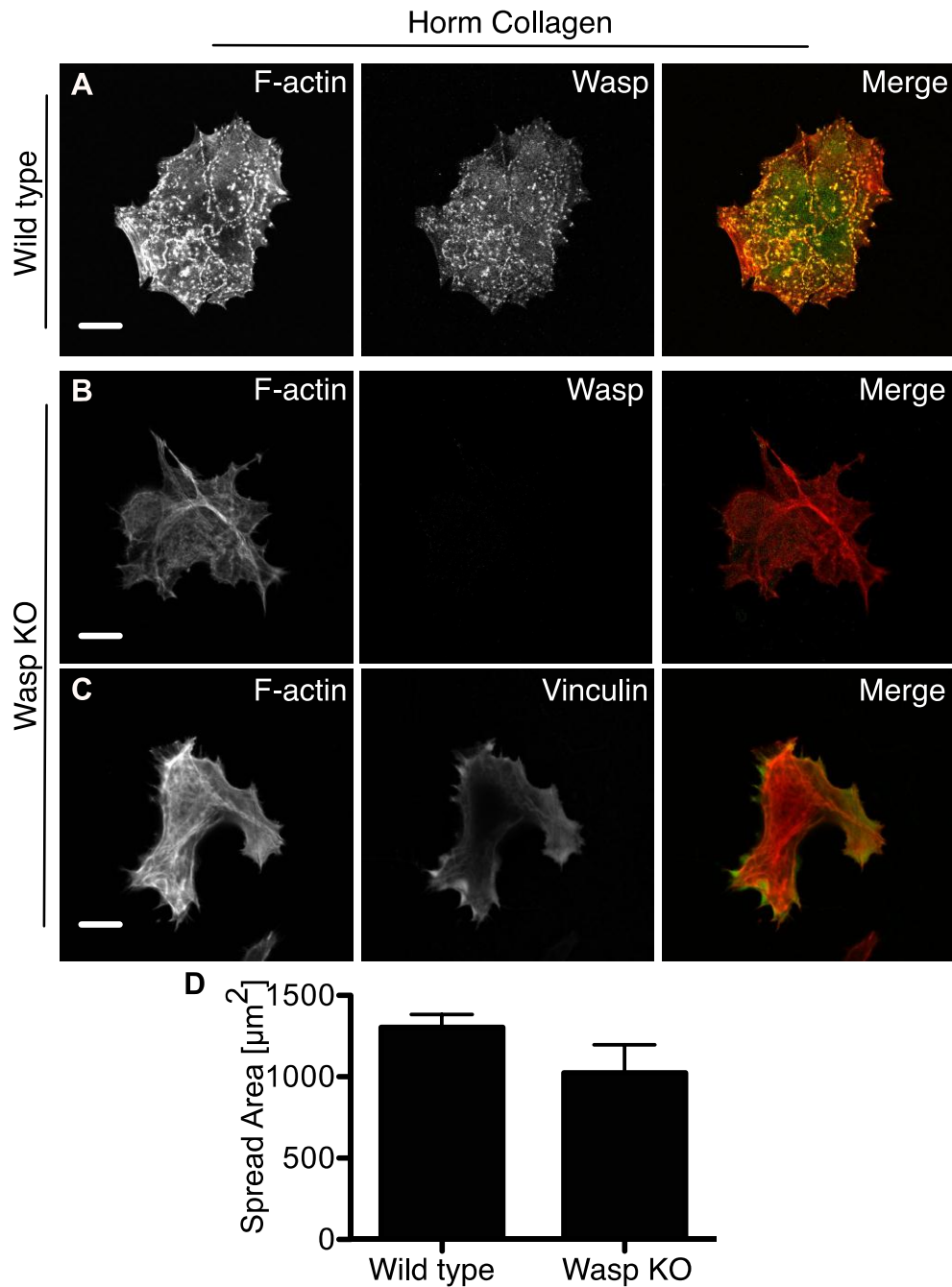


Figure 3.7: Wasp is necessary for podosome formation in Mks spreading on horm collagen.

Mks were allowed to spread for 3h on 100 $\mu\text{g}/\text{ml}$ horm collagen-coated surface in SFM. Litter-matched control cells (A) were stained for F-actin (red) and Wasp (green). Wasp KO Mks were stained for F-actin (red) and Wasp (B) or Vinculin (C) (green). The cell area of wild type and Wasp^{-/-} Mks was determined (D). Images were taken at the basolateral surface of the cell and are representative of at least three repeats. Scale bar represents 10 μm .

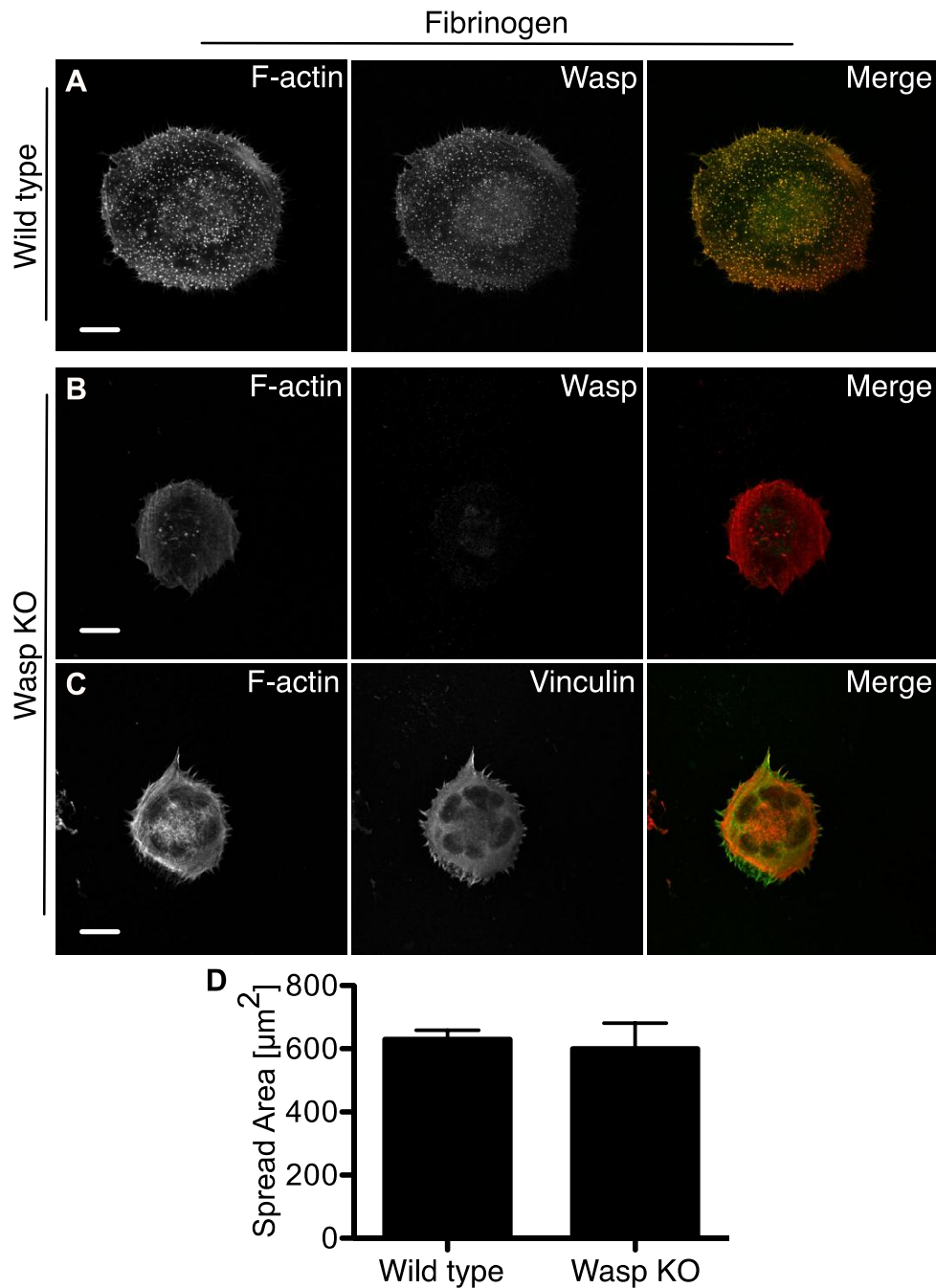


Figure 3.8: Wasp is necessary for podosome formation in Mks spreading on fibrinogen.

Mks were allowed to spread for 3h on 100 $\mu\text{g}/\text{ml}$ fibrinogen-coated surface in SFM. Litter-matched control cells (A) were stained for F-actin (red) and Wasp (green). Wasp KO Mks were stained for F-actin (red) and Wasp (B) or Vinculin (C) (green). The cell area of wild type and Wasp^{-/-} Mks was determined (D). Images were taken at the basolateral surface of the cell and are representative of at least three repeats. Scale bar represents 10 μm .

3.3.3 The presence of serum influences podosome assembly and the spreading behaviour of Mks seeded on collagen

Serum present in the culture medium contains a variety of growth factors, hormones and lipids, which could influence the spreading behaviour of Mks as well as the process of podosome assembly. To evaluate the influence of serum on Mk spreading and podosome assembly, I compared cells spread in complete medium with cells spread in serum-free medium (SFM) and determined the number of podosomes, the spread area, podosomes/ μm^2 and the podosome size based on a costaining for F-actin and Wasp. The morphology of the cells and single podosomes was unchanged and independent of the presence of serum (Figure 3.9A,B; Figure 3.10). Mks spread on collagen showed a reduction in podosome formation as well as a smaller spread area, which resulted in a reduced number of podosomes/ μm^2 but not in a difference in the actual size of single podosomes (Figure 3.9C-F). When Mks were plated on fibrinogen in the presence of complete medium or SFM, there was no difference in the number of podosomes. However, I observed that Mks spreading on fibrinogen in serum-free conditions did not attach as strongly to the matrix and were much more sensitive to sheer forces, which occurred due to processing for immunofluorescence staining.

The above data highlight the influence of serum on Mk spreading on collagen but not on fibrinogen. Serum contains fibrinogen (Wang *et al.*, 2011) so that the cell spreading in complete medium on collagen may also be activated by binding to fibrinogen. Furthermore, high variation in serum composition and content is very common (Bryan *et al.*, 2011). In order to get consistent results and to minimize the risk that factors in the serum influence cell adhesion, all the following experiments were performed in serum-free conditions.

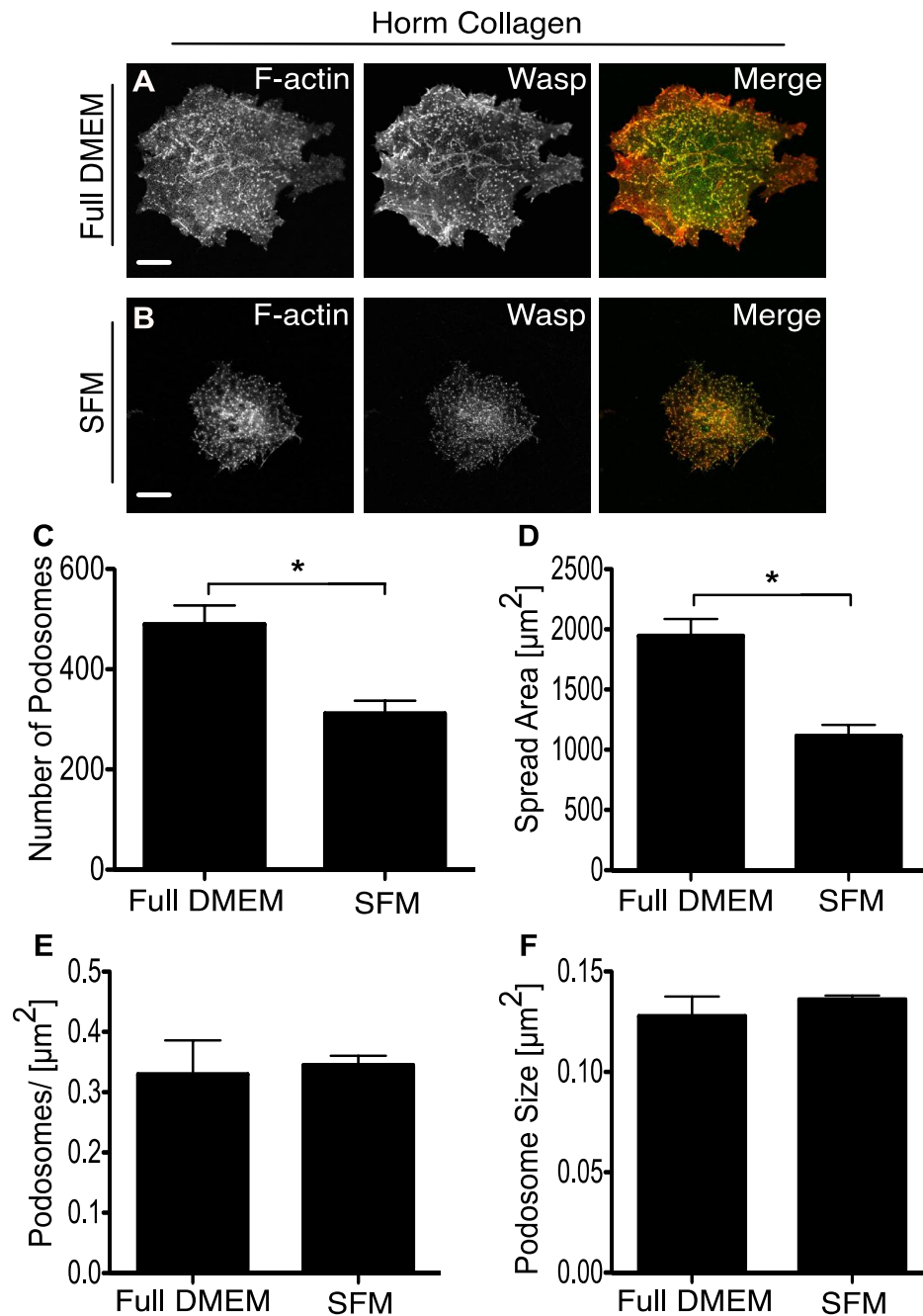


Figure 3.9: Serum influences podosome assembly and spreading behaviour of Mks plated on horm collagen.

Cells were spread for 3h on 100 $\mu\text{g}/\text{ml}$ horm collagen-coated surface in full DMEM containing serum (A) and in SFM (B). Mks were fixed and stained for F-actin (red) and Wasp (green), the right panel of images show the merge of both channels. The number of podosomes (C), the spread area (D), podosomes per μm^2 (E) and the size of podosomes (F) were determined. Images were taken at the basolateral surface of the cell and are representative of three repeats. Scale bar represents 10 μm . A two-tailed students t-test was performed, asterisk indicates a significant difference with a P-value<0.05. Error bars represent $\pm\text{SEM}$

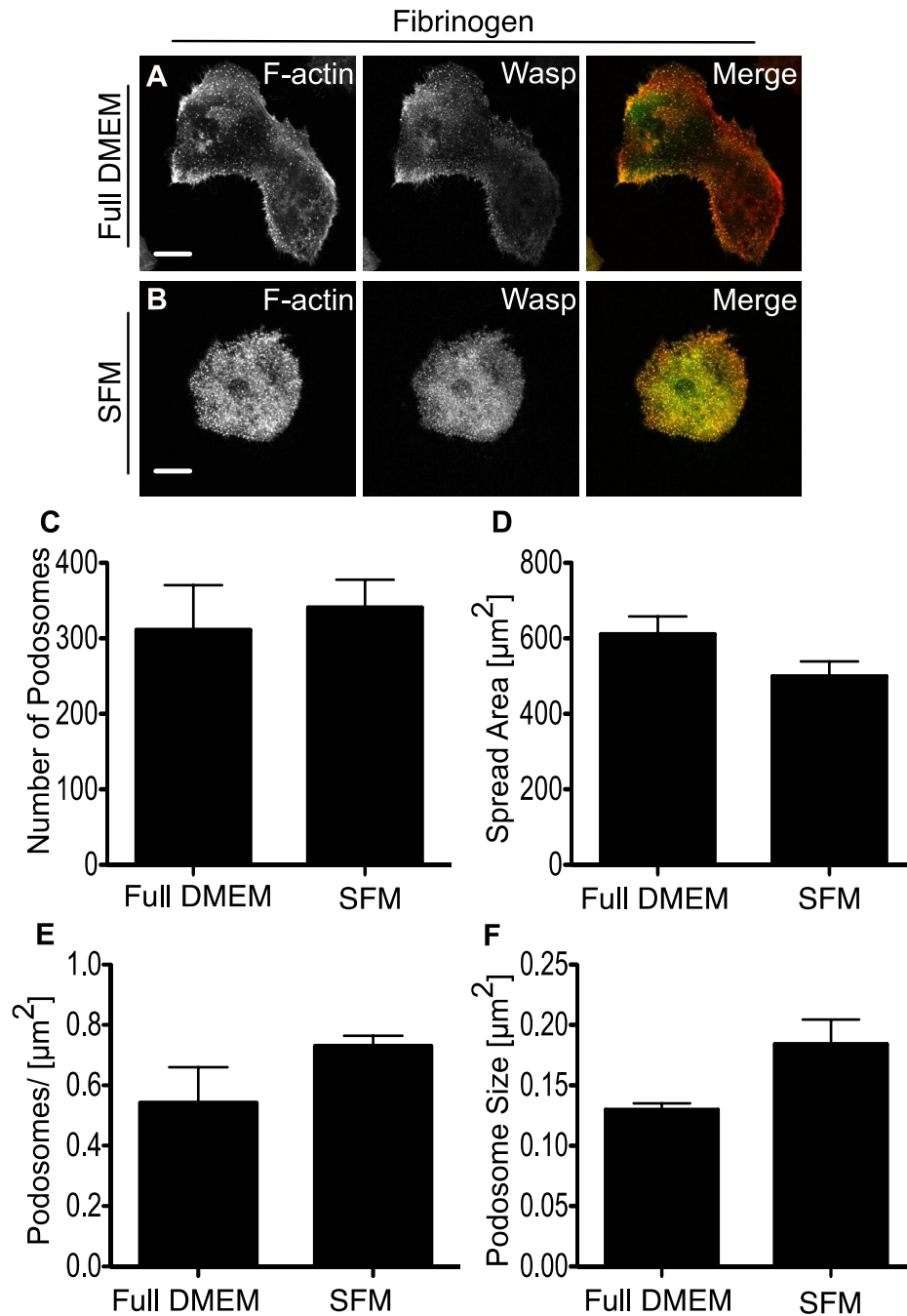


Figure 3.10: Serum does not influence podosome assembly in Mks spreading on fibrinogen.

Cells were spread for 3h on 100 $\mu\text{g}/\text{ml}$ fibrinogen-coated surface in full DMEM containing serum (A) and in SFM medium (B). Mks were fixed and stained for F-actin (red) and Wasp (green), the right panel of images show the merge of both channels. Images were taken at the basolateral surface of the cell and are representative of three repeats. The number of podosomes (C), the spread area (D), podosomes per μm^2 (E) and the size of podosomes (F) were determined. A two-tailed students t-test was performed, asterisk indicates a significant difference with a P-value <0.05 , no asterisk means no significant difference between the groups. Scale bar represents 10 μm , error bars show $\pm\text{SEM}$.

3.3.4 DMSO does not influence Mk podosome assembly

Not only can the factors in the serum influence the cell spreading behaviour, but also the chemical solution in which inhibitors were dissolved can have effects on cells. For the following experiments, a range of different inhibitors were used, which were predominantly dissolved in DMSO. As I had to use different concentrations of DMSO, it was important to evaluate the impact of this chemical on Mk spreading and podosome formation. Cells were spread on collagen in SFM in the presence of 0%, 0.1% and 1% DMSO (Figure 3.11). The different samples were costained for F-actin and Wasp. Overall, the cell morphology looked normal and podosome structures showed no difference in appearance (Figure 3.11A-C). No significant difference was detectable in the total number of podosomes, the spread area, podosomes/ μm^2 or the podosome size between the different concentrations of DMSO (Figure 3.11D-F).

These data verify that a DMSO concentration up to 1% does not detectably change the spreading behaviour or the number of podosomes in Mks.

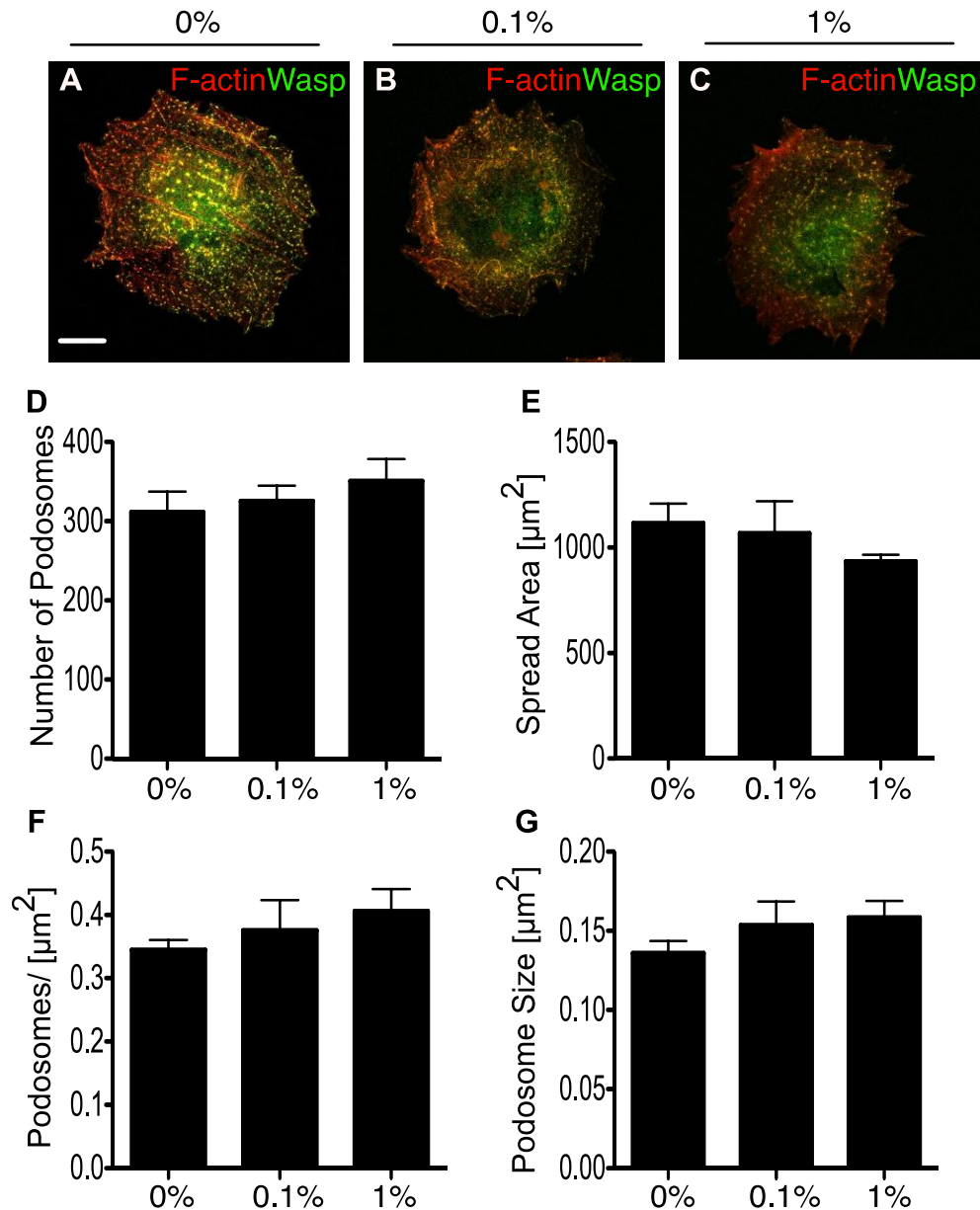


Figure 3.11: DMSO does not influence podosome formation or spreading behaviour of Mks.

Mks were allowed to spread for 3h on 100 $\mu\text{g}/\text{ml}$ horn collagen-coated surface in SFM in the presence of 0% (A), 0.1% (B) or 1% (C) DMSO. Cells were fixed and stained for F-actin (red) and Wasp (green), images show the merge of both channels. Pictures were taken at the basolateral surface of the cell and are representative of three repeats. The number of podosomes (C), the spread area (D), podosomes per μm^2 (E) and the size of podosomes (F) were determined. Scale bar represents 10 μm , error bars show $\pm\text{SEM}$.

3.3.5 Dose response curve for CK666 and Blebbistatin

The Arp2/3 complex is known to be involved in podosome assembly in different cell types like macrophages, dendritic cells and osteoclasts (Linder *et al.*, 2000a; Burns *et al.*, 2001; Hurst *et al.*, 2004). To validate the role of the Arp2/3 complex in Mk podosome formation, a specific inhibitor CK666 was applied to the cells during spreading. CK666 binds between Arp 2 and Arp3 and blocks the conformational change of the complex, which is necessary for its active state. In order to reach the maximum inhibitory effect, a dose response curve was performed with a range of concentrations as reported before (Nolen *et al.*, 2009). Cells treated with CK689, an inactive form of CK666 (methyl group and parts of a thiophene ring is missing), formed clear podosome structures positive for F-actin and Wasp with a normal cell morphology (Figure 3.12A). Furthermore, there was no significant difference between control cells and those treated with 40 μ M of CK689 in the number of podosomes or the cell surface detectable (Figure 3.13A,B, blue line). However, 10 μ M of Ck666 induced a significant reduction in the number of podosomes and the cell area (Figure 3.13A,B; red line). A further reduction in podosome numbers was reached with 20 μ M but no further decrease in the cell surface. The maximum inhibition of podosome formation was reached with 40 μ M of CK666 with a decrease in the cell surface of around 80%. In order to exclude a side effect, cells were spread for 2.5h and only treated for 30min with 20 μ M CK666. The number of podosomes was reduced in the same range as above but with no difference in the cell surface compared to control cells (Figure 3.13C,D).

Another protein of interest was Myosin II, which is known to be involved in podosome maintenance in macrophages (Bhuwania *et al.*, 2012). To evaluate the importance of Myosin II in Mk podosome assembly I used Blebbistatin, a chemical

compound that binds to the ATPase binding site of Myosin II and blocks the conformational change to its active state (Allingham *et al.*, 2005). A range of different concentrations was applied to determine an adequate dose of the inhibitor. The number of formed podosomes was not significantly affected but the area of the cell decreased with an increasing concentration of Blebbistatin (Figure 3.13A,B, green line). To exclude that Blebbistatin was acting via an effect only on Mks spreading, cells were treated with 10 μ M Blebbistatin after 2.5h spreading for 30min (Figure 3.13C,D). The analysis showed that the number of podosomes and also the area of the cell was unchanged compared to the control cells. This data verifies that Blebbistatin affects spreading but not podosome assembly. To demonstrate that Blebbistatin treatment blocks Myosin II activity, which is essential for stress fibre formation (Even-Ram *et al.*, 2007), the percentage of cells forming stress fibres was determined (Figure 3.13E, green line). Around 70% of control Mks spreading on collagen display stress fibres. In the presence of 10 μ M Blebbistatin, only 5% of the cells display stress fibre formation, confirming the inhibition of Myosin II activity. Mks treated with 20 μ M or 50 μ M Blebbistatin did not show a significant difference in stress fibre formation compared to cells treated with 10 μ M.

These data demonstrate that 20 μ M CK666 and 10 μ M Blebbistatin are appropriate concentrations to maximize the inhibitory effect of the target protein and to minimize other effects, such as a reduced spread area. Based on these results, I decided to use a concentration of 20 μ M CK666 and 10 μ M Blebbistatin for the following experiments.

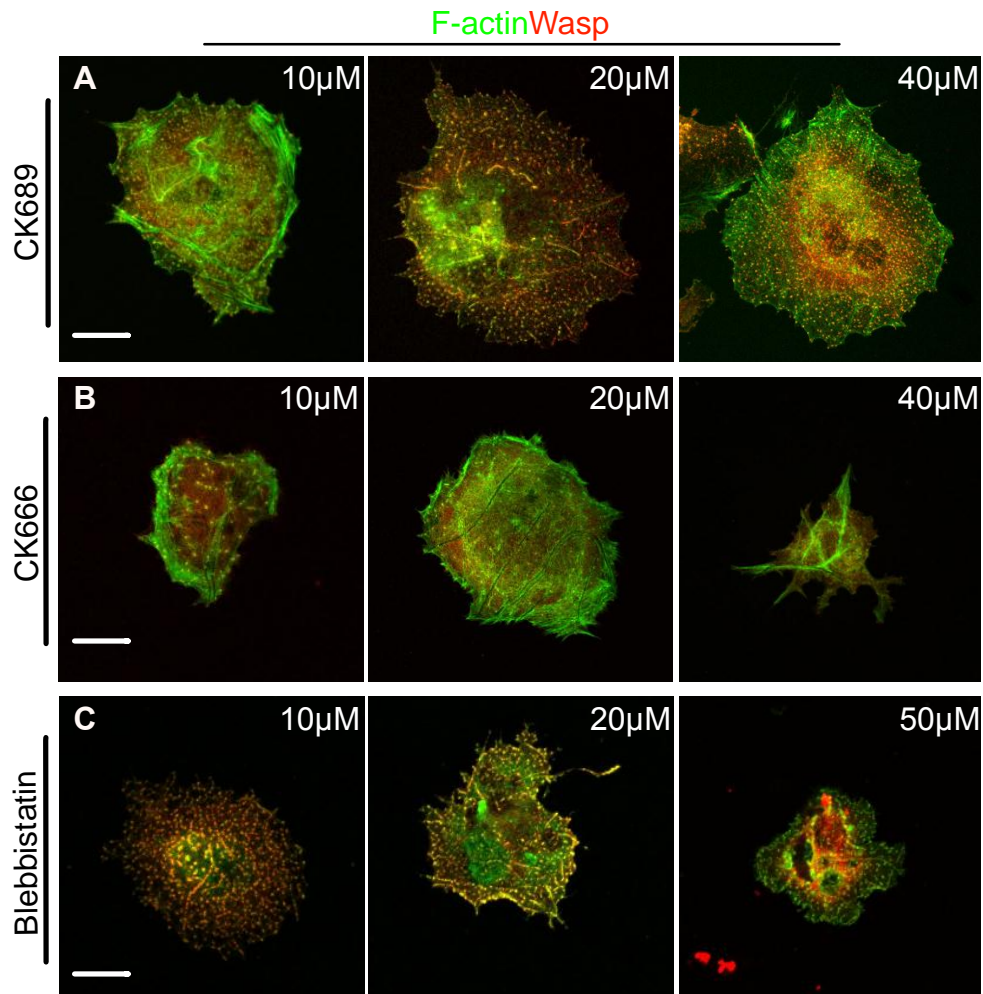


Figure 3.12: Dose response of actin related inhibitors on Mk podosome formation and cell spreading.

Mks were allowed to spread for 3h on 100μg/ml horn collagen-coated surface in SFM in the presence of CK689 (A), CK666 (B) or Blebbistatin in denoted concentrations. Cells were fixed and stained for F-actin (green) and Wasp (red), images show the merge of both channels. Pictures were taken at the basolateral surface of the cell and are representative of at least three repeats. Scale bar represents 10μm.

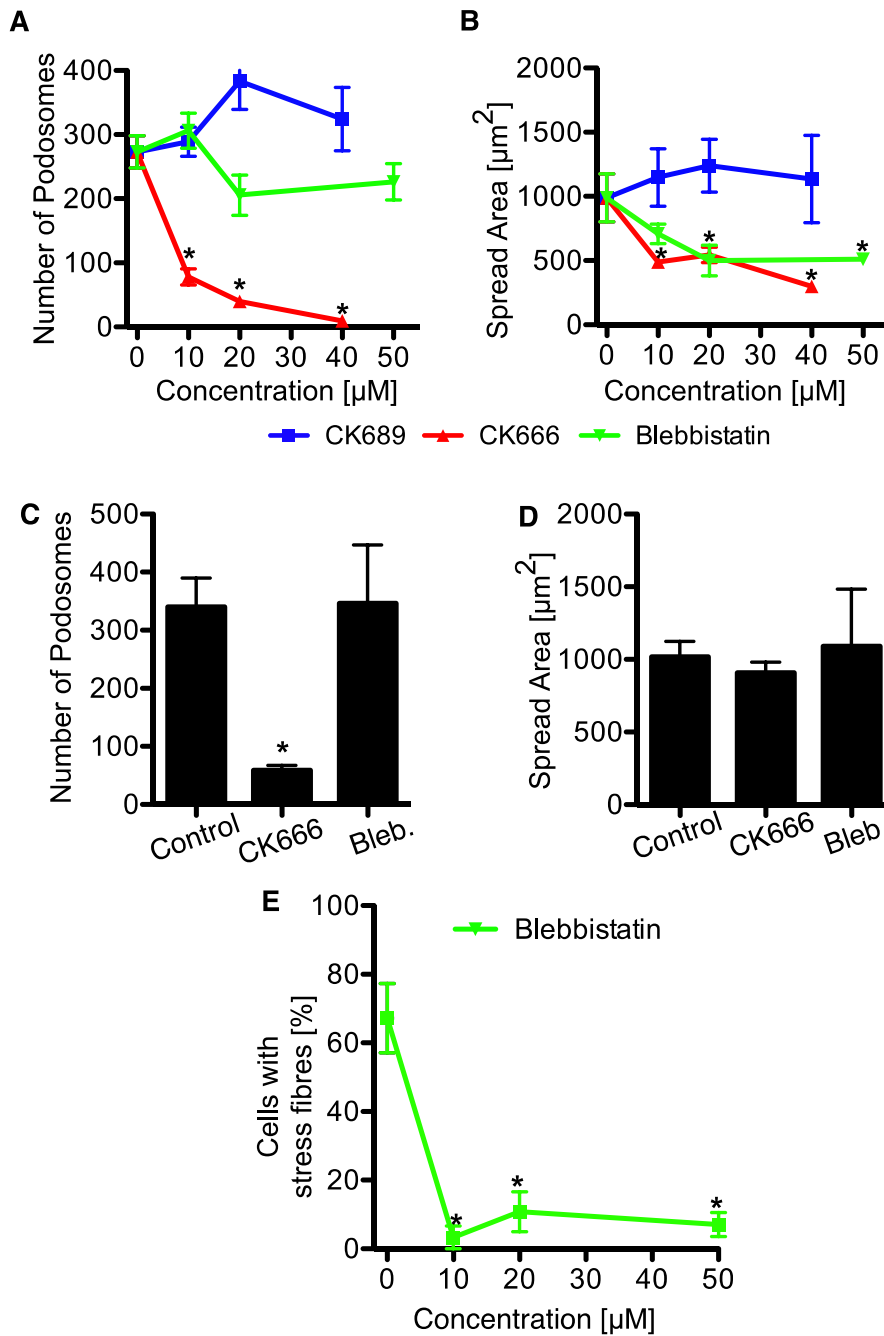


Figure 3.13: Dose response of actin related inhibitors on Mk podosome formation and cell spreading.

Mks were allowed to spread for 3h on 100 $\mu\text{g}/\text{ml}$ horn collagen-coated surface in SFM in the presence of different concentrations of CK689 (black line), CK666 (red line) or Blebbistatin (-) (green line). The number of podosomes (A) and the spread area (B) were determined. Cells were spread for 2.5h and were treated for 30min with 20 μM CK666 and 10 μM Blebbistatin, the number of podosomes (C) and the spread area (D) was determined. The percentage of cells forming stress fibres (E) in the presence of 10 μM Blebbistatin was analysed. A one-way ANOVA with a Dunnett test was performed, asterisk indicates a significant difference with a P -value <0.05 , no asterisk means no significant difference between the groups. Error bars indicate $\pm\text{SEM}$. Data represent at least three repeats.

3.3.6 F-actin nucleation and the Arp2/3 complex is essential for podosome assembly and spreading on collagen and fibrinogen

Podosome formation and dynamics are well described in different cell types, in order to compare the properties and the regulation of Mk podosomes I performed spreading analysis with inhibitors targeting with F-actin or F-actin interacting proteins such as the Arp2/3 complex and Myosin II. During inhibitor treatment, Mks were spread on horn collagen (Figure 3.14; Figure 3.15) or fibrinogen (Figure 3.16; Figure 3.17). Control samples contained DMSO and the specific control for CK666 was CK689, which showed no difference to the regular control sample. Control Mks formed clear dot-like structures positive for both F-actin and Wasp (Figure 3.14A, Figure 3.16A). Treatment with 3 μ M Latrunculin A (Latr. A), which blocks F-actin nucleation, showed the most dramatic effect with almost no podosome formation on both collagen and fibrinogen (Figure 3.14B; Figure 3.16B) and a clear reduction in the spreading area by more than 50% on collagen. The podosome size was not determined as the number was too low to perform an adequate analysis. A similar strong effect on podosome assembly was caused by the inhibition of the Arp2/3 complex activity with a decrease of podosomes per area by more than 75% (Figure 3.14D; Figure 3.16D and Figure 3.15A; Figure 3.17A) and a significant reduction in the spread area on collagen compared to the specific control CK689 (Figure 3.14C; Figure 3.15B). The surface area of Mks spreading on fibrinogen was not reduced (Figure 3.17B). With the inhibition of the Arp2/3 complex the podosome size was slightly smaller on both substrates (Figure 3.15D; Figure 3.17D), implicating that the full activity of the complex is necessary to reach full podosome size and intact functionality as well.

The activity of Myosin II was blocked by 10 μ M Blebbistatin, which did not affect the morphology of the cells or the formed podosomes (Figure 3.14E; Figure 3.16E). There was also no change in the number of podosomes but a slight decrease in the surface area of Mks spread on collagen (Figure 3.15B), which caused a significant difference in the number of podosomes per area (Figure 3.15C; Figure 3.17C). However, cells incubated with Blebbistatin for only 30min had a normal spreading area implicating that Myosin II activity is involved in the spreading behaviour of Mks but not in podosome formation (Figure 3.13C,D). This result underlines the longterm spreading effect of Blebbistatin. Because Myosin II is known to be involved in adhesion, maturation and maintenance it was surprising that there was no significant difference in the podosome size for Blebbistatin treated cells (Vicente-Manzanares *et al.*, 2011).

These data confirm an essential role of F-actin nucleation and underline the relevance of the Arp2/3 complex activity for podosome assembly. Furthermore, I determined a role for Myosin II in Mk spreading but not in podosome formation.

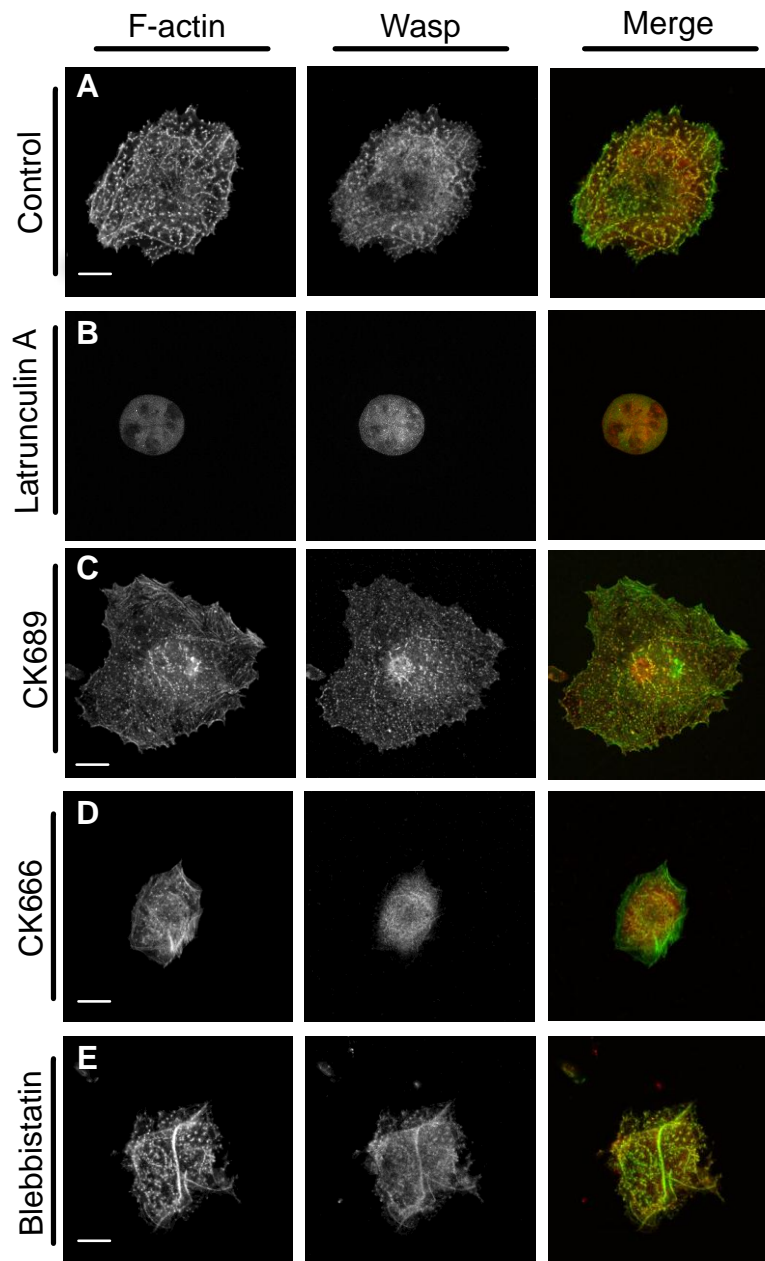


Figure 3.14: Inhibition of actin-associated proteins and the influence on Mks podosome formation and spreading on horm collagen.

Mks were allowed to spread for 3h on 100 μ g/ml horm collagen-coated surface in SFM in the presence of 0.1% DMSO (A), 3 μ M Latrunculin A (B), 20 μ M CK689 (C), 20 μ M CK666 (D) or 10 μ M Blebbistatin (-) (E). Latrunculin A was added after 1h of spreading. Ck689 is the inactive form of CK666 and the specific control. Images were taken at the basolateral surface of the cell and are representative of at least three repeats. Scale bar represents 10 μ m.

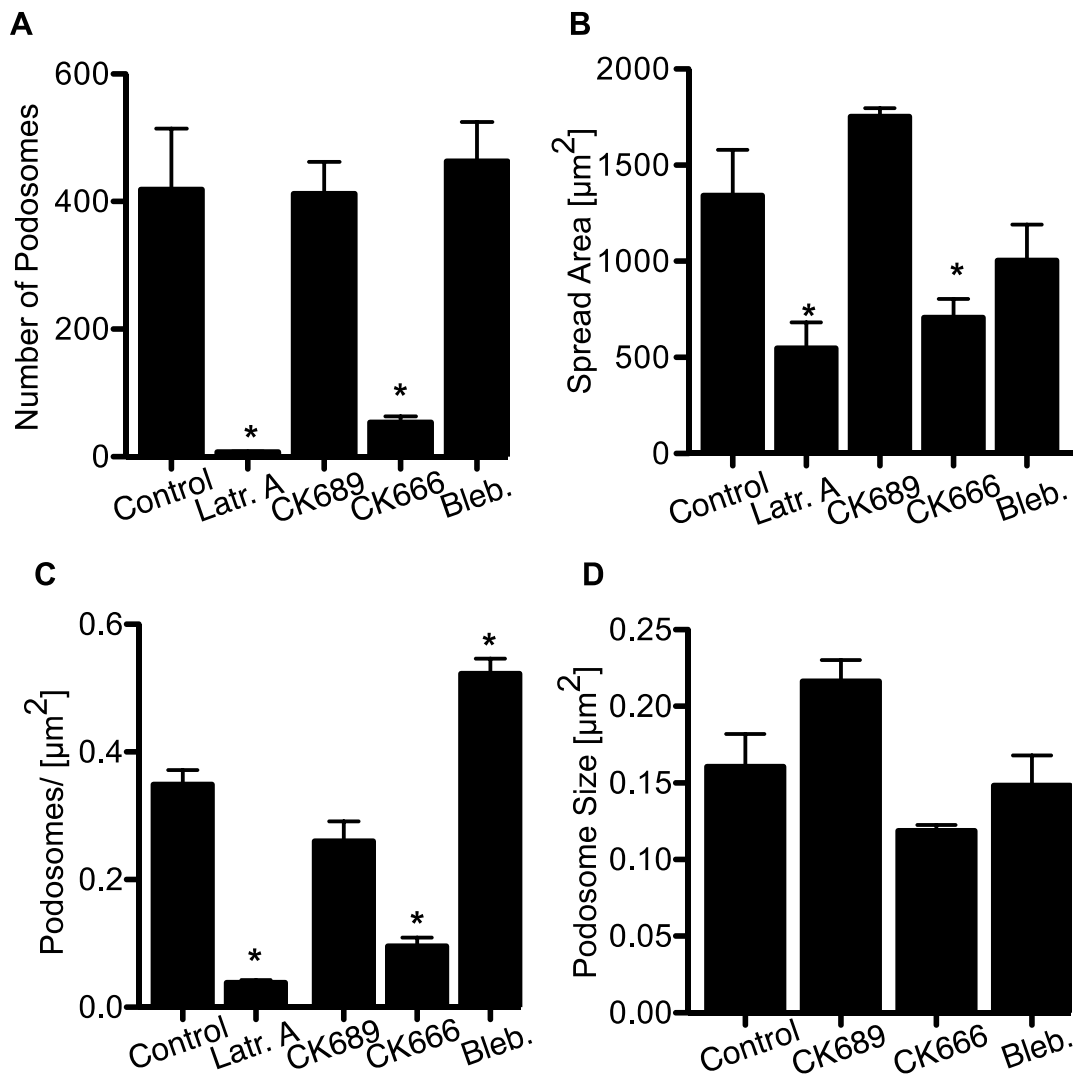


Figure 3.15: F-actin polymerization and Arp2/3 complex activity is essential for podosome formation on horm collagen.

Mks were allowed to spread for 3h on 100 $\mu\text{g}/\text{ml}$ horm collagen-coated surface in SFM in the presence of 3 μM Latrunculin A, 20 μM CK689, 20 μM CK666 or 10 μM Blebbistatin (-). The number of podosomes (A), the spread area (B), podosomes per μm^2 (C) and the size of podosomes (D) were determined. The size of podosomes in Mks treated with Latrunculin A could not be determined as not enough podosomes were formed. A one-way ANOVA with a Dunnett test was performed, asterisk indicates a significant difference with a P-value < 0.05. Error bars indicate $\pm\text{SEM}$. Data represent at least three repeats.

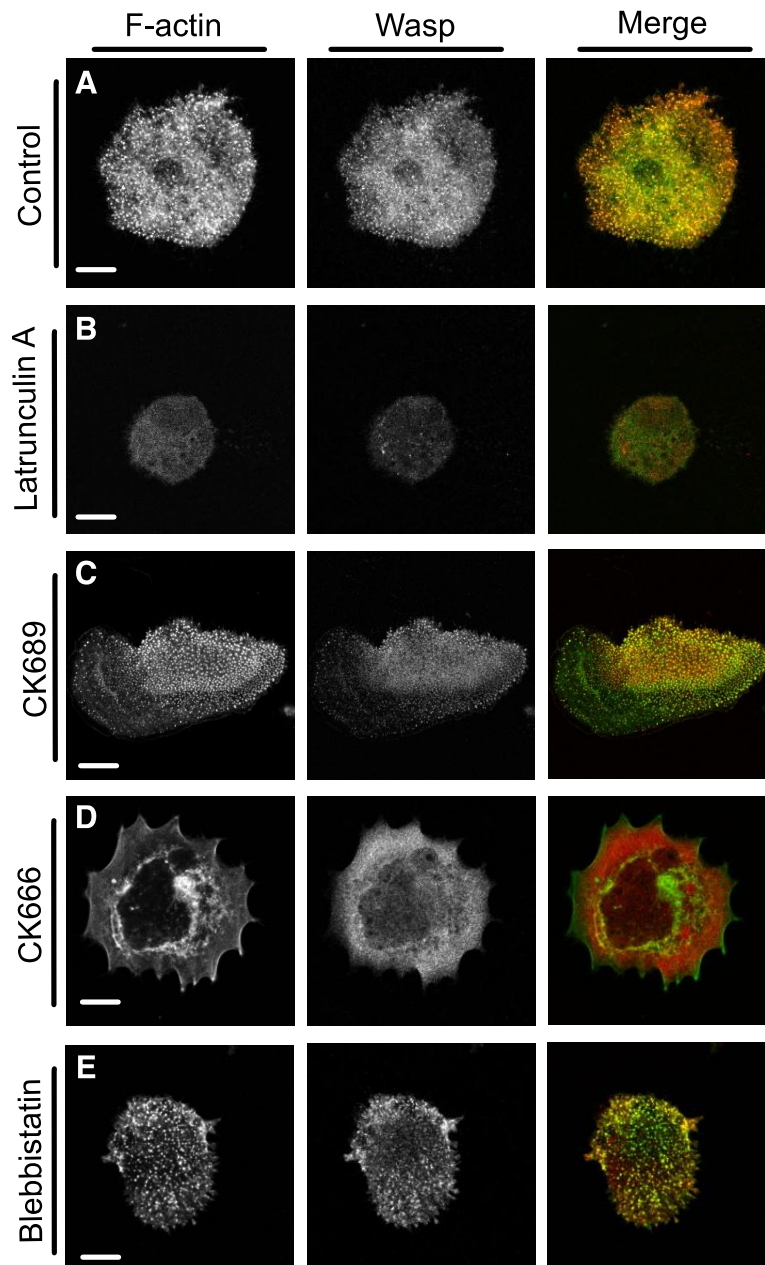


Figure 3.16: Inhibition of actin-associated proteins and the influence on Mk podosome formation and spreading on fibrinogen.

Mks were allowed to spread for 3h on 100 μ g/ml fibrinogen-coated surface in SFM in the presence of 0.1% DMSO (A), 3 μ M Latrunculin A (B), 20 μ M CK689 (C), 20 μ M CK666 (D) or 10 μ M Blebbistatin (-) (E). Latrunculin A was added after 1h of spreading. CK689 is the inactive form of CK666 and the specific control. Images were taken at the basolateral surface of the cell and are representative of at least three repeats. Scale bar represents 10 μ m.

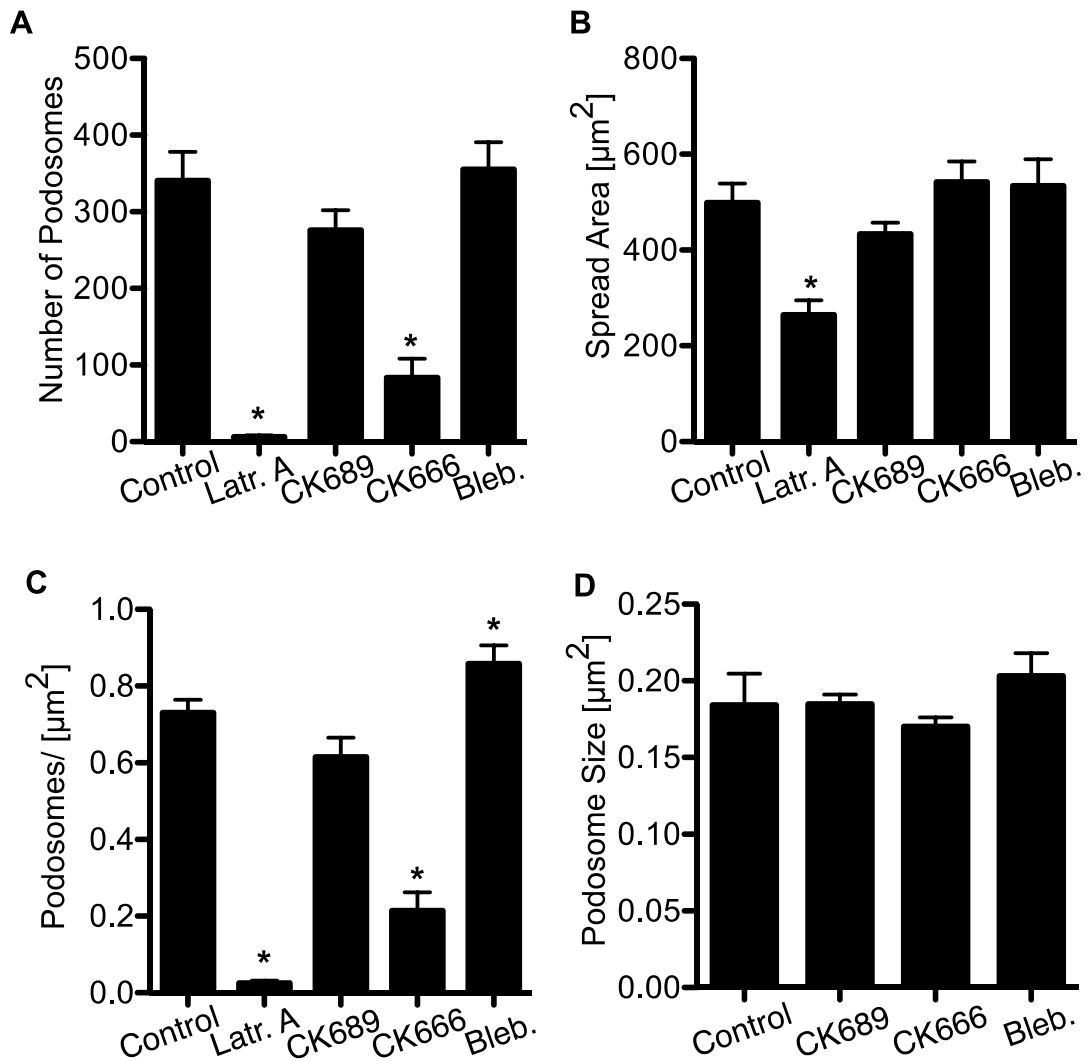


Figure 3.17: F-actin polymerization and Arp2/3 complex activity is essential for podosome formation on fibrinogen.

Mks were allowed to spread for 3h on 100 $\mu\text{g}/\text{ml}$ fibrinogen-coated surface in SFM in the presence of different inhibitors. The number of podosomes (A), the spread area (B), podosomes per μm^2 (C) and the size of podosomes (D) were determined. The size of podosomes in Mks treated with Latrunculin A could not be determined as not enough podosomes were formed. A one-way ANOVA with a Dunnett test was performed, asterisk indicates a significant difference with a P-value <0.05 . Data represent at least three repeats. Error bars represent $\pm\text{SEM}$.

3.3.7 MMP activity and microtubules are not fundamental for podosome formation in Mks spread on collagen or fibrinogen

The above analysis describes the role of F-actin and its interacting proteins in podosome assembly. However, there is another interesting group of potential key regulators for podosome assembly and matrix degradation, the matrix metalloproteases (MMP). MMPs play an essential role in invadopodia formation, but their importance in podosome assembly is not known. The localisation of MMPs at podosome structures was shown in different cell types before, however, their role in podosome organisation is unclear (Linder, 2007). To verify if MMP activity has an influence on podosome numbers in Mks, I used the broad-spectrum MMP inhibitor GM6001. GM6001 binds to the zinc dependent domain of different MMPs and blocks its protease activity. Because the inhibitor was only available in a certain concentration, I had to use a higher volume of the inhibitor and a corresponding volume of DMSO (0.1%, 0.2%, 0.4%) in the different samples. But as shown before (Figure 3.11) an increased volume of DMSO did not influence the spreading behaviour or podosome assembly in Mks. Cells were treated with 5 μ M, 10 μ M and 20 μ M GM6001 and were stained for F-actin and Wasp (Figure 3.18). The number of podosomes, the cell area and the podosome size were determined. Cells treated with different concentrations of GM6001 formed regular formed dot-like puncta, which did not differ from those observed in the control cells (Figure 3.18A,B). Furthermore, there was no difference in the number of podosomes, the spread area or the podosome size (Figure 3.18C-F).

These results confirm that MMP activity is not essential for podosome assembly in Mks. I used for the following experiments a concentration of 5 μ M (Figure 3.19), as this is a well-reported concentration for the inhibition of highly degradative

structures called invadopodia (Li *et al.*, 2010), and therefore an adequate evidence of MMP blockage.

Although podosomes are F-actin based structures there are some reports verifying the involvement of microtubules in podosome regulation (Destaing *et al.*, 2003; Linder *et al.*, 2000b). To test if the microtubule cytoskeleton plays a role in Mk podosome assembly I used Nocodazole, a chemical compound, which depolymerizes microtubule filaments (Wiesner *et al.*, 2010). Nocodazole is widely used in the Mk and platelet field, as it is known to block proplatelet formation with a concentration of 10 μ M; this concentration was used as well for the following experiments (Tablin *et al.*, 1990). However, microtubule depolymerisation did not influence the appearance of podosomes (Figure 3.19C; Figure 3.20C), their number, the spread area or the podosome size on both collagen and fibrinogen (Figure 3.19D-G; Figure 3.20D-G).

These data demonstrate a minor role for MMPs in podosomes, which make these structures fundamentally different from invadopodia formed by cancer cells (Ayala *et al.*, 2009). Furthermore, I showed that the microtubule cytoskeleton is not essential for podosome formation or maintenance in Mks, which highlights the cell-type specific properties of these structures, as in macrophages microtubules play a relevant role in de novo podosome assembly (Linder *et al.*, 2000b) as well as in the process of MMP-vesicle transport and therefore matrix degradation (Wiesner *et al.*, 2010).

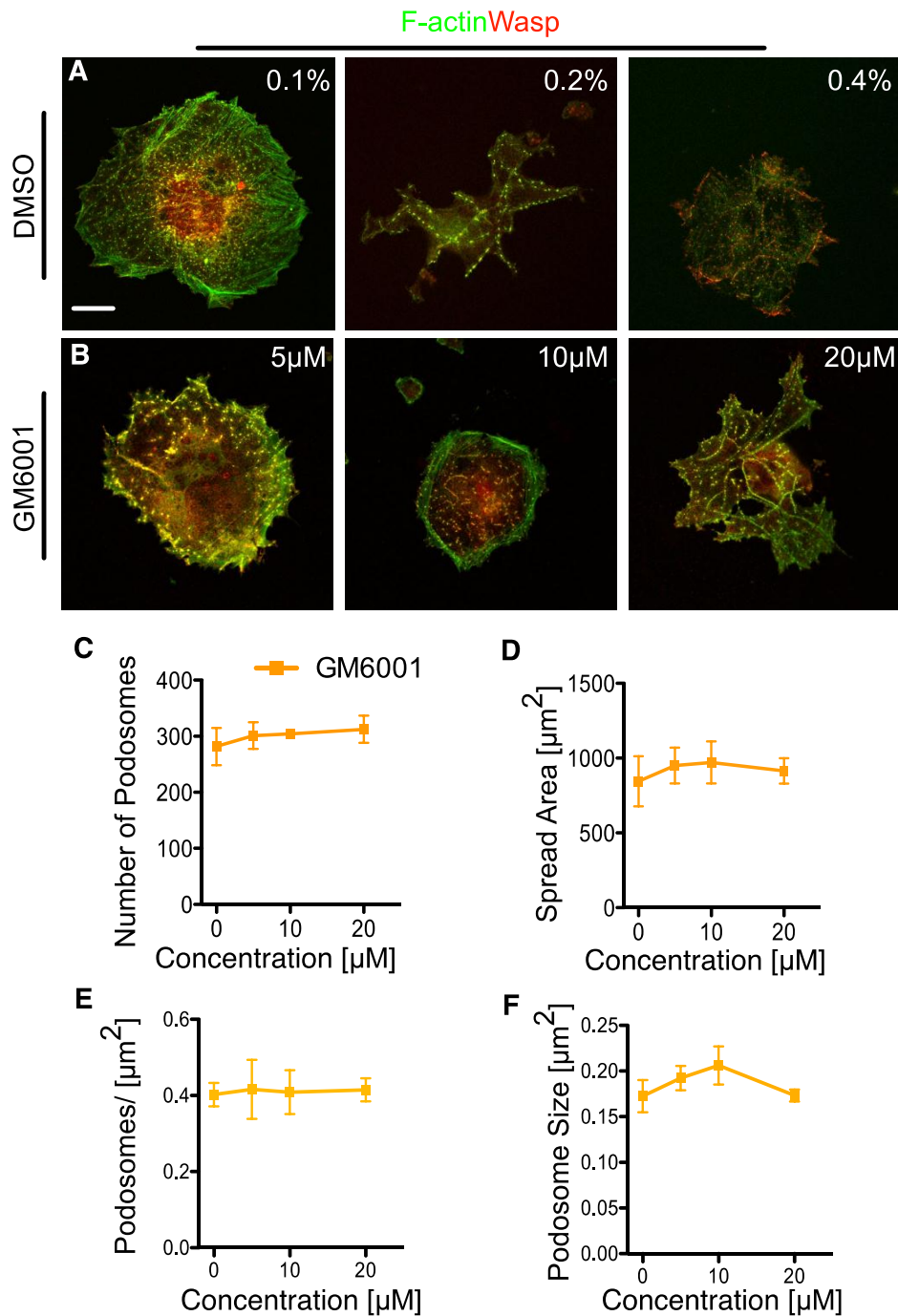


Figure 3.18: Dose response of GM6001 on Mk podosome formation and cell spreading.

Mks were allowed to spread for 3h on 100 μ g/ml horm collagen-coated surface in SFM in the presence of different concentrations of DMSO (A,C-F,black line) and GM6001 (B,C-F,blue line). Mks were fixed and stained for F-actin (green) and Wasp (red). Images were taken at the basolateral surface of the cell. The number of podosomes (C), the spread area (D), podosomes per μ m² (E) and the size of podosomes (F) were determined. A one-way ANOVA with a Dunnett test was performed, asterisk indicates a significant difference with a P-value<0.05. Data represent at least three repeats.

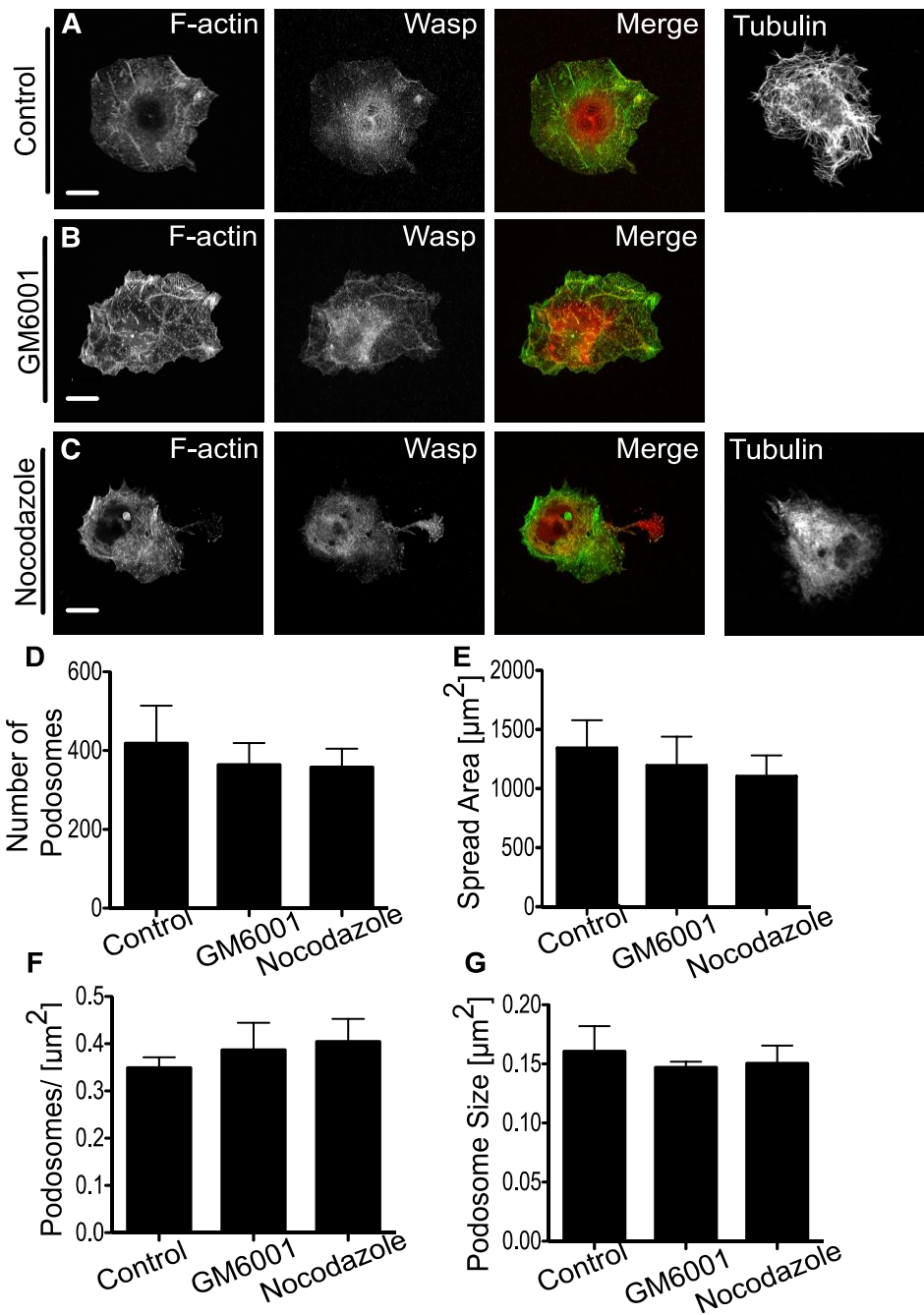


Figure 3.19: MMP activity and microtubule assembly is not involved in podosome formation in Mks spreading on horm collagen.

Mks were allowed to spread for 3h on 100 $\mu\text{g}/\text{ml}$ horm collagen-coated surface in SFM in the presence of 0.1% DMSO (A), 5 μM GM6001 (B) and 10 μM Nocodazole (C). Mks were fixed and stained for F-actin (green) and Wasp (red), the third panel of images shows the merge of both channels. The fourth image for the control and Nocodazole sample represents a cell stained for tubulin. The number of podosomes (D), the spread area (E), podosomes per μm^2 (F) and the size of podosomes (G) were determined. A one-way ANOVA with a Dunnett test was performed, asterisk indicates a significant difference with a P-value<0.05. Scale bar represents 10 μm . Data represent at least three repeats. Error bars indicates $\pm\text{SEM}$.

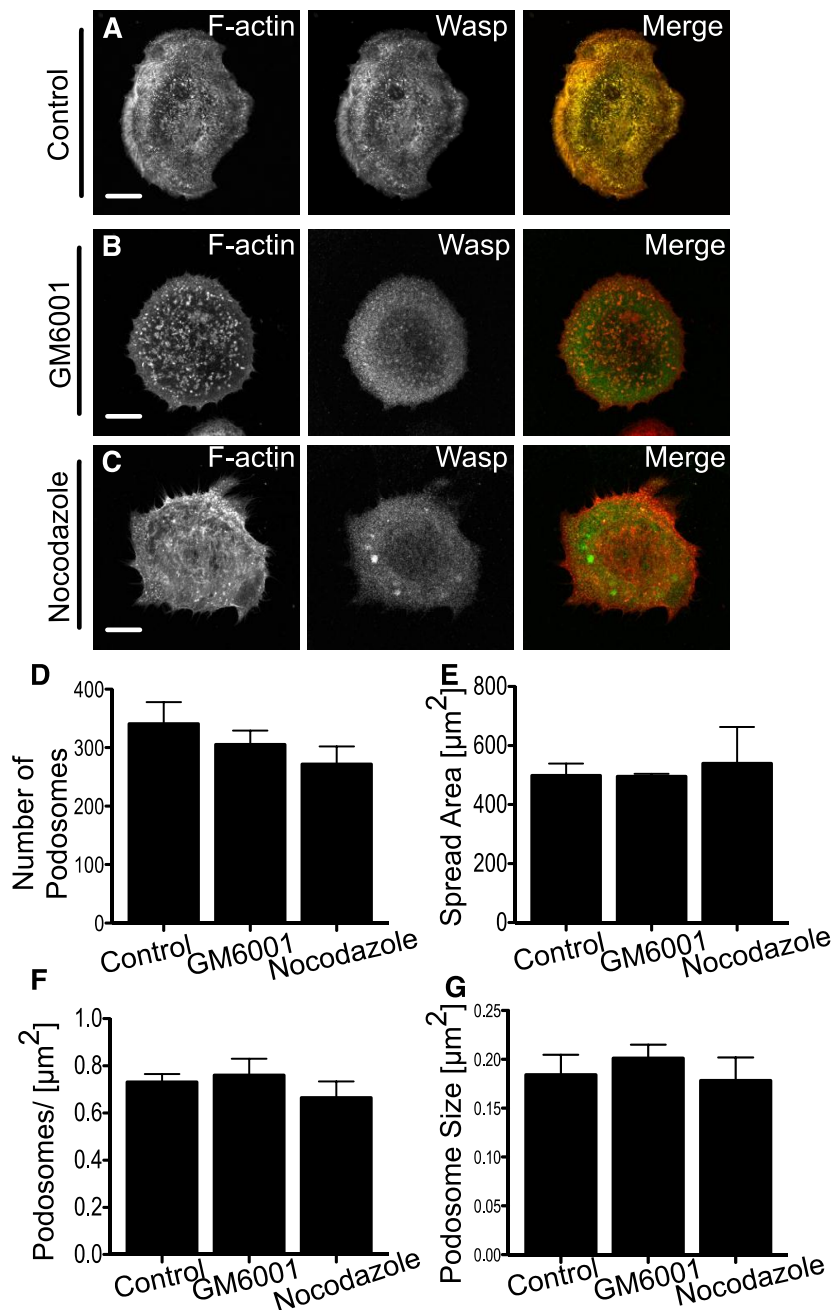


Figure 3.20: MMP activity and microtubule assembly is not involved in podosome formation in Mks spreading on fibrinogen.

Mks were allowed to spread for 3h on 100 $\mu\text{g}/\text{ml}$ fibrinogen-coated surface in SFM in the presence of 0.1% DMSO (A), 5 μM GM6001 (B) and 10 μM Nocodazole (C). Mks were fixed and stained for F-actin (red) and Wasp (green), the right panel of images shows the merge of both channels. Images were taken at the basolateral surface of the cell. The number of podosomes (D), the spread area (E), podosomes per μm^2 (F) and the size of podosomes (G) were determined. A one-way ANOVA with a Dunnett test was performed, asterisk indicates a significant difference with a P-value<0.05. Data represent at least three repeats. Scale bar shows 10 μm . Error bars indicate $\pm\text{SEM}$.

3.3.8 Integrin $\alpha_{IIb}\beta_3$ is involved in podosome formation on horn collagen

One main function of podosomes is cell adhesion to ECM proteins; this is maintained by Integrins, heterodimers of cell-matrix receptors. β_1 -, β_2 -, and β_3 -integrins are the most common Integrin subunits in podosome structures in cells such as macrophages, transformed fibroblasts, osteoclasts or dendritic cells (Linder and Aepfelbacher, 2003). Integrin $\alpha_{IIb}\beta_3$, a fibrinogen receptor, is specific for the megakaryocytic lineage and is known to play an important role in platelet activation (Watson *et al.*, 2005a). To verify if this specific Integrin is involved in Mk podosome formation, Lotrafiban, an antagonist of Integrin $\alpha_{IIb}\beta_3$, which blocks the substrate-binding site, was applied to Mks, spreading on collagen and fibrinogen. Mks on fibrinogen did not attach to the matrix, confirming that the inhibitor worked well with a concentration of 10 μ M. Cells spread on collagen formed normal podosomes positive for both F-actin and Wasp with no difference to the control cells (Figure 3.21A,B). However, a striking change was detected in the number of podosomes, which was reduced by 50% with a decreased spreading area. As both the number of podosomes and the surface area was reduced, the podosomes per area was unchanged, whereas the podosome size was slightly increased with Lotrafiban treatment (Figure 3.21C-F). However, the activation of $\alpha_{IIb}\beta_3$ integrin might not be due to binding to collagen but to other secreted substrates like von Willebrand factor (vWF).

With these results I demonstrate an important role for integrin $\alpha_{IIb}\beta_3$ in Mks in cell spreading and podosome assembly on collagen I. Furthermore, I demonstrate with these findings the involvement of a Mk specific integrin in podosome formation and therefore highlight a unique property of Mk podosomes.

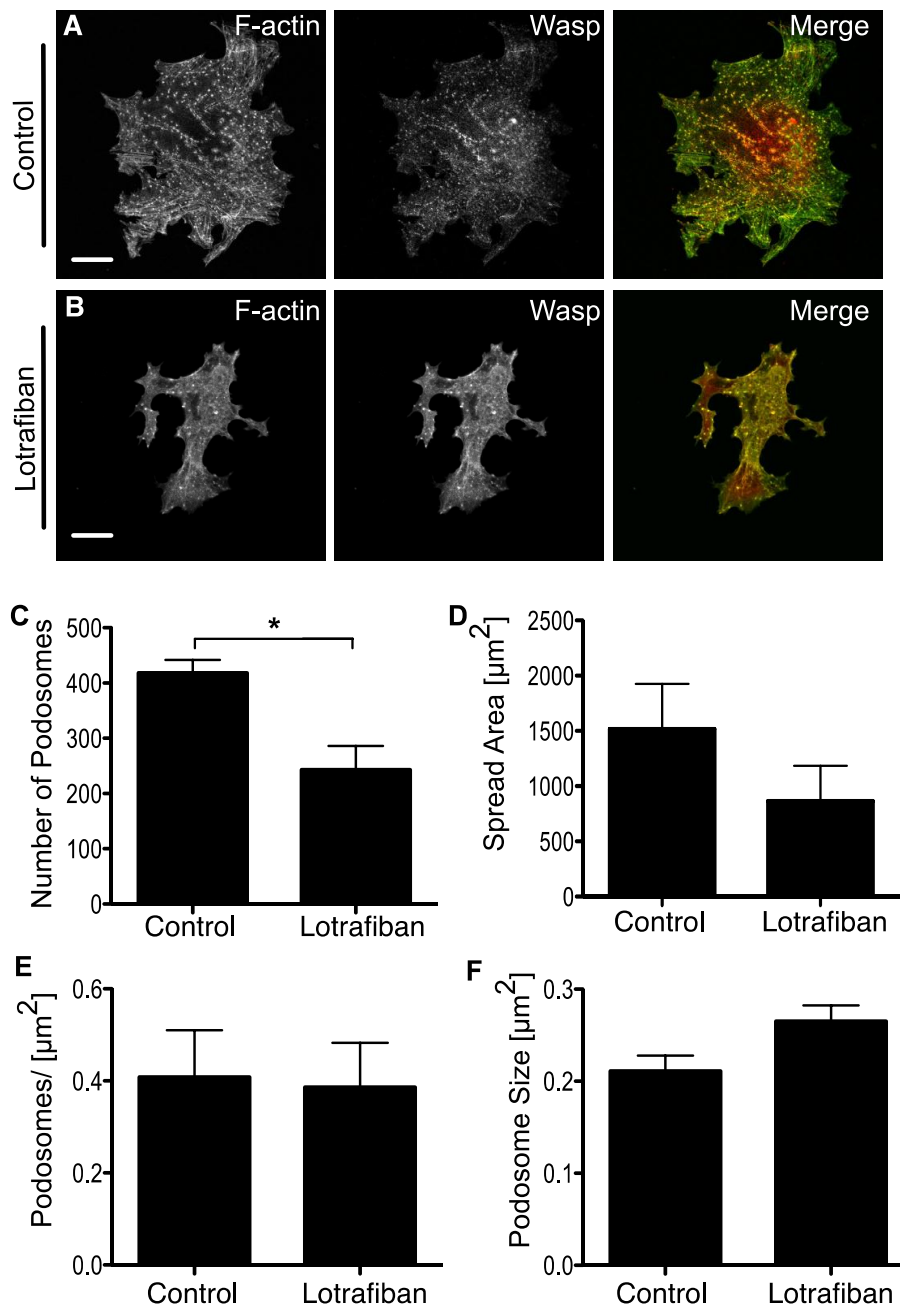


Figure 3.21: The inhibition of integrin $\alpha_{\text{IIb}}\beta_3$ induces a reduction in podosome assembly by Mks spreading on horm collagen.

Mks were allowed to spread for 3h on 100 $\mu\text{g}/\text{ml}$ horm collagen-coated surface in SFM in the presence of the control substance (H_2O) (A) and 10 μM Lotrafiban (B). Mks were fixed and stained for F-actin (green) and Wasp (red), the right panel of images shows the merge of both channels. Images were taken at the basolateral surface of the cell. The number of podosomes (C), the spread area (D), podosomes per μm^2 (E) and the size of podosomes (F) were determined. A one-tailed student's t-test test was performed, asterisk indicates a significant difference with a P-value<0.05. Data represent three repeats. Scale bar shows 10 μm . Error bars indicate $\pm\text{SEM}$.

3.4 Discussion

Podosomes are so named because they resemble cell feet in form and function, regulating adhesion, migration and matrix interactions of a variety of cell types. Typically, podosomes are found in highly motile monocytic lineage cells such as dendritic cells, osteoclasts and macrophages, where they are thought to be important for mediating the interactions between such cells and the extracellular matrix. In this chapter I describe a detailed structural characterization of megakaryocyte podosomes, their matrix specific formation, the protein composition determined with immunofluorescence tools and the involvement of key proteins tested with targeted inhibitors. Our results have important implications for understanding how Mks form podosomes and which proteins are involved. Our study also contributes to a broader understanding of podosome regulation in megakaryocytes.

I set up an immunofluorescence costaining for F-actin and Wasp and showed that Mks form classical podosome structures on both collagen I and fibrinogen. However, I also showed that the assembly of podosomes is dependent on the underlying matrix with a different number of podosomes per area on fibrinogen compared to collagen. This indicates that the density of podosomes is depending on the matrix protein but also its continuity and stiffness. An explanation for the high density of podosome structures could be the need for degradation of ECM or mechanosensory action for example during the process of proplatelet release. A thin layer of fibrinogen likely forms an inflexible monolayer on glass in contrast to more flexible collagen fibres. It is reported that more Integrins are clustered on stiffer substrates, suggesting a potential link between substrate elasticity and responsive adhesion assembly (Collin *et al.*, 2008; Peng *et al.*, 2012). Furthermore,

when macrophages were placed on different micropatterned substrata, podosome formation was actively encouraged on fibrinogen, while gelatin and a thin layer of collagen IV on glass were suppressive to podosome formation (Labernadie *et al.*, 2010). Some of the differences might also be accounted for the different integrins engaged by each matrix, with fibrinogen favouring $\alpha_{IIb}\beta_3$ Integrin and β_3 Integrin being the most abundant β -subunit in Mks, while collagen recruits β_1 Integrins, which are less abundant in platelets and Mks (Guo and Piguet, 1998). Interestingly, podosome size and shape did not appear to vary on the different matrices. However, in contrast to other podosome forming cells such as different monocytic cells, endothelial cells or smooth muscle cells, Mks assemble smaller podosomes, which are half the size (Linder, 2007). This could also be an explanation why Mks form around 4 times more podosome structures than other cell types like osteoclasts, macrophages and dendritic cells (Olivier *et al.*, 2006; Dovas *et al.*, 2009; Hammarfjord *et al.*, 2011).

The spatial localisation of podosomes is also dependent on the matrix. In contrast to uniform thin fibrinogen, where podosomes were more or less uniformly distributed in cells, Mks formed podosomes along collagen fibres in a linear fashion. The distribution of fibrinogen and collagen *in vivo* is very diverse as collagen is present in the entire bone marrow (Malara *et al.*, 2011a), whereas fibrinogen is only located at the vascular sinusoid (Larson and Watson, 2006b). This could have profound effects on the function of podosomes since such chain-like podosome structures could encourage not just adhesion but also guidance clues for protrusion, migration as well as degradation hotspots within megakaryocytes.

I investigated the protein composition of podosome structures with immunofluorescence tools and stained for typical core and ring proteins. Core proteins like Wasp, Cortactin and the Arp2/3 complex colocalized with the F-actin core in the same as in podosomes of other cell types (Gawden-Bone *et al.*, 2010; Luxenburg *et al.*, 2012). Classical ring structure associated proteins are Vinculin, Talin and Phosphotyrosine (Cox *et al.*, 2012; Linder, 2007), but only Vinculin showed a clear ring structure, confirming that the structural protein composition of podosomes differs from cell type to cell type. However, the staining for the different proteins were identical between spreading cells on collagen and fibrinogen.

Our data demonstrates the fundamental requirement for both actin polymerisation and the Wasp-Arp2/3 complex pathway for podosome formation and maintenance. As in other cell types the activity of the Arp2/3 complex was essential for Mk podosomes, as it regulates the constant turnover of F-actin (Luxenburg *et al.*, 2012). I thus show that Mks form podosomes by similar mechanisms as other cell types. Interestingly, the inhibition of Myosin-II had no significant effect on podosome formation and provides evidence that these structures are different from focal adhesions, which are dependent on Myosin-II activity. This is different for other podosome-forming cells like osteoclasts and macrophages, where Myosin II regulates the appearance or dynamics of podosomes or podosome-like structures (Collin *et al.*, 2006; Labernadie *et al.*, 2010; Van Helden *et al.*, 2008).

It is still a subject of debate whether invadopodia and podosomes are distinct or the same structures. In Mks, podosome formation is not affected upon the inhibition of MMP activity. This provides further evidence that podosomes are distinct from invadopodia, which are dependent on MMP activity. I suggest that

protease dependence might be one way to distinguish between invadopodia and podosomes, with the main architecture of podosomes being insensitive to protease inhibition and dependent on Wasp activity, while invadopodia do not assemble in the presence of MMP inhibitors and are independent of Wasp.

In some cell types microtubules were shown to be associated with podosomes (Linder *et al.*, 2011; Wiesner *et al.*, 2010). However, the treatment with Nocodazole had no effect on Mk podosome assembly. With this result, I show another cell specific property of these structures. This is in contrast to macrophages, where *de novo* podosome formation is dependent on microtubules (Linder *et al.*, 2000b).

Another Mk specific podosome feature, which I discovered, is the involvement of Integrin $\alpha_{IIb}\beta_3$ in podosome formation. Integrin $\alpha_{IIb}\beta_3$ is known to be a key regulator in platelet spreading but has not been described in the context of podosome formation. The adhesion via this Mk-specific Integrin activates Src-kinase (Watson *et al.*, 2005a), which is known to be involved in podosome assembly in transformed fibroblasts (Boateng *et al.*, 2012). However, further investigations are needed to determine the exact signalling through $\alpha_{IIb}\beta_3$ Integrins in Mk podosome formation.

In conclusion, I characterized the fundamental protein composition of podosomes in Mks, which was not different from podosomes in other cell types. Furthermore, I determined F-actin, the Arp2/3 complex and Wasp as essential key proteins for podosome assembly. This is also seen in other podosome-forming cells like in osteoclasts, dendritic cells or macrophages and implicates a universal consistency of regulation (Buccione *et al.*, 2004). However, with the identification of the involvement of $\alpha_{IIb}\beta_3$ Integrin in Mk podosomes I found a very distinctive feature

from podosome formed in other cell types. The above data established the base for a more detailed characterization of podosome structures, which is necessary to direct a functional role for podosomes in megakaryocytes and their physiological relevance.

4 Podosome lifetime and matrix degradation depends on the underlying substrate

4.1 Summary

Podosomes are highly dynamic F-actin based structures with a lifetime of a few minutes, which depends on the podosome structure, the cell type and the underlying matrix. Furthermore, they are able to degrade matrix proteins via MMPs. The aim of this chapter was to determine the lifetime of Mk podosomes on different substrates and to demonstrate if these structures are able to degrade ECM proteins. These findings highlight the role of the underlying matrix in terms of podosome dynamics and their degradative activity, which was never reported in Mks before.

4.1.1 Introduction

Podosome formations are characterized by an F-actin core surrounded by a ring of adhesion-associated proteins like Vinculin (Cox *et al.*, 2011; Linder *et al.*, 2011). However, there are more typical properties, which are specific for podosomes. One of these properties is the lifetime of podosome, which ranges between 2 and 12 minutes in average (Linder, 2007). The reason for this diversity in lifetime is not clearly defined. It might be a cell type specific feature, but it also could be influenced by the underlying matrix, its stiffness and the resulting difference in Integrin activation and therefore the trigger of various signalling pathways.

In addition to their role in adhesion, podosomes are well known to be hot spots of matrix degradation via MMP activity. Podosome mediated matrix degradation is

well established in a range of different cell types including osteoclasts (Saltel *et al.*, 2008) and dendritic cells (Dehring *et al.*, 2011), but not in Mks. The degradation of common ECM proteins like gelatin and fibronectin was shown in various podosome-forming cell types like macrophages or (Stolting *et al.*, 2012) dendritic cells (Banon-Rodriguez *et al.*, 2011; West *et al.*, 2008). Another physiologically relevant substrate are basement membranes (BM). Basement membranes are part of several structures lining organs and cavities such as in the skin, the peritoneum (mesentery), in blood vessels or lymphatic vessels (Detry *et al.*, 2011; Fuchs and Raghavan, 2002; Liliensiek *et al.*, 2009). The origin of the different basement membranes determines different properties in composition and structural coherence. The thickness for example of the aortic BM is double the size compared to the BM of the Vena Cava (Liliensiek *et al.*, 2009). Furthermore, different BMs are characterized by their continuity or so called low-expression regions (Voisin *et al.*, 2010). However, in general basement membranes are composed of a meshwork of more than 50 different proteins, with a scaffold of laminin and collagen IV (Hotary *et al.*, 2006). The location of the basement membrane is widely spread but generally it separates the epithelium from the stroma and is present at the basolateral side of the endothelium, like in blood vessels (Kalluri *et al.*, 2003). This membrane needs to be penetrated by cells migrating through different tissues, which is the case for Mks when they need to cross a vascular sinusoid in the bone marrow to release proplatelets into the blood stream (Pauly *et al.*, 1994).

In order to further characterize podosomes in Mks and to do a comparison with other cell types, I determined the lifetime of podosomes using Lifeact-GFP Mks. To investigate the influence of the underlying substrate, cells were spread on

fibrinogen and collagen. I also analysed the degradative activity of Mk podosomes on fibrinogen, collagen I and gelatin. Furthermore, I established an assay with a native basement membrane demonstrating the relevance of podosomes in MKs.

4.1.2 The Lifetime of podosomes is dependent on the underlying matrix

Podosomes are highly dynamic structures with a lifetime between 2 and 12 min in macrophages, dendritic cells and osteoclasts spreading on glass, fibronectin or collagen I. The lifetime of podosomes in Mks isolated from Lifeact-GFP mice using real time TIRF or confocal microscopy was measured. Mks form dynamic podosomes, which undergo rapid formation and dissolution as demonstrated on a fibrinogen surface (Figure 4.1A and supplemental movie 4). The mean lifetime of podosomes on fibrinogen was 5 ± 0.32 min (Figure 4.2A), with no podosome lasting for longer than 15 min (Figure 4.2B, black columns). In comparison, podosomes had a significantly longer half-life on collagen I of over 16 ± 1.14 min with more than 30% lasting beyond 20 min (Figure 4.2B supplemental movie 5). Furthermore, the podosomes sometimes assembled in a linear arrangement along the collagen fibres (Figure 4.1B).

These results suggest that Mks sense the matrix environment, its topography and stiffness and assemble podosomes along collagen fibres, which influences their lifetime.

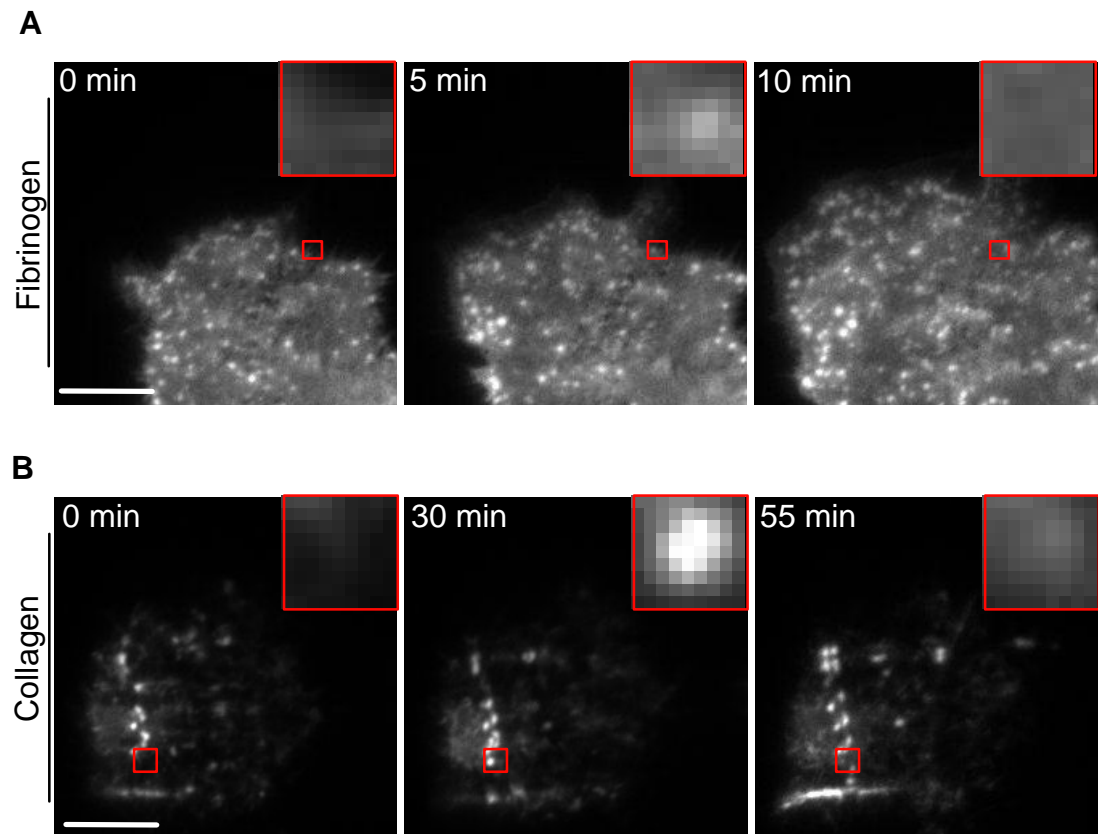
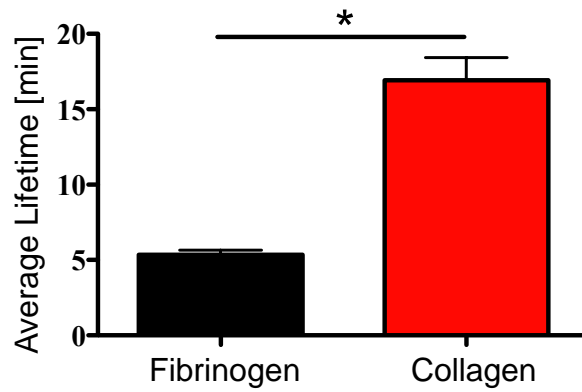


Figure 4.1: Podosome lifetime is dependent on the underlying matrix

Lifeact-GFP Mks were spread on a fibrinogen- (A) and collagen-coated surface (B). Cells were imaged with a TIRF microscope, imaging the lateral side of the cell. Images were taken every 20s up to 4h. The red squares indicate the magnified area of a single podosome. Scale bar represents 10 μ m. Complete movies are included in supplementary data (movie 4 and 5).

A



B

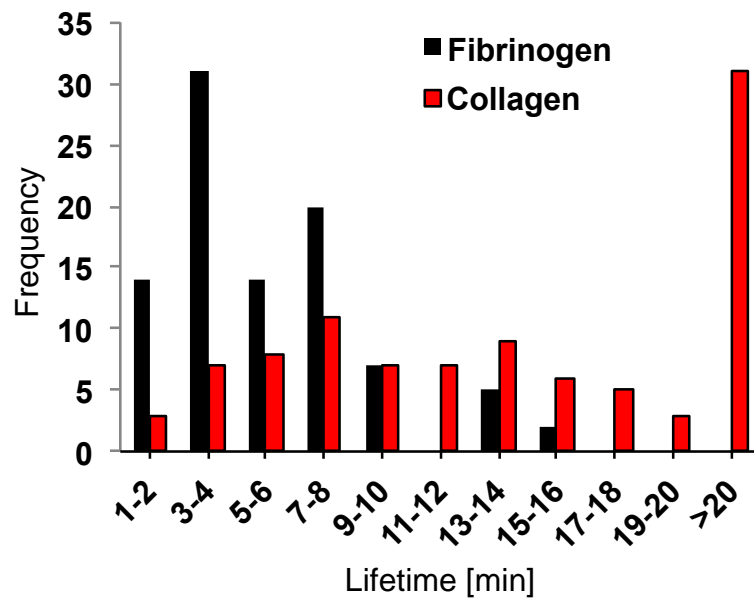


Figure 4.2: Podosome lifetime is dependent on the underlying matrix

The lifetime of podosomes (A) of Mks spreading on fibrinogen (black column) or collagen I (red column) was determined. The frequency of the different lifetimes was clustered into groups (B). The statistical analysis was done using a two-tailed student's t-test. Asterisk indicates a significant difference with a p-value <0.05. 100 podosomes were analysed from at least 10 different cells.

4.1.3 The activity of Myosin II plays a significant role in podosome turnover

I found that podosomes are influenced by the substratum on which cells are plated and next investigated whether contractile forces and MMP activity could also influence podosome lifetime. To further investigate the regulation of podosome dynamics on fibrinogen and collagen I, Lifeact-GFP Mks were treated with GM6001 (MMP blockage) and Blebbistatin (Myosin II inhibition) during real time spreading (Figure 4.3; Figure 4.5; supplemental movie 6-9). Mks formed normal podosomes on fibrinogen with an average lifetime of 4.5 min in control samples. In the presence of GM6001, podosomes of spreading Mks had an average lifetime of 3.9 min, which is not significantly different from the control (Figure 4.4A). However, the inhibition of Myosin II induced an increase in podosome lifetime by almost 40%, which is caused by a reduced frequency of short-living podosomes but an increase in long-living podosomes (Figure 4.4A,B). In comparison, similar results were determined for Mks spreading on collagen I. Podosomes formed on collagen I in control cells had a lifetime of around 12 min, which was not significantly changed upon MMP inhibition (Figure 4.6A). Interestingly, it was different for Myosin II blockage, which induced a change in lifetime up to 18.6 min with almost 50% of podosomes lasting for more than 20min (Figure 4.6B).

The results for the lifetime of podosomes in Mks spreading on the different matrix proteins and with the presence of MMP and Myosin II inhibitors were summarized (Figure 4.7A). Clusters were created to evaluate the different populations of short- (1-6min), medium- (7-13min), long- (14-20min) and very long-living (<20min) podosomes formed within different conditions (Figure 4.7B-D). MMP inhibition of Mks plated on fibrinogen caused a small change in the population of short- and medium-lifetime podosomes. In comparison to Myosin II blockage, which induced

an almost 20% increase of long-living podosomes. A more dramatic effect was observed in Mks spreading on collagen. The group of short lived podosomes was increased by 10% and at the same time the medium-lived podosomes were decreased by 50%. However, as mentioned before there was no significant difference detectable. The blockage of Myosin II had the most striking effect with a three times higher amount of very long-living podosomes. This identifies Myosin II as a crucial player in the regulation of podosomal lifetime. How Myosin II exactly functions in this process is not known and requires further investigations.

These data highlight, that the topography of the underlying substrate dictates the turnover of podosome in Mks and that these dynamics are regulated by Myosin II activity.

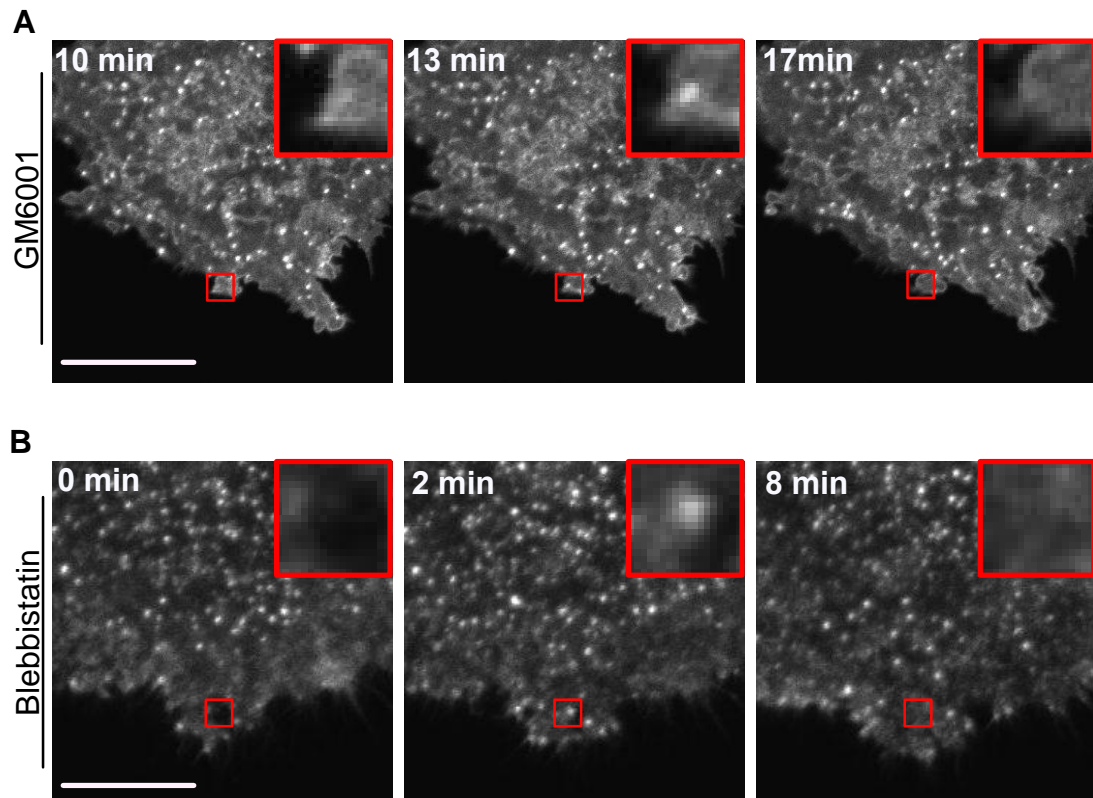


Figure 4.3: Podosome lifetime is independent of MMP activity but dependent on Myosin II in Mks spreading on fibrinogen

Lifeact-GFP Mks were spread on fibrinogen-coated surface and treated with 5 μ M GM6001 (A) and 10 μ M Blebbistatin (B). Cells were imaged with a confocal microscope, imaging the basolateral side of the cell. Images were taken every 20s up to 1h. The red squares indicate the magnified area of a single podosome. Scale bar represents 10 μ m. Complete movies are included in supplementary data (movie 6 and 7).

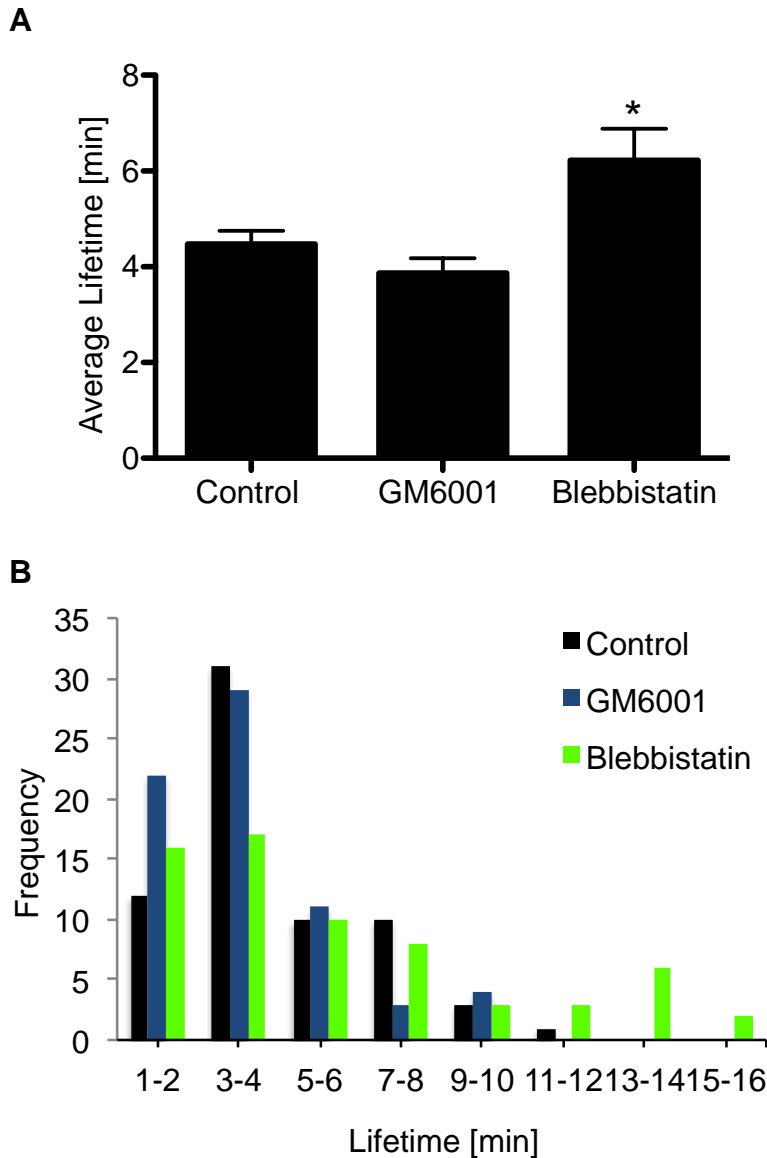


Figure 4.4: Podosome lifetime is independent of MMP activity but dependent on Myosin II in Mks spreading on fibrinogen

The lifetime of podosomes of Mks was determined (A). Cells spread on fibrinogen in the presence of 0.1% DMSO, 5 μ M GM6001 and 10 μ M Blebbistatin. The frequency of the different lifetimes was clustered into groups (B). The statistical analysis was done using an ANOVA test with a Dunnett post test, asterisk indicates a significant difference. At least 70 podosomes were analysed from at least 10 different cells. Complete movies are included in supplementary data.

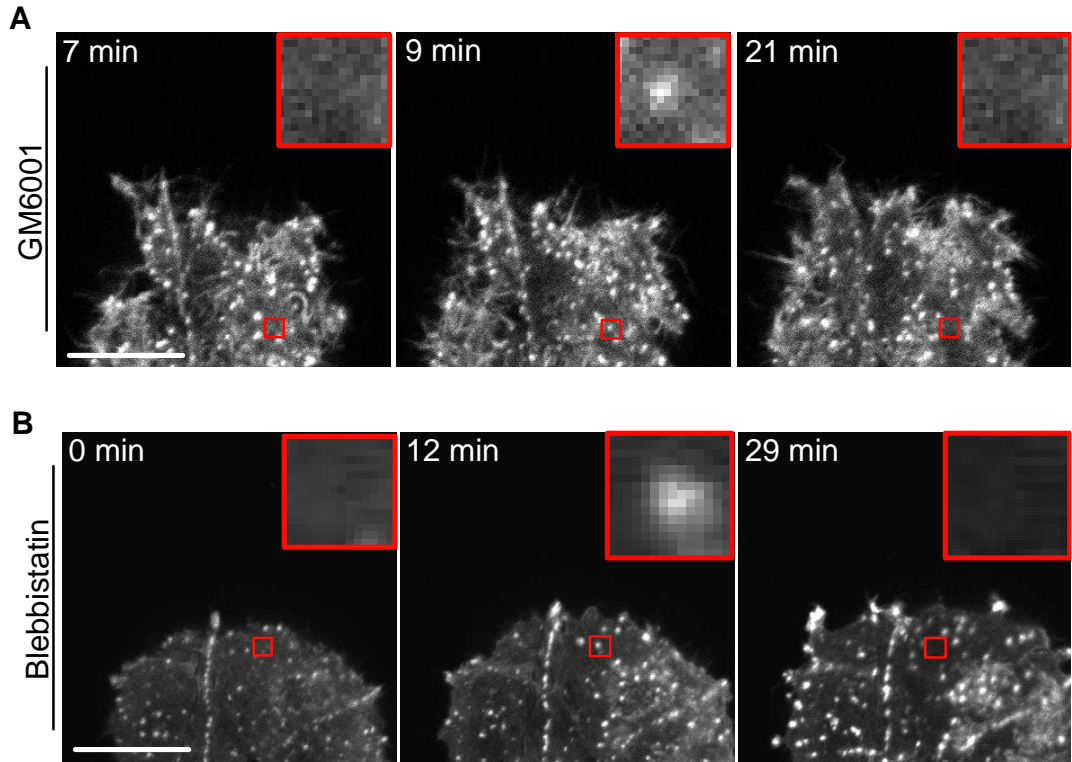


Figure 4.5: Podosome lifetime is independent of MMP activity but dependent on Myosin II in Mks spreading on collagen I

Lifect-GFP Mks were spread on collagen-coated surface and treated with 5 μ M GM6001 (A) and 10 μ M Blebbistatin (B). Cells were imaged with a confocal microscope, imaging the basolateral side of the cell. Images were taken every 20s up to 1h. The red squares indicate the magnified area of a single podosome. Scale bar represents 10 μ m. Complete movies are included in supplementary data.

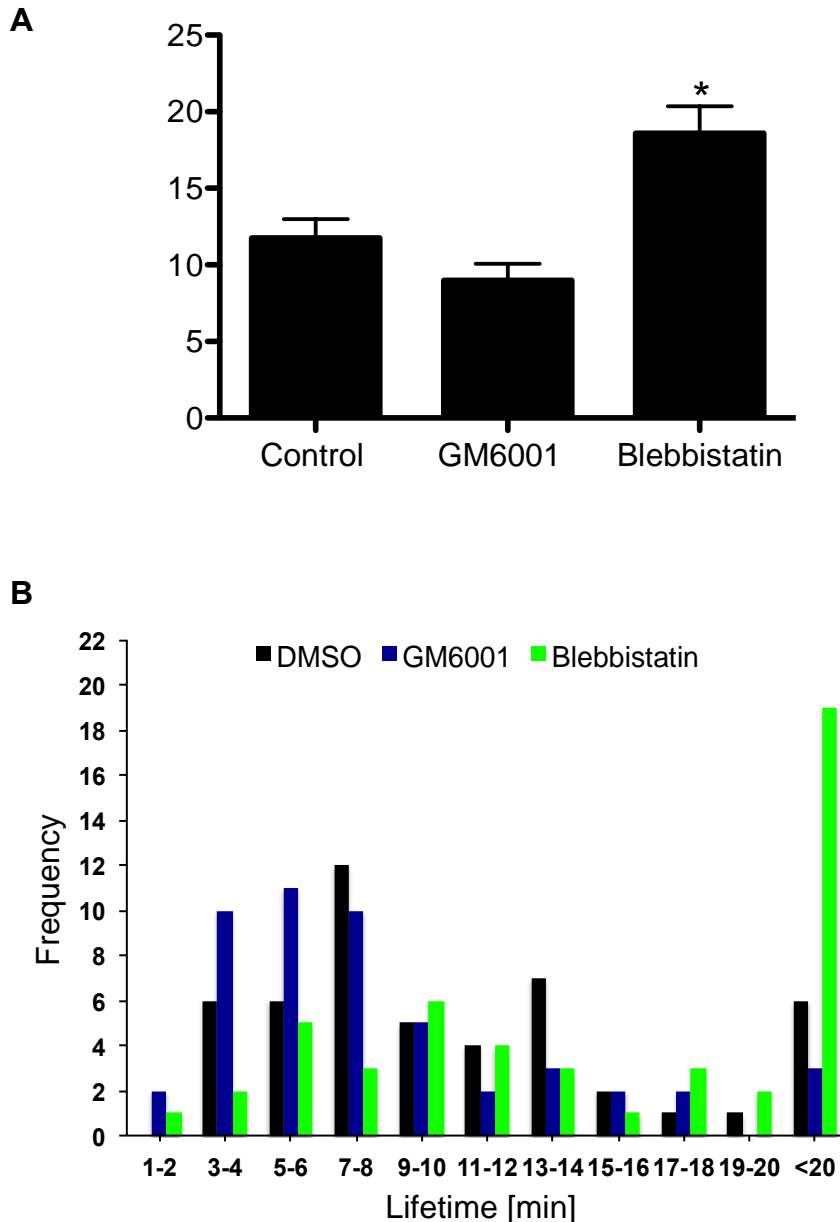


Figure 4.6: Podosome lifetime is independent of MMP activity but dependent on Myosin II in Mks spreading on collagen I

The lifetime of podosomes of Mks was determined (A). Cells spread on collagen I in the presence of 0.1% DMSO, 5 μ M GM6001 and 10 μ M Blebbistatin. The frequency of the different lifetimes was clustered into groups (B). The statistical analysis was done using an ANOVA test with a Dunnett post test, asterisk indicates a significant difference with a P-value <0.05. At least 50 podosomes were analysed from at least 8 different cells.

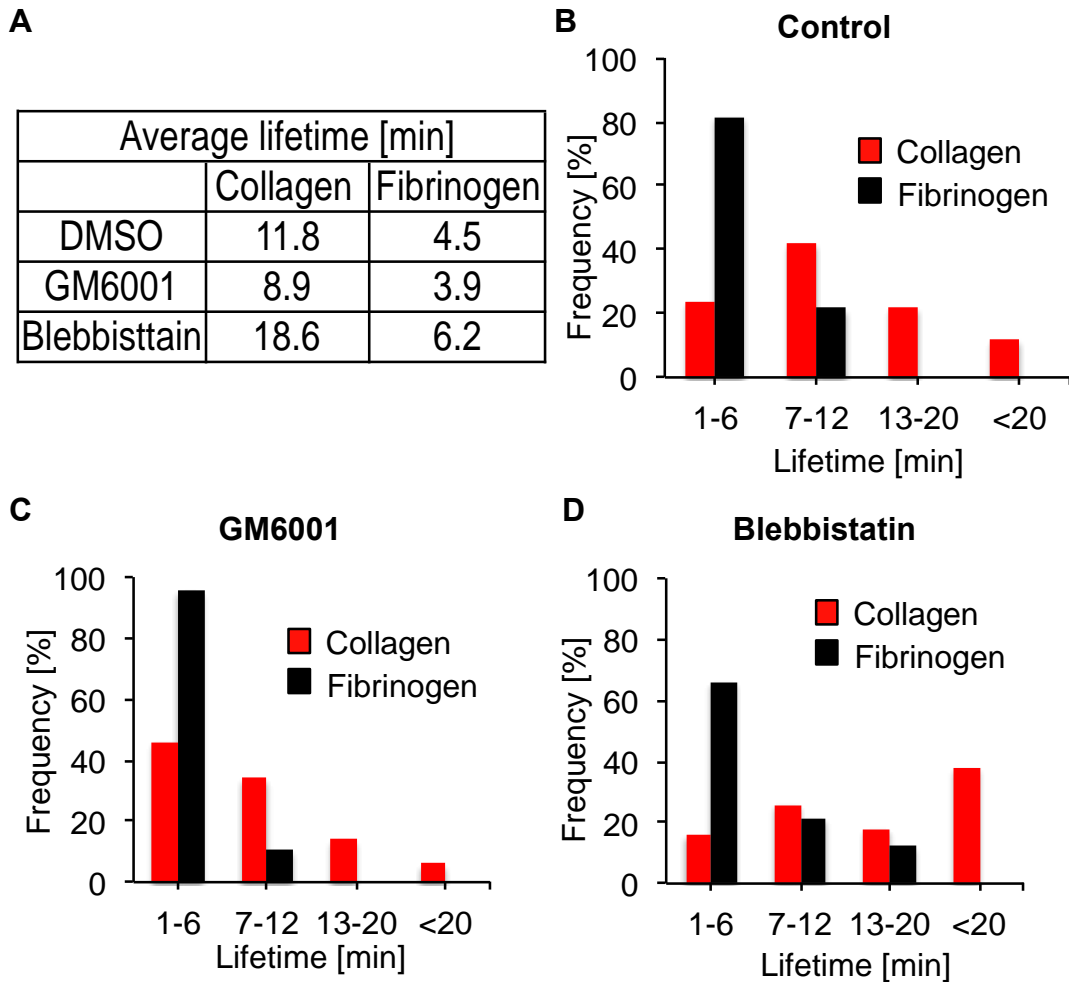


Figure 4.7: Summary of Mk podosome lifetime on collagen and fibrinogen with MMP and Myosin II inhibition

Average lifetime of podosomes on collagen I and fibrinogen in the presence of 0.1% DMSO, 5 μ M GM6001 and 10 μ M Blebbistatin (A). Percentaged grouping of short-living, medium-living, long-living and very long living podosomes on collagen (red columns) and fibrinogen (black columns) in the presence of DMSO (B), GM6001 (C) and Blebbistatin (D).

4.1.4 Mk Podosomes degrade fibrinogen but not gelatin or collagen I

One of the key features of podosomes is the proteolytic degradation of ECM proteins. Podosome driven degradation of ECM proteins like collagen or fibronectin is well established, however, it is not known if they can perform this function in Mks. To investigate if Mks perform podosome-mediated fibrinogen degradation, Mks were spread on Alexa 488-labelled fibrinogen and FITC-labelled gelatin (Figure 4.8). Mks formed clear F-actin rich podosomes, which could be partially localized to small holes in the fibrinogen monolayer (Figure 4.8A, red square). This is in contrast to gelatin, where only small cells with no podosomes could be detected (Figure 4.8B). Spread cells on gelatin showed only a low staining for CD41, a Mk-lineage specific receptor, determine that these are immature cells, which do not form podosomes (Figure 4.8C). Mks were also seeded on FITC-labelled collagen I (Figure 4.8D) but I was unable to visualize degradation of this matrix protein, most likely due to technical reasons as the fibres were thick and not flat aligned along the coverglass.

These data determine podosome-mediated degradation of fibrinogen. The lysis of gelatin or collagen I could not be detected. However, I do not want to exclude podosome-driven degradation of collagen I because the substrate did not form a continuous monolayer but were thick fibres, which made the detection of dot-like degradation patterns difficult to visualize.

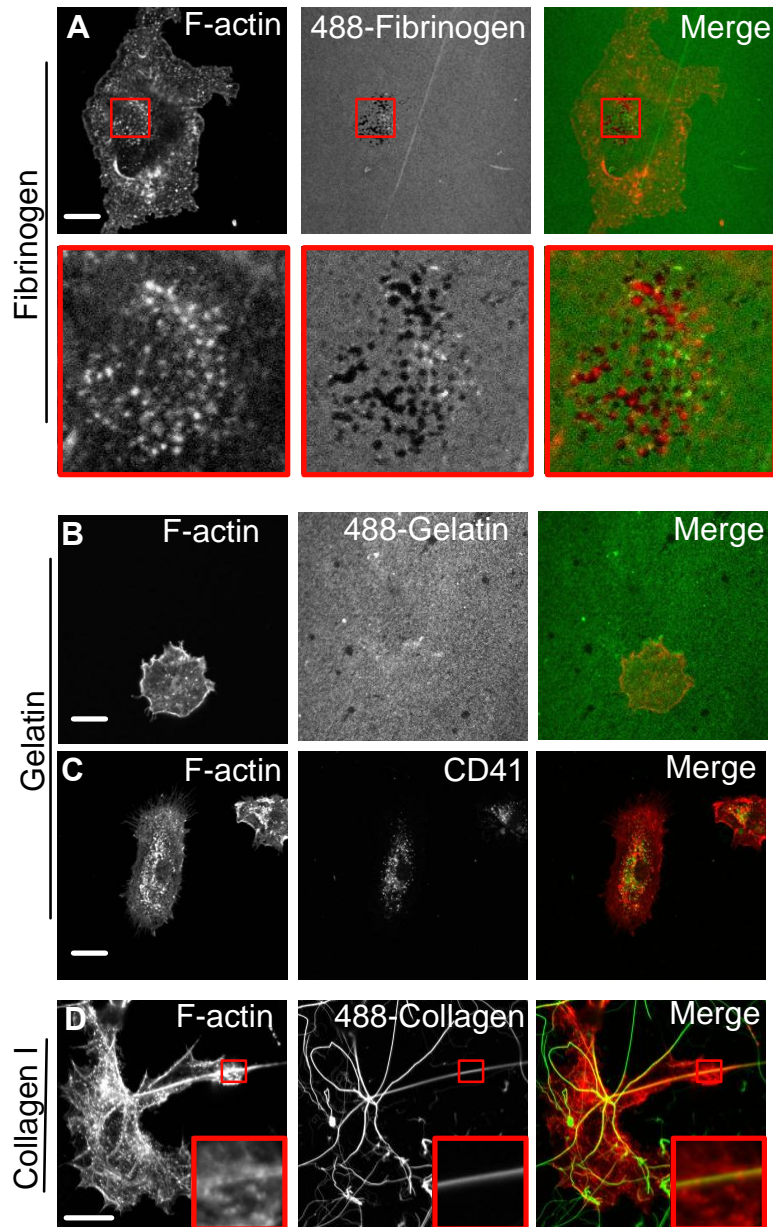


Figure 4.8: Podosomes degrade fibrinogen but not gelatin and collagen I

Mks spread on 488-labelled fibrinogen (A), 488-labelled gelatin (B) non-labelled gelatin (C) and 488-labelled collagen (D). Cells were fixed and stained for F-actin (red) and CD41 (green, only in C), merge shows the overlay of both channels. Images are representative for 3 repeats. Red squares show blow-up of images. Scale bar represents 10 μ m.

4.1.5 Podosome driven degradation of fibrinogen is MMP and Myosin II dependent

The analysis above describes podosome-mediated degradation of fibrinogen. To determine regulators of this degradation process Mks were treated with MMP and Myosin-IIA inhibitors during spreading on fibrinogen (Figure 4.9; Figure 4.10). Control cells formed clear podosomes, which were localized to holes in the fibrinogen matrix indicative of podosome-mediated degradation (Figure 4.9A). Not all podosomes could be located to holes in the matrix as podosomes are highly dynamic structures. Approximately 40% of Mks showed evidence of degradation (Figure 4.10A,B) and this was reduced in the presence of the MMP inhibitor GM6001 and the Myosin-IIA inhibitor blebbistatin by more than 50% (Figure 4.9A,B). Furthermore, the extent of matrix degradation was severely inhibited, most notably in the presence of GM6001 where the degradation was reduced by over 80% (Figure 4.10A, B).

This data show that Mks use both MMPs and Myosin-IIA to degrade fibrinogen via their podosomes, in which Myosin-IIA might not be directly involved in the lysis of the ECM but in cell contractility or the stiffness of single podosome associated with MMP-trafficking.

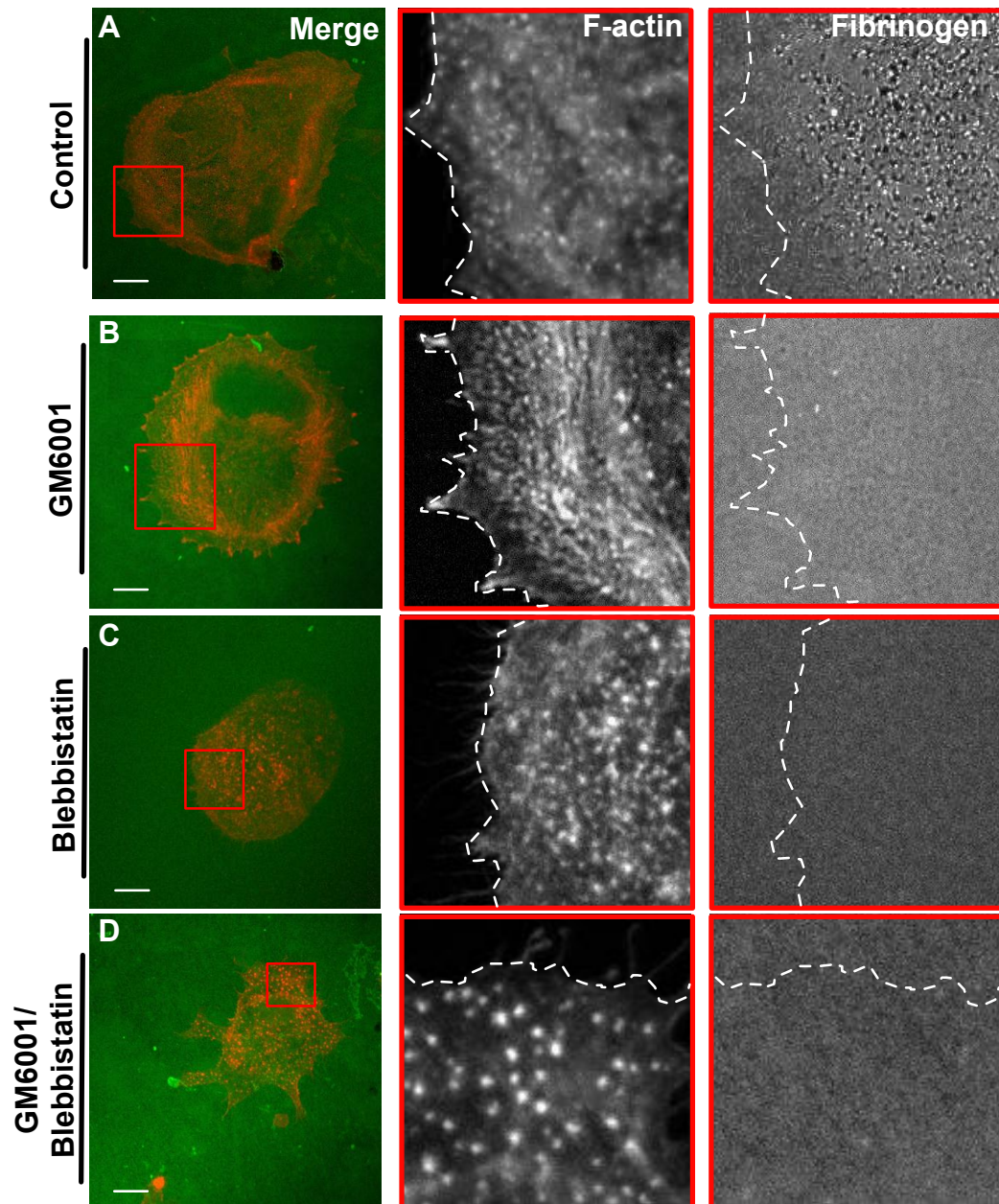


Figure 4.9: Podosome-mediated degradation of fibrinogen is dependent on MMP and Myosin II activity

Mks were spread on 488-labelled fibrinogen in the presence of 0.1% DMSO (A), 5 μM GM6001 (B), 10 μM Blebbistatin (C) and 5 μM GM6001 together with 10 μM Blebbistatin (D). Images show the merge of F-actin (red) and the fibrinogen (green), red square indicates area of interest, which is magnified in the second and third column of images. Dotted line outlines the cell rim, scale bar represents 10 μm. The experiment was repeated 6 times.

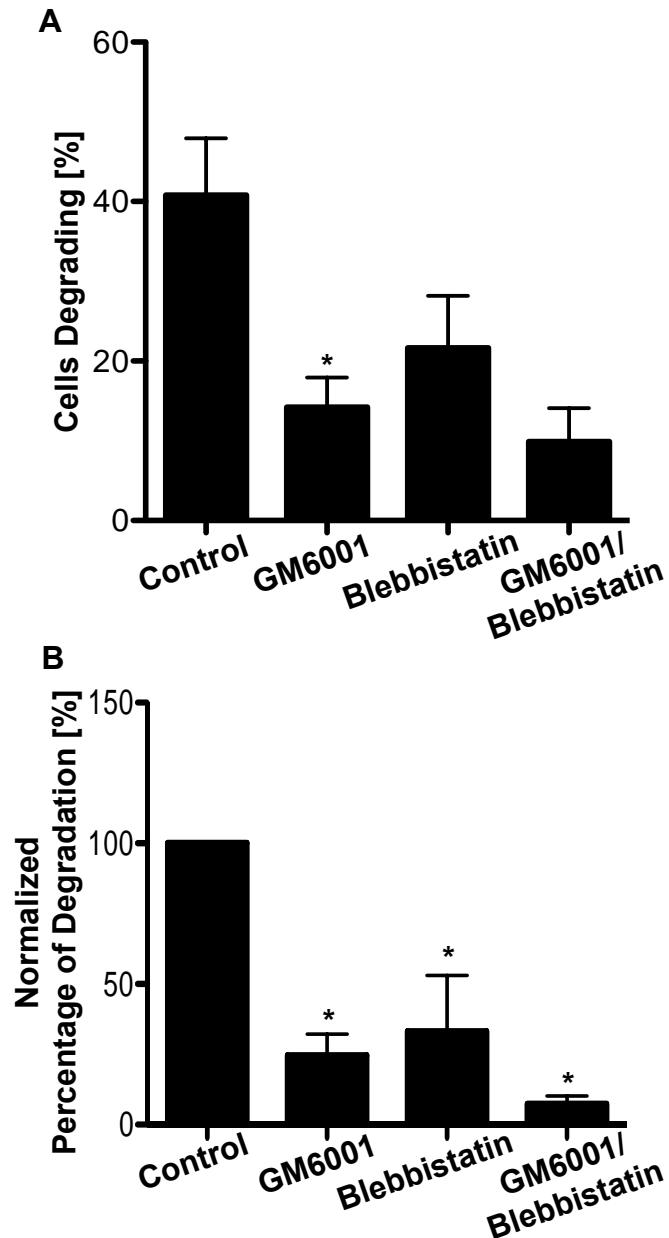


Figure 4.10: Podosome-mediated degradation of fibrinogen is dependent on MMP and Myosin II activity

Percentage of cells degrading fibrinogen (A) in the presence of 0.1% DMSO, 5 μ M GM6001, 10 μ M Blebbistatin and 5 μ M GM6001 together with 10 μ M Blebbistatin was determined. The amount of degradation was determined and normalized (B). The statistical analysis was done using an ANOVA test with a Dunnett post test, asterisk indicates a significant difference with a P-value <0.05. The experiment was repeated 6 times.

4.1.6 Establishment of a native basement membrane assay

The basement membrane is part of vascular sinusoids and is composed of a meshwork of different proteins with a scaffold of laminin and collagen IV (Rowe and Weiss, 2008). In order to release proplatelets (PPL), Mks have to cross this membrane. To investigate if Mks use podosomes to penetrate this membrane, native basement membrane from the murine peritoneum was isolated as previously described (Hotary *et al.*, 2006). The membrane was put on a filter cup (without the filter) treated, washed and set up for the experiment (Figure 4.11A). The membrane was stained for collagen IV and laminin showing the colocalization of the two proteins with small holes in the network, which was confirmed by electron microscopy performed in collaboration with Katharina Wolf (Radboud University, Nijmegen, Netherlands) (Figure 4.11B-D). Furthermore, no F-actin staining could be detected and only rudimentary DNA showing lysed nuclei were observed on empty native basement membranes (Figure 4.11E,F).

It was demonstrated previously, that Mks migrate towards a SDF-1 α gradient, which is associated with ECM degradation and proplatelet formation (Avecilla *et al.*, 2004; Hamada *et al.*, 1998). Thus, the presence of a SDF-1 α gradient would increase the physiological relevance. To verify, if it is possible to create a stable gradient, non-fluorescent buffer was put into the upper well with a fluorescent buffer in the lower well. Over time z-sections were taken in order to measure the fluorescence and the diffusion of the fluorescent buffer into the upper well through the basement membrane (Figure 4.12A,B). The fluorescence is the highest at the bottom of the z-stack, which represents the bottom of the dish. At the 1h-timepoint the fluorescence intensity is medium high to low at the area of the basement membrane (Figure 4.12B, upper image). However after 12h the fluorescence is

even lower but there is still a gradient visible (Figure 4.12B, lower image). To investigate how quickly a solution would diffuse from the top well through the basement membrane into the bottom well, reverse of the above experiment was performed (Figure 4.12C). The fluorescence intensity underneath a filter membrane was compared with a basement membrane in treated and untreated conditions (Figure 4.12D). After 3h most of the fluorescence buffer passed through the filter membrane. Around 40% of the FITC-dextran was able to pass the treated basement membrane and even less could cross the untreated basement membrane, indicating that the NH_4OH treatment damages the structure and permeability of the membrane.

The above data describe the setup of a new physiological assay, which was never been used in this way. I demonstrated that this assay maintained a stable gradient for 12h and that the membrane is less permeable over 3h than a commercial available $8\mu\text{m}$ filter membrane. This setup might be useful to detect the degradation of a native basement membrane. By the addition of a monolayer of endothelial cells to the membrane, it would be possible to mimic a vessel wall and to visualize transmigration processes.

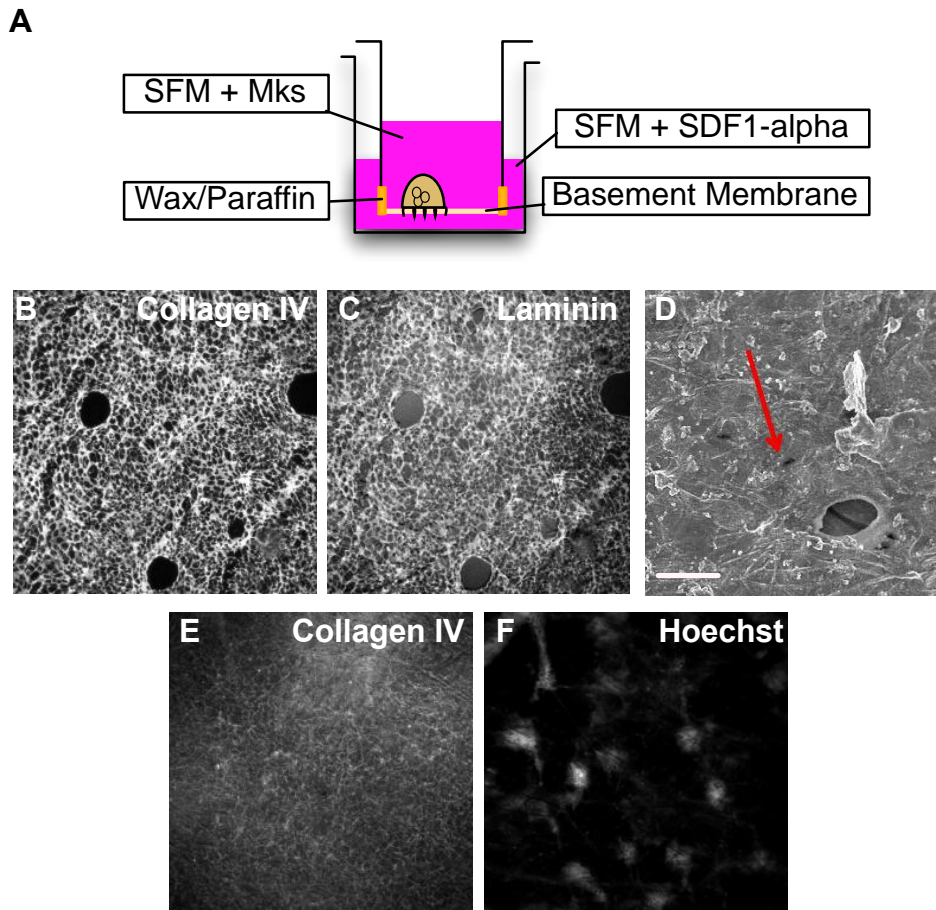


Figure 4.11: Establishment of a native basement membrane assay

Experimental set up of the basement membrane assay (A). Basement membrane was fixed and stained for Collagen IV (B), Laminin (C) and imaged with a confocal microscope. Electron microscopy (EM) was used to visualize pores in the membrane (D, red arrow) and was performed by K.Wolf. A 3D-reconstruction was done of the membrane after NH_3 treatment and was stained for Collagen IV and nuclei (E,F). EM was done once, confocal analysis was repeated at least 3 times.

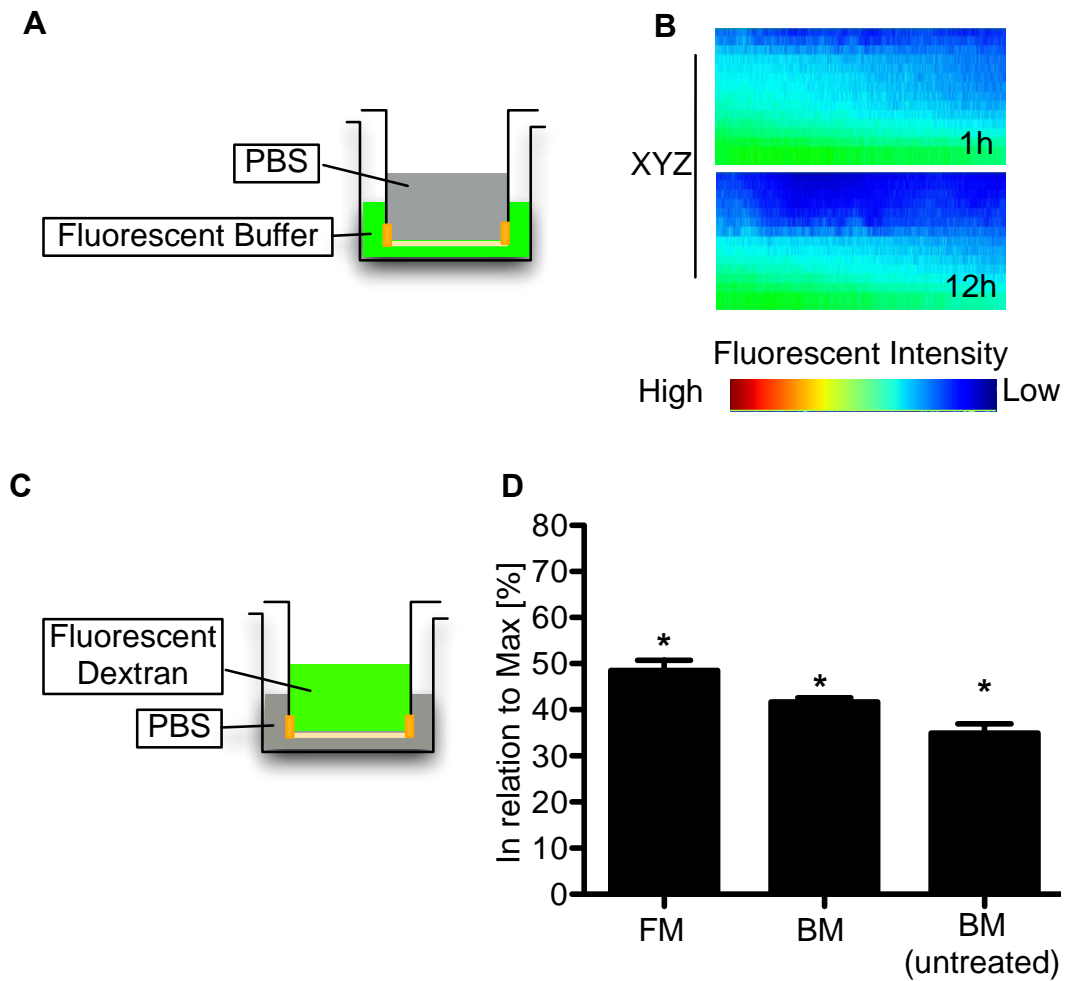


Figure 4.12: Permeability of the basement membrane

Diagram shows the experimental set up of the basement membrane assay with PBS in the upper well and fluorescent buffer in the lower well (A). XYZ-reconstruction of taken z-stacks of the basement membrane assay are shown, set up like in (A) described over 12h. Red represent high fluorescence, blue indicates low fluorescence (B). Set up of basement membrane assay with FITC-dextran in the upper well and PBS in the lower well (C). Fluorescence was measured with a spectrofluorometer and values were normalized to FITC-dextran control (D). The statistical analysis was done using an ANOVA test with a Dunnett post test, asterisk indicates a significant difference with a p-value <0.05. Set up in (A) was repeated twice, set up in (C) was performed 3 times.

4.1.7 Mks form podosomes and protrusive actin-rich structures to cross a native basement membrane

For Mks to release platelets into the bloodstream, they need to form protrusions known as proplatelets that can cross the basement membrane in the blood vessel wall. To study the potential role of podosomes in this process, I monitored megakaryocytes for spreading and podosome formation on native peritoneal basement membranes (Figure 4.13). The presence of podosomes was confirmed by immunofluorescence microscopy corresponding to the podosome markers, Cortactin and Vinculin, in combination with F-actin (Figure 4.13B,C). The Vinculin staining demonstrated a clear ring structure formation around the actin puncta (Figure 4.13C), whilst the Cortactin antibody showed clear staining in F-actin rich dot-like structures, which did not differ from podosomes formed on collagen I (Figure 4.13A,B). Furthermore, Mks spread on a native basement membrane to a similar extent as they did on collagen I (Figure 4.13D). Thus, Mks form similar podosomes on a native basement membrane to those formed on a 2D fibrinogen or collagen spread surface.

To investigate if Mks were able to form protrusions that crossed a native basement membrane, Lifeact-GFP Mks were spread on the membrane and imaged in real-time conditions. The spreading Mks formed clear actin-rich dots (Figure 4.14A-C). Furthermore, confocal imaging in the Z-plane revealed that over time actin protrusions were formed which were able to cross the membrane (Figure 4.14A-C, red arrow and supplemental movie 10).

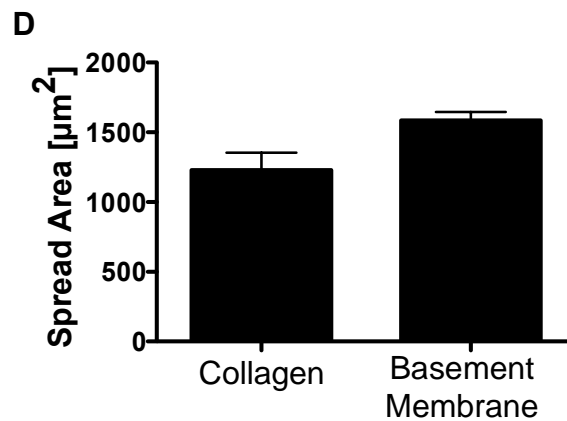
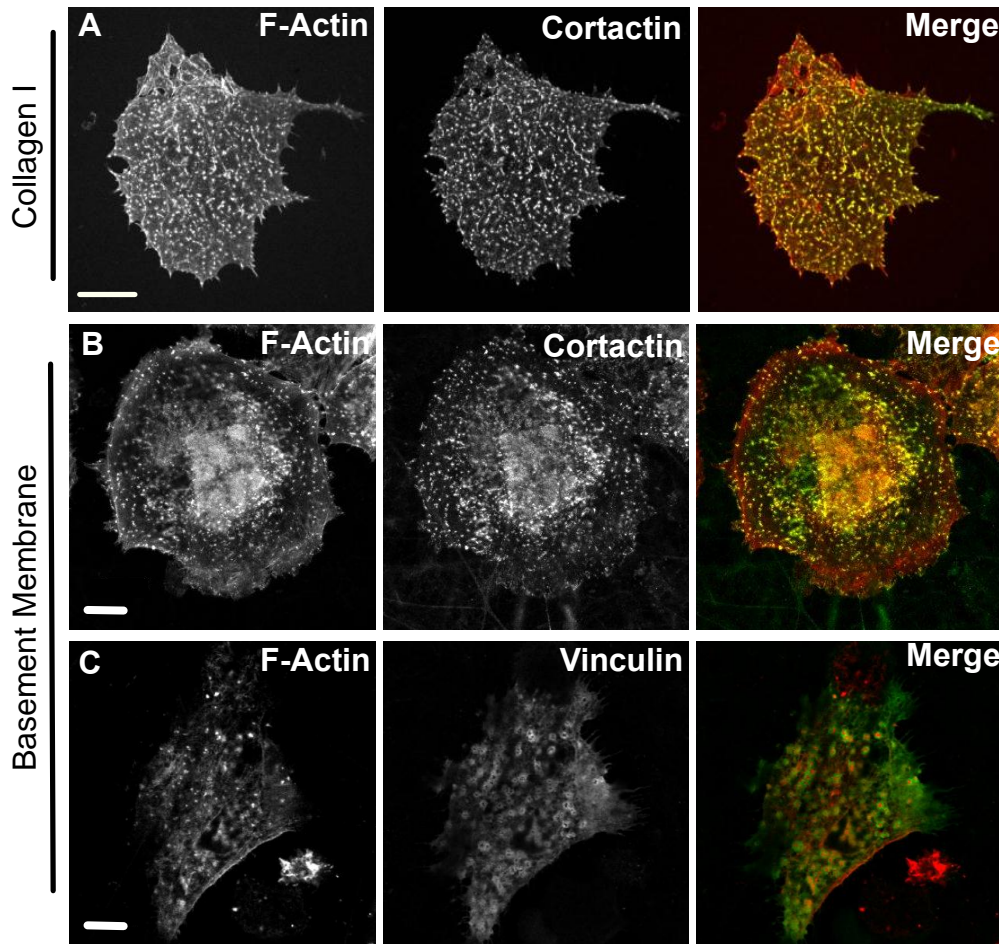


Figure 4.13: Mks form podosomes on a native basement membrane

Mks were allowed to spread on a collagen-coated surface for 3h (A) or on a native basement membrane (B,C). Mks were fixed and stained for F-actin (red) and Cortactin or Vinculin (green), merge shows the overlay of both channels. The cell surface area was determined of at least 20 cells spreading on collagen I and a native basement membrane (D). A two-tailed students t-test was performed, asterisk indicates significant differences with a p-value <0.05 . Images represent the results of at least 3 repeats. Scale bar indicates $10\mu\text{m}$.

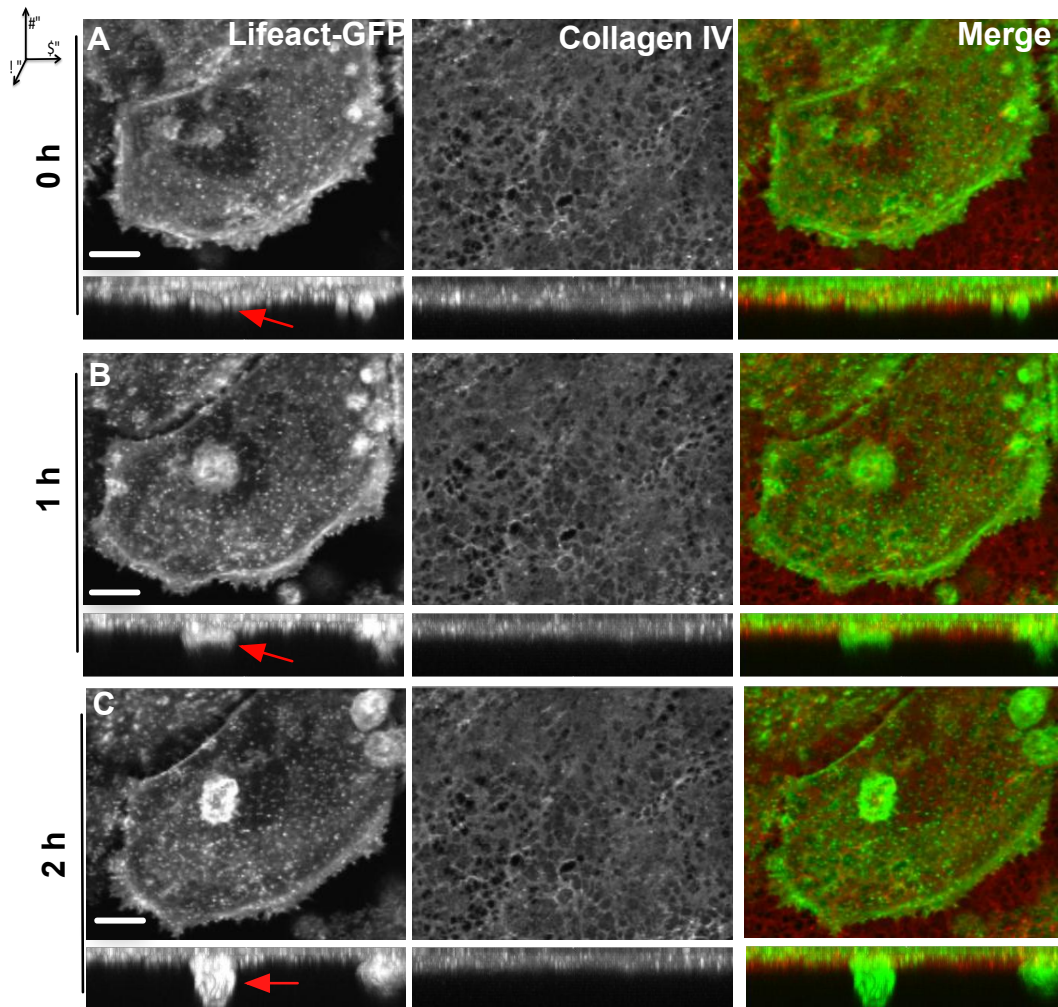


Figure 4.14: Mks form podosomes and actin-rich protrusions to cross a basement membrane

Real-time movie of GFP-Lifeact Mks (green) spreading on a native basement membrane, which was prestained for collagen IV (red). Panels of images show the XY-position and the corresponding Z-position at 0h (A), 1h (B) and 2h (C). Cells were preincubated for 1h. Red arrow indicates actin-rich protrusions crossing the basement membrane. Scale bar represents 20 μ m. Images show the maximum projection of Z-stacks. Triangle shows XYZ-directions. Complete movie is included in supplementary data (movie 10).

4.1.8 Mks form podosomes to cross a native basement membrane

To investigate the relevance of podosome assembly in the process of crossing a native basement membrane, Mks were treated with different inhibitors during spreading on the basement membrane. Control Mks spread fully on the membrane and formed actin rich dots corresponding to podosomes. The cross section of the Mk actin cytoskeleton showed actin-containing structures binding to the membrane as well as crossing through the membrane (Figure 4.15A, arrowhead). Around 25% of the control cells formed actin elongations, which were able to invade the membrane (Figure 4.17). The Arp2/3 complex inhibitor CK666 significantly decreased both the podosome formation and the percentage of protrusions that penetrated the membrane by almost 90% relative to the control (Figure 4.15B; Figure 4.17). I observed similar results with *Wasp*^{-/-} Mks indicating that podosomes are necessary to allow the protrusions to cross the basement membrane (Figure 4.15C). Furthermore, the inhibition of MMPs with 5 μ M GM6001 lead to a 50% reduction of actin-based protrusions across the basement membrane, implying that cells likely use protease activity to protrude actin processes through the basement membrane (Figure 4.16A; Figure 4.17). In contrast, inhibition of Myosin-IIA had no effect on the formation of protrusions across the membrane either in the absence or presence of MMP inhibition (Figure 4.16B,C; Figure 4.17). In chapter I I demonstrated that the microtubule cytoskeleton does not affect the formation of podosomes in Mks. However, microtubules are essential in the process of proplatelet formation. To investigate if the crossing protrusions are proplatelet extensions, Mks were treated with 10 μ M Nocodazole. Interestingly, this treatment induced a reduction of crossing protrusions by almost 50% (Figure 4.17A,B), implying that not only actin-based cell migratory events but maybe also

physiologically relevant processes like proplatelet formation might be observed in this assay.

The data above shows that the protrusion formation across native basement membranes is dependent on podosome formation, MMP activity and microtubules but not on Myosin-IIA.

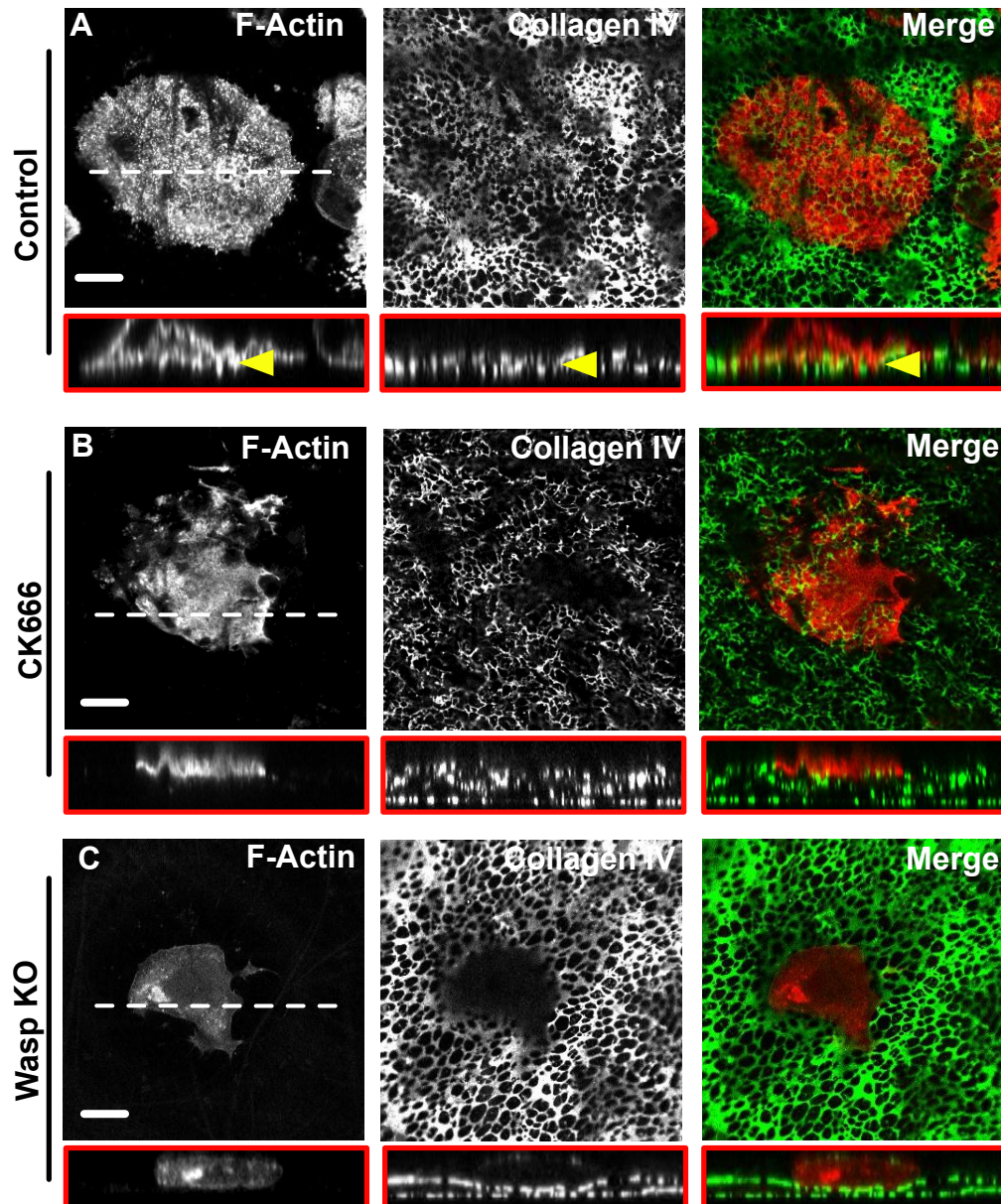


Figure 4.15: Mks use podosomes to cross a basement membrane

Mks were allowed to spread for 3h on a native basement membrane in the presence of 0.1% DMSO (A) and 20 μ M CK666 (B). *Wasp*^{-/-} Mks were seeded on the membrane (C). Cells were fixed and stained for F-actin (red) and collagen IV (green); merge shows overlay of both channels. Images show XY position and underneath the corresponding Z-direction. Dotted line indicates the location of the Z-position. Yellow arrowheads highlight the protrusions crossing the membrane. Scale bar represents 20 μ m. Experiments were repeated at least 3 times.

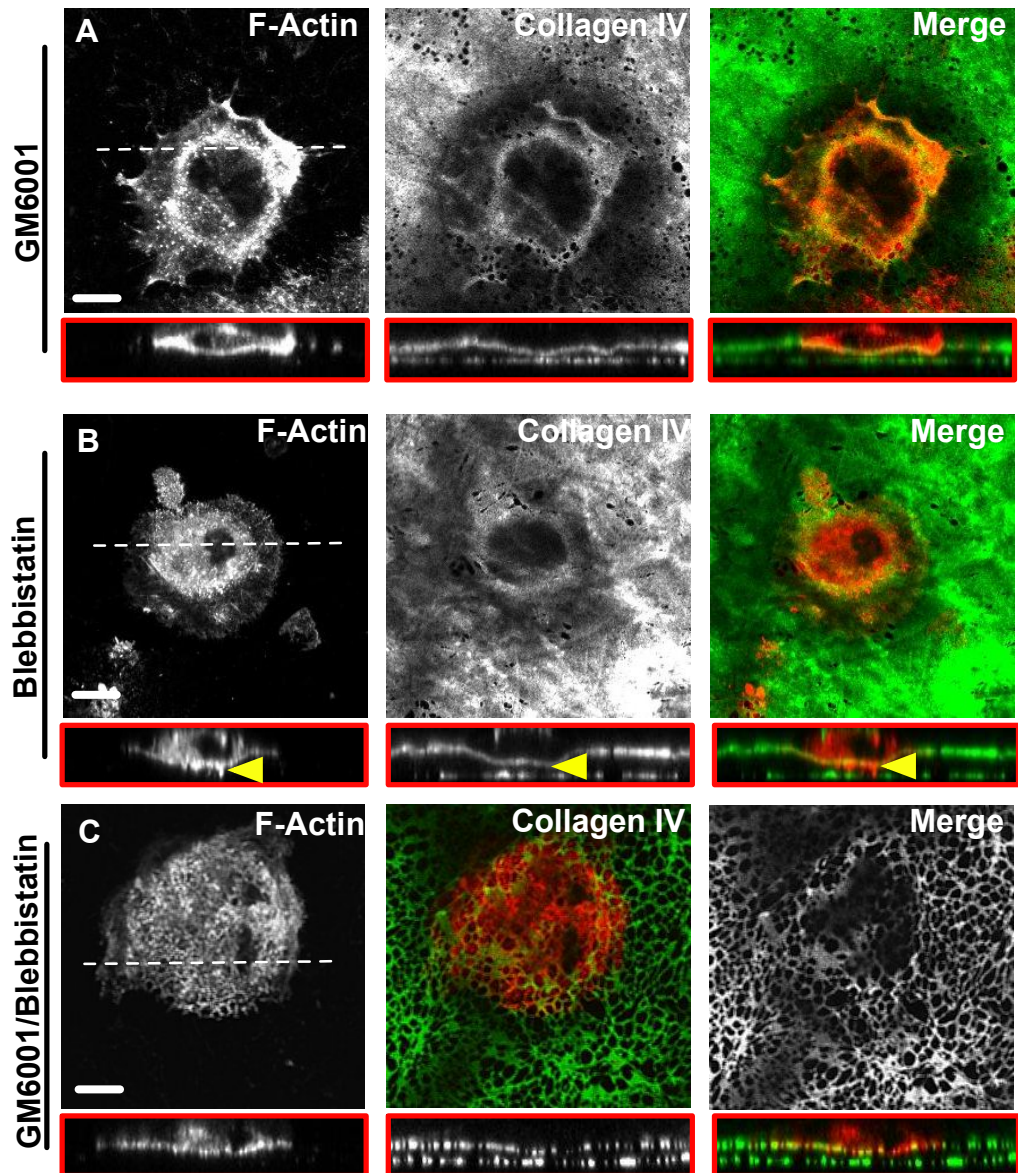


Figure 4.16: Mks use podosomes to cross a basement membrane

Mks were allowed to spread for 3h on a native basement membrane in the presence of 5 μ M GM6001 (A), 10 μ M Blebbistatin (B) and 5 μ M GM6001 together with 10 μ M Blebbistatin (C). Cells were fixed and stained for F-actin (red) and collagen IV (green), merge shows overlay of both channels. Images show XY position and underneath the corresponding Z-direction. Dotted line indicates the location of the Z-position. Yellow arrowheads highlight the protrusions crossing the membrane. Scale bar represents 20 μ m. Experiments were repeated at least 3 times.

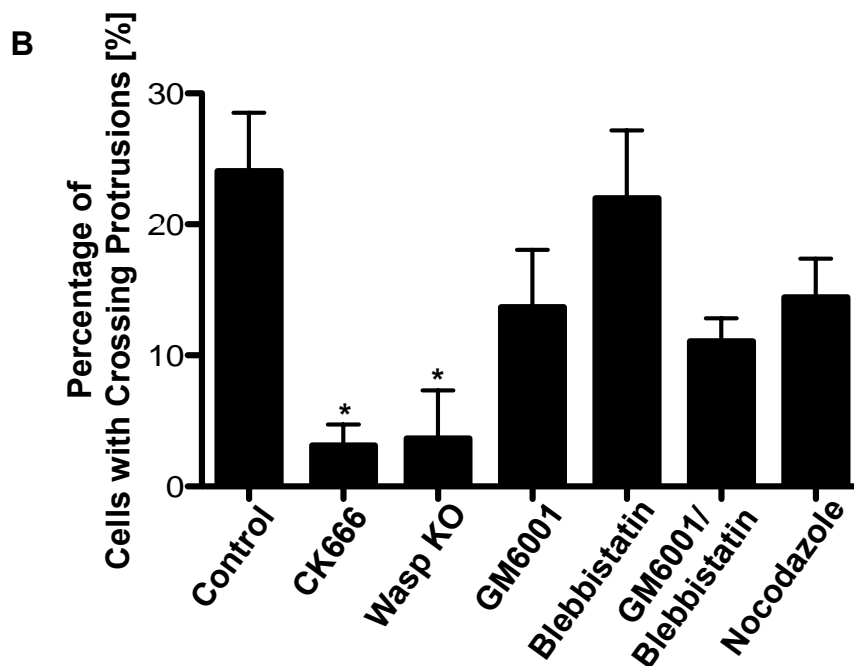
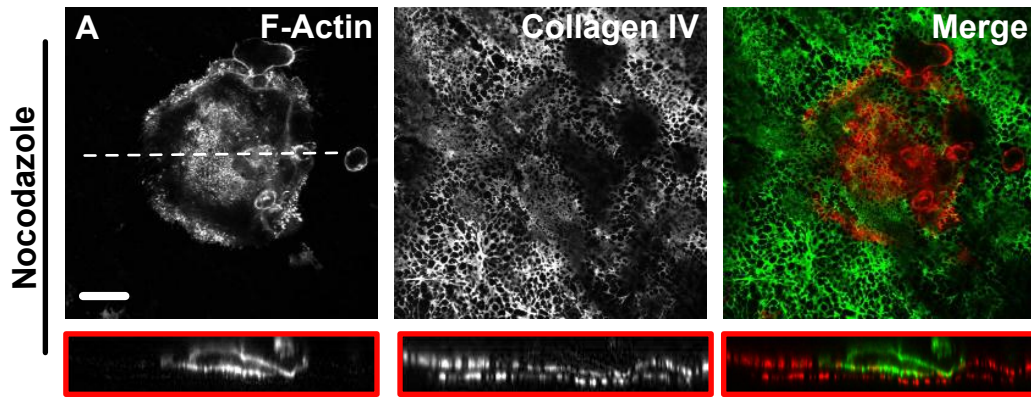


Figure 4.17: Mks use podosomes to cross a basement membrane

Mks were allowed to spread for 3h on a native basement membrane in the presence of 10 μ M Nocodazole (A). Cells were fixed and stained for F-actin (red) and collagen IV (green), merge shows overlay of both channels. Images show XY position and underneath the corresponding Z-direction. Dotted line indicates the location of the Z-position. Scale bar represents 20 μ m. The experiment was repeated at least 3 times. The percentage of crossing protrusions in the presence of different inhibitors and Wasp^{-/-} Mks was determined (B). The statistical analysis includes an ANOVA test with a Dunnett post test with asterisk indicating statistical significance with a P-value <0.05.

4.2 Discussion

Podosomes are highly dynamic F-actin based adhesion structures present in motile cells. The turnover of podosomes is cell type specific, macrophage podosomes for example undergo fission and fusion and their lifetime correlates with their position within the cell (Evans *et al.*, 2003). However, the lifetime of podosomes was predominantly determined in cells such as osteoclasts, dendritic cells or macrophages, spreading on glass but not on physiological relevant substrates like fibrinogen or collagen (Hammarfjord *et al.*, 2011; Destaing *et al.*, 2003; Bhuwania *et al.*, 2012). In this chapter I determined Mk podosome lifetime on collagen I and fibrinogen. Interestingly, podosomes on fibrinogen had a shorter lifetime than on collagen I implicating that the substratum dictates the turnover of podosome formations. Furthermore, it was recently reported that podosome-like structures in osteoclasts have a more dynamic turnover on a smooth surface compared to a rough surface (Geblinger *et al.*, 2012). With fluorescent microscopy I demonstrated that 488-labelled fibrinogen forms a “smooth” monolayer, whereas fluorescently-labelled collagen is present in chunks of fibres indicating a ‘rough’ surface topography. By imaging the different substrates with a bright field microscope it is possible to identify collagen fibres but not fibrinogen patterns. These observations indicate that podosomes in Mks might have a mechanosensory function. This functionality of podosomes is associated with Myosin II as a key regulator in podosome-forming cell types like macrophages or fibroblasts (Labernadie *et al.*, 2010; Collin *et al.*, 2006; Collin *et al.*, 2008). In Mks I showed that on both substrates the loss of Myosin II activity causes a significant increase in the lifetime of podosomes. The inhibition of Myosin II showed no

change in podosome assembly in terms of numbers. Nonetheless, the increased lifetime might indicate a role for Myosin II in podosome disassembly (Van Helden *et al.*, 2008). Furthermore, it was reported that Myosin II is present in radial fibres of podosomes and is involved in the stiffness of the podosome core (Bhuwania *et al.*, 2012; Labernadie *et al.*, 2010). In this context it might be possible that Myosin II regulates the turnover by contractility forces of radial fibres, which are dependent on the substrate topography.

A similar effect of blocking Myosin II activity was observed in osteoclasts treated with a MMP inhibitor resulting in an increase in podosome lifetime (Goto *et al.*, 2002). However, in Mks this treatment had no effect on the lifetime.

Nevertheless, MMPs are better known to be involved in the lysis of ECM components, than in the turnover of adhesion structures and as podosomes are also associated with the degradation of extracellular matrix, I wanted to test the degradative activity of podosomes in Mks (Gawden-Bone *et al.*, 2010; Linder, 2007). The results in this chapter clearly demonstrate that Mk podosomes can degrade ECM proteins, and that on fibrinogen this degradation is MMP and Myosin-IIA dependent. These results are in agreement with other reports showing MMP and Myosin-IIA involvement in podosome driven degradation (Bhuwania *et al.*, 2012; Gawden-Bone *et al.*, 2010). It is also reported that Mks take up fibrinogen through endocytic processes, which could be the mechanism of removing the degraded substrate (Deutsch and Tomer, 2006). Unfortunately I could not reliably detect podosome driven proteolysis of collagen I. Mks seeded on a FITC-labelled gelatin substratum were not able to attach in a sufficient number to allow quantification. In addition, Alexa 488-labelled horseradish collagen did not form a monolayer, which made the quantification of degradation technically unreliable.

However, it is likely that Mks do possess collagenase activity, as shown by Lane and colleagues (Lane *et al.*, 2000). There they show the expression of MMP-9, and a SAGE expression database further identified expression of MMP-14, MMP-24, MMP-25 as well as MMP-9 (M. Tomlinson and S. Watson unpublished data).

With the establishment of the basement membrane assay I created a novel experimental setup to observe podosome formation on a native, physiological relevant substrate. For the first time I could show in Mks an abundant formation of podosomes and actin-rich protrusions crossing a native basement membrane. Furthermore, the crossing of these actin protrusions was MMP dependent, implying the need for megakaryocyte driven matrix degradation. Strikingly the loss of podosomes caused by inhibition of the Arp2/3 complex or the deficiency in Wasp resulted in a significant reduction of the percentage of crossing protrusions. Nonetheless, the inhibition of the Arp2/3 complex does not only influence the formation of podosomes but all other branched actin structures such as lamellipodia, which are prominent for the involvement in cell migration (Bryce *et al.*, 2005). The inhibition of Myosin-IIA indicated that Myosin-mediated contractility played no role in protrusion formation suggesting that manipulation of the matrix through contraction forces was not required or that the extended podosomal lifetime is able to compensate this effect.

Interestingly, the blockage of microtubule polymerization, which also blocks proplatelet formation, showed a decrease in the percentage of crossing protrusions to a similar extent as MMP inhibition. This could mean that the crossing protrusions are proplatelet arms or that the microtubule cytoskeleton is involved in Mk motility.

These data clearly link podosomes, degradation of ECM proteins, with protrusions that can cross a basement membrane, which might be potential proplatelets. This link implies that podosomes could play a fundamental role in the effective delivery of platelets into the bloodstream during proplatelet formation. As such, it is tempting to hypothesize that the lack of podosomes in Wiskott-Aldrich syndrome (WAS) patients could contribute to the thrombocytopenia associated with this disorder (Ariga, 2012). However, the removal of the spleen of Was patients improves the number of platelets weakening this hypothesis (Corash *et al.*, 1985; Mullen *et al.*, 1993). This study illuminates the role of podosomes in Mks and extends the knowledge of their dynamics related to the underlying substrate. Further investigations are needed to understand these complex structures and their role in migration, adhesion and proplatelet formation.

5 The role of Cortactin and Abi in podosome formation

5.1 Summary

Cortactin is an F-actin binding protein and was demonstrated to be essential for podosome formation, in which it is also associated with ECM degradation. The loss of Cortactin in Mks resulted in the formation of bigger podosomes but caused no change in podosome numbers or their ability to degrade extracellular matrix proteins. Another F-actin interacting protein is Abi, which is a member of the Wave complex regulating Arp2/3 activity. Heterozygous Abi-1 expression and the loss of Abi-2 (Abi-1^{+/-}Abi-2^{-/-}) had no effect on podosome assembly in Mks. However, this genotype lead to impaired platelet activation on fibrinogen in the presence of thrombin.

5.2 Introduction

Cortactin interactions with Wasp or Wip are crucial for podosome assembly in smooth muscle cells (Webb *et al.*, 2006). Furthermore, Cortactin was shown to be essential in sealing zone accumulation in osteoclasts (Tehrani *et al.*, 2006) and is also involved in megakaryocyte maturation (Zhan *et al.*, 1997). Both Cortactin and its homologue hematopoietic lineage cell-specific protein 1 (HS1) are F-actin binding proteins involved in the rearrangement of the cytoskeleton and therefore in cell migration and adhesion (Cosen-Binker and Kapus, 2006; van Rossum *et al.*, 2005). Interestingly, Cortactin is associated with matrix metalloproteases (MMPs) in invadopodia-forming cancer cells and the inhibition of Cortactin expression

blocks matrix degradation and invadopodia formation (Artym *et al.*, 2006). In this context, Cortactin might not only be involved in F-actin polymerization but also in the trafficking of MMP vesicles towards the plasma membrane and/or vesicle budding (Clark *et al.*, 2007). Because of this role of Cortactin in invadopodia formation and cell motility, I was interested in the loss of Cortactin and its effect on cell spreading, podosome formation and matrix degradation in Mks.

The Arp2/3 complex mediated rearrangement of the actin cytoskeleton is not only important for Mk spreading and podosome formation but also for platelet activation and shape change (Li *et al.*, 2002). The Arp2/3 complex is regulated by Wasp family members, one of these members is the Wave complex, which is involved in the formation of lamellipodia (Pollitt and Insall, 2009). It was previously reported that the Wave complex is involved in the development of Mks and their spreading behavior as well as in glycoprotein VI (GPVI) mediated platelet activation (Calaminus *et al.*, 2007; Eto *et al.*, 2007). One member of the Wave complex is Abi, which is implicated in invadopodia formation in breast cancer cells (Sunt *et al.*, 2009) and interestingly, in the development and the spreading behavior of megakaryocytes (Eto *et al.*, 2007). In this context, I used Abi-1^{+/+}Abi-2^{-/-} and Abi-1^{+/-}Abi-2^{-/-} deficient Mks and platelets to evaluate the role of Abi-1/Abi-2 in spreading, podosome assembly, platelet activation and actin nodule formation.

5.3 Results

5.3.1 The loss of Cortactin in Mks changes podosome size but not its degradative activity

In order to demonstrate the relevance of Cortactin in Mk podosome formation, Mks derived from conditional Cortactin^{-/-} mice (Pf4Cre-Cortactin^{-/-}, platelet factor 4 (Pf4) is a Mk and platelet specific cytokine) were allowed to spread on fibrinogen (Figure 5.1). There was no difference in the localization of F-actin and Wasp between control and Cortactin^{-/-} cells. Furthermore, no change in the number of podosomes, the spread area or podosomes per area could be determined (Figure 5.2A-C). Although there was no change in the number of podosomes, the actual size of single podosomes increased in Cortactin deficient Mks by almost 40% (Figure 5.2D). Because the size changed and additionally Cortactin is known to interact with MMPs, I wanted to test the degradative activity of Cortactin^{-/-} Mks (Figure 5.3). Litter matched control cells spread normal on the 488-labelled fibrinogen matrix (Figure 5.3). Clear holes were visible in the substrate, which colocalized partially with F-actin rich spots indicating the degradation of fibrinogen by podosomes. However, the same was determined for Cortactin^{-/-} Mks spread 488-labelled fibrinogen (Figure 3B). There was no difference in the percentage of cells undergoing podosome-mediated fibrinogen degradation (Figure 5.3C).

These data indicate a regulative role for Cortactin in podosome size, but not in podosome assembly or ECM degradation mediated by Mks.

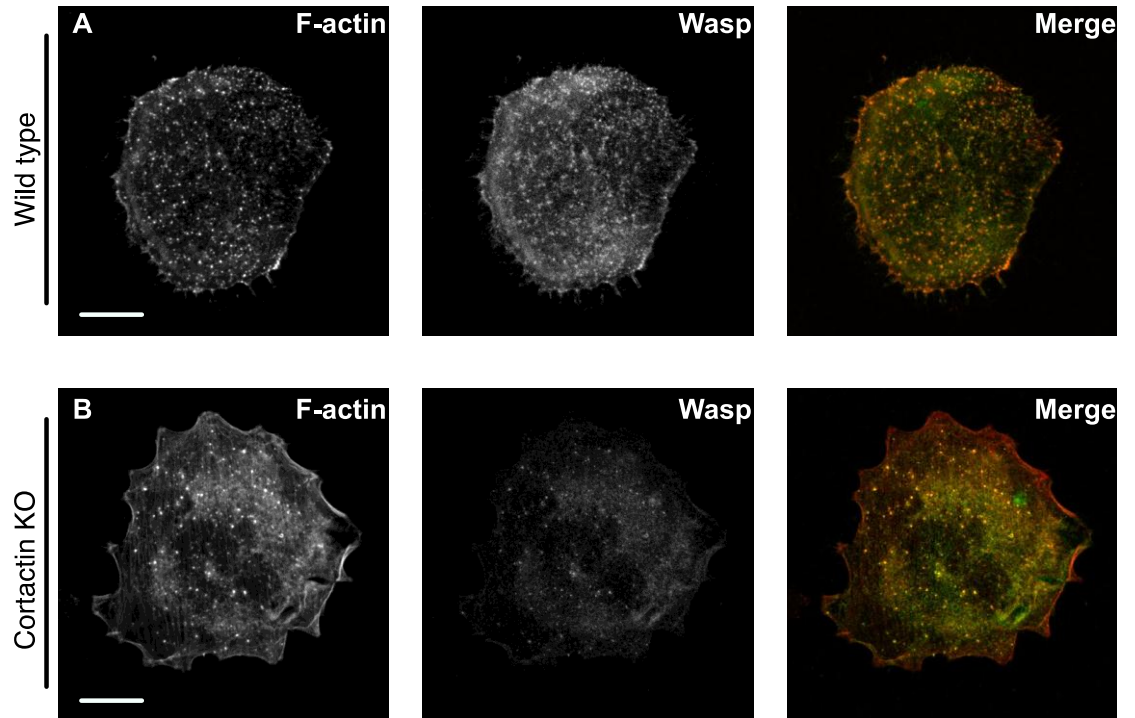


Figure 5.1: Cortactin^{-/-} Mks form podosomes on fibrinogen

Litter matched control (A) and Cortactin^{-/-} (B) Mks were allowed to spread for 3 h on a fibrinogen-coated surface. Cells were fixed and stained for F-actin (red) and Wasp (green), the overlay of both channels is shown in the third image of each row. Images are representative for a repeat of four experiments. Scale bar indicates 10µm.

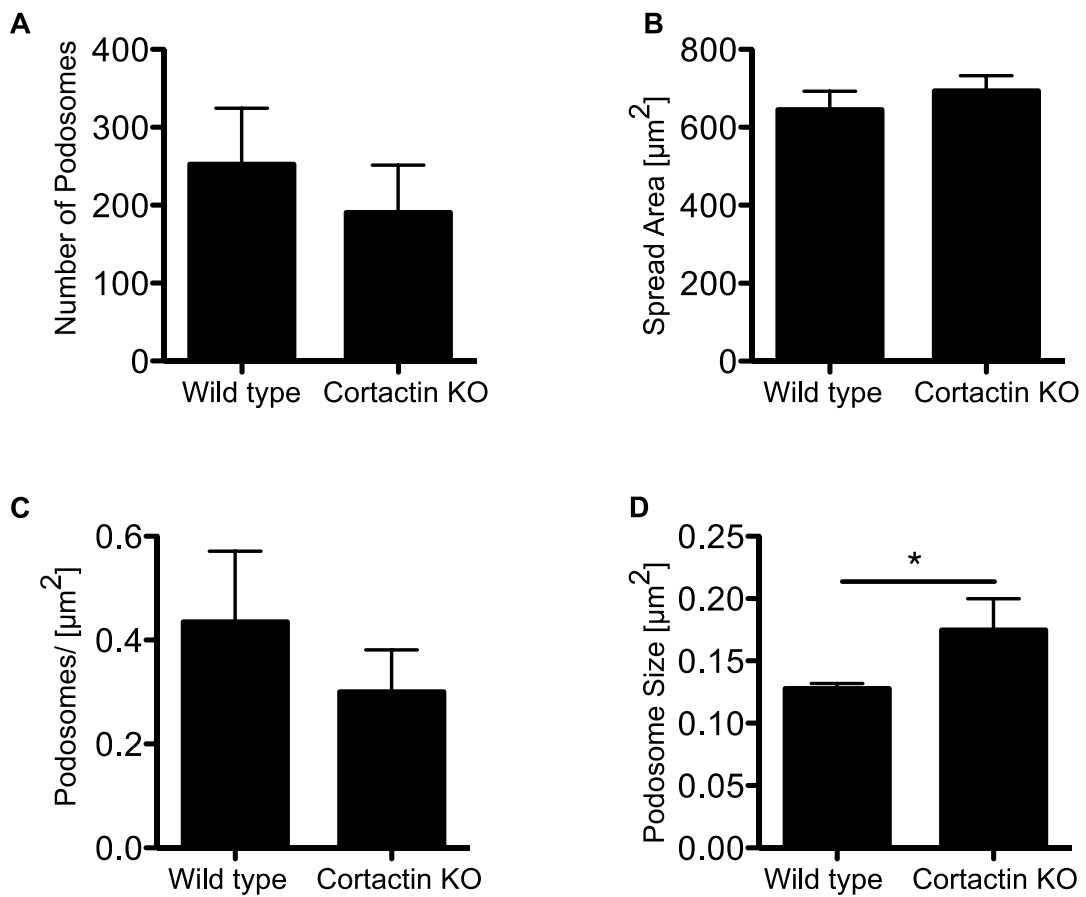


Figure 5.2: Cortactin^{-/-} Mks form podosomes on fibrinogen

The number of podosomes (A), the spread area (B), podosomes per area (C) and the podosome size (D) was determined for Cortactin^{-/-} and litter matched Mks spread on fibrinogen. A student's t-test was performed, asterisk indicates a significant difference with a P-value <0.05. Graphs include data of four experiments.

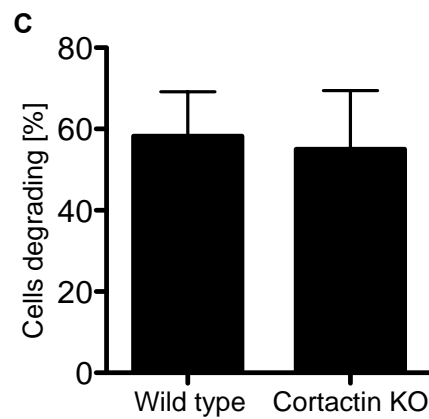
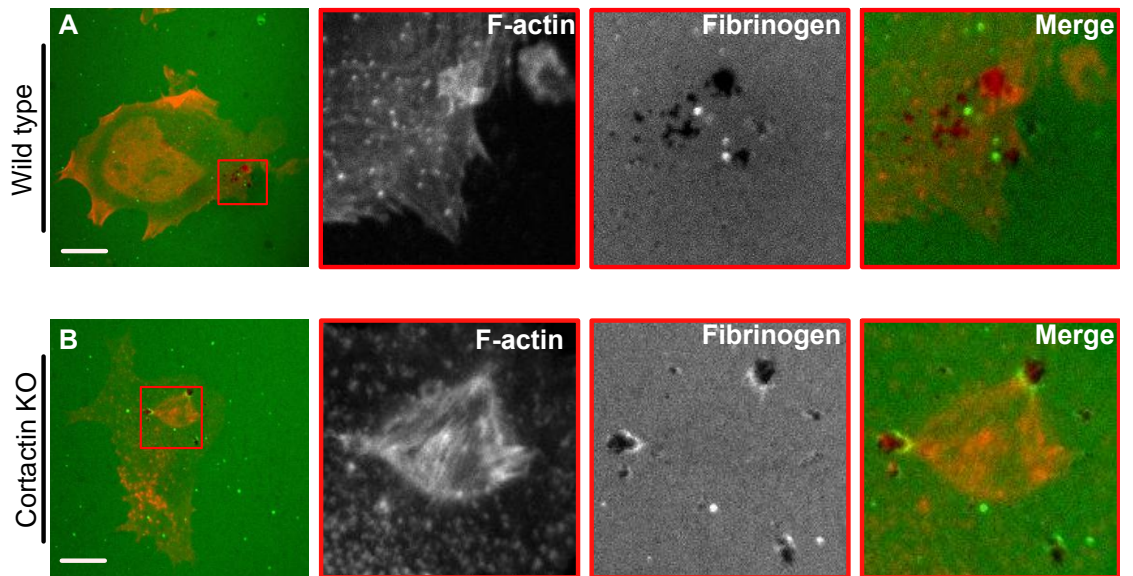


Figure 5.3: Cortactin^{-/-} Mks perform podosome mediated degradation of fibrinogen

Litter matched control (A) and Cortactin^{-/-} (B) Mks were allowed to spread for 3 h on a 488-labelled fibrinogen-coated surface. Cells were fixed and stained for F-actin. The red squares indicate the magnified area. Scale bar represents 10 μm. The percentage of degrading cells was determined (C). A student's t-test was performed, asterisk indicates a significant difference. Graph includes data of four experiments.

5.3.2 Podosome formation and spreading behavior is not changed in Abi-1^{+/-}Abi-2^{-/-} deficient Mks

To test the involvement of Abi-1 and Abi-2 and therefore the Wave complex in Mk spreading and podosome formation, Abi-1^{+/+}Abi-2^{-/-} and Abi-1^{+/-}Abi-2^{-/-} Mks were allowed to spread on a fibrinogen substrate. In both Abi-1^{+/+}Abi-2^{-/-} and Abi-1^{+/-}Abi-2^{-/-} deficient Mks, there was no change in the localization of the Arp2/3 complex or Wasp (Figure 5.4A-D). The morphology was not different from wild type MKs. The number of podosomes was slightly increased, but not by a significant amount (Figure 5.5A). The cell area was for all genotypes relatively high (compared to previous spreading experiments) for spreading on fibrinogen (Figure 5.5B), with corresponding low values for the amount of podosomes per area (Figure 5.5C). However, the size of podosomes was in an expected range and either Abi-1^{+/+}Abi-2^{-/-} or both Abi-1^{+/-}Abi-2^{-/-} Mks showed a difference compared to wild type Mks (Figure 5.5D).

These data demonstrate that Abi-2 has no major role in podosome formation and that Abi-1 can compensate the loss of Abi-2.

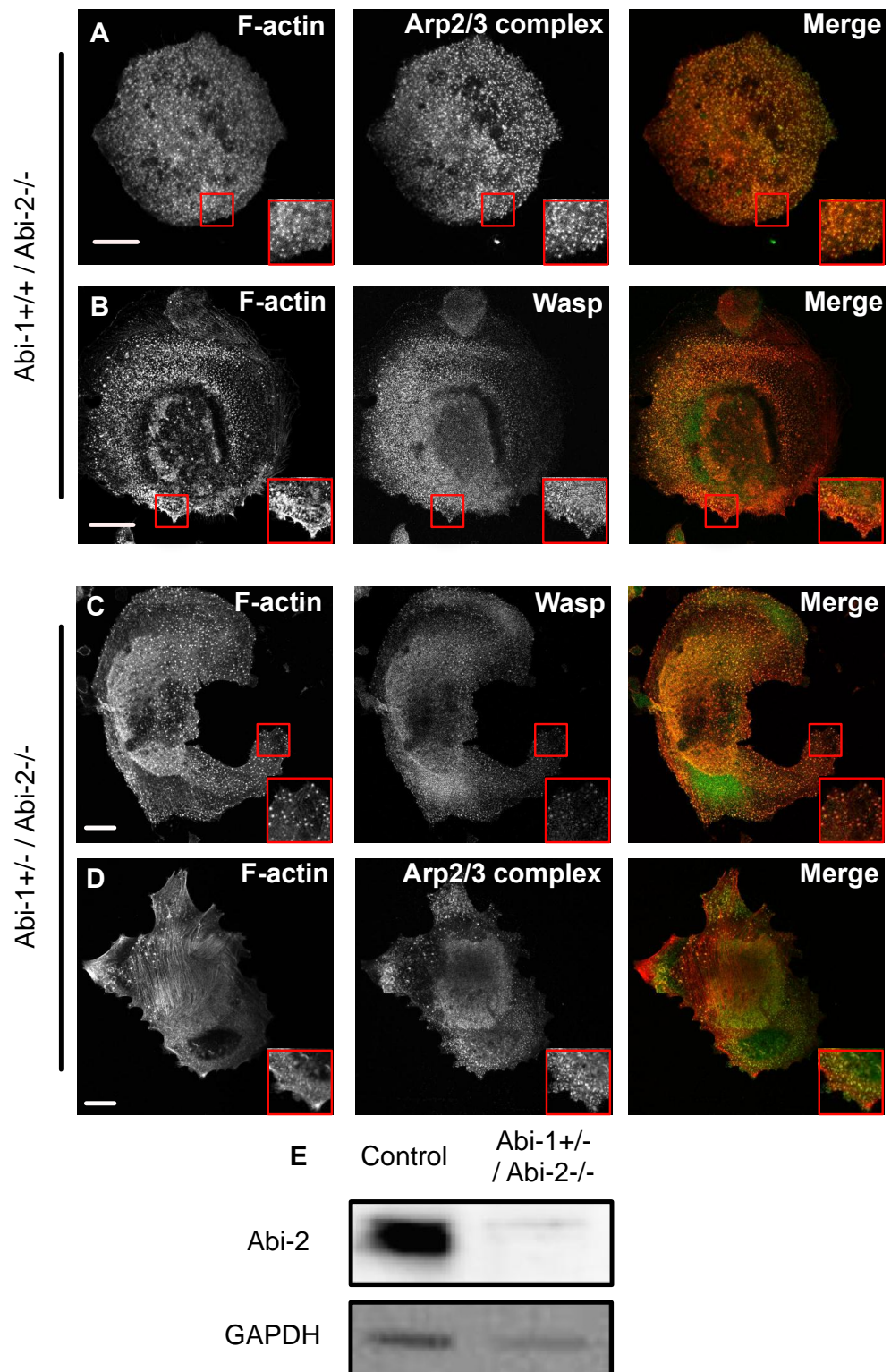


Figure 5.4: The loss of Abi-2 does not influence podosome formation in Mks

Abi-1^{+/+}/Abi-2^{-/-} (A,B) and *Abi-1^{+/-}/Abi-2^{-/-}* (C,D) Mks were allowed to spread for 3h on a fibrinogen-coated surface. Cells were fixed and stained for F-actin (red) and Wasp or the Arp2/3 complex (green), the overlay of both channels is shown in the third image of each row. Cell extracts of wild type control Mks and *Abi-1^{+/-}/Abi-2^{-/-}* Mks, subjected to SDS-PAGE and subsequently analyzed by Western blotting using indicated antibodies (E). Images are representative for a repeat of three experiments. Scale bar indicates 10 μ m.

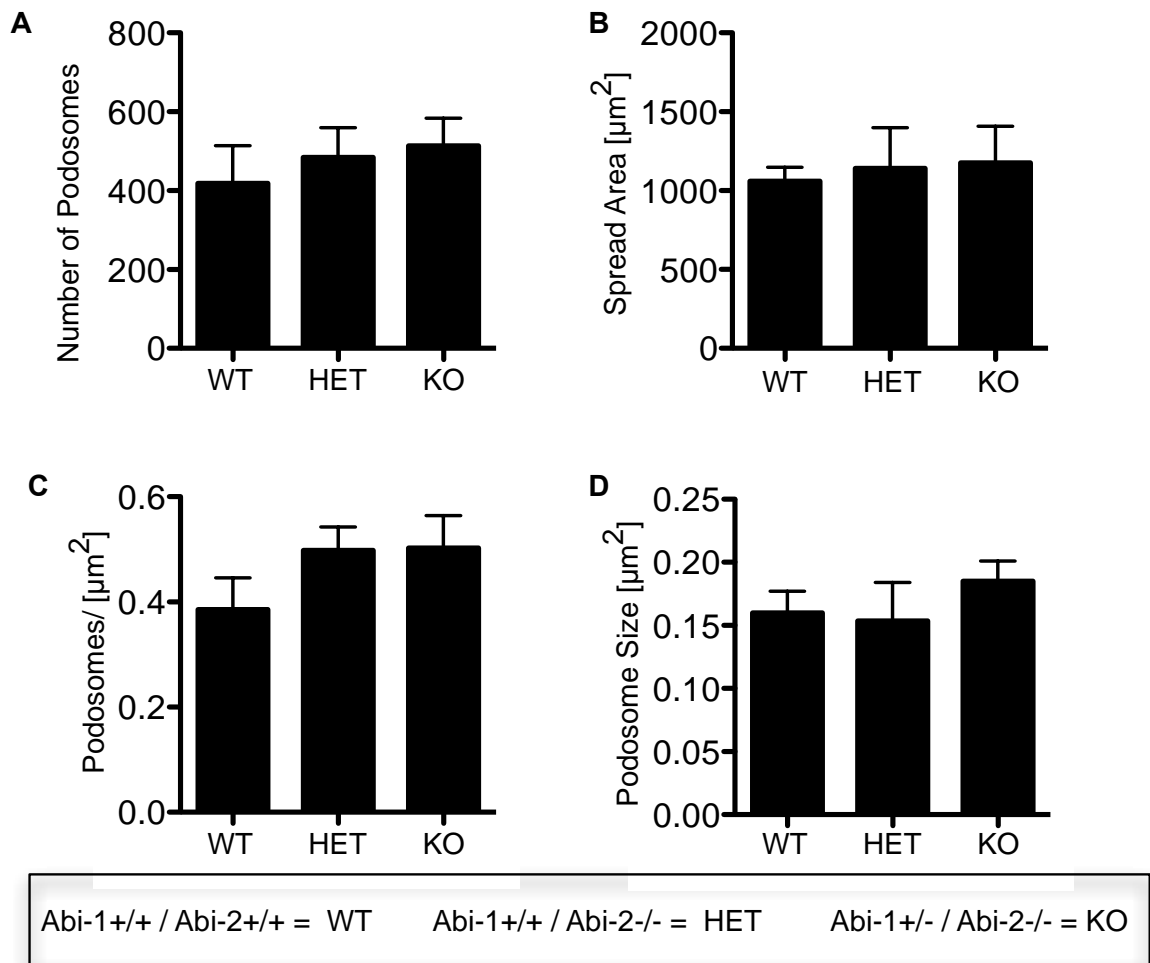


Figure 5.5: The loss of Abi-2 does not influence podosome formation in Mks

The number of podosomes (A), the spread area (B), podosomes per area (C) and the podosome size (D) was determined for Abi-1^{+/+}/Abi-2^{-/-} (HET), Abi-1^{+/+}/Abi-2^{-/-} (KO) Mks spread on fibrinogen. A student's t-test was performed, asterisk indicates a significant difference with a p-value <0.05. Graphs include data of three experiments.

5.3.3 **Abi-1^{+/-}Abi-2^{-/-} platelets have a reduced spread area on fibrinogen in the presence of thrombin**

To evaluate the involvement of Abi-1 and Abi-2 in the spreading behavior of platelets, as well as to illuminate the role of these proteins in the assembly of actin nodule structures, spreading experiments were performed on collagen and fibrinogen with and without thrombin (Figure 5.6; Figure 5.7 and Figure 5.8). As the loss of Abi-2 (Abi-1^{+/+}Abi-2^{-/-}) did not have a phenotype and Abi-1^{+/+}Abi-2^{-/-} platelets show the same spreading behavior as wild type platelets (compare McCarty *et al.*, 2005), Abi-1^{+/+}Abi-2^{-/-} platelets were used as control. Platelets of both genotypes were spread on collagen and stained for F-actin and the Arp2/3 complex, to verify if the partial loss of Abi-1 and the loss of Abi-2 (Abi-1^{+/-}Abi-2^{-/-}) induced a change in the localization of F-actin and the Arp2/3 complex. However, clear stress fibers were visible and the Arp2/3 complex located towards the rim of the spread platelets as expected (Figure 5.6A,B). No difference in the spreading area could be detected between the control and Abi-1^{+/-}Abi-2^{-/-} platelets (Figure 5.6C). The spreading behavior of Abi-1^{+/-}Abi-2^{-/-} platelets was also evaluated on fibrinogen, but no difference was determined for the localization of F-actin, the Arp2/3 complex or the spread area compared to litter matched control platelets (Figure 5.7A,B and C). Additionally, around 50% of both control and KO platelets formed actin nodules (Figure 5.7D). Control and Abi-1^{+/-}Abi-2^{-/-} platelets spread on fibrinogen were additionally treated with thrombin (Figure 5.8). The immunofluorescence staining for F-actin and the Arp2/3 complex was not different, but the Abi-1^{+/-}Abi-2^{-/-} cells had a more spiky morphology compared to the more rounded and coffee bean-shaped control platelets. Interestingly, the KO platelets had also a significantly smaller spread area (Figure 5.8C). However, there was no difference in the percentage of platelets forming actin nodules.

The above data demonstrate that Abi-2 is not relevant for platelet spreading and that its loss can be compensated by Abi-1. Nevertheless, the partial loss of Abi-1 and the complete loss of Abi-2 affect platelet spreading on fibrinogen with thrombin treatment.

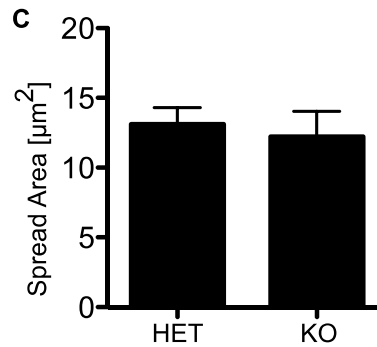
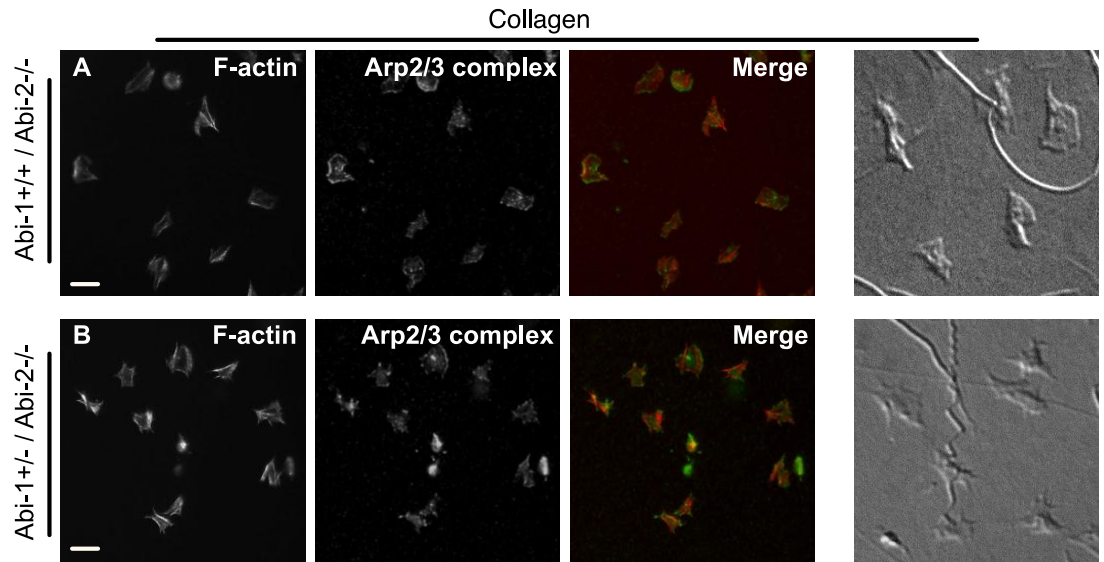


Figure 5.6: The heterozygous expression of Abi-1 does not affect platelet spreading on collagen I

Abi-1+/+/Abi-2-/- (A), Abi-1+/-/Abi-2-/- (B) platelets were allowed to spread for 45min on collagen I. Platelets were fixed and stained for F-actin (red) and the Arp2/3 complex (green). The spread area (C) of at least 60 platelets per experiment was determined. A student's t-test was performed, asterisk indicates a significant difference with a P-value <0.05. Graphs include data of three experiments.

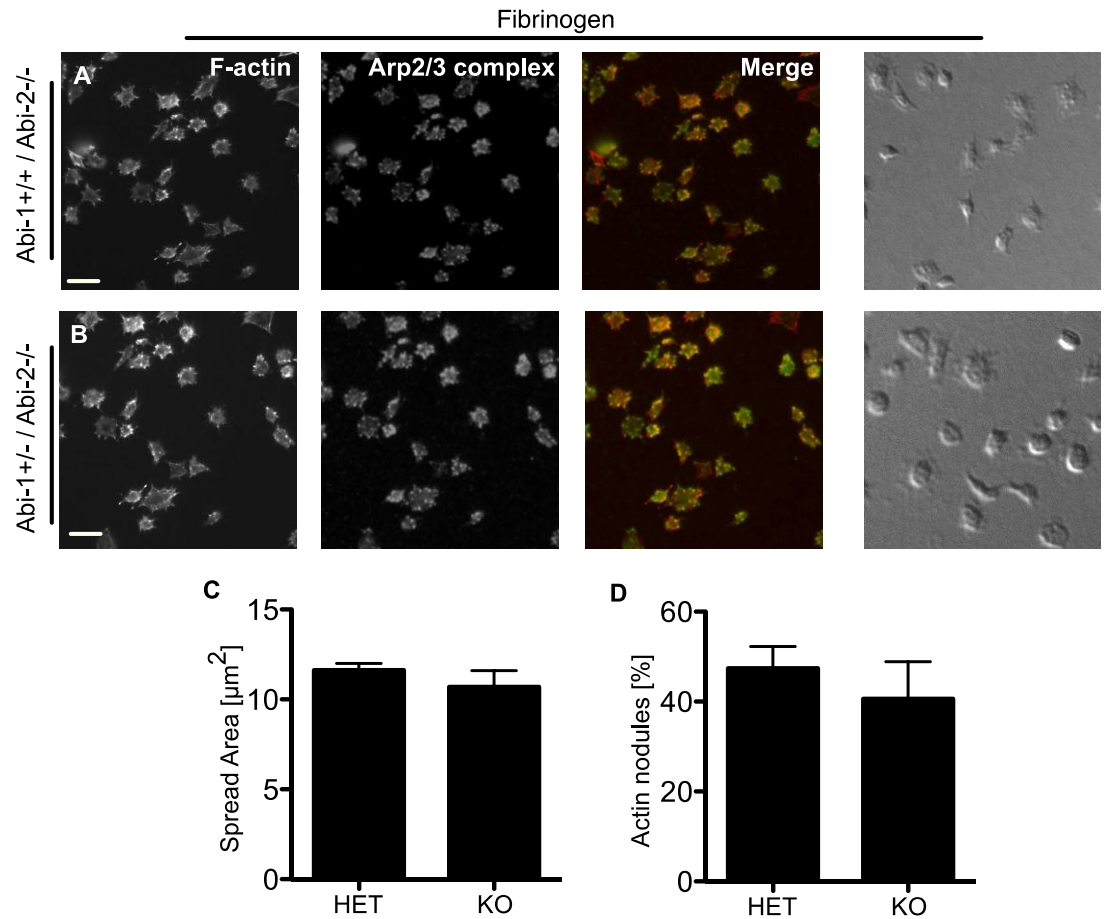


Figure 5.7: The heterozygous expression of Abi-1 does not affect platelet spreading or actin nodule formation on fibrinogen

Abi-1+/+/Abi-2-/- (A), Abi-1+/-/Abi-2-/- (B) platelets were allowed to spread for 45min on fibrinogen. Platelets were fixed and stained for F-actin (red) and the Arp2/3 complex (green). The spread area (C) and the appearance of actin nodules was determined by analyzing at least 60 platelets per experiment. A student's t-test was performed, asterisk indicates a significant difference with a P-value <0.05. Graphs include data of three experiments.

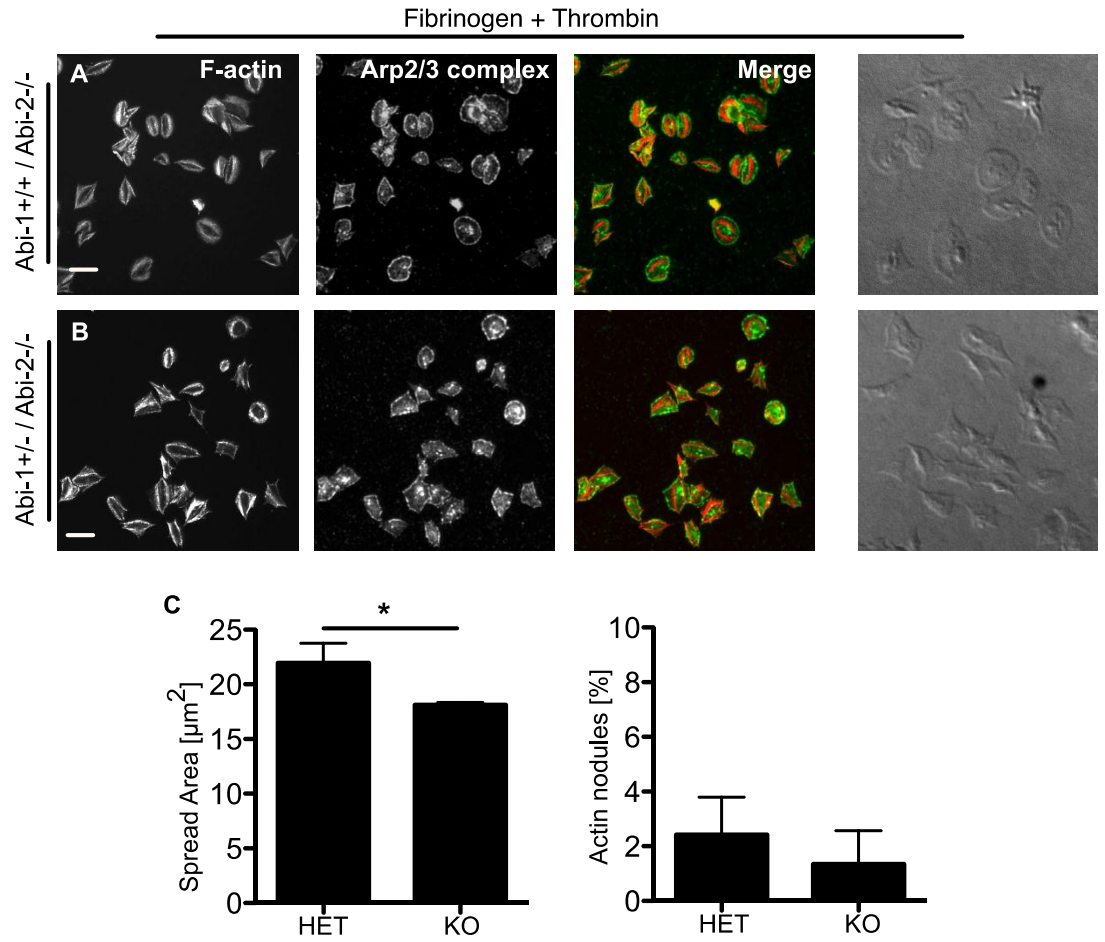


Figure 5.8: The heterozygous expression of Abi-1 does not affect platelet spreading or actin nodule formation on fibrinogen in the presence of thrombin

Abi-1^{+/+}/Abi-2^{-/-} (A), Abi-1^{+/-}/Abi-2^{-/-} (B) platelets were allowed to spread for 45min on fibrinogen in the presence of 1 U/ml thrombin. Platelets were fixed and stained for F-actin (red) and the Arp2/3 complex (green). The spread area (C) and the appearance of actin nodules were determined by analyzing at least 60 platelets per experiment. A student's t-test was performed, asterisk indicates a significant difference with a P-value < 0.05. Graphs include data of three experiments.

5.4 Discussion

The dynamic rearrangement of the F-actin cytoskeleton is the requirement for intact cell spreading and the formation of actin-based adhesion structures such as podosomes (Machesky *et al.*, 1999; Luxenburg *et al.*, 2012). The major player of these processes is the Arp2/3 complex, which is regulated by members of the Wasp family, but beside these proteins there are other potential Arp2/3 complex regulators. Such a potential regulator is Cortactin, which can bind directly to the Arp2/3 complex (Urano *et al.*, 2003b). In addition, Arp2/3 complex activation can be enhanced by Cortactin interactions with the Wasp-interacting protein (WIP) (Kinley *et al.*, 2003; Banon-Rodriguez *et al.*, 2010). In hematopoietic cells, there is a Cortactin homologue called hematopoietic lineage cell-specific protein I (HS1). However, Mks and platelets express both Cortactin and HS1 (van Rossum *et al.*, 2005). This fact might explain why Cortactin^{-/-} Mks show no spreading defect and no change in podosome numbers. However, the above results also demonstrate that the size of podosomes increased with the loss of Cortactin. In this context, it was reported that spleen derived dendritic cells deficient in Cortactin-binding domain of WIP induce the assembly of undefined podosome structures. Another report confirms these data with HS1^{-/-} bone marrow derived dendritic cells (Banon-Rodriguez *et al.*, 2005; Dehring *et al.*, 2011). This could mean that Cortactin has a regulatory function in the overall organization of a single podosome. Luxenburg and colleagues (Luxenburg *et al.*, 2012) described a similar role for Cortactin as a nucleation and stabilization factor of F-actin in podosome assembly and disassembly. Furthermore, the podosome lifetime was shown to be dependent on Src-mediated tyrosine phosphorylation of Cortactin (Luxenburg *et al.*, 2007). These data highlight the cell-type specific accumulation of podosomes, in contrast

to osteoclasts, which display a reduced Cortactin expression leaving them unable to assemble any podosomes (Tehrani *et al.*, 2006).

Besides its role as a potential regulator of podosome organization Cortactin is also associated with podosome- as well as invadopodia-mediated ECM degradation in dendritic cells or breast cancer cells (Banon-Rodriguez *et al.*, 2011; Artym *et al.*, 2006). Interestingly, Cortactin deficient Mks showed no change in the percentage of degrading cells. A possible explanation could be that Cortactin has no direct role in MMP-trafficking in Mks, but has a role in the structural organization and the turnover of podosomes. Another possibility is that the loss of Cortactin can be compensated by the upregulation of HS1.

Other potential proteins involved in spreading of Mks were Abi-1 and Abi-2, which are members of the Wave complex, which regulates the activity of the Arp2/3 complex and therefore F-actin nucleation. The knockout of Abi-1 is observed to be embryonic lethal at approximately embryonic day 11.5 (Dubielecka *et al.*, 2011). Furthermore Abi is known to be essential for the stability of the pentameric complex (Kunda *et al.*, 2003). In collaboration with M. Pendergast I used Abi-1^{+/+}/Abi-2^{-/-} and Abi-1^{+/-}/Abi-2^{-/-} mice and isolated bone marrow derived Mks as well as platelets from blood. Mks from both genotypes did not show a difference in spreading or podosome formation indicating that the Wave complex is not involved in these processes in Mks and that the redundant Abi-1 expression is adequate for the complex formation or that another member of the Wasp family can substitute it. These results are in contrast to other reports, which demonstrate a role for Wave-2/Abi-1 in lamellipodia formation (Eto *et al.*, 2007). However, these data are based on experiments with Mks derived from embryonic stem cells and not murine bone marrow.

Wave-1 was shown to play a major role in murine platelet spreading mediated by GPVI signaling on a collagen-related peptide (Calaminus *et al.*, 2007). Furthermore, it is reported that Abi-1^{+/-}/Abi-2^{-/-} cells have a decreased Wave-1 protein level (Echarri *et al.*, 2004). However, Abi-1^{+/+}/Abi-2^{-/-} and Abi-1^{+/-}/Abi-2^{-/-} platelets showed no difference in the spreading behavior on collagen or fibrinogen. Nevertheless, spreading of Abi-1^{+/-}/Abi-2^{-/-} platelets on fibrinogen with thrombin treatment was significantly decreased and the platelets had a more spiky appearance. The reduced level of the Wave-1 complex and therefore the reduced ability of lamellipodia formation could explain this result. However, this would be in contrast to previous studies, which demonstrated that the loss of Wave-1 does not influence platelet activation on fibrinogen (Calaminus *et al.*, 2007). Another explanation could be that the signaling via G-protein coupled receptor (activated by thrombin binding) recruits Abi interactions with the Wave-2 complex. Another hypothesis is that Abi interacts with formins like reported by Ryu and colleagues, describing the interaction of Abi-1/-2 with Diaphanous-related formins (Ryu *et al.*, 2009). To verify a clear function of Abi in platelet spreading as well as to understand the ongoing signaling cascades on the different substrates in more detail, more investigations need to be done such as the determination of the Wave complex expression level, the identification of other potential binding partners of Abi or the detection of Abi-3 expression.

6 General Discussion

6.1 Summary

In this thesis, I characterized podosomes in megakaryocytes in correlation with the underlying extracellular substrate. It demonstrate that the Arp2/3 complex and Wasp were essential for podosome assembly, that Mk podosomes were able to degrade matrix proteins and that their lifetime was dependent on Myosin-IIA as well as the topography of the substrate. Furthermore, I determined a crucial role for podosomes in the process of crossing a native basement membrane. The present results illuminate the structure and properties of podosome organelles in Mks and with these direct a possible function in migration and platelet production.

6.2 The ECM directs podosome properties and function

Previous studies demonstrated that the underlying or surrounding matrix influences the cellular behavior in the context of adhesion, migration and ECM degradation. I discussed above the potential function of podosomes as a mechanosensor. The first podosome components “sensing” the rigidity of the substrate are Integrin receptors or CD44 by binding to their ligand. This binding action potentially regulates the activity of prominent candidates of mechanosensory processes such as Myosin-II. Inhibiting Myosin-II increased the lifetime of podosomes in Mks. Other studies demonstrated that the loss of Myosin-II activity reduces the stiffness of the actin core and that Myosin-II is localized to radial actin fibers (Bhuwania *et al.*, 2012; Labernadie *et al.*, 2010). These results

emphasize the regulation of the lifetime but also the stiffness of the actin core by Myosin-II-driven contractility forces mediated by radial fibers. These radial fibers might be interconnected with other podosomes, building a sensing network throughout the whole cell, which facilitates the recognition of environmental changes. In line with this is a constant density of podosomes in Mks, which is dependent on the matrix protein and underlines the mechanosensory property of podosomes. Because the number and the lifetime of podosomes are affected by the substrate topology, it is likely that the migratory behavior is influenced as well.

Invadopodia were demonstrated to increase their degradative ability if formed on stiffer substrates (Alexander *et al.*, 2008). However, to my knowledge this was not demonstrated so far for podosome structures. Based on the above observations and the influence of ECM composition and flexibility on podosome properties, it could very well be true.

The physical properties of the different substrates need to be considered in order to understand the fundamental regulation of podosome assembly and to direct a substrate-dependent physiological role of these structures. In *in vivo* conditions cells encounter matrices of varying composition and mechanical properties, so it is important to explore this in *in vitro* conditions as well.

6.3 Podosome formation in 3D and *in vivo*

Podosome structures are well established on a 2D substrate. However, the formation in a more physiological relevant context such as in a 3D environment is needed and is the focus of recent studies (Cougoule *et al.*, 2010; Jevnikar *et al.*, 2012). Mks embedded in a 3D collagen I environment assembled podosome-like

structures similar to podosomes formed in 2D conditions (Figure 6.1). The formed structures are F-actin rich and align along the collagen fibers, which seem to be concentrated at those podosome-like organelles implying possible contraction forces mediated by the cell (Figure 6.1, arrows). This experimental setup indicates that Mks potentially form podosome-like structures in 3D, although further investigation are needed such as the staining for other podosome markers such as Vinculin, Paxillin or Cortactin. In addition, this data indicates that mature Mks use a mesenchymal rather than an amoeboid migration mode. This assay might be useful to explore the possible interactions between Mk and its environment, possibly mimicking a similar situation in the bone marrow niche.

The different appearance of podosomes in 2D versus 3D is possibly caused by change of the physical organization of the matrix into a gel structure. The stiffness of the 3D matrix can influence the podosome composition. A good example is the loss of the Vinculin ring structure, which could not be detected in 3D podosome formations (Goethem *et al.*, 2010). Another crucial subject in the podosome field is the evidence of these structures *in vivo*. Recently a study was published demonstrating the formation of podosomes by smooth muscle cells in aortic vessels visualized by electron microscopy (Quintavalle *et al.*, 2010). However, further investigations are needed focusing on matrix degradation, lifetime and protein composition in order to determine how similar and how comparable the podosome structures are, when formed in 2D, 3D or in *in vivo* conditions.

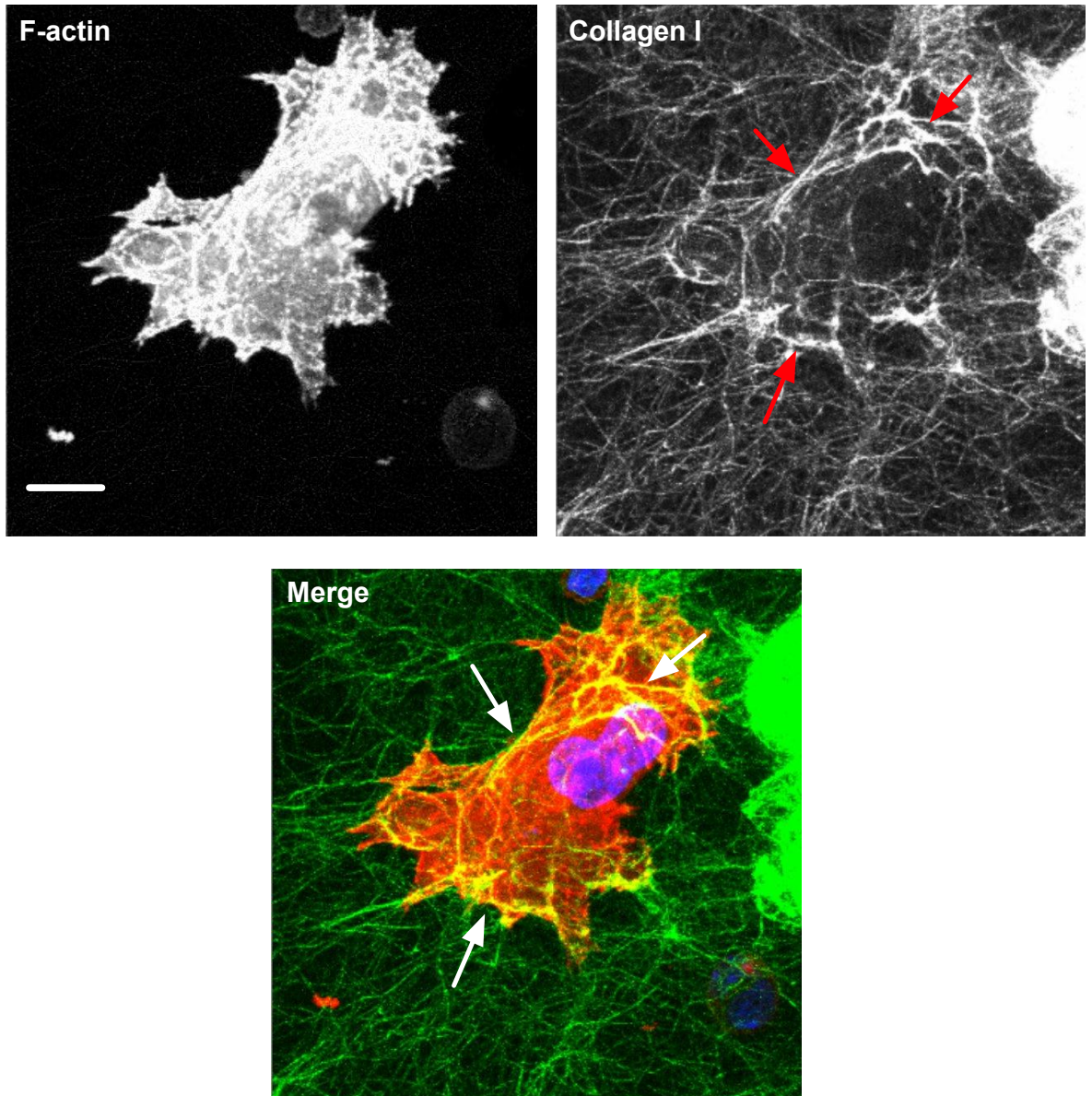


Figure 6.1: Mks form podosome-like structures in a 3D collagen I matrix

Mks were embedded into a FITC-labelled collagen I gel and incubated over night at 37°C in an incubator. The gel was fixed with formaldehyde for 30min, washed and stained for F-actin and DNA. Images represent maximum intensity projections of the taken Z-stack. Arrows show concentration of collagen fibers, which colocalize with F-actin rich structures. Scale bar indicates 10µm. A 3D reconstruction is included in the supplementary data.

6.4 Podosome structures in Mks – a direction of functionality

The previous report of podosome structures in Mks only performed limited and very basic description (Sabri *et al.*, 2006). The results of my study describe a fundamental analysis of podosome structure, organization, lifetime and degradative activity in Mks, which was not shown before. In comparison to single podosome structures in other cell types there was no elementary difference detectable. Although, Mks assemble higher numbers of podosomes compared to macrophages or dendritic cells (Stolting *et al.*, 2012; Olivier *et al.*, 2005). This observation might be explained by the bigger size of Mks compared to the other cell types and the correlative increase of podosome numbers. Another possible explanation might be an increased Integrin expression, which is maintained for the later released platelets. These Integrins might be used for podosome assembly and get recycled after disassembly to function in platelets.

In this context, I want to emphasize the potential function of podosomes in Mks. The described spreading data highlight the role of podosomes in adhesive actions. However, our experiments with Wasp KO Mks demonstrate that podosomes are not essential for spreading or adhesion. Nevertheless, the difference in podosome number and their lifetime on fibrinogen and collagen implies that these structures are able to sense differences in substrate composition. In correlation with the model of Mk maturation and platelet release, in which Mks need to migrate from the osteoblastic niche to the vascular niche, these results might indicate that podosomes have a role in Mk orientation, direction and migration by interacting with the different matrix proteins (Kopp *et al.*, 2005). Beside the mechanosensory

task of these structures, the degradation of the ECM is another crucial property of podosomes. The degradative ability of podosomes in Mks potentially functions to penetrate the collagen network in the bone marrow niche as well as the vascularity containing a basement membrane structure. I was not able to detect the degradation of collagen I fibers by Mk podosomes. However, I believe that this is based on technical issues rather than the inability of Mks to lyse collagen. The prolonged lifetime of podosomes on collagen I (Figure 4.7) might be explained by the fact that the Mk is possibly longer exposed to a rigid collagen environment than to a fibrinogen matrix. The degradation of a peritoneal basement membrane was difficult to detect because of the discontinuous staining of BM components and the variable nature of this assay. Nevertheless, the crossing of the basement membrane in an MMP-dependent manner and the detection of collagen IV positive staining inside the Mks (Figure 4.16B) indicate the removal of this matrix by Mks. The clear fibrinogen lysis by Mk podosomes enforces the hypothesis that podosomes facilitate the penetration through matrix and in the case of fibrinogen potentially the invasion into the blood vessel to release platelets. In addition, there is a significant difference in the nuclei size of degrading and non-degrading Mks (Figure 6.2). Potentially, this preliminary result implies that more mature Mks have an increased ability to degrade ECM proteins. This perfectly fits in our model, in which mature Mks use podosomes to migrate through the different niches, while immature Mks use an amoeboid migration mode, which is independent of MMP activity. However, further experiments are needed, such as investigating the correlation of podosome numbers and Mk maturity, to confirm this idea. I hypothesize, that observed functions of podosomes in Mks are crucial for Mk maturation and ultimately platelet formation. This hypothesis is enforced by Wasp KO mice, which form proplatelets and platelets in the bone marrow, and by

Wiskott-Aldrich syndrome patients, which suffer from microthrombocytopenia (Sabri *et al.*, 2006). However, the reduced platelet number can be improved by the removal of the spleen indicating multifaceted defects caused by the loss of Wasp. Nonetheless, the premature production of platelets is not recovered, which implies that podosomes could be essential for the direction of Mks towards the vascular niche.

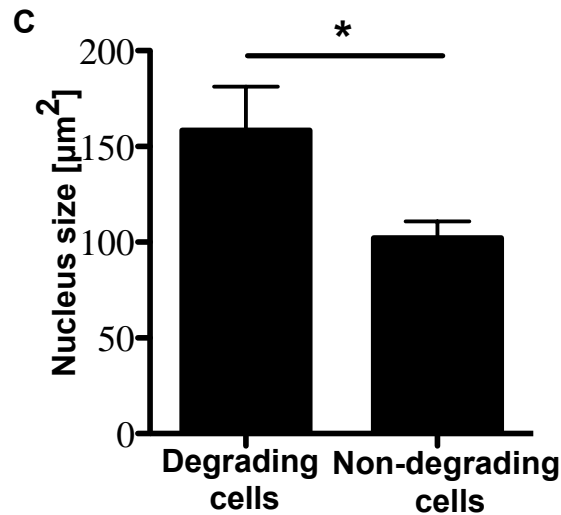
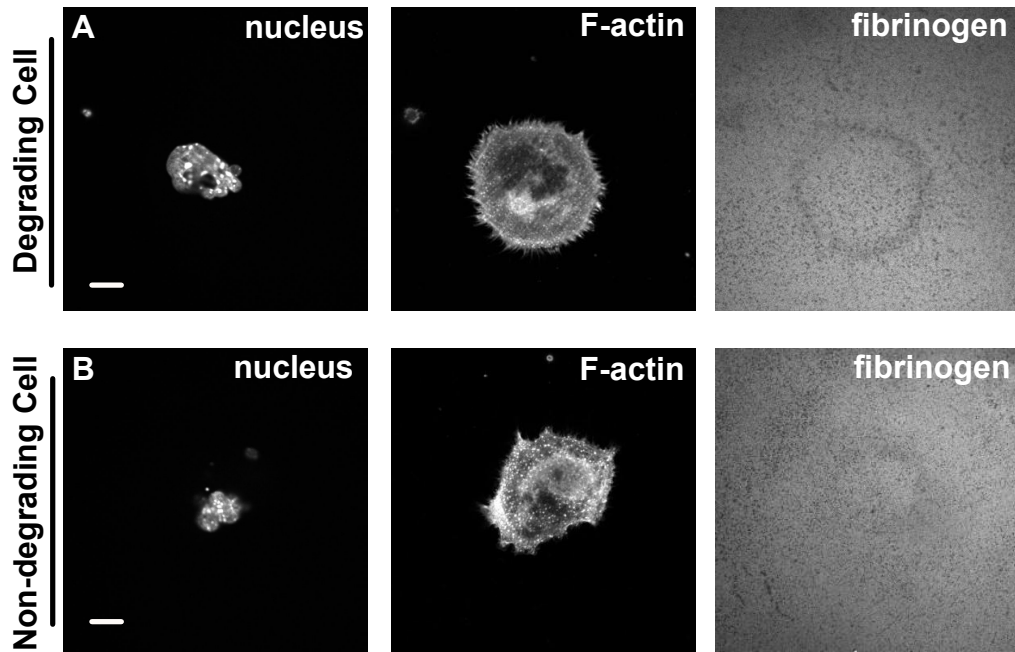


Figure 6.2: Mks with larger nuclei have an increased ability to degrade a fibrinogen matrix

Mks were spread on 100 $\mu\text{g}/\text{ml}$ 488-labelled fibrinogen-coated surfaces for 3h and stained for F-actin and DNA. The nuclear size of (A) degrading and (B) non-degrading cells was analysed (C). Per experiment 20 cells were analyzed. Statistical analysis was done with a student's t-test. Asterisk represents significant difference with a P-value <0.05 . Error bars indicate \pm SEM. Scale bars represent 10 μm .

6.5 Future directions

In this thesis I determined several characteristics of podosomes in Mks such as the amount of formed podosomes, their lifetime, their ability to degrade matrix proteins, regulative key proteins and their dynamics on different substrates. Nonetheless, these results only describe the basic attributes of these structures. Further studies are needed to extend the knowledge and the functional role of podosomes in Mks. Based on the described results it would be interesting to analyse podosomes in Mks undergoing directed migration and to explore a function for these structures also in migratory processes. Another key experiment would be the investigation of the correlation between podosome numbers and proplatelet formation. In addition, proplatelet and platelet formation could be studied with Mks forming podosomes and with Wasp KO Mks spreading on a native basement membrane. With this result, a direct role of podosomes could be related to platelet production and therefore a pivotal physiological function.

The application of further physiological relevant matrix proteins such as fibronectin and laminin could be used to direct the substrate specific behaviour of podosome structures. The use of several substrate stiffness levels and the influence on podosome numbers, the degree of matrix degradation and lifetime could be studied. These data could be analysed by atomic force microscopy to illuminate the correlation between substrate rigidity, podosome stiffness and podosome characteristics such as the lifetime or degradative activity. Myosin-II would be a particular interesting protein to look at.

Furthermore, detailed experiments of 3D podosome formation are needed with an extended analysis focusing on protein composition, lifetime and substrate specific ECM lysis.

Finally the role of podosomes *in vivo* needs to be illuminated. Complex *in vivo* imaging could be performed, with the use of Mk specific Lifeact expression, a vascular marker and the visualisation of the bone marrow ECM, which makes it possible to visualize podosome formation during migration and platelet release into the blood stream.

References

- Adams, J.C., 1997. Characterization of cell-matrix adhesion requirements for the formation of fascin microspikes. *Molecular biology of the cell* 8, 2345-2363.
- Aga, M., Bradley, J.M., Keller, K.E., Kelley, M.J., Acott, T.S., 2008. Specialized podosome- or invadopodia-like structures (PILS) for focal trabecular meshwork extracellular matrix turnover. *Investigative ophthalmology & visual science* 49, 5353-5365.
- Akisaka, T., Yoshida, H., Inoue, S., Shimizu, K., 2001. Organization of cytoskeletal F-actin, G-actin, and gelsolin in the adhesion structures in cultured osteoclast. *Journal of bone and mineral research : the official journal of the American Society for Bone and Mineral Research* 16, 1248-1255.
- Akisaka, T., Yoshida, H., Suzuki, R., Takama, K., 2008. Adhesion structures and their cytoskeleton-membrane interactions at podosomes of osteoclasts in culture. *Cell and tissue research* 331, 625-641.
- Albrechtsen, R., Stautz, D., Sanjay, A., Kveiborg, M., Wewer, U.M., 2011. Extracellular engagement of ADAM12 induces clusters of invadopodia with localized ectodomain shedding activity. *Experimental cell research* 317, 195-209.
- Alexander, N.R., Branch, K.M., Parekh, A., Clark, E.S., Iwueke, I.C., Guelcher, S.A., Weaver, A.M., 2008. Extracellular matrix rigidity promotes invadopodia activity. *Current biology : CB* 18, 1295-1299.
- Allavena, P., Paganin, C., Martin-Padura, I., Peri, G., Gaboli, M., Dejana, E., Marchisio, P.C., Mantovani, A., 1991. Molecules and structures involved in the adhesion of natural killer cells to vascular endothelium. *The Journal of experimental medicine* 173, 439-448.
- Allen, W.E., Zicha, D., Ridley, A.J., Jones, G.E., 1998. A role for Cdc42 in macrophage chemotaxis. *The Journal of cell biology* 141, 1147-1157.
- Allingham, J.S., Smith, R., Rayment, I., 2005. The structural basis of blebbistatin inhibition and specificity for myosin II. *Nature structural & molecular biology* 12, 378-379.
- Amano, T., Tanabe, K., Eto, T., Narumiya, S., Mizuno, K., 2001. LIM-kinase 2 induces formation of stress fibres, focal adhesions and membrane blebs, dependent on its activation by Rho-associated kinase-catalysed phosphorylation at threonine-505. *The Biochemical journal* 354, 149-159.

Anton, I.M., Jones, G.E., Wandosell, F., Geha, R., Ramesh, N., 2007. WASP-interacting protein (WIP): working in polymerisation and much more. *Trends in cell biology* 17, 555-562.

Ariga, T., 2012. Wiskott-Aldrich syndrome; an x-linked primary immunodeficiency disease with unique and characteristic features. *Allergology international : official journal of the Japanese Society of Allergology* 61, 183-189.

Artym, V.V., Zhang, Y., Seillier-Moiseiwitsch, F., Yamada, K.M., Mueller, S.C., 2006. Dynamic interactions of cortactin and membrane type 1 matrix metalloproteinase at invadopodia: defining the stages of invadopodia formation and function. *Cancer research* 66, 3034-3043.

Aspenstrom, P., 2002. The WASP-binding protein WIRE has a role in the regulation of the actin filament system downstream of the platelet-derived growth factor receptor. *Experimental cell research* 279, 21-33.

Athman, R., Louvard, D., Robine, S., 2002. The epithelial cell cytoskeleton and intracellular trafficking. III. How is villin involved in the actin cytoskeleton dynamics in intestinal cells? *American journal of physiology. Gastrointestinal and liver physiology* 283, G496-502.

Avecilla, S.T., Hattori, K., Heissig, B., Tejada, R., Liao, F., Shido, K., Jin, D.K., Dias, S., Zhang, F., Hartman, T.E., Hackett, N.R., Crystal, R.G., Witte, L., Hicklin, D.J., Bohlen, P., Eaton, D., Lyden, D., de Sauvage, F., Rafii, S., 2004. Chemokine-mediated interaction of hematopoietic progenitors with the bone marrow vascular niche is required for thrombopoiesis. *Nature medicine* 10, 64-71.

Avigdor, A., Goichberg, P., Shivtiel, S., Dar, A., Peled, A., Samira, S., Kollet, O., Hershkoviz, R., Alon, R., Hardan, I., Ben-Hur, H., Naor, D., Nagler, A., Lapidot, T., 2004. CD44 and hyaluronic acid cooperate with SDF-1 in the trafficking of human CD34+ stem/progenitor cells to bone marrow. *Blood* 103, 2981-2989.

Ayala, I., Baldassarre, M., Giacchetti, G., Caldieri, G., Tete, S., Luini, A., Buccione, R., 2008. Multiple regulatory inputs converge on cortactin to control invadopodia biogenesis and extracellular matrix degradation. *Journal of cell science* 121, 369-378.

Ayala, I., Giacchetti, G., Caldieri, G., Attanasio, F., Mariggio, S., Tete, S., Polishchuk, R., Castronovo, V., Buccione, R., 2009. Faciogenital dysplasia protein Fgd1 regulates invadopodia biogenesis and extracellular matrix degradation and is up-regulated in prostate and breast cancer. *Cancer research* 69, 747-752.

Baba, Y., Nonoyama, S., Matsushita, M., Yamadori, T., Hashimoto, S., Imai, K., Arai, S., Kunikata, T., Kurimoto, M., Kurosaki, T., Ochs, H.D., Yata, J., Kishimoto, T., Tsukada, S., 1999. Involvement of wiskott-aldrich syndrome protein in B-cell cytoplasmic tyrosine kinase pathway. *Blood* 93, 2003-2012.

Badowski, C., Pawlak, G., Grichine, A., Chabadel, A., Oddou, C., Jurdic, P., Pfaff, M., Albiges-Rizo, C., Block, M.R., 2008. Paxillin phosphorylation controls invadopodia/podosomes spatiotemporal organization. *Molecular biology of the cell* 19, 633-645.

Bakolitsa, C., Cohen, D.M., Bankston, L.A., Bobkov, A.A., Cadwell, G.W., Jennings, L., Critchley, D.R., Craig, S.W., Liddington, R.C., 2004. Structural basis for vinculin activation at sites of cell adhesion. *Nature* 430, 583-586.

Balduini, A., Pallotta, I., Malara, A., Lova, P., Pecci, A., Viarengo, G., Balduini, C.L., Torti, M., 2008. Adhesive receptors, extracellular proteins and myosin IIA orchestrate proplatelet formation by human megakaryocytes. *Journal of thrombosis and haemostasis : JTH* 6, 1900-1907.

Banon-Rodriguez, I., Monypenny, J., Ragazzini, C., Franco, A., Calle, Y., Jones, G.E., Anton, I.M., 2011. The cortactin-binding domain of WIP is essential for podosome formation and extracellular matrix degradation by murine dendritic cells. *European journal of cell biology* 90, 213-223.

Barry, S.T., Critchley, D.R., 1994. The RhoA-dependent assembly of focal adhesions in Swiss 3T3 cells is associated with increased tyrosine phosphorylation and the recruitment of both pp125FAK and protein kinase C-delta to focal adhesions. *Journal of cell science* 107 (Pt 7), 2033-2045.

Bear, J.E., Rawls, J.F., Saxe, C.L., 3rd, 1998. SCAR, a WASP-related protein, isolated as a suppressor of receptor defects in late Dictyostelium development. *The Journal of cell biology* 142, 1325-1335.

Beckstead, J.H., Stenberg, P.E., McEver, R.P., Shuman, M.A., Bainton, D.F., 1986. Immunohistochemical localization of membrane and alpha-granule proteins in human megakaryocytes: application to plastic-embedded bone marrow biopsy specimens. *Blood* 67, 285-293.

Bennett, J.S., Berger, B.W., Billings, P.C., 2009. The structure and function of platelet integrins. *Journal of thrombosis and haemostasis : JTH* 7 Suppl 1, 200-205.

Berdeaux, R.L., Diaz, B., Kim, L., Martin, G.S., 2004. Active Rho is localized to podosomes induced by oncogenic Src and is required for their assembly and function. *The Journal of cell biology* 166, 317-323.

Berman, A.E., Kozlova, N.I., Morozevich, G.E., 2003. Integrins: structure and signaling. *Biochemistry. Biokhimiia* 68, 1284-1299.

Bhadriraju, K., Yang, M., Alom Ruiz, S., Pirone, D., Tan, J., Chen, C.S., 2007. Activation of ROCK by RhoA is regulated by cell adhesion, shape, and cytoskeletal tension. *Experimental cell research* 313, 3616-3623.

- Bhuwania, R., Cornfine, S., Fang, Z., Kruger, M., Luna, E.J., Linder, S., 2012. Supravillin couples myosin-dependent contractility to podosomes and enables their turnover. *Journal of cell science* 125, 2300-2314.
- Bishop, A.L., Hall, A., 2000. Rho GTPases and their effector proteins. *The Biochemical journal* 348 Pt 2, 241-255.
- Block, M.R., Badowski, C., Millon-Fremillon, A., Bouvard, D., Bouin, A.P., Faurobert, E., Gerber-Scokaert, D., Planus, E., Albiges-Rizo, C., 2008. Podosome-type adhesions and focal adhesions, so alike yet so different. *European journal of cell biology* 87, 491-506.
- Boateng, L.R., Cortesio, C.L., Huttenlocher, A., 2012. Src-mediated phosphorylation of mammalian Abp1 (DBNL) regulates podosome rosette formation in transformed fibroblasts. *Journal of cell science* 125, 1329-1341.
- Bois, P.R., Borgon, R.A., Vornrhein, C., Izard, T., 2005. Structural dynamics of alpha-actinin-vinculin interactions. *Molecular and cellular biology* 25, 6112-6122.
- Bowden, E.T., Barth, M., Thomas, D., Glazer, R.I., Mueller, S.C., 1999. An invasion-related complex of cortactin, paxillin and PKCmu associates with invadopodia at sites of extracellular matrix degradation. *Oncogene* 18, 4440-4449.
- Brakebusch, C., Fassler, R., 2003. The integrin-actin connection, an eternal love affair. *The EMBO journal* 22, 2324-2333.
- Branch, K.M., Hoshino, D., Weaver, A.M., 2012. Adhesion rings surround invadopodia and promote maturation. *Biology open* 1, 711-722.
- Brazier, H., Stephens, S., Ory, S., Fort, P., Morrison, N., Blangy, A., 2006. Expression profile of RhoGTPases and RhoGEFs during RANKL-stimulated osteoclastogenesis: identification of essential genes in osteoclasts. *Journal of bone and mineral research : the official journal of the American Society for Bone and Mineral Research* 21, 1387-1398.
- Bresnick, A.R., 1999. Molecular mechanisms of nonmuscle myosin-II regulation. *Current opinion in cell biology* 11, 26-33.
- Bruzzaniti, A., Neff, L., Sanjay, A., Horne, W.C., De Camilli, P., Baron, R., 2005. Dynamin forms a Src kinase-sensitive complex with Cbl and regulates podosomes and osteoclast activity. *Molecular biology of the cell* 16, 3301-3313.
- Bryan, N., Andrews, K.D., Loughran, M.J., Rhodes, N.P., Hunt, J.A., 2011. Elucidating the contribution of the elemental composition of fetal calf serum to antigenic expression of primary human umbilical-vein endothelial cells in vitro. *Bioscience reports* 31, 199-210.

- Bryce, N.S., Clark, E.S., Leysath, J.L., Currie, J.D., Webb, D.J., Weaver, A.M., 2005. Cortactin promotes cell motility by enhancing lamellipodial persistence. *Current biology* : CB 15, 1276-1285.
- Bu, W., Lim, K.B., Yu, Y.H., Chou, A.M., Sudhakaran, T., Ahmed, S., 2010. Cdc42 interaction with N-WASP and Toca-1 regulates membrane tubulation, vesicle formation and vesicle motility: implications for endocytosis. *PLoS one* 5, e12153.
- Buccione, R., Orth, J.D., McNiven, M.A., 2004. Foot and mouth: podosomes, invadopodia and circular dorsal ruffles. *Nature reviews. Molecular cell biology* 5, 647-657.
- Burbelo, P.D., Drechsel, D., Hall, A., 1995. A conserved binding motif defines numerous candidate target proteins for both Cdc42 and Rac GTPases. *The Journal of biological chemistry* 270, 29071-29074.
- Burgess, S.A., Yu, S., Walker, M.L., Hawkins, R.J., Chalovich, J.M., Knight, P.J., 2007. Structures of smooth muscle myosin and heavy meromyosin in the folded, shutdown state. *Journal of molecular biology* 372, 1165-1178.
- Burgstaller, G., Gimona, M., 2004. Actin cytoskeleton remodelling via local inhibition of contractility at discrete microdomains. *Journal of cell science* 117, 223-231.
- Burns, S., Thrasher, A.J., 2004. Dendritic cells: the bare bones of immunity. *Current biology* : CB 14, R965-967.
- Burns, S., Thrasher, A.J., Blundell, M.P., Machesky, L., Jones, G.E., 2001. Configuration of human dendritic cell cytoskeleton by Rho GTPases, the WAS protein, and differentiation. *Blood* 98, 1142-1149.
- Calaminus, S.D., McCarty, O.J., Auger, J.M., Pearce, A.C., Insall, R.H., Watson, S.P., Machesky, L.M., 2007. A major role for Scar/WAVE-1 downstream of GPVI in platelets. *Journal of thrombosis and haemostasis* : JTH 5, 535-541.
- Calaminus, S.D., Thomas, S., McCarty, O.J., Machesky, L.M., Watson, S.P., 2008. Identification of a novel, actin-rich structure, the actin nodule, in the early stages of platelet spreading. *Journal of thrombosis and haemostasis* : JTH 6, 1944-1952.
- Calle, Y., Burns, S., Thrasher, A.J., Jones, G.E., 2006. The leukocyte podosome. *European journal of cell biology* 85, 151-157.
- Calle, Y., Chou, H.C., Thrasher, A.J., Jones, G.E., 2004. Wiskott-Aldrich syndrome protein and the cytoskeletal dynamics of dendritic cells. *The Journal of pathology* 204, 460-469.

Carrier, M.F., Pantaloni, D., 1997. Control of actin dynamics in cell motility. *Journal of molecular biology* 269, 459-467.

Cassimeris, L., Safer, D., Nachmias, V.T., Zigmond, S.H., 1992. Thymosin beta 4 sequesters the majority of G-actin in resting human polymorphonuclear leukocytes. *The Journal of cell biology* 119, 1261-1270.

Cau, J., Hall, A., 2005. Cdc42 controls the polarity of the actin and microtubule cytoskeletons through two distinct signal transduction pathways. *Journal of cell science* 118, 2579-2587.

Chabadel, A., Banon-Rodriguez, I., Cluet, D., Rudkin, B.B., Wehrle-Haller, B., Genot, E., Jurdic, P., Anton, I.M., Saltel, F., 2007. CD44 and beta3 integrin organize two functionally distinct actin-based domains in osteoclasts. *Molecular biology of the cell* 18, 4899-4910.

Chan, K.T., Cortesio, C.L., Huttenlocher, A., 2009. FAK alters invadopodia and focal adhesion composition and dynamics to regulate breast cancer invasion. *The Journal of cell biology* 185, 357-370.

Cheeseman, I.M., Desai, A., 2008. Molecular architecture of the kinetochore-microtubule interface. *Nature reviews. Molecular cell biology* 9, 33-46.

Chellaiah, M.A., 2006. Regulation of podosomes by integrin α v β 3 and Rho GTPase-facilitated phosphoinositide signaling. *European journal of cell biology* 85, 311-317.

Chen, F., Ma, L., Parrini, M.C., Mao, X., Lopez, M., Wu, C., Marks, P.W., Davidson, L., Kwiatkowski, D.J., Kirchhausen, T., Orkin, S.H., Rosen, F.S., Mayer, B.J., Kirschner, M.W., Alt, F.W., 2000. Cdc42 is required for PIP(2)-induced actin polymerization and early development but not for cell viability. *Current biology : CB* 10, 758-765.

Chen, W.T., Olden, K., Bernard, B.A., Chu, F.F., 1984. Expression of transformation-associated protease(s) that degrade fibronectin at cell contact sites. *The Journal of cell biology* 98, 1546-1555.

Chen, Z., Borek, D., Padrick, S.B., Gomez, T.S., Metlagel, Z., Ismail, A.M., Umetani, J., Billadeau, D.D., Otwinowski, Z., Rosen, M.K., 2010. Structure and control of the actin regulatory WAVE complex. *Nature* 468, 533-538.

Chereau, D., Kerff, F., Graceffa, P., Grabarek, Z., Langsetmo, K., Dominguez, R., 2005. Actin-bound structures of Wiskott-Aldrich syndrome protein (WASP)-homology domain 2 and the implications for filament assembly. *Proceedings of the National Academy of Sciences of the United States of America* 102, 16644-16649.

Chou, H.C., Anton, I.M., Holt, M.R., Curcio, C., Lanzardo, S., Worth, A., Burns, S., Thrasher, A.J., Jones, G.E., Calle, Y., 2006. WIP regulates the stability and localization of WASP to podosomes in migrating dendritic cells. *Current biology* : CB 16, 2337-2344.

Chrzanowska-Wodnicka, M., Burridge, K., 1996. Rho-stimulated contractility drives the formation of stress fibers and focal adhesions. *The Journal of cell biology* 133, 1403-1415.

Clark, E.S., Whigham, A.S., Yarbrough, W.G., Weaver, A.M., 2007. Cortactin is an essential regulator of matrix metalloproteinase secretion and extracellular matrix degradation in invadopodia. *Cancer research* 67, 4227-4235.

Collin, O., Na, S., Chowdhury, F., Hong, M., Shin, M.E., Wang, F., Wang, N., 2008. Self-organized podosomes are dynamic mechanosensors. *Current biology* : CB 18, 1288-1294.

Collin, O., Tracqui, P., Stephanou, A., Usson, Y., Clement-Lacroix, J., Planus, E., 2006. Spatiotemporal dynamics of actin-rich adhesion microdomains: influence of substrate flexibility. *Journal of cell science* 119, 1914-1925.

Corash, L., Shafer, B., Blaese, R.M., 1985. Platelet-associated immunoglobulin, platelet size, and the effect of splenectomy in the Wiskott-Aldrich syndrome. *Blood* 65, 1439-1443.

Cornfine, S., Himmel, M., Kopp, P., El Azzouzi, K., Wiesner, C., Kruger, M., Rudel, T., Linder, S., 2011. The kinesin KIF9 and reggie/flotillin proteins regulate matrix degradation by macrophage podosomes. *Molecular biology of the cell* 22, 202-215.

Cosen-Binker, L.I., Kapus, A., 2006. Cortactin: the gray eminence of the cytoskeleton. *Physiology (Bethesda)* 21, 352-361.

Cotta-de-Almeida, V., Westerberg, L., Maillard, M.H., Onaldi, D., Wachtel, H., Meelu, P., Chung, U.I., Xavier, R., Alt, F.W., Snapper, S.B., 2007. Wiskott Aldrich syndrome protein (WASP) and N-WASP are critical for T cell development. *Proceedings of the National Academy of Sciences of the United States of America* 104, 15424-15429.

Cougoule, C., Le Cabec, V., Poincloux, R., Al Saati, T., Mege, J.L., Tabouret, G., Lowell, C.A., Laviolette-Malirat, N., Maridonneau-Parini, I., 2010. Three-dimensional migration of macrophages requires Hck for podosome organization and extracellular matrix proteolysis. *Blood* 115, 1444-1452.

Cougoule, C., Van Goethem, E., Le Cabec, V., Lafouresse, F., Dupre, L., Mehraj, V., Mege, J.L., Lastrucci, C., Maridonneau-Parini, I., 2012. Blood leukocytes and

macrophages of various phenotypes have distinct abilities to form podosomes and to migrate in 3D environments. *European journal of cell biology* 91, 938-949.

Cox, S., Rosten, E., Monypenny, J., Jovanovic-Taliman, T., Burnette, D.T., Lippincott-Schwartz, J., Jones, G.E., Heintzmann, R., 2012. Bayesian localization microscopy reveals nanoscale podosome dynamics. *Nature methods* 9, 195-200.

Critchley, D.R., Gingras, A.R., 2008. Talin at a glance. *Journal of cell science* 121, 1345-1347.

Cukierman, E., Pankov, R., Yamada, K.M., 2002. Cell interactions with three-dimensional matrices. *Current opinion in cell biology* 14, 633-639.

Datta, A., Shi, Q., Boettiger, D.E., 2001. Transformation of chicken embryo fibroblasts by v-src uncouples beta1 integrin-mediated outside-in but not inside-out signaling. *Molecular and cellular biology* 21, 7295-7306.

Debili, N., Issaad, C., Masse, J.M., Guichard, J., Katz, A., Breton-Gorius, J., Vainchenker, W., 1992. Expression of CD34 and platelet glycoproteins during human megakaryocytic differentiation. *Blood* 80, 3022-3035.

DeFife, K.M., Jenney, C.R., Colton, E., Anderson, J.M., 1999. Cytoskeletal and adhesive structural polarizations accompany IL-13-induced human macrophage fusion. *The journal of histochemistry and cytochemistry : official journal of the Histochemistry Society* 47, 65-74.

Dehring, D.A., Clarke, F., Ricart, B.G., Huang, Y., Gomez, T.S., Williamson, E.K., Hammer, D.A., Billadeau, D.D., Argon, Y., Burkhardt, J.K., 2011. Hematopoietic lineage cell-specific protein 1 functions in concert with the Wiskott-Aldrich syndrome protein to promote podosome array organization and chemotaxis in dendritic cells. *J Immunol* 186, 4805-4818.

Delaisse, J.M., Engsig, M.T., Everts, V., del Carmen Ovejero, M., Ferreras, M., Lund, L., Vu, T.H., Werb, Z., Winding, B., Lochter, A., Karsdal, M.A., Troen, T., Kirkegaard, T., Lenhard, T., Heegaard, A.M., Neff, L., Baron, R., Foged, N.T., 2000. Proteinases in bone resorption: obvious and less obvious roles. *Clinica chimica acta; international journal of clinical chemistry* 291, 223-234.

Destaing, O., Planus, E., Bouvard, D., Oddou, C., Badowski, C., Bossy, V., Raducanu, A., Fourcade, B., Albiges-Rizo, C., Block, M.R., 2010. beta1A integrin is a master regulator of invadosome organization and function. *Molecular biology of the cell* 21, 4108-4119.

Destaing, O., Saltel, F., Geminard, J.C., Jurdic, P., Bard, F., 2003. Podosomes display actin turnover and dynamic self-organization in osteoclasts expressing actin-green fluorescent protein. *Molecular biology of the cell* 14, 407-416.

Destaing, O., Saltel, F., Gilquin, B., Chabadel, A., Khochbin, S., Ory, S., Jurdic, P., 2005. A novel Rho-mDia2-HDAC6 pathway controls podosome patterning through microtubule acetylation in osteoclasts. *Journal of cell science* 118, 2901-2911.

Detry, B., Bruyere, F., Ericum, C., Paupert, J., Lamaye, F., Maillard, C., Lenoir, B., Foidart, J.M., Thiry, M., Noel, A., 2011. Digging deeper into lymphatic vessel formation in vitro and in vivo. *BMC cell biology* 12, 29.

Deutsch, V.R., Tomer, A., 2006. Megakaryocyte development and platelet production. *British journal of haematology* 134, 453-466.

Dorfleutner, A., Cho, Y., Vincent, D., Cunnick, J., Lin, H., Weed, S.A., Stehlik, C., Flynn, D.C., 2008. Phosphorylation of AFAP-110 affects podosome lifespan in A7r5 cells. *Journal of cell science* 121, 2394-2405.

Dovas, A., Gevrey, J.C., Grossi, A., Park, H., Abou-Kheir, W., Cox, D., 2009. Regulation of podosome dynamics by WASp phosphorylation: implication in matrix degradation and chemotaxis in macrophages. *Journal of cell science* 122, 3873-3882.

Dubielecka, P.M., Ladwein, K.I., Xiong, X., Migeotte, I., Chorzalska, A., Anderson, K.V., Sawicki, J.A., Rottner, K., Stradal, T.E., Kotula, L., 2011. Essential role for Abi1 in embryonic survival and WAVE2 complex integrity. *Proceedings of the National Academy of Sciences of the United States of America* 108, 7022-7027.

Dumon, S., Heath, V.L., Tomlinson, M.G., Gottgens, B., Frampton, J., 2006. Differentiation of murine committed megakaryocytic progenitors isolated by a novel strategy reveals the complexity of GATA and Ets factor involvement in megakaryocytopoiesis and an unexpected potential role for GATA-6. *Experimental hematology* 34, 654-663.

Duong, L.T., Rodan, G.A., 2000. PYK2 is an adhesion kinase in macrophages, localized in podosomes and activated by beta(2)-integrin ligation. *Cell motility and the cytoskeleton* 47, 174-188.

Echarri, A., Lai, M.J., Robinson, M.R., Pendergast, A.M., 2004. Abl interactor 1 (Abi-1) wave-binding and SNARE domains regulate its nucleocytoplasmic shuttling, lamellipodium localization, and wave-1 levels. *Molecular and cellular biology* 24, 4979-4993.

Eilers, U., Klumperman, J., Hauri, H.P., 1989. Nocodazole, a microtubule-active drug, interferes with apical protein delivery in cultured intestinal epithelial cells (Caco-2). *The Journal of cell biology* 108, 13-22.

Eto, K., Nishikii, H., Ogaeri, T., Suetsugu, S., Kamiya, A., Kobayashi, T., Yamazaki, D., Oda, A., Takenawa, T., Nakauchi, H., 2007. The WAVE2/Abi1 complex differentially regulates megakaryocyte development and spreading:

implications for platelet biogenesis and spreading machinery. *Blood* 110, 3637-3647.

Evans, J.G., Correia, I., Krasavina, O., Watson, N., Matsudaira, P., 2003. Macrophage podosomes assemble at the leading lamella by growth and fragmentation. *The Journal of cell biology* 161, 697-705.

Even-Ram, S., Doyle, A.D., Conti, M.A., Matsumoto, K., Adelstein, R.S., Yamada, K.M., 2007. Myosin IIA regulates cell motility and actomyosin-microtubule crosstalk. *Nature cell biology* 9, 299-309.

Eves, R., Webb, B.A., Zhou, S., Mak, A.S., 2006. Caldesmon is an integral component of podosomes in smooth muscle cells. *Journal of cell science* 119, 1691-1702.

Faccio, R., Grano, M., Colucci, S., Villa, A., Giannelli, G., Quaranta, V., Zallone, A., 2002. Localization and possible role of two different alpha v beta 3 integrin conformations in resting and resorbing osteoclasts. *Journal of cell science* 115, 2919-2929.

Falet, H., Hoffmeister, K.M., Neujahr, R., Hartwig, J.H., 2002. Normal Arp2/3 complex activation in platelets lacking WASp. *Blood* 100, 2113-2122.

Ferkowicz, M.J., Starr, M., Xie, X., Li, W., Johnson, S.A., Shelley, W.C., Morrison, P.R., Yoder, M.C., 2003. CD41 expression defines the onset of primitive and definitive hematopoiesis in the murine embryo. *Development* 130, 4393-4403.

Frame, M.C., 2002. Src in cancer: deregulation and consequences for cell behaviour. *Biochimica et biophysica acta* 1602, 114-130.

Friedl, P., Wolf, K., 2010. Plasticity of cell migration: a multiscale tuning model. *The Journal of cell biology* 188, 11-19.

Fuchs, E., Raghavan, S., 2002. Getting under the skin of epidermal morphogenesis. *Nature reviews. Genetics* 3, 199-209.

Galvez, B.G., Matias-Roman, S., Yanez-Mo, M., Sanchez-Madrid, F., Arroyo, A.G., 2002. ECM regulates MT1-MMP localization with beta1 or alphavbeta3 integrins at distinct cell compartments modulating its internalization and activity on human endothelial cells. *The Journal of cell biology* 159, 509-521.

Garcia-Bernal, D., Wright, N., Sotillo-Mallo, E., Nombela-Arrieta, C., Stein, J.V., Bustelo, X.R., Teixido, J., 2005. Vav1 and Rac control chemokine-promoted T lymphocyte adhesion mediated by the integrin alpha4beta1. *Molecular biology of the cell* 16, 3223-3235.

Gawden-Bone, C., Zhou, Z., King, E., Prescott, A., Watts, C., Lucocq, J., 2010. Dendritic cell podosomes are protrusive and invade the extracellular matrix using metalloproteinase MMP-14. *Journal of cell science* 123, 1427-1437.

Geblinger, D., Addadi, L., Geiger, B., 2010. Nano-topography sensing by osteoclasts. *Journal of cell science* 123, 1503-1510.

Gimona, M., Kaverina, I., Resch, G.P., Vignal, E., Burgstaller, G., 2003. Calponin repeats regulate actin filament stability and formation of podosomes in smooth muscle cells. *Molecular biology of the cell* 14, 2482-2491.

Goley, E.D., Welch, M.D., 2006. The ARP2/3 complex: an actin nucleator comes of age. *Nature reviews. Molecular cell biology* 7, 713-726.

Golubkov, V.S., Cieplak, P., Chekanov, A.V., Ratnikov, B.I., Aleshin, A.E., Golubkova, N.V., Postnova, T.I., Radichev, I.A., Rozanov, D.V., Zhu, W., Motamedchaboki, K., Strongin, A.Y., 2010. Internal cleavages of the autoinhibitory prodomain are required for membrane type 1 matrix metalloproteinase activation, although furin cleavage alone generates inactive proteinase. *The Journal of biological chemistry* 285, 27726-27736.

Goto, T., Maeda, H., Tanaka, T., 2002. A selective inhibitor of matrix metalloproteinases inhibits the migration of isolated osteoclasts by increasing the life span of podosomes. *Journal of bone and mineral metabolism* 20, 98-105.

Grashoff, C., Hoffman, B.D., Brenner, M.D., Zhou, R., Parsons, M., Yang, M.T., McLean, M.A., Sligar, S.G., Chen, C.S., Ha, T., Schwartz, M.A., 2010. Measuring mechanical tension across vinculin reveals regulation of focal adhesion dynamics. *Nature* 466, 263-266.

Grill, B., Schrader, J.W., 2002. Activation of Rac-1, Rac-2, and Cdc42 by hemopoietic growth factors or cross-linking of the B-lymphocyte receptor for antigen. *Blood* 100, 3183-3192.

Gross, B.S., Wilde, J.I., Quek, L., Chapel, H., Nelson, D.L., Watson, S.P., 1999. Regulation and function of WASp in platelets by the collagen receptor, glycoprotein VI. *Blood* 94, 4166-4176.

Guo, J., Piguet, P.F., 1998. Stimulation of thrombocytopoiesis decreases platelet beta2 but not beta1 or beta3 integrins. *British journal of haematology* 100, 712-719.

Hakem, A., Sanchez-Sweatman, O., You-Ten, A., Duncan, G., Wakeham, A., Khokha, R., Mak, T.W., 2005. RhoC is dispensable for embryogenesis and tumor initiation but essential for metastasis. *Genes & development* 19, 1974-1979.

Hamada, T., Mohle, R., Hesselgesser, J., Hoxie, J., Nachman, R.L., Moore, M.A., Rafii, S., 1998. Transendothelial migration of megakaryocytes in response to stromal cell-derived factor 1 (SDF-1) enhances platelet formation. *The Journal of experimental medicine* 188, 539-548.

Hammarfjord, O., Falet, H., Gurniak, C., Hartwig, J.H., Wallin, R.P., 2011. Gelsolin-independent podosome formation in dendritic cells. *PloS one* 6, e21615.

Has, C., Herz, C., Zimina, E., Qu, H.Y., He, Y., Zhang, Z.G., Wen, T.T., Gache, Y., Aumailley, M., Bruckner-Tuderman, L., 2009. Kindlin-1 Is required for RhoGTPase-mediated lamellipodia formation in keratinocytes. *The American journal of pathology* 175, 1442-1452.

Heasman, S.J., Ridley, A.J., 2008. Mammalian Rho GTPases: new insights into their functions from in vivo studies. *Nature reviews. Molecular cell biology* 9, 690-701.

Herz, C., Aumailley, M., Schulte, C., Schlotzer-Schrehardt, U., Bruckner-Tuderman, L., Has, C., 2006. Kindlin-1 is a phosphoprotein involved in regulation of polarity, proliferation, and motility of epidermal keratinocytes. *The Journal of biological chemistry* 281, 36082-36090.

Hirokawa, N., Noda, Y., Tanaka, Y., Niwa, S., 2009. Kinesin superfamily motor proteins and intracellular transport. *Nature reviews. Molecular cell biology* 10, 682-696.

Hotary, K., Li, X.Y., Allen, E., Stevens, S.L., Weiss, S.J., 2006. A cancer cell metalloprotease triad regulates the basement membrane transmigration program. *Genes & development* 20, 2673-2686.

Hotulainen, P., Lappalainen, P., 2006. Stress fibers are generated by two distinct actin assembly mechanisms in motile cells. *The Journal of cell biology* 173, 383-394.

Hou, P., Estrada, L., Kinley, A.W., Parsons, J.T., Vojtek, A.B., Gorski, J.L., 2003. Fgd1, the Cdc42 GEF responsible for Faciogenital Dysplasia, directly interacts with cortactin and mAbp1 to modulate cell shape. *Human molecular genetics* 12, 1981-1993.

Hu, J., Mukhopadhyay, A., Truesdell, P., Chander, H., Mukhopadhyay, U.K., Mak, A.S., Craig, A.W., 2011. Cdc42-interacting protein 4 is a Src substrate that regulates invadopodia and invasiveness of breast tumors by promoting MT1-MMP endocytosis. *Journal of cell science* 124, 1739-1751.

Huang, C., Ni, Y., Wang, T., Gao, Y., Haudenschild, C.C., Zhan, X., 1997. Down-regulation of the filamentous actin cross-linking activity of cortactin by Src-

mediated tyrosine phosphorylation. *The Journal of biological chemistry* 272, 13911-13915.

Hurst, I.R., Zuo, J., Jiang, J., Holliday, L.S., 2004. Actin-related protein 2/3 complex is required for actin ring formation. *Journal of bone and mineral research : the official journal of the American Society for Bone and Mineral Research* 19, 499-506.

Huss, R., 2000. Isolation of primary and immortalized CD34-hematopoietic and mesenchymal stem cells from various sources. *Stem Cells* 18, 1-9.

Huveneers, S., Danen, E.H., 2009. Adhesion signaling - crosstalk between integrins, Src and Rho. *Journal of cell science* 122, 1059-1069.

Isaac, B.M., Ishihara, D., Nusblat, L.M., Gevrey, J.C., Dovas, A., Condeelis, J., Cox, D., 2010. N-WASP has the ability to compensate for the loss of WASP in macrophage podosome formation and chemotaxis. *Experimental cell research* 316, 3406-3416.

Ishii, M., Egen, J.G., Klauschen, F., Meier-Schellersheim, M., Saeki, Y., Vacher, J., Proia, R.L., Germain, R.N., 2009. Sphingosine-1-phosphate mobilizes osteoclast precursors and regulates bone homeostasis. *Nature* 458, 524-528.

Ishikawa, R., Yamashiro, S., Kohama, K., Matsumura, F., 1998. Regulation of actin binding and actin bundling activities of fascin by caldesmon coupled with tropomyosin. *The Journal of biological chemistry* 273, 26991-26997.

Ismail, A.M., Padrick, S.B., Chen, B., Umetani, J., Rosen, M.K., 2009. The WAVE regulatory complex is inhibited. *Nature structural & molecular biology* 16, 561-563.

Italiano, J.E., Jr., Lecine, P., Shivdasani, R.A., Hartwig, J.H., 1999. Blood platelets are assembled principally at the ends of proplatelet processes produced by differentiated megakaryocytes. *The Journal of cell biology* 147, 1299-1312.

Italiano, J.E., Jr., Patel-Hett, S., Hartwig, J.H., 2007. Mechanics of proplatelet elaboration. *Journal of thrombosis and haemostasis : JTH* 5 Suppl 1, 18-23.

Jevnikar, Z., M, M., Jamnik, P., Doljak, B., Fonovic, U.P., Kos, J., 2012a. Cathepsin H mediates the processing of talin and regulates migration of prostate cancer cells. *The Journal of biological chemistry*.

Jevnikar, Z., Mirkovic, B., Fonovic, U.P., Zidar, N., Svajger, U., Kos, J., 2012b. Three-dimensional invasion of macrophages is mediated by cysteine cathepsins in protrusive podosomes. *European Journal of Immunology*

Johansson, M.W., Lye, M.H., Barthel, S.R., Duffy, A.K., Annis, D.S., Mosher, D.F., 2004. Eosinophils adhere to vascular cell adhesion molecule-1 via podosomes. *American journal of respiratory cell and molecular biology* 31, 413-422.

Jordan, M.A., Wilson, L., 2004. Microtubules as a target for anticancer drugs. *Nature reviews. Cancer* 4, 253-265.

Juin, A., Billottet, C., Moreau, V., Destaing, O., Albiges-Rizo, C., Rosenbaum, J., Genot, E., Saltel, F., 2012a. Physiological type I collagen organization induces the formation of a novel class of linear invadosomes. *Molecular biology of the cell* 23, 297-309.

Juin, A., Planus, E., Guillemot, F., Horakova, P., Albiges-Rizo, C., Genot, E., Rosenbaum, J., Moreau, V., Saltel, F., 2012b. Extracellular matrix rigidity controls podosome induction in microvascular endothelial cells. *Biology of the cell / under the auspices of the European Cell Biology Organization*.

Junt, T., Schulze, H., Chen, Z., Massberg, S., Goerge, T., Krueger, A., Wagner, D.D., Graf, T., Italiano, J.E., Jr., Shivdasani, R.A., von Andrian, U.H., 2007. Dynamic visualization of thrombopoiesis within bone marrow. *Science* 317, 1767-1770.

Jurdic, P., Saltel, F., Chabadel, A., Destaing, O., 2006. Podosome and sealing zone: specificity of the osteoclast model. *European journal of cell biology* 85, 195-202.

Kalfa, T.A., Pushkaran, S., Mohandas, N., Hartwig, J.H., Fowler, V.M., Johnson, J.F., Joiner, C.H., Williams, D.A., Zheng, Y., 2006. Rac GTPases regulate the morphology and deformability of the erythrocyte cytoskeleton. *Blood* 108, 3637-3645.

Kalluri, R., 2003. Basement membranes: structure, assembly and role in tumour angiogenesis. *Nature reviews. Cancer* 3, 422-433.

Karakose, E., Schiller, H.B., Fassler, R., 2010. The kindlins at a glance. *Journal of cell science* 123, 2353-2356.

Katayama, K., Melendez, J., Baumann, J.M., Leslie, J.R., Chauhan, B.K., Nemkul, N., Lang, R.A., Kuan, C.Y., Zheng, Y., Yoshida, Y., 2011. Loss of RhoA in neural progenitor cells causes the disruption of adherens junctions and hyperproliferation. *Proceedings of the National Academy of Sciences of the United States of America* 108, 7607-7612.

Kato, M., Miki, H., Kurita, S., Endo, T., Nakagawa, H., Miyamoto, S., Takenawa, T., 2002. WICH, a novel verprolin homology domain-containing protein that functions cooperatively with N-WASP in actin-microspike formation. *Biochemical and biophysical research communications* 291, 41-47.

Kato, M., Takenawa, T., 2005. WICH, a member of WASP-interacting protein family, cross-links actin filaments. *Biochemical and biophysical research communications* 328, 1058-1066.

Kaushansky, K., Lok, S., Holly, R.D., Broudy, V.C., Lin, N., Bailey, M.C., Forstrom, J.W., Buddle, M.M., Oort, P.J., Hagen, F.S., *et al.*, 1994. Promotion of megakaryocyte progenitor expansion and differentiation by the c-Mpl ligand thrombopoietin. *Nature* 369, 568-571.

Kaverina, I., Stradal, T.E., Gimona, M., 2003. Podosome formation in cultured A7r5 vascular smooth muscle cells requires Arp2/3-dependent de-novo actin polymerization at discrete microdomains. *Journal of cell science* 116, 4915-4924.

King, S.M., Reed, G.L., 2002. Development of platelet secretory granules. *Seminars in cell & developmental biology* 13, 293-302.

Kinley, A.W., Weed, S.A., Weaver, A.M., Karginov, A.V., Bissonette, E., Cooper, J.A., Parsons, J.T., 2003. Cortactin interacts with WIP in regulating Arp2/3 activation and membrane protrusion. *Current biology : CB* 13, 384-393.

Kirchenbuchler, D., Born, S., Kirchgessner, N., Houben, S., Hoffmann, B., Merkel, R., 2010. Substrate, focal adhesions, and actin filaments: a mechanical unit with a weak spot for mechanosensitive proteins. *Journal of physics. Condensed matter : an Institute of Physics journal* 22, 194109.

Kirkbride, K.C., Hong, N.H., French, C.L., Clark, E.S., Jerome, W.G., Weaver, A.M., 2012. Regulation of late endosomal/lysosomal maturation and trafficking by cortactin affects Golgi morphology. *Cytoskeleton (Hoboken)* 69, 625-643.

Klein, G., 1995. The extracellular matrix of the hematopoietic microenvironment. *Experientia* 51, 914-926.

Konno, A., Kirby, M., Anderson, S.A., Schwartzberg, P.L., Candotti, F., 2007. The expression of Wiskott-Aldrich syndrome protein (WASP) is dependent on WASP-interacting protein (WIP). *International immunology* 19, 185-192.

Kopp, P., Lammers, R., Aepfelbacher, M., Woehlke, G., Rudel, T., Machuy, N., Steffen, W., Linder, S., 2006. The kinesin KIF1C and microtubule plus ends regulate podosome dynamics in macrophages. *Molecular biology of the cell* 17, 2811-2823.

Kostoulas, G., Lang, A., Nagase, H., Baici, A., 1999. Stimulation of angiogenesis through cathepsin B inactivation of the tissue inhibitors of matrix metalloproteinases. *FEBS letters* 455, 286-290.

Kremerskothen, J., Stolting, M., Wiesner, C., Korb-Pap, A., van Vliet, V., Linder, S., Huber, T.B., Rottiers, P., Reuzeau, E., Genot, E., Pavenstadt, H., 2011. Zona

occludens proteins modulate podosome formation and function. *FASEB journal : official publication of the Federation of American Societies for Experimental Biology* 25, 505-514.

Kumar, C.C., 1998. Signaling by integrin receptors. *Oncogene* 17, 1365-1373.

Kunda, P., Craig, G., Dominguez, V., Baum, B., 2003. Abi, Sra1, and Kette control the stability and localization of SCAR/WAVE to regulate the formation of actin-based protrusions. *Current biology : CB* 13, 1867-1875.

Labernadie, A., Thibault, C., Vieu, C., Maridonneau-Parini, I., Charriere, G.M., 2010. Dynamics of podosome stiffness revealed by atomic force microscopy. *Proceedings of the National Academy of Sciences of the United States of America* 107, 21016-21021.

Laevsky, G., Knecht, D.A., 2003. Cross-linking of actin filaments by myosin II is a major contributor to cortical integrity and cell motility in restrictive environments. *Journal of cell science* 116, 3761-3770.

Lal, H., Verma, S.K., Foster, D.M., Golden, H.B., Reneau, J.C., Watson, L.E., Singh, H., Dostal, D.E., 2009. Integrins and proximal signaling mechanisms in cardiovascular disease. *Frontiers in bioscience : a journal and virtual library* 14, 2307-2334.

Lane, W.J., Dias, S., Hattori, K., Heissig, B., Choy, M., Rabbany, S.Y., Wood, J., Moore, M.A., Rafii, S., 2000. Stromal-derived factor 1-induced megakaryocyte migration and platelet production is dependent on matrix metalloproteinases. *Blood* 96, 4152-4159.

Larson, M.K., Watson, S.P., 2006a. A product of their environment: do megakaryocytes rely on extracellular cues for proplatelet formation? *Platelets* 17, 435-440.

Larson, M.K., Watson, S.P., 2006b. Regulation of proplatelet formation and platelet release by integrin alpha IIb beta3. *Blood* 108, 1509-1514.

Lee, S.H., Dominguez, R., 2010. Regulation of actin cytoskeleton dynamics in cells. *Molecules and cells* 29, 311-325.

Levinson, N.M., Seeliger, M.A., Cole, P.A., Kuriyan, J. Structural basis for the recognition of c-Src by its inactivator Csk. 2008. *Cell*

Ley, K., Laudanna, C., Cybulsky, M.I., Nourshargh, S., 2007. Getting to the site of inflammation: the leukocyte adhesion cascade updated. *Nature reviews. Immunology* 7, 678-689.

- Li, A., Dawson, J.C., Forero-Vargas, M., Spence, H.J., Yu, X., Konig, I., Anderson, K., Machesky, L.M., 2010. The actin-bundling protein fascin stabilizes actin in invadopodia and potentiates protrusive invasion. *Current biology* : CB 20, 339-345.
- Li, A., Ma, Y., Yu, X., Mort, R.L., Lindsay, C.R., Stevenson, D., Strathdee, D., Insall, R.H., Chernoff, J., Snapper, S.B., Jackson, I.J., Larue, L., Sansom, O.J., Machesky, L.M., 2011. Rac1 drives melanoblast organization during mouse development by orchestrating pseudopod- driven motility and cell-cycle progression. *Developmental cell* 21, 722-734.
- Li, J., Zhang, Y., Yao, X., Zhang, B., Du, J., Tang, C., 2002a. Effect of homocysteine on the L-arginine/nitric oxide synthase/nitric oxide pathway in human platelets. *Heart and vessels* 16, 46-50.
- Li, Z., Kim, E.S., Bearer, E.L., 2002b. Arp2/3 complex is required for actin polymerization during platelet shape change. *Blood* 99, 4466-4474.
- Lijnen, H.R., 2001. Plasmin and matrix metalloproteinases in vascular remodeling. *Thrombosis and haemostasis* 86, 324-333.
- Liliensiek, S.J., Nealey, P., Murphy, C.J., 2009. Characterization of endothelial basement membrane nanotopography in rhesus macaque as a guide for vessel tissue engineering. *Tissue engineering. Part A* 15, 2643-2651.
- Lim, K.B., Bu, W., Goh, W.I., Koh, E., Ong, S.H., Pawson, T., Sudhakaran, T., Ahmed, S., 2008. The Cdc42 effector IRSp53 generates filopodia by coupling membrane protrusion with actin dynamics. *The Journal of biological chemistry* 283, 20454-20472.
- Linder, S., 2007. The matrix corroded: podosomes and invadopodia in extracellular matrix degradation. *Trends in cell biology* 17, 107-117.
- Linder, S., Aepfelbacher, M., 2003. Podosomes: adhesion hot-spots of invasive cells. *Trends in cell biology* 13, 376-385.
- Linder, S., Higgs, H., Hufner, K., Schwarz, K., Pannicke, U., Aepfelbacher, M., 2000a. The polarization defect of Wiskott-Aldrich syndrome macrophages is linked to dislocalization of the Arp2/3 complex. *J Immunol* 165, 221-225.
- Linder, S., Hufner, K., Wintergerst, U., Aepfelbacher, M., 2000b. Microtubule-dependent formation of podosomal adhesion structures in primary human macrophages. *Journal of cell science* 113 Pt 23, 4165-4176.
- Linder, S., Wiesner, C., Himmel, M., 2011. Degrading devices: invadosomes in proteolytic cell invasion. *Annual review of cell and developmental biology* 27, 185-211.

- Liu, A.X., Rane, N., Liu, J.P., Prendergast, G.C., 2001. RhoB is dispensable for mouse development, but it modifies susceptibility to tumor formation as well as cell adhesion and growth factor signaling in transformed cells. *Molecular and cellular biology* 21, 6906-6912.
- Lordier, L., Bluteau, D., Jalil, A., Legrand, C., Pan, J., Rameau, P., Jouni, D., Bluteau, O., Mercher, T., Leon, C., Gachet, C., Debili, N., Vainchenker, W., Raslova, H., Chang, Y., 2012. RUNX1-induced silencing of non-muscle myosin heavy chain IIB contributes to megakaryocyte polyploidization. *Nature communications* 3, 717.
- Lorenz, M., Yamaguchi, H., Wang, Y., Singer, R.H., Condeelis, J., 2004. Imaging sites of N-wasp activity in lamellipodia and invadopodia of carcinoma cells. *Current biology : CB* 14, 697-703.
- Luo, B.H., Carman, C.V., Springer, T.A., 2007. Structural basis of integrin regulation and signaling. *Annual review of immunology* 25, 619-647.
- Luxenburg, C., Geblinger, D., Klein, E., Anderson, K., Hanein, D., Geiger, B., Addadi, L., 2007. The architecture of the adhesive apparatus of cultured osteoclasts: from podosome formation to sealing zone assembly. *PLoS one* 2, e179.
- Luxenburg, C., Winograd-Katz, S., Addadi, L., Geiger, B., 2012. Involvement of actin polymerization in podosome dynamics. *Journal of cell science* 125, 1666-1672.
- Machesky, L.M., Gould, K.L., 1999. The Arp2/3 complex: a multifunctional actin organizer. *Current opinion in cell biology* 11, 117-121.
- Malara, A., Gruppi, C., Pallotta, I., Spedden, E., Tenni, R., Raspanti, M., Kaplan, D., Tira, M.E., Staii, C., Balduini, A., 2011a. Extracellular matrix structure and nano-mechanics determine megakaryocyte function. *Blood* 118, 4449-4453.
- Malara, A., Gruppi, C., Rebuzzini, P., Visai, L., Perotti, C., Moratti, R., Balduini, C., Tira, M.E., Balduini, A., 2011b. Megakaryocyte-matrix interaction within bone marrow: new roles for fibronectin and factor XIII-A. *Blood* 117, 2476-2483.
- Marchand, J.B., Kaiser, D.A., Pollard, T.D., Higgs, H.N., 2001. Interaction of WASP/Scar proteins with actin and vertebrate Arp2/3 complex. *Nature cell biology* 3, 76-82.
- Marchisio, P.C., Bergui, L., Corbascio, G.C., Cremona, O., D'Urso, N., Schena, M., Tesio, L., Caligaris-Cappio, F., 1988. Vinculin, talin, and integrins are localized at specific adhesion sites of malignant B lymphocytes. *Blood* 72, 830-833.

- Martel, V., Racaud-Sultan, C., Dupe, S., Marie, C., Paulhe, F., Galmiche, A., Block, M.R., Albiges-Rizo, C., 2001. Conformation, localization, and integrin binding of talin depend on its interaction with phosphoinositides. *The Journal of biological chemistry* 276, 21217-21227.
- Martinez-Quiles, N., Ho, H.Y., Kirschner, M.W., Ramesh, N., Geha, R.S., 2004. Erk/Src phosphorylation of cortactin acts as a switch on-switch off mechanism that controls its ability to activate N-WASP. *Molecular and cellular biology* 24, 5269-5280.
- Mattia, G., Vulcano, F., Milazzo, L., Barca, A., Macioce, G., Giampaolo, A., Hassan, H.J., 2002. Different ploidy levels of megakaryocytes generated from peripheral or cord blood CD34+ cells are correlated with different levels of platelet release. *Blood* 99, 888-897.
- Mazharian, A., Watson, S.P., Severin, S., 2009. Critical role for ERK1/2 in bone marrow and fetal liver-derived primary megakaryocyte differentiation, motility, and proplatelet formation. *Experimental hematology* 37, 1238-1249 e1235.
- McCarty, O.J., Larson, M.K., Auger, J.M., Kalia, N., Atkinson, B.T., Pearce, A.C., Ruf, S., Henderson, R.B., Tybulewicz, V.L., Machesky, L.M., Watson, S.P., 2005. Rac1 is essential for platelet lamellipodia formation and aggregate stability under flow. *The Journal of biological chemistry* 280, 39474-39484.
- McClive, P.J., Sinclair, A.H., 2001. Rapid DNA extraction and PCR-sexing of mouse embryos. *Molecular reproduction and development* 60, 225-226.
- McGough, A., Pope, B., Chiu, W., Weeds, A., 1997. Cofilin changes the twist of F-actin: implications for actin filament dynamics and cellular function. *The Journal of cell biology* 138, 771-781.
- Melendez, J., Stengel, K., Zhou, X., Chauhan, B.K., Debidda, M., Andreassen, P., Lang, R.A., Zheng, Y., 2011. RhoA GTPase is dispensable for actomyosin regulation but is essential for mitosis in primary mouse embryonic fibroblasts. *The Journal of biological chemistry* 286, 15132-15137.
- Mellor, H., 2010. The role of formins in filopodia formation. *Biochimica et biophysica acta* 1803, 191-200.
- Mersich, A.T., Miller, M.R., Chkourko, H., Blystone, S.D., 2010. The formin FRL1 (FMNL1) is an essential component of macrophage podosomes. *Cytoskeleton (Hoboken)* 67, 573-585.
- Merten, M., Thiagarajan, P., 2000. P-selectin expression on platelets determines size and stability of platelet aggregates. *Circulation* 102, 1931-1936.

- Mierke, C.T., Kollmannsberger, P., Zitterbart, D.P., Diez, G., Koch, T.M., Marg, S., Ziegler, W.H., Goldmann, W.H., Fabry, B., 2010. Vinculin facilitates cell invasion into three-dimensional collagen matrices. *The Journal of biological chemistry* 285, 13121-13130.
- Mitra, S.K., Schlaepfer, D.D., 2006. Integrin-regulated FAK-Src signaling in normal and cancer cells. *Current opinion in cell biology* 18, 516-523.
- Mitsios, J.V., Prevost, N., Kasirer-Friede, A., Gutierrez, E., Groisman, A., Abrams, C.S., Wang, Y., Litvinov, R.I., Zemljic-Harpe, A., Ross, R.S., Shattil, S.J., 2010. What is vinculin needed for in platelets? *Journal of thrombosis and haemostasis* : JTH 8, 2294-2304.
- Mizutani, K., Miki, H., He, H., Maruta, H., Takenawa, T., 2002. Essential role of neural Wiskott-Aldrich syndrome protein in podosome formation and degradation of extracellular matrix in src-transformed fibroblasts. *Cancer research* 62, 669-674.
- Mohamed, M.M., Sloane, B.F., 2006. Cysteine cathepsins: multifunctional enzymes in cancer. *Nature reviews. Cancer* 6, 764-775.
- Monsky, W.L., Kelly, T., Lin, C.Y., Yeh, Y., Stetler-Stevenson, W.G., Mueller, S.C., Chen, W.T., 1993. Binding and localization of M(r) 72,000 matrix metalloproteinase at cell surface invadopodia. *Cancer research* 53, 3159-3164.
- Montanez, E., Ussar, S., Schifferer, M., Bosl, M., Zent, R., Moser, M., Fassler, R., 2008. Kindlin-2 controls bidirectional signaling of integrins. *Genes & development* 22, 1325-1330.
- Monypenny, J., Chou, H.C., Banon-Rodriguez, I., Thrasher, A.J., Anton, I.M., Jones, G.E., Calle, Y., 2011. Role of WASP in cell polarity and podosome dynamics of myeloid cells. *European journal of cell biology* 90, 198-204.
- Moreau, V., Tatin, F., Varon, C., Genot, E., 2003. Actin can reorganize into podosomes in aortic endothelial cells, a process controlled by Cdc42 and RhoA. *Molecular and cellular biology* 23, 6809-6822.
- Morrell, C.N., Matsushita, K., Chiles, K., Scharpf, R.B., Yamakuchi, M., Mason, R.J., Bergmeier, W., Mankowski, J.L., Baldwin, W.M., 3rd, Faraday, N., Lowenstein, C.J., 2005. Regulation of platelet granule exocytosis by S-nitrosylation. *Proceedings of the National Academy of Sciences of the United States of America* 102, 3782-3787.
- Moser, M., Nieswandt, B., Ussar, S., Pozgajova, M., Fassler, R., 2008. Kindlin-3 is essential for integrin activation and platelet aggregation. *Nature medicine* 14, 325-330.

- Mullen, C.A., Anderson, K.D., Blaese, R.M., 1993. Splenectomy and/or bone marrow transplantation in the management of the Wiskott-Aldrich syndrome: long-term follow-up of 62 cases. *Blood* 82, 2961-2966.
- Mullins, R.D., Pollard, T.D., 1999. Rho-family GTPases require the Arp2/3 complex to stimulate actin polymerization in *Acanthamoeba* extracts. *Current biology* : CB 9, 405-415.
- Murakami, N., Healy-Louie, G., Elzinga, M., 1990. Amino acid sequence around the serine phosphorylated by casein kinase II in brain myosin heavy chain. *The Journal of biological chemistry* 265, 1041-1047.
- Nagahisa, H., Nagata, Y., Ohnuki, T., Osada, M., Nagasawa, T., Abe, T., Todokoro, K., 1996. Bone marrow stromal cells produce thrombopoietin and stimulate megakaryocyte growth and maturation but suppress proplatelet formation. *Blood* 87, 1309-1316.
- Nascimento, F.D., Rizzi, C.C., Nantes, I.L., Stefe, I., Turk, B., Carmona, A.K., Nader, H.B., Juliano, L., Tersariol, I.L., 2005. Cathepsin X binds to cell surface heparan sulfate proteoglycans. *Archives of biochemistry and biophysics* 436, 323-332.
- Natale, D.R., Watson, A.J., 2002. Rac-1 and IQGAP are potential regulators of E-cadherin-catenin interactions during murine preimplantation development. *Mechanisms of development* 119 Suppl 1, S21-26.
- Neubauer, H., Cumano, A., Muller, M., Wu, H., Huffstadt, U., Pfeffer, K., 1998. Jak2 deficiency defines an essential developmental checkpoint in definitive hematopoiesis. *Cell* 93, 397-409.
- Nicholson-Dykstra, S., Higgs, H.N., Harris, E.S., 2005. Actin dynamics: growth from dendritic branches. *Current biology* : CB 15, R346-357.
- Nilsson, S.K., Debatis, M.E., Dooner, M.S., Madri, J.A., Quesenberry, P.J., Becker, P.S., 1998. Immunofluorescence characterization of key extracellular matrix proteins in murine bone marrow in situ. *The journal of histochemistry and cytochemistry : official journal of the Histochemistry Society* 46, 371-377.
- Nishimura, T., Yamaguchi, T., Kato, K., Yoshizawa, M., Nabeshima, Y., Ohno, S., Hoshino, M., Kaibuchi, K., 2005. PAR-6-PAR-3 mediates Cdc42-induced Rac activation through the Rac GEFs STEF/Tiam1. *Nature cell biology* 7, 270-277.
- Niu, G., Chen, X., 2011. Why integrin as a primary target for imaging and therapy. *Theranostics* 1, 30-47.

Nobes, C.D., Hall, A., 1995. Rho, rac, and cdc42 GTPases regulate the assembly of multimolecular focal complexes associated with actin stress fibers, lamellipodia, and filopodia. *Cell* 81, 53-62.

Nolen, B.J., Tomasevic, N., Russell, A., Pierce, D.W., Jia, Z., McCormick, C.D., Hartman, J., Sakowicz, R., Pollard, T.D., 2009. Characterization of two classes of small molecule inhibitors of Arp2/3 complex. *Nature* 460, 1031-1034.

Nonoyama, S., Ochs, H.D., 2001. Wiskott-Aldrich syndrome. *Current allergy and asthma reports* 1, 430-437.

Nourshargh, S., Hordijk, P.L., Sixt, M., 2010. Breaching multiple barriers: leukocyte motility through venular walls and the interstitium. *Nature reviews. Molecular cell biology* 11, 366-378.

Olivier, A., Jeanson-Leh, L., Bouma, G., Compagno, D., Blondeau, J., Seye, K., Charrier, S., Burns, S., Thrasher, A.J., Danos, O., Vainchenker, W., Galy, A., 2006. A partial down-regulation of WASP is sufficient to inhibit podosome formation in dendritic cells. *Molecular therapy : the journal of the American Society of Gene Therapy* 13, 729-737.

Ory, S., Brazier, H., Pawlak, G., Blangy, A., 2008. Rho GTPases in osteoclasts: orchestrators of podosome arrangement. *European journal of cell biology* 87, 469-477.

Otey, C.A., Pavalko, F.M., Burridge, K., 1990. An interaction between alpha-actinin and the beta 1 integrin subunit in vitro. *The Journal of cell biology* 111, 721-729.

Page-McCaw, A., Ewald, A.J., Werb, Z., 2007. Matrix metalloproteinases and the regulation of tissue remodelling. *Nature reviews. Molecular cell biology* 8, 221-233.

Pan, Y.R., Chen, C.L., Chen, H.C., 2011. FAK is required for the assembly of podosome rosettes. *The Journal of cell biology* 195, 113-129.

Pant, K., Chereau, D., Hatch, V., Dominguez, R., Lehman, W., 2006. Cortactin binding to F-actin revealed by electron microscopy and 3D reconstruction. *Journal of molecular biology* 359, 840-847.

Parekh, A., Weaver, A.M., 2009. Regulation of cancer invasiveness by the physical extracellular matrix environment. *Cell adhesion & migration* 3, 288-292.

Pasapera, A.M., Schneider, I.C., Rericha, E., Schlaepfer, D.D., Waterman, C.M., 2010. Myosin II activity regulates vinculin recruitment to focal adhesions through FAK-mediated paxillin phosphorylation. *The Journal of cell biology* 188, 877-890.

Patel-Hett, S., Wang, H., Begonja, A.J., Thon, J.N., Alden, E.C., Wandersee, N.J., An, X., Mohandas, N., Hartwig, J.H., Italiano, J.E., Jr., 2011. The spectrin-based

membrane skeleton stabilizes mouse megakaryocyte membrane systems and is essential for proplatelet and platelet formation. *Blood* 118, 1641-1652.

Pauly, R.R., Passaniti, A., Bilato, C., Monticone, R., Cheng, L., Papadopoulos, N., Gluzband, Y.A., Smith, L., Weinstein, C., Lakatta, E.G., *et al.*, 1994. Migration of cultured vascular smooth muscle cells through a basement membrane barrier requires type IV collagenase activity and is inhibited by cellular differentiation. *Circulation research* 75, 41-54.

Pelham, R.J., Jr., Wang, Y., 1997. Cell locomotion and focal adhesions are regulated by substrate flexibility. *Proceedings of the National Academy of Sciences of the United States of America* 94, 13661-13665.

Pelletier, O., Pokidysheva, E., Hirst, L.S., Bouxsein, N., Li, Y., Safinya, C.R., 2003. Structure of actin cross-linked with alpha-actinin: a network of bundles. *Physical review letters* 91, 148102.

Peng, X., Huang, J., Xiong, C., Fang, J., 2012. Cell adhesion nucleation regulated by substrate stiffness: a Monte Carlo study. *Journal of biomechanics* 45, 116-122.

Pestonjamasp, K.N., Pope, R.K., Wulfschlegel, J.D., Luna, E.J., 1997. Supervillin (p205): A novel membrane-associated, F-actin-binding protein in the villin/gelsolin superfamily. *The Journal of cell biology* 139, 1255-1269.

Pfaff, M., Jurdic, P., 2001. Podosomes in osteoclast-like cells: structural analysis and cooperative roles of paxillin, proline-rich tyrosine kinase 2 (Pyk2) and integrin alphaVbeta3. *Journal of cell science* 114, 2775-2786.

Plow, E.F., Qin, J., Byzova, T., 2009. Kindling the flame of integrin activation and function with kindlins. *Current opinion in hematology* 16, 323-328.

Polanowska-Grabowska, R., Gibbins, J.M., Gear, A.R., 2003. Platelet adhesion to collagen and collagen-related peptide under flow: roles of the [alpha]2[beta]1 integrin, GPVI, and Src tyrosine kinases. *Arteriosclerosis, thrombosis, and vascular biology* 23, 1934-1940.

Pollitt, A.Y., Insall, R.H., 2009. WASP and SCAR/WAVE proteins: the drivers of actin assembly. *Journal of cell science* 122, 2575-2578.

Ponta, H., Sherman, L., Herrlich, P.A., 2003. CD44: from adhesion molecules to signalling regulators. *Nature reviews. Molecular cell biology* 4, 33-45.

Price, G.J., Jones, P., Davison, M.D., Patel, B., Bendori, R., Geiger, B., Critchley, D.R., 1989. Primary sequence and domain structure of chicken vinculin. *The Biochemical journal* 259, 453-461.

- Psaila, B., Lyden, D., Roberts, I., 2012. Megakaryocytes, malignancy and bone marrow vascular niches. *Journal of thrombosis and haemostasis : JTH* 10, 177-188.
- Quintavalle, M., Elia, L., Condorelli, G., Courtneidge, S.A., 2010. MicroRNA control of podosome formation in vascular smooth muscle cells in vivo and in vitro. *The Journal of cell biology* 189, 13-22.
- Raftopoulou, M., Hall, A., 2004. Cell migration: Rho GTPases lead the way. *Developmental biology* 265, 23-32.
- Reddi, A.H., Gay, R., Gay, S., Miller, E.J., 1977. Transitions in collagen types during matrix-induced cartilage, bone, and bone marrow formation. *Proceedings of the National Academy of Sciences of the United States of America* 74, 5589-5592.
- Reed, G.L., Fitzgerald, M.L., Polgar, J., 2000. Molecular mechanisms of platelet exocytosis: insights into the "secrete" life of thrombocytes. *Blood* 96, 3334-3342.
- Ren, X.D., Kiosses, W.B., Sieg, D.J., Otey, C.A., Schlaepfer, D.D., Schwartz, M.A., 2000. Focal adhesion kinase suppresses Rho activity to promote focal adhesion turnover. *Journal of cell science* 113 (Pt 20), 3673-3678.
- Revenu, C., Athman, R., Robine, S., Louvard, D., 2004. The co-workers of actin filaments: from cell structures to signals. *Nature reviews. Molecular cell biology* 5, 635-646.
- Richardson, J.L., Shivdasani, R.A., Boers, C., Hartwig, J.H., Italiano, J.E., Jr., 2005. Mechanisms of organelle transport and capture along proplatelets during platelet production. *Blood* 106, 4066-4075.
- Riedl, J., Crevenna, A.H., Kessenbrock, K., Yu, J.H., Neukirchen, D., Bista, M., Bradke, F., Jenne, D., Holak, T.A., Werb, Z., Sixt, M., Wedlich-Soldner, R., 2008. Lifeact: a versatile marker to visualize F-actin. *Nature methods* 5, 605-607.
- Robinson, R.C., Turbedsky, K., Kaiser, D.A., Marchand, J.B., Higgs, H.N., Choe, S., Pollard, T.D., 2001. Crystal structure of Arp2/3 complex. *Science* 294, 1679-1684.
- Rottiers, P., Saltel, F., Daubon, T., Chaigne-Delalande, B., Tridon, V., Billottet, C., Reuzeau, E., Genot, E., 2009. TGFbeta-induced endothelial podosomes mediate basement membrane collagen degradation in arterial vessels. *Journal of cell science* 122, 4311-4318.
- Rowe, R.G., Weiss, S.J., 2008. Breaching the basement membrane: who, when and how? *Trends in cell biology* 18, 560-574.

Ryu, J.R., Echarri, A., Li, R., Pendergast, A.M., 2009. Regulation of cell-cell adhesion by Abi/Diaphanous complexes. *Molecular and cellular biology* 29, 1735-1748.

Sabri, S., Foudi, A., Boukour, S., Franc, B., Charrier, S., Jandrot-Perrus, M., Farndale, R.W., Jalil, A., Blundell, M.P., Cramer, E.M., Louache, F., Debili, N., Thrasher, A.J., Vainchenker, W., 2006. Deficiency in the Wiskott-Aldrich protein induces premature proplatelet formation and platelet production in the bone marrow compartment. *Blood* 108, 134-140.

Saftig, P., Hunziker, E., Wehmeyer, O., Jones, S., Boyde, A., Rommerskirch, W., Moritz, J.D., Schu, P., von Figura, K., 1998. Impaired osteoclastic bone resorption leads to osteopetrosis in cathepsin-K-deficient mice. *Proceedings of the National Academy of Sciences of the United States of America* 95, 13453-13458.

Sagot, I., Klee, S.K., Pellman, D., 2002. Yeast formins regulate cell polarity by controlling the assembly of actin cables. *Nature cell biology* 4, 42-50.

Sakai, T., Jove, R., Fassler, R., Mosher, D.F., 2001. Role of the cytoplasmic tyrosines of beta 1A integrins in transformation by v-src. *Proceedings of the National Academy of Sciences of the United States of America* 98, 3808-3813.

Saltel, F., Chabadel, A., Bonnelye, E., Jurdic, P., 2008. Actin cytoskeletal organisation in osteoclasts: a model to decipher transmigration and matrix degradation. *European journal of cell biology* 87, 459-468.

Sanjay, A., Houghton, A., Neff, L., DiDomenico, E., Bardelay, C., Antoine, E., Levy, J., Gailit, J., Bowtell, D., Horne, W.C., Baron, R., 2001. Cbl associates with Pyk2 and Src to regulate Src kinase activity, alpha(v)beta(3) integrin-mediated signaling, cell adhesion, and osteoclast motility. *The Journal of cell biology* 152, 181-195.

Sasahara, Y., Rachid, R., Byrne, M.J., de la Fuente, M.A., Abraham, R.T., Ramesh, N., Geha, R.S., 2002. Mechanism of recruitment of WASP to the immunological synapse and of its activation following TCR ligation. *Molecular cell* 10, 1269-1281.

Sato, T., del Carmen Ovejero, M., Hou, P., Heegaard, A.M., Kumegawa, M., Foged, N.T., Delaisse, J.M., 1997. Identification of the membrane-type matrix metalloproteinase MT1-MMP in osteoclasts. *Journal of cell science* 110 (Pt 5), 589-596.

Schaller, M.D., 2001. Paxillin: a focal adhesion-associated adaptor protein. *Oncogene* 20, 6459-6472.

Schlaepfer, D.D., Mitra, S.K., 2004. Multiple connections link FAK to cell motility and invasion. *Current opinion in genetics & development* 14, 92-101.

Schmidt, S., Nakchbandi, I., Ruppert, R., Kawelke, N., Hess, M.W., Pfaller, K., Jurdic, P., Fassler, R., Moser, M., 2011. Kindlin-3-mediated signaling from multiple integrin classes is required for osteoclast-mediated bone resorption. *The Journal of cell biology* 192, 883-897.

Schober, M., Raghavan, S., Nikolova, M., Polak, L., Pasolli, H.A., Beggs, H.E., Reichardt, L.F., Fuchs, E., 2007. Focal adhesion kinase modulates tension signaling to control actin and focal adhesion dynamics. *The Journal of cell biology* 176, 667-680.

Schoumacher, M., Goldman, R.D., Louvard, D., Vignjevic, D.M., 2010. Actin, microtubules, and vimentin intermediate filaments cooperate for elongation of invadopodia. *The Journal of cell biology* 189, 541-556.

Schulze, H., Korpai, M., Hurov, J., Kim, S.W., Zhang, J., Cantley, L.C., Graf, T., Shivdasani, R.A., 2006. Characterization of the megakaryocyte demarcation membrane system and its role in thrombopoiesis. *Blood* 107, 3868-3875.

Scott, M.P., Zappacosta, F., Kim, E.Y., Annan, R.S., Miller, W.T., 2002. Identification of novel SH3 domain ligands for the Src family kinase Hck. Wiskott-Aldrich syndrome protein (WASP), WASP-interacting protein (WIP), and ELMO1. *The Journal of biological chemistry* 277, 28238-28246.

Scott, R.W., Hooper, S., Crighton, D., Li, A., Konig, I., Munro, J., Trivier, E., Wickman, G., Morin, P., Croft, D.R., Dawson, J., Machesky, L., Anderson, K.I., Sahai, E.A., Olson, M.F., 2010. LIM kinases are required for invasive path generation by tumor and tumor-associated stromal cells. *The Journal of cell biology* 191, 169-185.

Sehgal, S., Storrie, B., 2007. Evidence that differential packaging of the major platelet granule proteins von Willebrand factor and fibrinogen can support their differential release. *Journal of thrombosis and haemostasis : JTH* 5, 2009-2016.

Selden, L.A., Kinosian, H.J., Newman, J., Lincoln, B., Hurwitz, C., Gershman, L.C., Estes, J.E., 1998. Severing of F-actin by the amino-terminal half of gelsolin suggests internal cooperativity in gelsolin. *Biophysical journal* 75, 3092-3100.

Sellers, J.R., Eisenberg, E., Adelstein, R.S., 1982. The binding of smooth muscle heavy meromyosin to actin in the presence of ATP. Effect of phosphorylation. *The Journal of biological chemistry* 257, 13880-13883.

Sen, B., Johnson, F.M., 2011. Regulation of SRC family kinases in human cancers. *Journal of signal transduction* 2011, 865819.

Serrels, B., Serrels, A., Brunton, V.G., Holt, M., McLean, G.W., Gray, C.H., Jones, G.E., Frame, M.C., 2007. Focal adhesion kinase controls actin assembly via a

FERM-mediated interaction with the Arp2/3 complex. *Nature cell biology* 9, 1046-1056.

Shi, G.P., Villadangos, J.A., Dranoff, G., Small, C., Gu, L., Haley, K.J., Riese, R., Ploegh, H.L., Chapman, H.A., 1999. Cathepsin S required for normal MHC class II peptide loading and germinal center development. *Immunity* 10, 197-206.

Shimaoka, M., Takagi, J., Springer, T.A., 2002. Conformational regulation of integrin structure and function. *Annual review of biophysics and biomolecular structure* 31, 485-516.

Shivdasani, R.A., Fujiwara, Y., McDevitt, M.A., Orkin, S.H., 1997. A lineage-selective knockout establishes the critical role of transcription factor GATA-1 in megakaryocyte growth and platelet development. *The EMBO journal* 16, 3965-3973.

Shortman, K., Liu, Y.J., 2002. Mouse and human dendritic cell subtypes. *Nature reviews. Immunology* 2, 151-161.

Sim, D.S., Merrill-Skoloff, G., Furie, B.C., Furie, B., Flaumenhaft, R., 2004. Initial accumulation of platelets during arterial thrombus formation in vivo is inhibited by elevation of basal cAMP levels. *Blood* 103, 2127-2134.

Sit, S.T., Manser, E., 2011. Rho GTPases and their role in organizing the actin cytoskeleton. *Journal of cell science* 124, 679-683.

Snapper, S.B., Rosen, F.S., Mizoguchi, E., Cohen, P., Khan, W., Liu, C.H., Hagemann, T.L., Kwan, S.P., Ferrini, R., Davidson, L., Bhan, A.K., Alt, F.W., 1998. Wiskott-Aldrich syndrome protein-deficient mice reveal a role for WASP in T but not B cell activation. *Immunity* 9, 81-91.

Somlyo, A.P., Somlyo, A.V., 2003. Ca²⁺ sensitivity of smooth muscle and nonmuscle myosin II: modulated by G proteins, kinases, and myosin phosphatase. *Physiological reviews* 83, 1325-1358.

Sossey-Alaoui, K., Su, G., Malaj, E., Roe, B., Cowell, J.K., 2002. WAVE3, an actin-polymerization gene, is truncated and inactivated as a result of a constitutional t(1;13)(q21;q12) chromosome translocation in a patient with ganglioneuroblastoma. *Oncogene* 21, 5967-5974.

Staiger, C.J., Blanchoin, L., 2006. Actin dynamics: old friends with new stories. *Current opinion in plant biology* 9, 554-562.

Steffen, A., Faix, J., Resch, G.P., Linkner, J., Wehland, J., Small, J.V., Rottner, K., Stradal, T.E., 2006. Filopodia formation in the absence of functional WAVE- and Arp2/3-complexes. *Molecular biology of the cell* 17, 2581-2591.

Stolting, M., Wiesner, C., van Vliet, V., Butt, E., Pavenstadt, H., Linder, S., Kremerskothen, J., 2012. Lasp-1 regulates podosome function. *PloS one* 7, e35340.

Stradal, T., Courtney, K.D., Rottner, K., Hahne, P., Small, J.V., Pendergast, A.M., 2001. The Abl interactor proteins localize to sites of actin polymerization at the tips of lamellipodia and filopodia. *Current biology : CB* 11, 891-895.

Straight, A.F., Cheung, A., Limouze, J., Chen, I., Westwood, N.J., Sellers, J.R., Mitchison, T.J., 2003. Dissecting temporal and spatial control of cytokinesis with a myosin II Inhibitor. *Science* 299, 1743-1747.

Stylli, S.S., Stacey, T.T., Verhagen, A.M., Xu, S.S., Pass, I., Courtneidge, S.A., Lock, P., 2009. Nck adaptor proteins link Tks5 to invadopodia actin regulation and ECM degradation. *Journal of cell science* 122, 2727-2740.

Suetsugu, S., Banzai, Y., Kato, M., Fukami, K., Kataoka, Y., Takai, Y., Yoshida, N., Takenawa, T., 2007. Male-specific sterility caused by the loss of CR16. *Genes to cells : devoted to molecular & cellular mechanisms* 12, 721-733.

Sugihara, K., Nakatsuji, N., Nakamura, K., Nakao, K., Hashimoto, R., Otani, H., Sakagami, H., Kondo, H., Nozawa, S., Aiba, A., Katsuki, M., 1998. Rac1 is required for the formation of three germ layers during gastrulation. *Oncogene* 17, 3427-3433.

Sun, H., Schlondorff, J.S., Brown, E.J., Higgs, H.N., Pollak, M.R., 2011. Rho activation of mDia formins is modulated by an interaction with inverted formin 2 (INF2). *Proceedings of the National Academy of Sciences of the United States of America* 108, 2933-2938.

Sun, H.Q., Yamamoto, M., Mejillano, M., Yin, H.L., 1999. Gelsolin, a multifunctional actin regulatory protein. *The Journal of biological chemistry* 274, 33179-33182.

Sun, L., Hwang, W.Y., Aw, S.E., 2006. Biological characteristics of megakaryocytes: specific lineage commitment and associated disorders. *The international journal of biochemistry & cell biology* 38, 1821-1826.

Sun, X., Li, C., Zhuang, C., Gilmore, W.C., Cobos, E., Tao, Y., Dai, Z., 2009. Abl interactor 1 regulates Src-Ik1-matrix metalloproteinase 9 axis and is required for invadopodia formation, extracellular matrix degradation and tumor growth of human breast cancer cells. *Carcinogenesis* 30, 2109-2116.

Suraneni, P., Rubinstein, B., Unruh, J.R., Durnin, M., Hanein, D., Li, R., 2012. The Arp2/3 complex is required for lamellipodia extension and directional fibroblast cell migration. *The Journal of cell biology* 197, 239-251.

Svitkina, T.M., Bulanova, E.A., Chaga, O.Y., Vignjevic, D.M., Kojima, S., Vasiliev, J.M., Borisy, G.G., 2003. Mechanism of filopodia initiation by reorganization of a dendritic network. *The Journal of cell biology* 160, 409-421.

Symons, M., Derry, J.M., Karlak, B., Jiang, S., Lemahieu, V., McCormick, F., Francke, U., Abo, A., 1996. Wiskott-Aldrich syndrome protein, a novel effector for the GTPase CDC42Hs, is implicated in actin polymerization. *Cell* 84, 723-734.

Tablin, F., Castro, M., Leven, R.M., 1990. Blood platelet formation in vitro. The role of the cytoskeleton in megakaryocyte fragmentation. *Journal of cell science* 97 (Pt 1), 59-70.

Tajika, K., Ikebuchi, K., Inokuchi, K., Hasegawa, S., Dan, K., Sekiguchi, S., Nakahata, T., Asano, S., 1998. IL-6 and SCF exert different effects on megakaryocyte maturation. *British journal of haematology* 100, 105-111.

Takenawa, T., Miki, H., 2001. WASP and WAVE family proteins: key molecules for rapid rearrangement of cortical actin filaments and cell movement. *Journal of cell science* 114, 1801-1809.

Takenawa, T., Suetsugu, S., 2007. The WASP-WAVE protein network: connecting the membrane to the cytoskeleton. *Nature reviews. Molecular cell biology* 8, 37-48.

Tarone, G., Cirillo, D., Giancotti, F.G., Comoglio, P.M., Marchisio, P.C., 1985. Rous sarcoma virus-transformed fibroblasts adhere primarily at discrete protrusions of the ventral membrane called podosomes. *Experimental cell research* 159, 141-157.

Tatin, F., Varon, C., Genot, E., Moreau, V., 2006. A signalling cascade involving PKC, Src and Cdc42 regulates podosome assembly in cultured endothelial cells in response to phorbol ester. *Journal of cell science* 119, 769-781.

Tehrani, S., Tomasevic, N., Weed, S., Sakowicz, R., Cooper, J.A., 2007. Src phosphorylation of cortactin enhances actin assembly. *Proceedings of the National Academy of Sciences of the United States of America* 104, 11933-11938.

Theriot, J.A., 1997. Accelerating on a treadmill: ADF/cofilin promotes rapid actin filament turnover in the dynamic cytoskeleton. *The Journal of cell biology* 136, 1165-1168.

Thomas, S.G., Calaminus, S.D., Auger, J.M., Watson, S.P., Machesky, L.M., 2007. Studies on the actin-binding protein HS1 in platelets. *BMC cell biology* 8, 46.

Thon, J.N., Macleod, H., Begonja, A.J., Zhu, J., Lee, K.C., Mogilner, A., Hartwig, J.H., Italiano, J.E., Jr., 2012. Microtubule and cortical forces determine platelet size during vascular platelet production. *Nature communications* 3, 852.

Thon, J.N., Montalvo, A., Patel-Hett, S., Devine, M.T., Richardson, J.L., Ehrlicher, A., Larson, M.K., Hoffmeister, K., Hartwig, J.H., Italiano, J.E., Jr., 2010.

Cytoskeletal mechanics of proplatelet maturation and platelet release. *The Journal of cell biology* 191, 861-874.

Tolde, O., Rosel, D., Vesely, P., Folk, P., Brabek, J., 2010. The structure of invadopodia in a complex 3D environment. *European journal of cell biology* 89, 674-680.

Tomer, A., 2004. Human marrow megakaryocyte differentiation: multiparameter correlative analysis identifies von Willebrand factor as a sensitive and distinctive marker for early (2N and 4N) megakaryocytes. *Blood* 104, 2722-2727.

Tsuboi, S., Takada, H., Hara, T., Mochizuki, N., Funyu, T., Saitoh, H., Terayama, Y., Yamaya, K., Ohyama, C., Nonoyama, S., Ochs, H.D., 2009. FBP17 Mediates a Common Molecular Step in the Formation of Podosomes and Phagocytic Cups in Macrophages. *The Journal of biological chemistry* 284, 8548-8556.

Tu, C., Ortega-Cava, C.F., Chen, G., Fernandes, N.D., Cavallo-Medved, D., Sloane, B.F., Band, V., Band, H., 2008. Lysosomal cathepsin B participates in the podosome-mediated extracellular matrix degradation and invasion via secreted lysosomes in v-Src fibroblasts. *Cancer research* 68, 9147-9156.

Turner, C.E., Glenney, J.R., Jr., Burridge, K., 1990. Paxillin: a new vinculin-binding protein present in focal adhesions. *The Journal of cell biology* 111, 1059-1068.

Urano, T., Liu, J., Li, Y., Smith, N., Zhan, X., 2003a. Sequential interaction of actin-related proteins 2 and 3 (Arp2/3) complex with neural Wiscott-Aldrich syndrome protein (N-WASP) and cortactin during branched actin filament network formation. *The Journal of biological chemistry* 278, 26086-26093.

Urano, T., Zhang, P., Liu, J., Hao, J.J., Zhan, X., 2003b. Haematopoietic lineage cell-specific protein 1 (HS1) promotes actin-related protein (Arp) 2/3 complex-mediated actin polymerization. *The Biochemical journal* 371, 485-493.

Vaananen, H.K., Horton, M., 1995. The osteoclast clear zone is a specialized cell-extracellular matrix adhesion structure. *Journal of cell science* 108 (Pt 8), 2729-2732.

Van Goethem, E., Guet, R., Balor, S., Charriere, G.M., Poincloux, R., Labrousse, A., Maridonneau-Parini, I., Le Cabec, V., 2011. Macrophage podosomes go 3D. *European journal of cell biology* 90, 224-236.

Van Goethem, E., Poincloux, R., Gauffre, F., Maridonneau-Parini, I., Le Cabec, V., 2010. Matrix architecture dictates three-dimensional migration modes of human macrophages: differential involvement of proteases and podosome-like structures. *J Immunol* 184, 1049-1061.

van Helden, S.F., Oud, M.M., Joosten, B., Peterse, N., Figdor, C.G., van Leeuwen, F.N., 2008. PGE2-mediated podosome loss in dendritic cells is dependent on actomyosin contraction downstream of the RhoA-Rho-kinase axis. *Journal of cell science* 121, 1096-1106.

van Rossum, A.G., Schuurin-Scholtes, E., van Buuren-van Seggelen, V., Kluin, P.M., Schuurin, E., 2005. Comparative genome analysis of cortactin and HS1: the significance of the F-actin binding repeat domain. *BMC genomics* 6, 15.

Varon, C., Tatin, F., Moreau, V., Van Obberghen-Schilling, E., Fernandez-Sauze, S., Reuzeau, E., Kramer, I., Genot, E., 2006. Transforming growth factor beta induces rosettes of podosomes in primary aortic endothelial cells. *Molecular and cellular biology* 26, 3582-3594.

Vicente-Manzanares, M., Ma, X., Adelstein, R.S., Horwitz, A.R., 2009. Non-muscle myosin II takes centre stage in cell adhesion and migration. *Nature reviews. Molecular cell biology* 10, 778-790.

Vicente-Manzanares, M., Newell-Litwa, K., Bachir, A.I., Whitmore, L.A., Horwitz, A.R., 2011. Myosin IIA/IIB restrict adhesive and protrusive signaling to generate front-back polarity in migrating cells. *The Journal of cell biology* 193, 381-396.

Vidal, C., Geny, B., Melle, J., Jandrot-Perrus, M., Fontenay-Roupie, M., 2002. Cdc42/Rac1-dependent activation of the p21-activated kinase (PAK) regulates human platelet lamellipodia spreading: implication of the cortical-actin binding protein cortactin. *Blood* 100, 4462-4469.

Visse, R., Nagase, H., 2003. Matrix metalloproteinases and tissue inhibitors of metalloproteinases: structure, function, and biochemistry. *Circulation research* 92, 827-839.

Voisin, M.B., Probstl, D., Nourshargh, S., 2010. Venular basement membranes ubiquitously express matrix protein low-expression regions: characterization in multiple tissues and remodeling during inflammation. *The American journal of pathology* 176, 482-495.

Volkman, B.F., Prehoda, K.E., Scott, J.A., Peterson, F.C., Lim, W.A., 2002. Structure of the N-WASP EVH1 domain-WIP complex: insight into the molecular basis of Wiskott-Aldrich Syndrome. *Cell* 111, 565-576.

Volkman, N., DeRosier, D., Matsudaira, P., Hanein, D., 2001. An atomic model of actin filaments cross-linked by fimbrin and its implications for bundle assembly and function. *The Journal of cell biology* 153, 947-956.

Wang, J.F., Liu, Z.Y., Gropman, J.E., 1998. The alpha-chemokine receptor CXCR4 is expressed on the megakaryocytic lineage from progenitor to platelets and modulates migration and adhesion. *Blood* 92, 756-764.

Wang, R., Lajevardi-Khosh, A., Choi, S., Chae, J., 2011. Regenerative Surface Plasmon Resonance (SPR) biosensor: real-time measurement of fibrinogen in undiluted human serum using the competitive adsorption of proteins. *Biosensors & bioelectronics* 28, 304-307.

Wang, Y., McNiven, M.A., 2012. Invasive matrix degradation at focal adhesions occurs via protease recruitment by a FAK-p130Cas complex. *The Journal of cell biology* 196, 375-385.

Watson, S.P., Auger, J.M., McCarty, O.J., Pearce, A.C., 2005a. GPVI and integrin α IIb β 3 signaling in platelets. *Journal of thrombosis and haemostasis : JTH* 3, 1752-1762.

Watson, S.P., Bahou, W.F., Fitzgerald, D., Ouwehand, W., Rao, A.K., Leavitt, A.D., 2005b. Mapping the platelet proteome: a report of the ISTH Platelet Physiology Subcommittee. *Journal of thrombosis and haemostasis : JTH* 3, 2098-2101.

Webb, B.A., Eves, R., Mak, A.S., 2006. Cortactin regulates podosome formation: roles of the protein interaction domains. *Experimental cell research* 312, 760-769.

Webb, D.J., Donais, K., Whitmore, L.A., Thomas, S.M., Turner, C.E., Parsons, J.T., Horwitz, A.F., 2004. FAK-Src signalling through paxillin, ERK and MLCK regulates adhesion disassembly. *Nature cell biology* 6, 154-161.

Weed, S.A., Karginov, A.V., Schafer, D.A., Weaver, A.M., Kinley, A.W., Cooper, J.A., Parsons, J.T., 2000. Cortactin localization to sites of actin assembly in lamellipodia requires interactions with F-actin and the Arp2/3 complex. *The Journal of cell biology* 151, 29-40.

Weekes, J., Barry, S.T., Critchley, D.R., 1996. Acidic phospholipids inhibit the intramolecular association between the N- and C-terminal regions of vinculin, exposing actin-binding and protein kinase C phosphorylation sites. *The Biochemical journal* 314 (Pt 3), 827-832.

Weiss, E.E., Kroemker, M., Rudiger, A.H., Jockusch, B.M., Rudiger, M., 1998. Vinculin is part of the cadherin-catenin junctional complex: complex formation between α -catenin and vinculin. *The Journal of cell biology* 141, 755-764.

Welch, M.D., DePace, A.H., Verma, S., Iwamatsu, A., Mitchison, T.J., 1997. The human Arp2/3 complex is composed of evolutionarily conserved subunits and is localized to cellular regions of dynamic actin filament assembly. *The Journal of cell biology* 138, 375-384.

West, M.A., Prescott, A.R., Chan, K.M., Zhou, Z., Rose-John, S., Scheller, J., Watts, C., 2008. TLR ligand-induced podosome disassembly in dendritic cells is ADAM17 dependent. *The Journal of cell biology* 182, 993-1005.

Westphal, R.S., Soderling, S.H., Alto, N.M., Langeberg, L.K., Scott, J.D., 2000. Scar/WAVE-1, a Wiskott-Aldrich syndrome protein, assembles an actin-associated multi-kinase scaffold. *The EMBO journal* 19, 4589-4600.

Wheeler, A.P., Wells, C.M., Smith, S.D., Vega, F.M., Henderson, R.B., Tybulewicz, V.L., Ridley, A.J., 2006. Rac1 and Rac2 regulate macrophage morphology but are not essential for migration. *Journal of cell science* 119, 2749-2757.

Wickenhauser, C., Lorenzen, J., Thiele, J., Hillienhof, A., Jungheim, K., Schmitz, B., Hansmann, M.L., Fischer, R., 1995. Secretion of cytokines (interleukins-1 alpha, -3, and -6 and granulocyte-macrophage colony-stimulating factor) by normal human bone marrow megakaryocytes. *Blood* 85, 685-691.

Wiesner, C., Faix, J., Himmel, M., Bentzien, F., Linder, S., 2010. KIF5B and KIF3A/KIF3B kinesins drive MT1-MMP surface exposure, CD44 shedding, and extracellular matrix degradation in primary macrophages. *Blood* 116, 1559-1569.

Xiao, H., Bai, X.H., Wang, Y., Kim, H., Mak, A.S., Liu, M., 2013. MEK/ERK pathway mediates PKC activation-induced recruitment of PKCzeta and MMP-9 to podosomes. *Journal of cellular physiology* 228, 416-427.

Xiao, H., Eves, R., Yeh, C., Kan, W., Xu, F., Mak, A.S., Liu, M., 2009. Phorbol ester-induced podosomes in normal human bronchial epithelial cells. *Journal of cellular physiology* 218, 366-375.

Xu, W., Baribault, H., Adamson, E.D., 1998. Vinculin knockout results in heart and brain defects during embryonic development. *Development* 125, 327-337.

Yablonski, D., Kane, L.P., Qian, D., Weiss, A., 1998. A Nck-Pak1 signaling module is required for T-cell receptor-mediated activation of NFAT, but not of JNK. *The EMBO journal* 17, 5647-5657.

Yamaguchi, H., Lorenz, M., Kempiak, S., Sarmiento, C., Coniglio, S., Symons, M., Segall, J., Eddy, R., Miki, H., Takenawa, T., Condeelis, J., 2005. Molecular mechanisms of invadopodium formation: the role of the N-WASP-Arp2/3 complex pathway and cofilin. *The Journal of cell biology* 168, 441-452.

Yamakita, Y., Matsumura, F., Lipscomb, M.W., Chou, P.C., Werlen, G., Burkhardt, J.K., Yamashiro, S., 2011. Fascin1 promotes cell migration of mature dendritic cells. *J Immunol* 186, 2850-2859.

Yamana, N., Arakawa, Y., Nishino, T., Kurokawa, K., Tanji, M., Itoh, R.E., Monypenny, J., Ishizaki, T., Bito, H., Nozaki, K., Hashimoto, N., Matsuda, M., Narumiya, S., 2006. The Rho-mDia1 pathway regulates cell polarity and focal adhesion turnover in migrating cells through mobilizing Apc and c-Src. *Molecular and cellular biology* 26, 6844-6858.

- Yamashiro, S., Yamakita, Y., Ono, S., Matsumura, F., 1998. Fascin, an actin-bundling protein, induces membrane protrusions and increases cell motility of epithelial cells. *Molecular biology of the cell* 9, 993-1006.
- Yan, C., Martinez-Quiles, N., Eden, S., Shibata, T., Takeshima, F., Shinkura, R., Fujiwara, Y., Bronson, R., Snapper, S.B., Kirschner, M.W., Geha, R., Rosen, F.S., Alt, F.W., 2003. WAVE2 deficiency reveals distinct roles in embryogenesis and Rac-mediated actin-based motility. *The EMBO journal* 22, 3602-3612.
- Ye, F., Hu, G., Taylor, D., Ratnikov, B., Bobkov, A.A., McLean, M.A., Sligar, S.G., Taylor, K.A., Ginsberg, M.H., 2010. Recreation of the terminal events in physiological integrin activation. *The Journal of cell biology* 188, 157-173.
- Yu, X., Machesky, L.M., 2012. Cells assemble invadopodia-like structures and invade into matrigel in a matrix metalloprotease dependent manner in the circular invasion assay. *PloS one* 7, e30605.
- Yu, X., Zech, T., McDonald, L., Gonzalez, E.G., Li, A., Macpherson, I., Schwarz, J.P., Spence, H., Futo, K., Timpson, P., Nixon, C., Ma, Y., Anton, I.M., Visegrady, B., Insall, R.H., Oien, K., Blyth, K., Norman, J.C., Machesky, L.M., 2012. N-WASP coordinates the delivery and F-actin-mediated capture of MT1-MMP at invasive pseudopods. *The Journal of cell biology* 199, 527-544.
- Zhan, X., Haudenschild, C.C., Ni, Y., Smith, E., Huang, C., 1997. Upregulation of cortactin expression during the maturation of megakaryocytes. *Blood* 89, 457-464.
- Zhou, S., Webb, B.A., Eves, R., Mak, A.S., 2006. Effects of tyrosine phosphorylation of cortactin on podosome formation in A7r5 vascular smooth muscle cells. *American journal of physiology. Cell physiology* 290, C463-471.
- Ziegler, W.H., Liddington, R.C., Critchley, D.R., 2006. The structure and regulation of vinculin. *Trends in cell biology* 16, 453-460.

Appendix

The following supplementary movies can be found in the CD in the back sleeve:

Movie 1 – Chapter 3, Figure 3.1A: Mk spreading on fibrinogen

Movie 2 – Chapter 3, Figure 3.1B: Mk spreading on Horm collagen

Movie 3 – Chapter 3, Figure 3.4D: RFP-Lifeact/GFP-Wasp expressing Mk spreading on fibrinogen

Movie 4 – Chapter 4, Figure 4.1A: GFP-Lifeact Mk spreading on fibrinogen

Movie 5 – Chapter 4, Figure 4.1B: GFP-Lifeact Mk spreading on Horm collagen

Movie 6 – Chapter 4, Figure 4.3A: GFP-Lifeact Mk spreading on fibrinogen in the presence of 5 μ M GM6001

Movie 7 – Chapter 4, Figure 4.3B: GFP-Lifeact Mk spreading on fibrinogen in the presence of 10 μ M Blebbistatin

Movie 8 – Chapter 4, Figure 4.5A: GFP-Lifeact Mk spreading on collagen I in the presence of 5 μ M GM6001

Movie 9 – Chapter 4, Figure 4.5B: GFP-Lifeact Mk spreading on collagen I in the presence of 10 μ M Blebbistatin

Movie 10 – Chapter 4, Figure 4.14: GFP-Lifeact Mk spreading on a native basement membrane prestained for collagen IV

Movie 11 – Chapter 6, Figure 6.1: 3D reconstruction of Mk in 3D FITC-collagen I gel, stained for F-actin (red) and DNA (blue)